World Renewable Energy Congress – Sweden

8–13 May, 2011
Linköping, Sweden

Editor

Professor Bahram Moshfegh

Copyright

Linköping Electronic Conference Proceedings, 57
Linköping University Electronic Press
Linköping, Sweden, 2011

http://www.ep.liu.se/ecp_home/index.en.aspx?issue=057
ISBN: 978-91-7393-070-3
ISSN 1650-3740 (online)
ISSN 1650-3686 (print)

Volume 2

Climate Change Issues

Table of Contents

Risk based adaptation to climate change

Kjell Eriksson[1,*], Peter Friis-Hansen[1]

[1] *DNV Research & Innovation, Veritasveien 1, 1363 Høvik, Norway*
** Corresponding author. Tel: +47 95468338, E-mail: Kjell.Eriksson@DNV.COM*

Abstract: Climate change is real and owners and operators of critical infrastructures need to adapt to a different environment. Decisions will have to be made under large degree of uncertainty. There are today no specific methods that combine global climate models with infrastructure design methods. Hence the uncertainty in the decisions becomes even larger.

The paper presents a method for combining state-of-the-art climate modelling, meteorological approaches, with state-of-the-art structural design methods in a decision theoretic frame. This has, to our knowledge, not been done before. The decision framework will help authorities to make complicated and critical decisions with respect to how to prepare for future changes in the environment. The work is based on the climate models used in the current and updated IPCC Reports, regional and local meteorological and oceanographic models, and the DNV Recommended Practice on environmental loads, DNV-RP-C205.

The decision theoretic frame is risk-based where expected loss will be expressed in monetary terms. The approach is applicable to critical infrastructures, power generation and transmission, and offshore oil and gas installations.

The paper will address key design parameters, likely climate change scenarios, time horizon of the infrastructure or installation in question, limitations of existing climate models, combination of global and regional climate models, how to downscale results and, ultimately, how to convert the results into a design basis.
The methodology presented in the paper is based on ongoing research partly financed by the Norwegian Research Council and partly by DNV.

Keywords: *Climate change, Adaptation, Risk management, Infrastructures*

1. Introduction

"*Every year, climate change claims lives and seriously affects much of our planet. The scale and breadth of the challenge as identified by the Climate Vulnerability Monitor is already immense. So is the explosive growth of its negative effects on human society. Everyone should be aware of the risks we are running by not tackling the climate crisis, and how simple it is in many cases to avoid damage now and tomorrow. Still, only truly urgent action will prevent increasingly irreversible harm to the earth and the life it sustains. Equally urgent support is currently needed to help populations in places most vulnerable to the worst effects of climate change. They are on today's frontlines of our common struggle with a now rapidly changing planet.*" This citation is taken from the DARA [1] homepage, where their recently published report "Climate Vulnerability Monitor 2010" is published. The *Climate Vulnerability Monitor 2010* report draws attention to approximately 350,000 lives already lost each year as a result of global warming and changes to our climate. The annual number of lives lost is forecasted to increase to nearly 1 million by year 2030. The report further estimates that US$ 150 billion is lost in today's economy as a result of climate changes. These losses will increase in the future. More than half of the total economic losses will occur in industrialized countries. Moreover, DARA estimates that around 170 countries (i.e. most of the world) have high vulnerability to climate change in at least one key impact area already today.

The evidence in the DARA report highlights that decision-makers worldwide will face huge challenges in selecting effective means for adapting costly infrastructures to the changing climate. If decision makers fail to properly adapt infrastructures in time, the potential losses

may well exceed far beyond the cost of the infrastructure itself. Lost infrastructures such as part of e.g. a transport system, energy system, or vital public facilities (for instance hospitals), may paralyse society for a long time and therefore create a setback for the economy and a whole community.

What aggravates the decision making is the overwhelming amount of uncertainties that the decision maker is facing. The decision maker must not only consider uncertainties in relation to future climatic changes (temperature, storms, precipitation, waves, subsidence, etc.) and how these correlate, but also the health state of the degrading infrastructure prior to the occurrence of the events, as well as estimate direct and indirect consequences that follow. However, uncertainties are not limited to this. Mathematical models that use semi-empirical models of vegetation, soils, ice-sheets, etc., are invoked to forecast future climate change effects. These models are imprecise and will add further uncertainty into the decision problem.

The forecasting of the climate is based on four representative CO2 emission scenarios; however, we do not know which scenario that best will describe the future. Finally, it is the extreme events that govern failure of the structures, and these extremes are by nature hard to predict. Therefore, also statistical uncertainty enters the decision problem.

Although most decision-makers are increasingly concerned with the adverse impacts of climate variability and change, decision-makers rarely possess the composite knowledge needed to understand the complexity, interconnectivity, and limitations of uncertainty modelling, to make effective decisions to manage current and future climate risks. The challenge in establishing this technical understanding requires that risk-based adaptation to climate change assume a new level of integration and coordination.

DNV is currently developing a Recommended Practice (RP) for risk-based adaptation to climate change. The objective of the RP is to assist decision makers, such as public authorities, to exercise critical and sound decision-making on how to prepare and adapt to future changes in the environment. This is sought achieved through the formulation of a structured method that combines state-of-the-art climate modelling, meteorological approaches, with state-of-the-art structural design methods. The method is based on the climate models used in the current and updated IPCC Reports, regional and local meteorological and oceanographic models; and finally, it is risk-based where all uncertainties are accounted for. Such a recommended practice has, to our knowledge, never been developed before.

Since the majority of the uncertainties to a large extent are rooted in expert judgement in combination with mathematical modelling, the recommended practice will also include methods for identification of what uncertainties affect the decision making the most, and provide guidance for reducing these uncertainties. This is central since decisions made on adapting infrastructures to climate change are very costly in general; wherefore it is of paramount importance for decision-makers to identify means to effectively reduce the probability of making a wrong decision.

DNV is aware of the work undertaken by the World Meteorological Organization under the Global Framework for Climate Services (GFCS) [2]. GFCS was established by the Heads of State and Government, Ministers and Heads of Delegations present at the UN World Climate Conference-3 (WCC-3) in September 2009 with the mandate to: "*Enable better management of the risks of climate variability and change and adaptation to climate change at all levels, through development and incorporation of science-based climate information and prediction into planning, policy and practice.*" As such, the GFCS activity may seem identical to the

work that DNV is undertaking to establish an RP. However, the work of GFCS appears (at present) to have focus on strengthening the global observing capability of the members by optimising the density and spatial distribution of observing networks, ensuring data compatibility and increasing the quality of observations. Such work is very important to arrive at better and more reliable predictions in climate modelling, which will also be undertaken by GFCS. However, in our work on the RP, focus is on formulating a structured method that effectively will allow decision makers to effectively control and handle all uncertainties involved in the decision-making and as such to arrive at better decision. Hence, the RP and the GFCS work complement each other. At present our RP is not based on the GFCS work, but this may change in future.

In this paper we describe the general background and applied principles behind the recommended practice. The paper is compiled as follows: In section 2 the applied terminology for risk related elements are defined. Here it is argued why risk is defined as expected monetary loss. In section 3, we discuss climate modelling and how to arrive at a description of the outmost important assessment of extreme events of the climate impacts as well as the correlation among different climate impacts. Section 4 discusses the existing design principles for infrastructures. It is highlighted that extreme events for such structures have a completely different meaning than that applied in the IPCC reports. Section 5 shortly presents the risk modelling and describes how the dominating uncertainties in the model can be identified. For this set of dominating uncertainties effective uncertainty reductions can be made. In section 6, we present a graphical overview of the overall method, and finally in section 7, we summarise and conclude the expected benefits from establishing and applying the recommended practice to costly decisions on adaptation of important infrastructures to a chancing climate.

2. Risk related terminology

2.1. Risk

Intuitively a measure of risk should be some increasing function of both the probability of occurrence of the adverse event and the consequence of the adverse event represented on some numerical (monetary) scale. If an adverse event A occurs once within a year with probability p, and two or more occurrences of A within a year have negligible probability as compared to p and, moreover, the consequence of the occurrence of A can be represented by a loss L equal to a known monetary cost c, then the expected value of the yearly cost is $pc+(1-p)0=pc$, because there is no cost from A if A does not occur. There is a decision theoretical reason[i] to take this *expected cost* as the definition of the yearly risk $r(A)$ associated with the event A, i.e. $r(A)=pc$. This definition may easily be relaxed to apply for events that occur in time with frequency λ, to become $r(A)=\lambda c$.

Typically, risk analysis is performed without a clear definition of how to measure risk, and only displayed by a simple, crude colour coding. Such an approach is not sufficient to be applied for decision making of complex costly structures. In the RP we advocate for detailed modelling of both frequencies and consequences.

[i] The decision theoretical argument is, of course, that decisions on risk reduction initiatives are measured on monetary scale, and that risk as such directly is in agreement with the fundament of decision theory.

2.2. Vulnerability

There exist several definitions for "vulnerability" that all depend upon the type of system they relate to (e.g. technical, computer, networks, organisational and societal systems). The set of definitions all refer to *weaknesses* or *flaws* embedded within the system caused by some event combined with the capability of the environment (or external circumstances) to *exploit such weaknesses* to impair the functioning of the system [3,4,5].

The provided definitions of vulnerability are imprecise, and are not operable within the quantitative framework of the RP being established. Therefore, we define *vulnerability* as the *conditional expected loss*; that is, the risk calculated conditional on the occurrence of the unwanted event. This implies that vulnerability will be decreasing when the failure probability of any implemented barrier decreases or when the consequences decreases. This definition is operable and is in agreement with common use of the word *vulnerability*.

2.3. Resilience

There exist several definitions of resilience in literature. Within the resilience engineers there seem to be consensus along the line that is well defined by Wreathall [6]: "*Resilience is the ability of an organization (system) to keep, or recover quickly to, a stable state, allowing it to continue operation during and after a major mishap, or in the presence of continuous significant stresses*".

Unfortunately, this definition makes it difficult to measure resilience. We therefore propose the definition: "Resilience is the *ability to control* the risk that follows after a major mishap. The risk includes operational loss, emergency recovery, etc., of the continuously stressed system." This implies that resilience also can be defined as controlling the vulnerability that follows after the occurrence of the direct losses, i.e. controlling the follow consequences.

3. Climate models

The assessment of statistics on extreme events in weather variables influenced by a changing climate is of outmost importance to adaptation decisions for future infrastructures. This is a complex task. Firstly, it is difficult to estimate the extreme value statistics, since it by nature is hard to get reliable statistics of rare events from available observations. Secondly, for a changing climate, statistics based on past observations cannot directly be extrapolated, and we must rely on theories, models and past analogies. Research shows that some of the largest impacts of climate change will be through more extreme climate events [7].

The primary tool for assessing climate changes is emission scenario simulations using General Circulation Models (GCM), which in a rather coarse resolution solve the flow and energy equations for the atmosphere and oceans. Furthermore, these models are combined with semi-empirical models of vegetation, soils, ice-sheets etc, to form Earth System Models. The models are extremely costly to run at a level with reliable predictive power, which creates two types of limitations. Firstly, while they provide reasonable predictions at the large scales, they generally underestimate extremes. This is both due to the fact that the coarse resolution makes the meteorological fields unrealistically smooth and the fact that the models are too costly to run for reliable simulation of the extreme tails of the probability distributions of the meteorological fields. Secondly, the global models do not provide the probabilistic information of extreme local climate events needed for risk analysis. For the task of assessing the statistics of a specific climatologic variable, relevant for a specific location (say 10m wind over the North Sea), there are some main techniques:

Dynamical downscaling is based on Regional Climate Models (RCM) that uses GCMs as boundary conditions to simulate the state of the atmosphere in a region with a smaller grid resolution than used in the GCM. RCM models are usually defined at a grid size of 10-50 km and are able to better represent topography and land use than GCM models. However, these models inherit some of the biases of the GCM, and in most cases further statistical downscaling and adjustment is required.

Statistical downscaling techniques are needed to obtain bias-corrected, high-resolution local projections from GCM and RCM simulations. The basic idea behind statistical downscaling is to define a relationship between large scale and local scale climate variables. Presently little emphasis has been put towards downscaling of extremes.

Stochastic weather generators have been applied for downscaling precipitation and derivation of extreme value statistics. These models are typically empirical Markov chain models for generating surrogate climate variables based on parameters estimations from observations and models. Downscaling using stochastic weather generator may change the GCM results considerable. Semenov and Barrow [8] reports an increase in monthly average precipitation by up to a factor of three in some areas.

Climate statistics derives distributions based on past observations. These are based on the assumption of stationarity where past observations are used to estimate the extreme value distributions and associated risks. IPPC operates with approximately 25 GCM models, among which around 8 differ in the underlying semi-empirical models. This implies that that these models do have different competences in capturing different climate change effects in different regions. Similarly there exist of the order of 15 different RCM models that again each have their own competences and weaknesses in different areas.

One of the objectives of the RP that we are developing is to identify what climate change effects are important (for offshore structures in the first version) at different locations around the world. This is used to highlight the relevant weather features that the chosen GCMs and RCMs must be able to capture to arrive at trustworthy climate change predictions. For instance, for the Barents Sea it is important that the models capture polar lows, synoptic lows, and sea ice extent, otherwise extreme winds and waves may be grossly underestimated.

Meehl et al. [9] discussed that though the climate models can simulate many aspects of climate variability and extremes, they still are characterized by systematic simulation errors and limitations in accurately simulating regional climate such that appropriate caveats must accompany any discussion of future changes in weather and climate extremes. However, as computers become more powerful this allow for taking into account more climatological effects and at the same time increasing the grid size. However, when errors are systematic, then the increase in computer power may be of limited use.

Depending on the structures that are evaluated the climate predictions shall be evaluated for the following time periods: present, 20, 50 and 100 years forecasting. Infrastructures are typically designed for 100 year lifetime, whereas offshore structures generally have an expected lifetime of 50 years. The need for all periods for infrastructures is due to dominating uncertainties may change at the different time scales and result in a different mixture of extremes. This may initiate new failure modes to the infrastructures.

Today the climate models are evaluated only for the extreme emission scenarios (currently the A1B-scenario). This may result in too conservative adaptive measures are implemented. This

may result in unjustified large investments being allocated at the expense of other initiatives not being implemented. For this reason it is desirable to have climate model runs for all emission scenarios and to assign a probability distribution over the set of analysed scenarios.

4. Design principles for infrastructures

The structural dimensioning of civil infrastructures is made according to requirements formulated in a structural design code. The code requirements are interpreted and formulated within a mathematical model for the geometric and mechanical properties of the structure and for the actions on the structure. For a carefully selected set of the (random) variables that independently contribute to that part of the mathematical model that concerns geometry, strength properties and actions, the code committee calibrates the set of (random) variables such that the design code can control the safety level of a broad class of structures for which the code is meant to cover. The variables are called *design variables*. Control over the safety level is achieved by selecting a *characteristic value* for all design variables (this is typically the 98% or 2-5% fractile value of the random variable) and calibrating *partial safety factors* that amplify the design variables such that the desired safety level is obtained.

For example, consider a simple steel rod with load that pulls at the end of the rod. Let the random strength of the rod be R and the random load be S. The critical situation is clearly when the strength is small and the load is high. Therefore the characteristic value, r_c, of the strength is defined as the 5% fractile value of R and the characteristic value, s_c, of the load takes the 98% fractile of S. The partial safety factor on r_c is γ_r and γ_s on s_c. The design equation in this example becomes:

$$g = \frac{r_c}{\gamma_r} - s_c \gamma_s \geq 0 .$$

The magnitude of the partial safety factors depend on how critical the required safety level of the structure is. Table 1 presents the required reliability (safety) index requirements for building structures.

Table 1. Example of reliability index requirements. From NKB [10].Values in parenthesis is the failure probability.

		Type of failure		
(Reference period 1 year)		Ductile with reserves	Ductile without reserves	Brittle
Safety class	Low	3.1 ($1.0 \cdot 10^{-3}$)	3.7 ($1.1 \cdot 10^{-4}$)	4.2 ($1.3 \cdot 10^{-5}$)
	Normal	3.7 ($1.1 \cdot 10^{-4}$)	4.2 ($1.3 \cdot 10^{-5}$)	4.7 ($1.3 \cdot 10^{-6}$)
	High	4.2 ($1.3 \cdot 10^{-5}$)	4.7 ($1.3 \cdot 10^{-6}$)	5.2 ($1.0 \cdot 10^{-7}$)

The table shows that the required reliability (safety) level depends both on safety class and type of failure. Both the safety class and type of failure refer to consequences of failure. The levels have been identified and validated through cost-benefit analysis of a large suite of structures. Low safety level refers to warehouses whereas the high safety class refers to grandstands and critical infrastructures. The work by NKB forms the basis for all structural codes in Scandinavia, and the principle is now also applied in the Eurocode [2] for structural design.

The table provide valuable information about the fractile level of the extreme value distribution that is of real interest. Critical infrastructures will typically be designed to reliability level of 4.2 to 4.7. It can be shown that this level corresponds to annual exceedance probabilities of the order of $1.3 \cdot 10^{-3}$ to $1.3 \cdot 10^{-5}$.

In the document IPPC [11] rare events are defined as: "*An event that is rare at a particular place and time of year. Definitions of 'rare' vary, but an extreme weather event would normally be as rare as or rarer than the 10th or 90th percentile of the observed probability density function. By definition, the characteristics of what is called extreme weather may vary from place to place in an absolute sense.*" It is seen that what IPPC consider as rare events significantly differs from the extreme values that is required in structural design, which is a factor of 100 to 10.000 less than the IPPC definition of rare events. The need to extend extremes far beyond what is normally classed as rare within the climatological terminology is very important and a very challenging task.

5. Risk modelling and identification of the dominating uncertainties

The risk modelling contains two interconnected parts: one is to estimate the annual probability of the structure failing and the second is to identify the spectrum of consequences that may materialise following the occurrence of unwanted events. The considered consequence spectrum shall cover both direct and indirect losses, and loss types will not only address loss of life and material losses, but shall also account for production losses and environmental losses. When estimating the indirect losses it is important to consider how the evaluated infrastructure relates and impinge on the surrounding society.

We consider three means for running the risk analysis: The first approach is to establish a Bayesian network (BN) construct for the entire problem. This approach requires a descretisation of the random variables and losses. The second is to apply a full structural reliability approach that use continuous distribution. The third approach is to apply Monte Carlo simulation to estimate the risk. This approach may be combined with the two former through discrete event simulations.

The two first approaches almost directly facilitate identification of the most dominating uncertainties as this can be extracted almost as a bi-product of the analysis. For the BN approach we use so-called *max-propagation* to identify dominating uncertainties, and for the second approach the importance factors directly provide the information. The third approach is somewhat more involved as it requires multiple runs to evaluate the 'value of information' for each random variable. Means will be identified for reducing the uncertainties for the set of variables that dominate the risk modelling, since it will be those variables influences the probability of making a wrong decision the most. Hence, this information gathering may represent a significant cost savings at limited cost.

6. Overview of the risk based method

Figure 1 presents a graphical overview of the overall method. The procedure has 6 steps. The first step is to identify a probability distribution over the emission scenarios thereafter to identify relevant GCMs and RCMs to predict the distributions of future climate. The risk analysis completed by first completing a vulnerability analysis. This facilitates future updates due to changes in emission scenarios, GCM/RCM choices, implementation of adaptation measures.

7. Summary and conclusion

Climate change is real and owners and operators of critical infrastructures need to adapt to a different environment. Climate change is analysed by different global climate models. One fundamental difference between global climate models and design codes for infrastructure is that the climate models operate with average values, whereas one needs extreme values for design codes. It should be noted that the definition of a rare event used by IPCC is fundamentally different from the definition of an extreme event in a design code. There is a significant

difference in designing a roof for total of 10% more snowfall if the additional snowfall is evenly distributed throughout the winter versus if the additional snowfall is concentrated for a few days. Designing infrastructure for future climate conditions will involve handling a large number of factors with significant uncertainties. We propose to use a risk based method to handle these uncertainties, and as a means to building a bridge between the climate models and design methods used for infrastructure. More work is needed to clearly describe and quantify the characteristics of the different climate models, better understand the limitations different downscaling methods and to identify the dominating uncertainties.

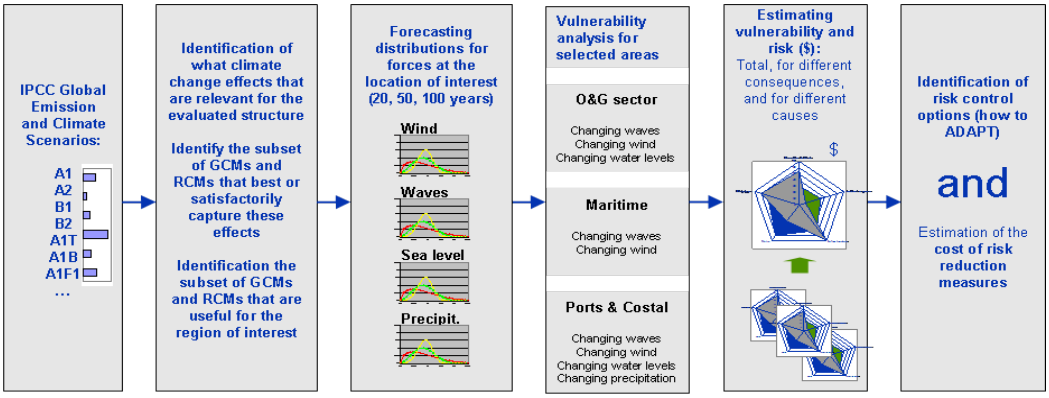

Fig. 1. Overall methodology.

References

[1] DARA, Climate Vulnerability Monitor 2010, http://daraint.org/climate-vulnerability-monitor/climate-vulnerability-monitor-2010/download-the-report/, 2010.

[2] GFCS, Position Paper on Global Framework for Climate Services. Submitted by the World Meteorological Organization. 2010. http://www.wmo.int/pages/gfcs/documents/GFCS_Position_Paper_DRAFT_REV_1_en_1.pdf

[3] ISO 27005, ISO 27000 Directory, http://www.27000.org/iso-27005.htm 2008.

[4] European Network and Information Security Agency (ENISA). www.enisa.europa.eu

[5] The Open Group (an industry consortium to set vendor- and technology-neutral open standards for computing infrastructure)

[6] Wreathall, J. Properties of Resilient Organisations. An Initial View. In Resilience Engineering Concepts and Precepts". pp. 275-285. Eds. E. Hollnagel, D.D. Woods, and N. Leveson,. Ashgate, 2008.

[7] IPCC, 2007, http://www.ipcc.ch/publications_and_data/publications_and_data.htm

[8] M.A. Semenov and E. M. Barrow, Use of Stochastic Weather Generators in the Development of Climate Change Scenarios. Climatic Change 35: 397–414, 1997.

[9] G.A. Meehl, F. Zwiers, J. Evans, T. Knutson. L. Mearns, and P. Whetton, Trends in Extreme Weather and Climate Events: Issues Related to Modeling Extremes in Projections of Future Climate Change. Bulletin of the American Meteorological Society, Vol. 81, No. 3. 2000. Pp. 427-436

[10] Nordic Committee for building structures (NKB), Recommendations for Loading and Safety Regulations for Structural Design. NKB Report No. 36, 1978.

[11] IPCC report … On extreme events and definition of rare, 2007

How much energy can we consume?

Oleg P.Dimitriev*

V.Lashkaryov Institute of Semiconductor Physics, Kiev, Ukraine
** Corresponding author. Tel: +38 044 5259706, Fax: +38 044 5255530, E-mail: dimitr@isp.kiev.ua*

Abstract: This report considers the global energy consumption from the viewpoint of thermodynamic balance between the Earth and the cosmic environment. To follow such a balance is postulated to be necessary to maintain proper functioning of the biosphere and stable climate conditions on the Earth. This viewpoint implies the following principles of energy consumption: (i) the energy should be consumed from the renewable sources only and (ii) the amount of the consumed energy should not exceed the amount of energy that incomes to the Earth. Three major sources of the renewable energy are considered, i.e., a direct incoming solar irradiation, a chemical energy through products of photosynthesis and, finally, an outgoing radiation from the Earth as a heated body. It is shown that the first and the third sources are potentially the most effective ways of the energy consumption. The last one, however, is not properly developed now. With the first two sources, the energy consumption rate cannot exceed a limit of 10^{17} W, but practically due to technical restrictions it can be set as 10^{14} W, which is approximately an order higher of the contemporary rate of energy consumption by the mankind. Development of the third source of energy is shown to allow us to increase the above limit up to one order of magnitude more. However, one should take great care of using this source of energy since it can affect climate changes also.

Keywords: *Thermodynamic balance, Renewable energy, Consumption limit*

Nomenclature

P_{sun} *energy power incoming from the sun to the earth-atmosphere system* ..... *W*
P_{earth} *energy power incoming to/outgoing from the earth surface* ..... *W*
$P^{\downarrow}_{org}$ *energy power stored via photosynthesis* .. *W*
P_{sc} *energy power produced by solar cells* ..... *W*
P_{O2} *energy power to produce oxygen through photosynthesis* ..... *W*
η_{org} *power conversion efficiency of photosynthesis* ..... *%*
η_{indir} *power conversion efficiency of solar energy used via produ*
η_{sc} *power conversion efficiency of solar cells %*
N_A *Avogadro's constant*..... mol^{-1}

1. Introduction

The global strategy of energy consumption has not ever been developed or widely accepted yet. However, there are several signals indicating in favor of such a strategy to be assumed in the near future. One signal comes from the fact that the organic fuel supplies (oil and gas) are exhausted and will come to the end in a few tens of years, and even the coal reserves will run out faster than many believe [1]. The second signal comes from the fact that the global climate is now sensitive to the increasing level of energy consumption and carbon dioxide production as a result of such kind of activity, respectively.

This report considers the principles of the global energy consumption from the viewpoint of thermodynamic balance between the Earth and the cosmic environment, which is necessary to maintain stable and unchanged conditions for proper functioning of the biosphere on the Earth. This viewpoint implies the following principles: (i) The energy should be consumed from the renewable sources only; (ii) The amount of the consumed energy should not exceed the natural production of energy through formation of organic fuel, income of solar energy, etc.

Solar energy is considered as a global supplier of the renewable energy on the Earth, which gives rise to formation of all sources of the organic fuel through photosynthesis, as well as

energy of wind, hydro-energy through local heating of the earth surface, melting of ice, etc. Nuclear energy is not included in this balance since nuclear materials are not renewable and, moreover, nuclear waste still represents a very dangerous factor for the biosphere.

We consider three possible ways of using a solar energy, namely, the use of a direct incoming solar irradiation, the use of an indirect solar energy through products of photosynthesis and, finally, the use of a reemitted energy from the Earth after the heating of the planet and its irradiation as a black body at the heated temperature. It is considered for the first way that although the power of incoming solar irradiation to the Earth is of the order of 10^{17} W, only a small part of that, approximately 10^{14} W, can be utilized by solar cells due to limitations in their power conversion efficiency, as well as limitation in surface area on the Earth suitable for their displacement. The second way of using the energy through products of photosynthesis can also yield a maximum consumption of 10^{14} W which is equivalent to the energy power production by the biosphere. The total power of human energy consumption is of the order of 10^{13} W at the moment [2]. With the modern 4% annual increase of the energy consumption on the Earth it will take about 60 years to reach the maximal possible limit of 10^{14} W. Finally, there is a large domain of the renewable energy resource in the form of the outgoing terrestrial radiation which could yield additional income and shift the above limit of consumption to higher values. The methods to develop this domain will be discussed below. However, such a shift in energy consumption can be accompanied with unpredictable changes in temperature regimes on the Earth surface. Therefore, the energy consumption limit should be postulated anyway as soon as possible in the near future.

2. Methodology: the energy balance on the Earth

The law of energy conservation states that any energy can be spent for performing some work and/or heating. The main source of the incoming energy on the Earth is the Sun. The solar radiation reaching the earth surface has an average power per square meter of about 230 W/m^2 and its spectrum extends from the UV to the IR, with the major part of energy lying in the visible range which has the maximum at the wavelength of about 0.5 μm (Fig.1). Eventually, an equal amount of energy must be lost from the Earth-atmosphere system if the internal energy of this system remains constant and the climate is stable. Therefore, the Earth emits the terrestrial radiation as a heated body. However, the spectral range of this outgoing radiation is shifted to the IR since the average temperature of the radiative body, i.e., the Earth, is 288^0 K (Fig.1). Although the peak amount of the outgoing terrestrial radiation (which is at the wavelength of 10 μm) is much smaller as compared to the corresponding peak of the incoming solar radiation at 0.5 μm, namely, *ca.* $7\text{x}10^{-3}$ (calculated using the data from ref. [3]) versus $1.5\text{x}10^3$ W/(m^{2}μm), respectively, the outgoing radiation has a much wider spectral range, so that the total amounts of the both radiations are equal in accordance with the thermodynamic balance of the planet.

On the other hand, the amount of photons incoming to and outgoing from the Earth is rather different according to the balance of the incoming and outgoing energy, i.e.,

$$E(\nu)=\int h n d\nu = (\sum h\nu_i n_i)_{sun} = (\sum h\nu_k n_k)_{earth},$$

where n_i is the amount of photons with the frequency ν_i, h the Planck constant. It can be roughly evaluated this relationship as $N_{earth}/N_{sun}=20$, where N_{earth} is the average number of photons with the wavelength 10 μm emitted by the earth-atmosphere system and N_{sun} is the average number of photons with the wavelength 0.5 μm from the Sun.

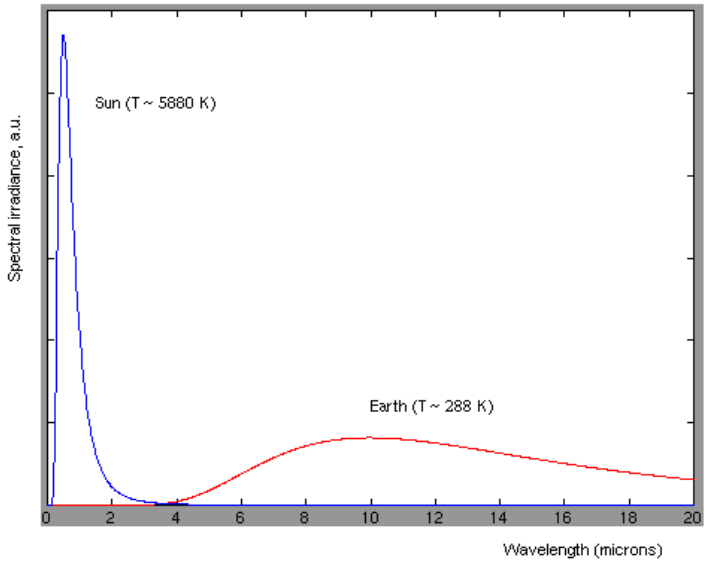

Fig.1. Relationship between incoming solar (blue curve) and outgoing terrestrial (red curve) radiation. The magnitude of the terrestrial radiation is magnified by a factor of 500,000.

However, a small part of photons from the Sun is stored in the form of chemical energy due to photosynthesis. This part of photons can be evaluated taking into account the energy conversion efficiency of photosynthesis to be of the order of 0.1% (see section 3 for details) that results in only a single stored photon of the thousand ones that are coming from the Sun. As a result, the relationship of the incoming, stored and outgoing energies can be presented schematically in Fig.2. Since only one incoming photon of one thousand gives rise to formation of all organic minerals and fuel, such as coal, natural gas, and petroleum as the products of photosynthesis, it can be easy to understand that only a small part of the incoming energy is mainly consumed now by the mankind.

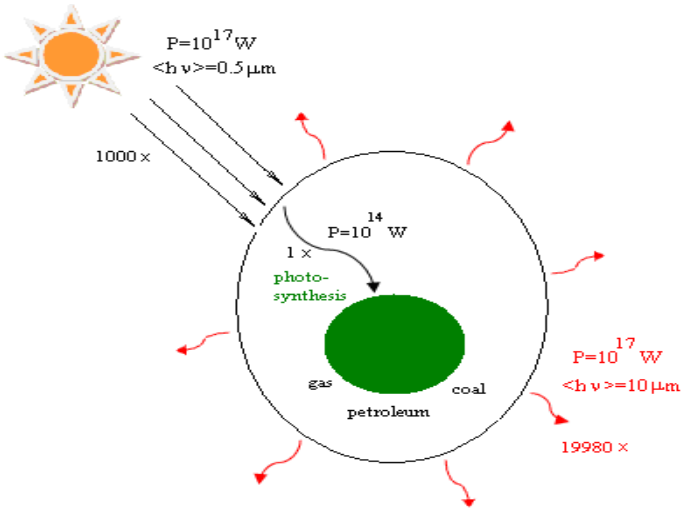

Fig.2. Relationship between incoming, stored, and outgoing energy rates per each 1000 incoming photons from the Sun.

3. Use of renewable sources of energy

3.1. Indirect consumption of solar energy through products of photosynthesis

The energy flux utilized by photosynthesis is $P^{\downarrow}_{org} \sim 10^{14}$ W. This value can be calculated from the photosynthesis equation, i.e.

$$CO_2 + H_2O \Rightarrow CHOH + O_2 \qquad (1).$$

The process described by Eq. (1) involves 4 electrons to be transferred; each of them requires the energy of 1.2 eV per electron. Therefore, formation of an O_2 molecule requires consumption of 4.8 eV. However, quantum efficiency of the system requires 8 to 12 quanta of light to be adsorbed which results in synthesis of one molecule of oxygen. Therefore, the total energy consumed by the photosynthetic system to produce one molecule of O_2 will be approximately $E_{O2} \sim 10$ quanta x 2 eV = 20 eV. Green plants produce totally 10^{14} kg of O_2 per year on the Earth, or $m_{O2} = 3x10^9$ g per second. The energy power necessary to produce O_2, therefore, will be

$$P_{O2} = E_{O2}(m_{O2}/M)N_A = 1.8 \cdot 10^{14}\ W \qquad (2),$$

where M=32 is the molar mass of O_2. Using this result and the power of solar energy reaching the Earth surface which is

$$P_{sun} - albedo\ (\sim 28\%) = P_{earth} \sim 1.2 \cdot 10^{17} W,$$

one can evaluate the average efficiency of photosynthesis as

$$\eta_{org} = P_{O2}/P_{earth} \sim 1.5 \cdot 10^{-3} = 0.15\ \% \qquad (3).$$

The same value for η_{org} can be also obtained via expression $P^{\downarrow}_{org} = \eta_{org}\ S_{earth} \cdot 230\ W/m^2$, where an assumption is made that the plants cover the overall earth surface S_{earth}. In fact, this assumption is rather crude, because there are large deserts, ice or mountain areas free of plants, but which can be overcompensated, however, by plant diversity in forests which occupy a few levels of space from the earth surface.

The efficiency value (3) can also vary depending on l ocal conditions of grow of plant organisms, for example, reaching up to 2% for water-plants grown in special pools [4].

It is natural to assume that the rate of energy consumption based on products of photosynthesis (gas, oil, coal, etc.), if the concept of energy consumption sets these resources as the basic sources of energy, cannot exceed the rate of formation of the organic products through photosynthesis calculated above. Thus, the energy consumption rate should be limited to $P_{org} < 10^{14}$ W which is only one order of magnitude exceeds the total power of all industrial energy producers currently on the Earth of about 10^{13} W [5]. The contemporary rate of energy consumption by the mankind can be calculated also by using the data on total mass of burning of dry fuel equivalent to $5 \cdot 10^{12}$ kg of carbon per year. The energy of reaction $C+O_2 \Rightarrow CO_2$ is $3.3 \cdot 10^7$ J/kg which gives the energy power of $5 \cdot 10^{12}$ W, which is consistent also with the year energy consumption data of the order of 10^{17} W·h [2]. It is easy to calculate, assuming the annual increase of the contemporary energy consumption of about 4% [5] that the above limit will be reached in the next 60 years ($(1.04)^N = 10$, from where N=59).

Finally, the efficiency of conversion of the solar energy by indirect way through burning of the organic products of photosynthesis, assuming that power conversion efficiency of the burning process is about 40%, will be only

$$\eta_{indir} = 6 \cdot 10^{-2}\% \qquad (4).$$

3.2. Direct consumption of incoming solar radiation

The power of solar energy irradiated the Earth is of the order of 10^{17} W. That means that the theoretical maximum of the solar energy consumption can be of the same order, i.e., $P_{sc} \sim 10^{17}$ W, if the power conversion efficiency of the corresponding devices approaches 100%. There are limitations, however, because power conversion efficiency of the conventional solar cells is far lower, of the order of η_{sc} ~10%, and because these cells cannot be set over the whole surface of the Earth. For example, in order to produce energy comparable with that stored by photosynthesis, the area of the solar cells S_{sc} should be as much as 1% of the Earth surface S_{earth}, which can be calculated from the following expressions with account of power conversion efficiency for photosynthesis (Eq.(3)),

$$P_{sc} = P^{\downarrow}_{org} \Rightarrow \eta_{sc} S_{sc} \cdot 230\ W/m^2 = \eta_{org} S_{earth} \cdot 230\ W/m^2 \Rightarrow S_{sc}/S_{earth} = \eta_{org}/\eta_{sc} \qquad (5)$$

1% of the earth surface is rather big, but reasonable value which seems to not significantly affect the biosphere and cropland areas. For comparison, the total urban area on the Earth is now approximately $3.4 \cdot 10^2$ km^2 [6] which cover approximately 0.07 % of the Earth surface. To cover an approximately one order of magnitude higher surface seems to be a challenging, but achievable task. However, additional studies are needed to confirm that this value is acceptable and compatible with the living areas on the Earth.

Thus, the energy production through a direct consumption of the solar irradiation energy can reach theoretically one order of magnitude higher value as compared with the contemporary production of energy through burning of organic fuel (see previous section). In addition, power conversion efficiency of the direct conversion of solar energy (η_{sc} ~10%) is three orders of magnitude higher as compared with that of the indirect production of energy (see Eq.(4)). Thus, a direct consumption of the solar energy is more efficient than the apparent efficiency of burning of the carbon-containing products.

3.3. Consumption of outgoing terrestrial radiation

There is a large part of IR energy, $P^{\uparrow}_{earth}$, which is reemitted from the earth surface in the form of the terrestrial radiation the Earth emits as the black body with the temperature of $T_{earth} = 255^0$ K. The amount of this energy is huge and comparable with that coming from the sun to the earth surface, due to the thermodynamic balance of the planet (see Fig.1),

$$P^{\uparrow}_{earth} \sim P_{sun} \sim 10^{17}\ W$$

There are several candidates that can serve as converters of this IR energy to electricity, such as pyroelectric and thermoelectric materials, gapless semiconductors, thermocouples, etc.; however, their application in respect to the terrestrial energy has not been developed yet. The advantages of the consumption of the terrestrial radiation is, first, that this radiation is highly scattered and therefore there is no need for orientation of the corresponding IR receivers or this orientation is not so critical as compared with the solar cells converting direct solar irradiation, so that the IR receivers can occupy several levels upward and, second, they do not

compete for the solar light with green plants. Below we consider three classes of materials which can be potentially used for the above energy domain.

It is well known that some organic compounds, such as metal complexes, ionic dyes, extended π-conjugated chromophores, and donor–acceptor charge transfer chromophores can absorbs near-IR (NIR) light with the wavelengths up to 1 μm [7]. Recent effort of chemists, however, resulted in development of a new series of donor-acceptor and donor-acceptor-donor D-π-A-π-D NIR compounds whose absorption can be tuned within the wavelength region of 0.6–1.4 μm [7]. Even more exciting examples include donor-acceptor covalently linked compounds of tetrathiafulvalene-tetracyanoquinodimethane (TTF-σ-TCNQ), fused porphyrin ribbons and TTF-dithiolato metal complexes, which demonstrate the absorption spectra extended to the middle-IR with the absorption maxima at 1.6, 2.9, and 4.6 μm, respectively, where the thermo-excited electron transfer has been observed experimentally [8]. Great opportunity can be expected also from the carbon materials and particularly graphene [9] which has a zero band gap and, therefore, can absorb photons from the whole IR range. Thus, design of energy converters based on organic molecules which combine high stability and electronic absorption extended to the middle and far IR is an exciting and challenging problem.

The second class of materials to be used for IR absorption is gapless or narrow-gap semiconductors whose band gap is smaller than 1 eV (equivalent to ~0.8 μm). Many of semiconductors, such as InSb (0.17 eV), InAs (0.36 eV), PbSe (0.82 eV), PbTe (0.31 eV) have the band gap values (shown in parenthesis) that allow them to absorb in the near-IR range. However, there are few candidates, i.e., HgSe, HgTe, which can collect energy from the middle IR range also. These last compounds, however, are toxic, and their application, therefore, are to be restricted. Nevertheless, development of these materials in the form of colloidal particles [10] packed in the inert matrix might overcome this problem. The advantages of the nanoparticle application also will give the opportunity to tune the range of absorption by simple change of the particle size.

The above types of the IR receivers produce an electron-hole pair upon absorption of an IR quantum. Their advantage as compared with the solar cells operating in the visible spectrum is that the amount of IR quanta is much larger as compared with the quanta of visible light (see Fig.2); therefore, the IR devices can potentially collect more quanta and produce a larger amount of electron-hole pairs as compared with the conventional solar cells. On the other hand, the devices which can respond in the middle and far IR still should be developed to collect quanta from a more extended spectral range.

The third class of materials perspective for harvesting IR radiation is thermoelectric materials. The thermoelectric energy conversion unit normally consists of two different (n- and p-type) semiconducting materials connected together in the form of a thermocouple; these materials are now actively developed [11], although some skepticism concerning their perspective in the energy solution domain exists [12]. It should be noted that the advantage of thermoelectric devices is that these can consume IR energy of practically all wavelengths and they do not have a quantum threshold restriction from which the device becomes active. However, a sufficiently large thermal gradient is needed for their effective work.

It is a question which part of the IR spectrum is most suitable to consume. If, for example, the corresponding devices will collect IR energy which normally leaves the Earth through the transparency window of the atmosphere (i.e., within the wavelength range of 8-13 μm) their work can promote the increase in the temperature regime at the earth surface. On the other

hand, if the IR converters will collect energy in the region of absorption of greenhouse gases and scatter it in the transparency window, their work can weaken the green-house effect and decrease the temperature, respectively. Therefore, the use of the above converters could help in controlling the climate regimes. However, such effects, if any, can be expected only if the converters of IR energy are applied on the large scale.

4. Conclusions

The energy consumption rate limit should be set as a necessary concept in the near future to conserve thermodynamic balance on the Earth. Such a limit, if based on the major production of energy through burning of organic fuel, has been shown to exceed the contemporary rate of energy consumption by approximately one order of magnitude and can be reached in the next 60 years. Consumption of direct solar energy and reemitted IR radiation from the Earth-atmosphere system on the large scale can somewhat extend the above limit. Optimistic estimates above show that use of the direct solar energy can double this limit. There is no estimate at the moment how much terrestrial radiation can be consumed, since the respective energy converters are at the beginning of their development. It is known, however, that power conversion efficiency of thermoelectric devices is of the order of few percents [12]. The same order of magnitude is typical for the best photovoltaic cells based on organic materials, therefore, it can be expected the same value for power conversion efficiency of the best organic IR converters also. Taking into account some advantages of the IR energy converters discussed above we can suppose very tentatively that their use on the large scale might yield another portion of energy of the order of 10^{14} W. Thus, the overall increase of the total limit of the renewable energy production rate can be very modest, being within 10^{14}-10^{15} W range. Therefore, the necessary political and economical steps should be undertaken towards the necessity of the energy consumption constraint to keep the living conditions on the Earth constant.

References

[1] R. Heinberg, D. Fridley, The end of cheap coal, Nature 468, 2010, pp. 367-369.

[2] S.K. Aggarwal, A.K. Gupta, D.G. Lilley, Terrestrial energy, Aerospace America, Dec. 2006, p.70.

[3] C.G. Abbot, Terrestrial temperature and atmospheric absorption, Proc. Natl. Acad. Sci. USA 4, 1918, pp. 104-106.

[4] V.V.Alexeev, K.V.Chekarev, Solar energetics, Nauka, 1991, 60 p.

[5] K.Ya. Kondratyev, I. Galindo, Contemporary stage of civilization development and its perspectives, Univ. of Colima Press, 2002, 139 p.; K. Ya. Kondratyev, I. Galindo, Global change situation: today and tomorrow, Univ. of Colima Press, 2002, 164 p; K.Ya.Kondratyev, Key aspects of global climate change, Energy and Environment 15, 2004, pp. 467-501.

[6] Demographia world urban areas & population projections: Edition 6.1, July 2010, pp.1-128 (www.demographia.com/db-worldua.pdf).

[7] G. Qian, Z. Y. Wang, Near-infrared organic compounds and emerging applications, Chem. Asian J. 5, 2010, pp. 1006–1029.

[8] D. F. Perepichka, M. R. Bryce, Molecules with exceptionally small HOMO–LUMO gaps, Angew. Chem. Int. Ed. 44, 2005, pp. 5370–5373.

[9] J.M. Dawlaty, S. Shivaraman, J. Strait, P. George, M. Chandrashekhar, F. Rana, M.G. Spencer, D. Veksler, Y. Chen, Measurement of the optical absorption spectra of epitaxial graphene, Appl. Phys. Lett. 93, 2008, 13195.

[10] M. T. Harrison, S. V. Kershaw, M. G. Burt, A. L. Rogach, A. Kornowski, A. Eychmüller, and H. Weller, Colloidal nanocrystals for telecommunications. Complete coverage of the low-loss fiber windows by mercury telluride quantum dots, Pure Appl. Chem. 72, 2000, pp. 295-307.

[11] J.F. Li, W.S. Liu, L.D. Zhao, M.Zhou, High-performance nanostructured thermoelectric materials, NPG Asia Mater. 2, 2010, pp. 152-158.

[12] C.B.Vining, An inconvenient truth about thermoelectrics, Nature Mater., 8, 2009, pp. 83-85.

Effective Urban Energy Planning and Governance: A New Conceptual Framework

Yosef R. Jabareen[1*]

[11] *Technion – Israel Institute of Technology, Haifa, Israel*
** Corresponding author. Tel: +922 52865336, Fax: +972 48294617, E-mail:jabareen@technion.ac.il*

Abstract: Beyond any doubt *climate change* and its resulting uncertainties challenge the concepts, procedures, and scope of conventional approaches to the planning of our cities. Thus, demanding from us to situate the energy issue in the central when planning urban spaces. Yet, the literature is vague in the context of urban energy, and there is a lack of a theoretical framework that conceptualizes urban energy planning. Therefore, the aim of this paper is to propose a new multifaceted conceptual framework for theorizing urban energy planning based on multidisciplinary literature. Eventually, this study elaborates a conceptual framework that consists of eight concepts that were identified through a conceptual analysis of interdisciplinary literature on sustainability, climate change, ecology, economics, and urban planning. These concepts, which together constitute the theoretical framework of urban energy planning for climate change, are: *Utopian Vision*, *Equity*, *Uncertainty*, *Natural Capital*, *Eco-Form*, *Integrative Approach*, *Ecological Energy*, and *Ecological Economics*.

Keywords: *Urban Planning, Energy, Theory, Conceptual Framework*

1. Introduction

Climate change poses new risks and uncertainties that often lie outside our range of experience (IPCC, 2007: 719) and that have the potential to affect the social, economic, ecological, and physical systems of any given city. In this way, climate change and its resulting uncertainties challenge the concepts, procedures, and scope of conventional approaches to city planning, creating a need to rethink and revise current approaches. Decisively, it demands from us to situate the energy issue in the central when planning urban spaces. Yet, a striking weakness of the scholarship on the subject is its lack of multifaceted theorizing and the fact that it typically overlooks the multidisciplinary and complex nature of urban energy planning. Moreover, the literature is vague in the context of urban energy, and there is a lack of a theoretical framework that conceptualizes urban energy planning. Therefore, the aim of this paper is to propose a new multifaceted conceptual framework for theorizing urban energy planning based on multidisciplinary literature.

2. Methodology

A *conceptual analysis method* was used to build the conceptual framework (Jabareen 2009). This method is a grounded theory technique that aims "to generate, identify, and trace a phenomenon's major concepts, which together constitute its theoretical framework" (Jabareen 2009). Each concept possesses its own attributes, characteristics, assumptions, limitations, distinct perspectives, and specific function within the conceptual framework. The methodology delineates the following stages in conceptual framework building: a) mapping selected data sources; b) reviewing the literature and categorizing the selected data; c) identifying and naming the concepts; d) deconstructing and categorizing the concepts; e) integrating the concepts; f) synthesis, resynthesis, and making it all make sense; g) validating the conceptual framework; and h) rethinking the conceptual framework (Jabareen 2009).

3. Results

The Concepts of the Conceptual Framework

The conceptual framework is composed of eight concepts (see Jabareen, 2006), as Fig1 shows. These concepts are:

a. Utopian Vision: This concept is concerned with a plan's future vision. Usually, urban planning seeks to bring about a different and more desirable future. Theoretically, the power of visionary or utopian thinking lies in its inherent ability to envision the future in terms of radically new forms and values (de Geus, 1999). An urban vision incorporating climate change as a central theme is of the utmost importance to practitioners, decision makers, and the public. Visionary frames are important in climate change, as they serve to identify problematic conditions and the need for change, to propose future alternatives, and to urge all stakeholders to act in concert to affect change. Climate change planning visions must provide people with an interpretive framework that enables them to understand how the issue is related to their own lives in the present and future, and to the world at large (Taylor, 2000; Benford and Snow, 2000: 614). This concept addresses the visionary and utopian aspects regarding future urban life, the city's potential role in climate change mitigation, and the city vision regarding energy production and consumption as well.

b. Equity: Equity is a key concept in evaluating climate change policies (IPCC, 2001). The impacts of climate change and climate change mitigation policies are "socially differentiated," and are therefore matters of local and international distributional equity and justice (Adger, 2001: 929; O'Brien et. al., 2004; Paavola et al., 2006). Some argue that inequality leads to greater environmental degradation and that a more equitable distribution of power and resources would result in improved environmental quality (Boyce et al. 1999; Agyeman et al., 2002; Solow 1991, Stymne and Jackson, 2000). Moreover, there are individuals and groups within all societies who are more vulnerable than others and lack the capacity to adapt to climate change (IPCC, 2007: 719). A society's vulnerability is influenced by its development path, physical exposure, resource distribution, social networks, government institutions, and technological development (, 2007: 719-720). The concept of equity addresses social aspects, including: environmental justice; public participation; and methods of addressing each community's vulnerability to climate change (urban vulnerability matrix).

c. Uncertainty Management: Uncertainty "is a perceived lack of knowledge, by an individual or group, which is relevant to the purpose or action being undertaken and its outcomes" (Abbot, 2009: 503). The new urban uncertainties posed by climate change challenge the concepts, procedures, and scope of planning. In order to cope with the new challenges, planners must develop a greater awareness and place mitigation and policies for "adaptation," or actual adjustments that might eventually enhance resilience and reduce vulnerability to expected climate changes, at the center of the planning process (Adger et. Al., 2007: 720). Planners must also develop a better understanding of the risks climate change poses for infrastructure, households, and communities. To address these risks, planners have two types of uncertainty or adaptation management at their disposal: 1) Ex-ante management, or actions taken to reduce and/or prevent risky events; and 2) Ex-post management, or actions taken to recover losses after a risky event (Heltberg et al., 2009).

d. Natural Capital: Natural capital refers to "the stock of all environmental and natural resource assets, from oil in the ground to the quality of soil and groundwater, from the stock of fish in the ocean to the capacity of the globe to recycle and absorb carbon" (Pearce et. al., 1990: 1). Maintaining constant natural capital is an important criterion for sustainability

(Pearce and Turner, 1990: 44; Geldrop and Withagen, 2000). The stock of natural capital should not decrease, as this could endanger the ecological system and threaten the ability of future generations to generate wealth and maintain their well-being. This concept addresses the consumption and - equally as important - the renewal of natural assets that are used for development, such as land, water, air, and open spaces.

***e. Integrative Approach*:** Planning for climate change is more complex than the conventional approach to planning as it is undertaken in a context of great uncertainty. This context poses new challenges for collaboration among public, private, and civil institutions and organizations on all levels. Integrating the many different stakeholders and agents into planning is essential for achieving climate change objectives. The "ability of a governance system to adapt to uncertain and unpredicted conditions is a new notion" (Mirfenderesk and Corkill, 2009: 152). Therefore, adaptive management requires new planning strategies and procedures that transcend conventional planning approaches by integrating uncertainties into the planning process and prioritizing stakeholders' expectations in an uncertain environment. Plans should also be "flexible enough to quickly adapt to our rapidly changing environment" (Mirfenderesk and Corkill, 2009).

***f. Ecological Energy*:** The clean, renewable, and efficient use of energy is a central theme in planning for the achievement of climate change objectives. This concept evaluates how a plan addresses the energy sector and whether it proposes strategies to reduce energy consumption and to use new, alternative, and clean energy sources.

***g. Ecological Economics*:** This concept is based on the assumption that environmentally sound economics can play a decisive role in achieving climate change objectives in a capitalist world. Cities that are committed to climate change mitigation and sustainability should stimulate markets for 'green' products and services, promote environmentally friendly consumption, and contribute to urban economic development by creating a cleaner environment (Hsu, 2006: 11; Mercer Human Resources Consulting, 2005). In this spirit, the American Recovery and Reinvestment Plan, proposed by President Barack Obama, calls for spurring "job creation while making long-term investments in energy, and infrastructure," and increasing "production of alternative energy" (White House, 2009).

h. Eco-Form: The physical form of a city affects its habitats and ecosystems, the everyday activities and spatial practices of its inhabitants, and, eventually, climate change. This concept evaluates spatial planning, architecture, design, and the ecologically-desired form of the city and its components (such as buildings and neighborhoods). Jabareen (2006) suggests the following set of nine planning typologies, or criteria of evaluation, which are helpful in evaluating plans from the perspective of eco-form as follows:

Compactness refers to urban contiguity and connectivity and suggests that future urban development should take place adjacent to existing urban structures (Wheeler, 2002). Compact urban space can minimize the need to transport energy, materials, products, and people (Elkin et. al., 1991). Intensification, a major strategy for achieving compactness, uses urban land more efficiently by increasing the density of development and activity, and involves: developing previously undeveloped urban land; redeveloping existing buildings or previously developed sites; subdivisions and conversions; and additions and extensions (Jenks, 2000: 243).

Sustainable Transport suggests that planning should promote sustainable modes of transportation through traffic reduction; trip reduction; the encouragement of non-motorized travel (such as walking and cycling); transit-oriented development; safety; equitable access for all; and renewable energy sources, (Cervero, 2003; Clercq and Bertolini, 2003).

Density is the ratio of people or dwelling units to land area. Density affects climate change through differences in the consumption of energy, materials, and land for housing, transportation, and urban infrastructure. High density planning can save significant amounts of energy (Carl, 2000; Walker and Rees, 1997; Newman and Kenworthy, 1989).

Mixed Land Uses indicates the diversity of functional land uses, such as residential, commercial, industrial, institutional, and transportation. It allows planners to locate compatible land uses in close proximity to one another in order to decrease the travel distance to between activities. This encourages walking and cycling and reduces the need for car travel, as jobs, shops, and leisure facilities are located in close proximity of one another (Parker, 1994; Alberti, 2000; Van and Senior, 2000; Thorne and Filmer-Sankey, 2003).

Diversity is "a multidimensional phenomenon" that promotes other desirable urban features, including a larger variety of housing types, building densities, household sizes, ages, cultures, and incomes (Turner and Murray, 2001: 320). Diversity is vital for cities. Without it, the urban system declines as a living place (Jacobs 1961) and the resulting homogeneity of built forms, which often produces unattractive monotonous urban landscapes, leads to increased segregation, car travel, congestion, and air pollution (Wheeler, 2002).

Passive Solar Design aims to reduce energy demands and to provide the best use of passive energy through specific planning and design measures, such as orientation, layout, landscaping, building design, urban materials, surface finish, vegetation, and bodies of water. This facilitates optimum use of solar gain and microclimatic conditions and reduces the need for the heating and cooling of buildings by means of conventional energy sources (Owens, 1992; Thomas, 2003; Yannis, 1998: 43).

Greening, or bringing "nature into the city," makes positive contributions to many aspects of the urban environment, including: biodiversity; the lived-in urban environment; urban climate; economic attractiveness; community pride; and health and education (Beatley 2000; Swanwick et al., 2003; Forman, 2002; Dumreicher et al., 2000; Beer et. al.,, 2003; Ulrich, 1999).

Renewal and Utilization refers to the process of reclaiming the many sites that are no longer appropriate for their original intended use and can be reclaimed for a new purpose, such as brownfields. Cleaning, rezoning, and developing contaminated sites are key aspects of revitalizing cities and neighbourhoods and contribute to their sustainability and to a healthier urban environment.

Planning Scale influences and is influenced by climate change. For this reason, desirable planning scale should be considered and integrated in plans for regional, municipal, district, neighbourhood, street, site, and building levels. Planning that moves from macro to micro levels has a more holistic and positive impact on climate change.

4. Discussion and/or Conclusions

The *conceptual framework* is not a mere collection of concepts. Rather, all concepts are interrelated and interwoven with one another; each plays an important role in the framework as a whole. The conceptual framework consists of eight concepts of assessment that were identified through conceptual analyses of interdisciplinary literature on sustainability and climate change. Together, these concepts – each of which represents a distinctive aspect of urban energy planning - form the conceptual framework. Importantly, each concept contributes to the planning of urban energy in its domain. The positive contribution o all concepts together will lead to effective urban energy governance. The overlooking of one concept or more will cause various negative externalities to climate change.

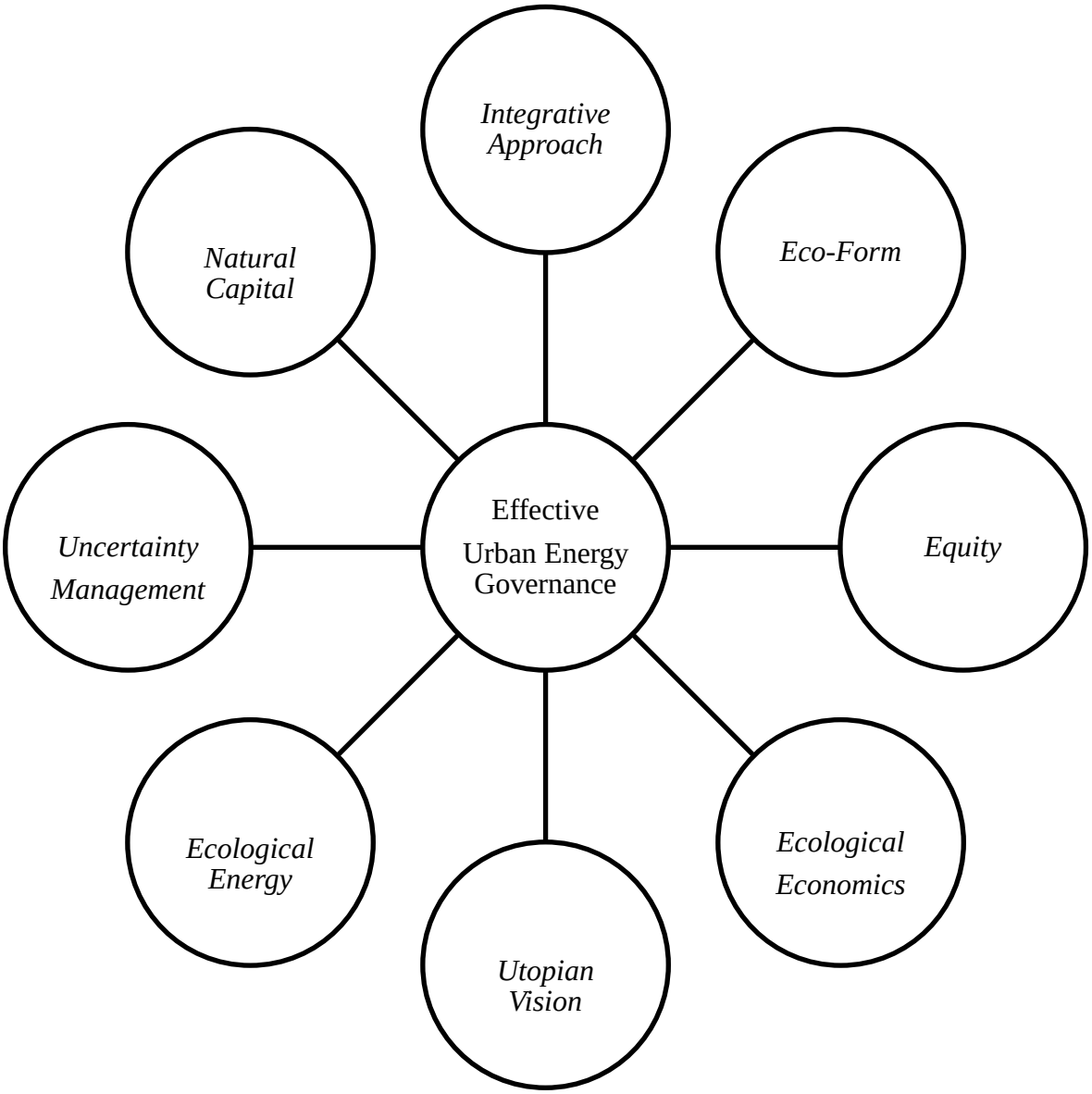

Fig. 1 Conceptual framework for urban energy.

References

[1] IPCC - S.H. Schneider, S. Semenov, A. Patwardhan, I. Burton, C.H.D. Magadza, M. Oppenheimer, A.B. Pittock, A. Rahman, J.B. Smith, A. Suarez and F. Yamin, Assessing key vulnerabilities and the risk from climate change. Climate Change 2007: Impacts,

Adaptation and Vulnerability. Contribution of Working Group II to the Fourth Assessment Report of the Intergovernmental Panel on Climate Change, M.L. Parry, O.F. Canziani, J.P. Palutikof, P.J. van der Linden and C.E. Hanson, Eds., Cambridge University Press, Cambridge, UK, 2007, pp. 779-810.

[2] Y. Jabareen, Building Conceptual Framework: Philosophy, Definitions and Procedure, International Journal of Qualitative Methods, Vol 8(4), 2009, pp. 49-62.

[3] Y. Jabareen, Sustainable Urban Forms: Their Typologies, Models, and Concepts, Journal of Planning Education and Research, Vol. 26 (1), 2006, pp. 38-52.

[4] M. de. Geus, Ecological Utopias: Envisioning the Sustainable Society. Utrecht: International Books, 1999.

[5] D. E. Taylor, The Rise of the Environmental Justice Paradigm: Injustice Framing and the Social Construction of Environmental Discourses American Behavioral Scientist 43, 2000, pp. 508-580.

[6] Benford Robert D. and Snow David A. 2000. Framing Processes and Social Movements: An Overview and Assessment. *Annual Review of Sociology*, Vol. 26: 611-639

[7] IPCC.Third Assessment Report: Climate Change 2001 (TAR).

[8] W.N Adger,. S. Agrawala, M.M.Q. Mirza, C. Conde, K. O'Brien, J. Pulhin, R. Pulwarty, B. Smit and K. Takahashi, Assessment of adaptation practices, options, constraints and capacity. Climate Change 2007: Impacts, Adaptation and Vulnerability. Contribution of Working Group II to the Fourth Assessment Report of the Intergovernmental Panel on Climate Change, M.L. Parry, O.F. Canziani, J.P. Palutikof, P.J. van der Linden and C.E. Hanson, Eds., Cambridge University Press, Cambridge, UK, 2007, pp. 717-743.

[9] R. O'Brien, Leichenko, U. Kelkar, H. Venema, G. Aandahl, H. Tompkins, A. Javed, S. Bhadwal, A. Barg, L.P. Nygaard and J. West, Mapping vulnerability to multiple stressors: climate change and globalization in India, Global Environmental Change 14, 2004, pp. 303–313.

[10] J. Paavola, and Adger W. Neil, Fair adaptation to climate change. Ecological Economics. Volume 56, Issue 4, 2006, pp. 594-609.

[11] J.K. Boyce, Klemer, A.R., Templet, P.H. and Willis, C.E, Power distribution, the environment, and public health: a state-level analysis. Ecological Economics. 29, 1, 1999, pp. 127–140.

[12] J. Agyeman, Bullard, R. D., & Evans, B. Exploring the nexus: Bringing together sustainability, environmental justice and equity. Space & Polity, Vol 6(1), 2002, pp. 77-90.

[13] R. Solow, Sustainability: An Economist's Perspective. The Eighteenth J. Seward Johnson Lecture. Woods Hole, MA: Woods Hole Oceanographic Institution, 1999.

[14] J. Abbott. Planning for complex metropolitan regions: A better future or a more certain one? Journal of Planning Education and Research, vol.28, 2009, 503-517.

[15] W.N. Adger, Scales of governance and environmental justice for adaptation and mitigation of climate change. Journal of International Development, Vol. 13(7), 2001, pp. 921-931.

[16] R. Heltberg, Paul Bennett Siegel, Steen Lau Jorgensen. 2009. Addressing human vulnerability to climate change: Toward a 'no-regrets' approach. Global Environmental Change, 19, 2009, pp. 89–99.

[17] D. Pearce, Edward, Barbier., and Anil Markandya. Sustainable development: Economics and environment in the Third World. London: Earthscan Publications, 1990.

[18] Geldrop, J. and C. Withagen, Natural capital and sustainability. *Ecological Economics*, Vol. 32 (3), 2000, pp. 445-455.

[19] H. Mirfenderesk and Corkill David, Sustainable management of risks associated with climate change. *International Journal of Climate Change Strategies and Management*, Vol. 1(2), 2009, pp.146-159.

[20] D. Hsu David, *Sustainable New York City.* New York City: Design Trust for Public Space and the New York City Office of Environmental Coordination, 2006.

[21] Mercer Human Resources Consulting, Quality of Living Survey: New York City. Private communication, 2004.

[22] White House http://www.whitehouse.gov/issues/Economy; see also http://www.recovery.gov/Pages/home.aspx, 2009.

[23] S. Wheeler, Stephen. M. Constructing sustainable development/safeguarding our common future: Rethinnking sustainable development. *Journal of the American Planning Association* 68:1, 2002, pp. 110-111.

[24] T. Elkin, McLaren, Duncan, and Hillman, Mayer, *Reviving the city: Towards sustainable urban development*, Friends of the Earth, London, 1991.

[25] M. Jenks, The acceptability of urban intensification. In *Achieving sustainable urban form*, edited by Williams K., Burton E., and Jenks M., London: E & FN SPON, 2000.

[26] S. Owens, Energy, environmental sustainability and land-use planning. In *Sustainable development and urban form*, edited by Michael, Breheny. London: Pion, 1992, pp. 79-105,

[27] R. Cervero, RobertCoping with Complexity in America's Urban Transport Sector. *The 2nd International Conference on the Future of Urban Transport*, Göteborg, Sweden, 2003.

[28] F. Clercq, and L. Bertolini, Achieving sustainable accessibility: An evaluation of policy measures in the Amsterdam area. *Built Environment* 29:1, 2003, pp. 36-47.

[29] P. Carl, Urban density and block metabolism. In *Architecture, city, environment. Proceedings of PLEA 2000*, edited by Steemers Koen and Simos Yannas, London: James & James, 2000, pp. 343-347.

[30] L. Walker, and Rees William. Urban density and ecological footprints – An analysis of Canadian households. In *Eco-city dimensions: Healthy communities, healthy planet*, edited by Roseland Mark, New Society Publishers, 1997.

[31] P. Newman, and Kenworthy, J. Gasoline consumption and cities: a comparison of US cities with a global survey. *Journal of the American Planning Association* 55, 1989, pp. 23-37.

[32] T. Parker, *The land use—air quality linkage: How land use and transportation affect air quality*. Sacramento: California Air Resources Board. 1994.

[33] Alberti, M. (2000) Urban form and ecosystem dynamics: Empirical evidence and practical implications. In *Achieving sustainable urban form*, edited by Williams K., Burton E., and Jenks M., London: E & FN Spon. 2000, pp. 84-96.

[34] Van Uyen-Phan and Martyn Senior. The contribution of mixed land uses to sustainable travel in cities. In *Achieving sustainable urban form*, edited by Williams K., Burton E., and Jenks M., London: E & FN Spon, 2000, pp. 139-148.

[35] R. Thorne, and William, Filmer-Sankey, Transportation. In *Sustainable urban design*, edited by Thomas Randall, 25-32, London: Spon Press, 2003.

[36] S. R. Turner S. and Margaret. S. Murray, Managing growth in a climate of urban diversity: South Florida's Eastward ho! Initiative. Journal of Planning Education and Research 20, 2001, 308-328

[37] J. Jacobs, Jane, The death and life of great American cities, New York: Random House, 1961.

[38] R. Thomas, Building design. Sustainable urban design: An environmental approach, edited by In Thomas R. and Fordham M., 46-88, London: Spon Press, 2003.

[39] S. Yanns, Living with the city: Urban design and environmental sustainability. In Environmantly friendly cities, edited by Maldonado Eduardo and Simon Yannas, 41-48, London: James & James, 1998.

[40] T. Beatley, Green urbanism: Learning from European cities. Washington, D.C.: Island Press, 2000.

[41] C. Swanwick, , Nigel Dunnett., and Helen Woolley, Nature, role and value of green space in towns and cities: An overview, Built Environment 29:2, 2003, pp. 94-106.

[42] R. T. Forman, Richard, The missing catalyst: Design and planning with ecology. In Ecology and design: Frameworks for learning, edited by Johnson Bart T. and Hill Kristina, Washington, DC: Island Press, 2000.

[43] H. Dumreicher, Heidi, L. Richard S., and Yanarella, Ernest J, The appropriate scale for "low energy": Theory and practice at the Westbahnhof. In Architecture, city, environment. Proceedings of PLEA 2000, edited by Steemers Koen and Simos Yannas, London: James & James. 2000, pp. 359-363.

[44] A. Beer, T. Delshammar, and P. Schildwacht, A changing understanding of the role of greenspace in high-density housing: A European perspective. Built Environment, 29:2, 2003, pp. 132-143.

[45] R. S. Ulrich, Roger, Effects of gardens on health outcomes: theory and research, in Healing gardens: Therapeutic benefits and design recommendations, edited by Marcus, Clare Cooper. and Marni Barnes., New York: Whiley, 1999.

Simple Statistical Model for Complex Probabilistic Climate Projections: Overheating Risk and Extreme Events

Sandhya Patidar[1,*], David Jenkins[2], Phil Banfill[2], Gavin Gibson[1]

[1] *Maxwell Institute for Mathematical Sciences , School of Mathematical and Computer Sciences, Heriot-Watt University, Edinburgh, UK*
[2] *Urban Energy Research Group, School of Built Environment (address as above)*
* *Corresponding author. Tel: +44 1314514365, E-mail: S.Patidar@hw.ac.uk*

Abstract: Climate change could substantially impact the performance of the buildings in providing thermal comfort to occupants. Recently launched UK climate projections (UKCP09), clearly indicate that all areas of the UK will get warmer in future with the possibility of more frequent and severe extreme events, such as heat waves. This study, as part of the Low Carbon Futures (LCF) Project, explores the consequent risk of overheating and the vulnerability of a building to extreme events. A simple statistical model proposed by the LCF project elsewhere has been employed to emulate the outputs of the dynamic building simulator (ESP-r) which cannot feasibly be used itself with thousands of available probabilistic climate database. Impact of climate change on the daily external and internal temperature profiles has been illustrated by means of 3D plots over the entire overheating period (May - October) and over 3000 equally probable future climates. Frequency of extreme heat events in changing climate and its impact on overheating issues for a virtual case study domestic house has been analyzed. Results are presented relative to a baseline climate (1961-1990) for three future timelines (2030s, 2050s, and 2080s) and three emission scenarios (Low, Medium, and High).

Keywords: *Probabilistic climate projections, Building and Adaptation, Overheating*

1. Introduction

Experiments based on an advanced scientific methodology and general circulation models (GCM), commonly known as global climate models, reveal that there is an exponential increase in the global concentration of greenhouse gases [1]. According to a UK Climate Projections (UKCP09) [2] briefing report, central England's temperature has already increased by 1 ^{o}C since the 1970s and this increase is most likely due to anthropogenic emission of greenhouse gases [3]. This excessive addition of the greenhouse gasses in the atmosphere is warming up the Earth's surface causing climate change and thus altering the weather pattern. Climate change could hasten species extinction, cause coastal flooding, and lead to more frequent and severe storms and extreme temperature events such as heat waves. Such extreme temperature events could cause catastrophic losses to both human and natural systems and thereby have dramatic ecological, economic and sociological impact [3-8].

For the UK, projections for future changes to climate are provided by the UK Climate Projections (UKCP09) and are available in probabilistic format to address the uncertainty associated with future climate change. To include a measure for the uncertainty, these climate projections are generated by multiple simulations of global climate models (in particular HadCM3 [9]) combined with a new methodology designed by the Met Office. The projections also include the results of other IPCC [1] climate models, and are constrained by observations of past climate. Thus to describe just any single future climate scenario a range (in fact thousands) of possible climates are available where each climate has a certain probability of occurring.

Extreme events, by definition, are in the tails of such probability distributions. Interestingly, events in the tail of the distribution are the ones that change most in frequency of occurrence as the distribution shifts due to global warming [10-11]. The work presented in this paper will

focus on the potential impact of future climate changes on the frequency of the extreme temperature regimes (heat wave) and how this could influence the overheating issues in the UK's domestic house sectors.

The suite of probabilistic climates projection available from UKCP09 for a London location at three future timelines, namely 2030's, 2050s, and 2080s, including a baseline [1960-1990] has been carefully analyzed to quantify the future change in the frequency of extreme heat events. The impact of extreme heat events on indoor comfort temperatures of a domestic building case study has been assessed by means of a simple statistical model proposed by the Low Carbon Futures (LCF) project [12] elsewhere [13-14]. This simple statistical tool is mainly based on multiple regression techniques and could efficiently emulate the outputs of traditional dynamics building simulation software ESP-r [15], which cannot be practically used with thousands of potential climates available for each future scenario.

This project is sponsored by the Adaptation and Resilience in a Changing Climate (ARCC) Programme [16], looking at possible methods, i.e. adaptations, for coping with a future climate.

2. Methodology

To analyze complex probabilistic climate information and to generate corresponding indoor temperature profiles for a case study dwelling, an elegant regression tool has been developed by the LCF project which is described in detail elsewhere [14]. The simple regression tool which is based on data reduction methods such as Principal Component Analysis (PCA) and multiple regressions is validated at an hourly scale to provide a close match (within a range of 1 °C) for the outputs of dynamic building simulation software (ESP-r). More details on the development procedure of the regression tool are found elsewhere [13].

This section should present a brief description of probabilistic climatic information available from UKCP09, profiles of the domestic building case study simulated with ESP-r, and a short note on the regression tool which has been employed to emulate outputs of ESP-r for quantifying extreme heat events and its impact on overheating issues in the case-study building. A short review on the possible definitions of the heat wave is also included.

2.1. Probabilistic Climate Projections and Regression Tool

The UKCP09 provides climate change information focused on the UK. The projections are presented for seven 30 years time periods ("2020s" denoting as 2010 – 2039, "2030s" denoting 2020 – 2049, … , up to "2080s" denoting 2070 - 2099), and at three different future greenhouse gas emissions scenarios represented as "High", "Medium" and "Low". These projections are based on change relative to a baseline time period (1961–1990) and, by means of a *Weather Generator* (WG) [17] tool, are available at an hourly temporal resolution with a 5×5 km^2 spatial resolution for any user defined UK location.

For the work presented in this article, climatic information has been downloaded from UKCP09's WG tool for a London location corresponding to all three greenhouse gas emissions scenarios and at three future time periods, namely 2030s, 2050s and 2080s, including baseline. Notably for any user specified future scenario, the WG tool could provide at least 3000 equally probable hourly climate files (each climate file represents a prototype climate year for that scenario) in the form of 100 statistically equivalent time series, where each of the time series is equally probable and of 30 years in length. For each of the future scenarios under investigation a representative sample of 100 climate years is formed by means

of a random sampling algorithm, which selects one year randomly from each of the 100 time series.

To formulate the regression tool, a 3-bedroom cavity-wall house with a total floor area of 144 m^2 has been simulated with ESP-r for one randomly chosen climate file from the 100 available climate years (additional information on the virtual case study building can be found elsewhere [18]). The regression tool is based on the concept of underpinning the existing relationship between available climate variants and the indoor temperatures, where each climate variant first need to be carefully analyzed and simplified by means of PCA. The model has been formulated to capture indoor temperature profiles during the period of May to October only. To allow time-based sensitivity analysis, the idea of segmented modelling has been applied and data fitted in parts, namely a) May – June; b) July-August; and c) September – October, to cover the entire period (May-October) [13].

A regression tool which could be formulated from the one climate file had been validated across all the available 100 climates files and corresponding to all different future scenarios as described above. Moreover, the proposed statistical regression tool has been demonstrated to efficiently estimate the outputs of ESP-r at an hourly scale within a single degree centigrade for up to 90% of the entire data set [13-14]. Thus, it is reasonable to consider an application of the proposed simple and efficient regression tool for quantifying frequency of heat waves and analyzing overheating issues in that context.

2.2. Heat waves and Overheating

Research conducted by Met Office clearly shows that even in the UK heat waves could be lethal, when hotter summers are predicted in foreseeable future [19]. There is no universal definition of a heat wave, however a heat wave could be considered as a prolonged period of excessively hot weather accompanied by high humidity, where temperatures are outside the normal climate pattern for that period [20]. For the UK, the Met Office defines summer heat wave duration as "***the sum of days with daily maximum temperature more than 3 °C above 1961–90 daily normal for ≥5 consecutive days (May–October)***" [21].

As stated previously, extreme events formulate tails of the probability distribution and therefore for the present study of heat waves and overheating analysis, it is essential to consider all 3000 climates corresponding to each available future scenario. An initial analysis of 3000 baseline climate files identified 15.6 ^{o}C as the daily normal temperature for 1961 – 1990. For each climate file daily normal temperature has been averaged over the overheating period and then again averaged over all equally probable 3000 climate years.

Thus, **summer heat wave duration** could be defined as – "*sum of days with daily maximum temperature more than 18.6 ^{o}C for 5 or more days during May to October*". In this context, to examine the impact of heat waves on indoor temperatures, two overheating criterion had been designed and compared with corresponding heat wave durations:
Overheating Criterion 1 - "*Sum of the days with average of night time (11pm – 7am) bedroom temperature more than 24 ^{o}C for 5 or more days during May to October*".
Overheating Criterion 2 - "*Sum of the days with average of night time (11pm – 7am) bedroom temperature more than 28 ^{o}C for 5 or more days during May to October*".

Notably, overheating Criteria 1 and 2 are designed by the author and are mainly motivated from the Met Office definition of summer heat wave in order to compare the influence of external climates on the indoor comfort temperatures.

3. Result

Following the above definition of a heat wave and overheating criteria, some key results has been presented in this section for a London location.

3.1. External and Internal Temperatures

An analysis of external and internal temperatures are performed at an hourly scale and presented at daily scale corresponding to 3000 climate years (during summer period, May - October) by means of 3D color coded plots in Figs. 1 and 2. Climatic files have been analyzed to measure change in daily maximum external temperature and corresponding average night time (11pm – 7am) bedroom temperatures in three future time periods: 2030s, 2050s and 2080s, in relation to a baseline period for the medium emission scenario.

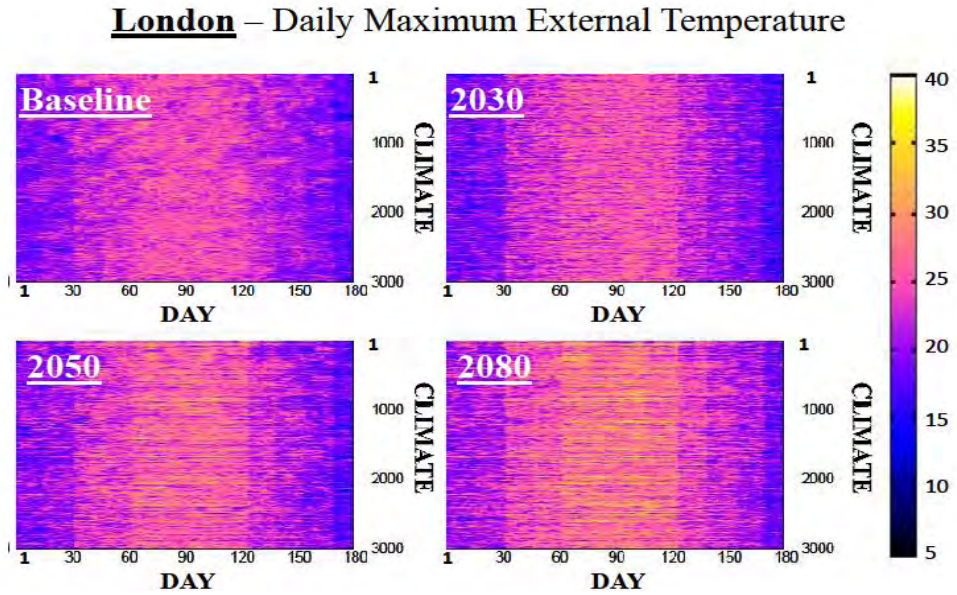

Fig. 1. Daily maximum of external temperature measured over 3000 climates for London - Medium Emission Scenario.

A visual inspection of Fig. 1 suggests that, for the baseline period daily maximum external temperature varies between 10 - 20 ^{o}C. Notably, temperatures around 10 ^{o}C could be observed as a less probable event on a distribution curve of the entire dataset, however it can be easily confirmed from the 3D plots that 10 ^{o}C is the most probable temperature for the start and end of the period i.e. May and October. During the 2030s, a temperature range of 15 - 20 ^{o}C appears to predominate, whereas during the 2050s, maximum external temperature could reach 30 ^{o}C, though less often and mainly during peak summer time (July – August). Events of maximum external temperature reaching 30 ^{o}C during peak summer period (July-August) could become more frequent in 2080s.

A simple statistical tool (as described in Section 2) has been used to reflect the changes in the averaged night time bedroom temperatures over the corresponding three future time periods: 2030s, 2050s and 2080s, in relation to the baseline period Fig. 2. Visual inspection of Fig. 2 suggests that for the baseline period the most probable average night time bedroom temperature ranges is 15 - 20 ^{o}C (May and October), 20 - 25 ^{o}C (June and September), and 25 - 27 °C (July and August). However, for the 2030s the most probable temperature range appears to be 20 - 25 ^{o}C, whereas 25 - 30 ^{o}C appear to be dominating during peak summer period (July - August). In the 2050s, the most probable temperature range still appears to be

20 - 25 °C with more probabilities, in comparison to 2030s, shifted to the temperature range 25 - 30 °C during peak summer period (July - August). The impact of climate change could further raise the probability attached to temperature ranges 25 - 30 °C in 2080s with the peak summer period (July and August) mainly dominated by the temperatures above 30 °C.

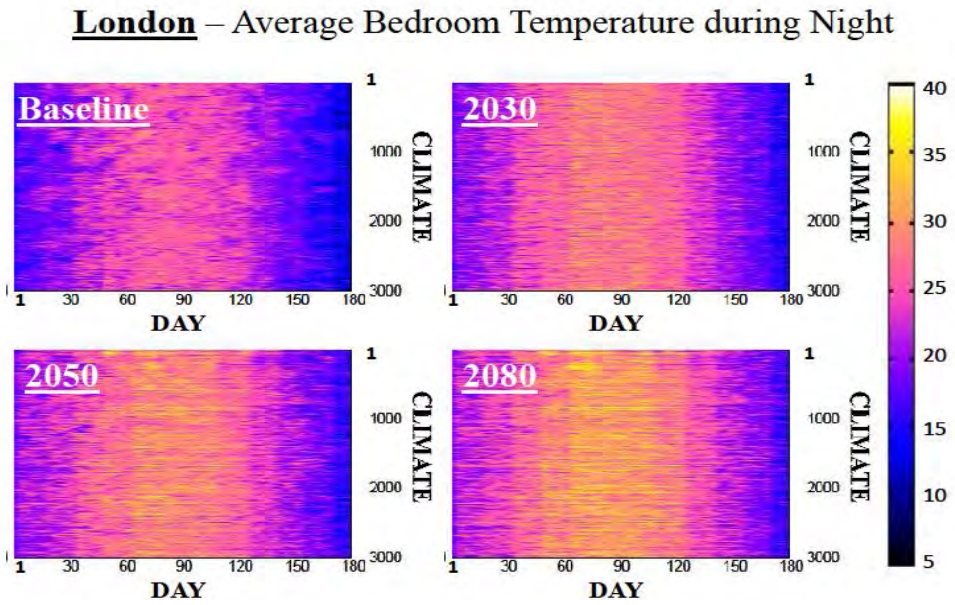

Fig. 2. Daily average of bedroom temperature during night (11pm – 7am) measured over 3000 climates for London - Medium Emission Scenario.

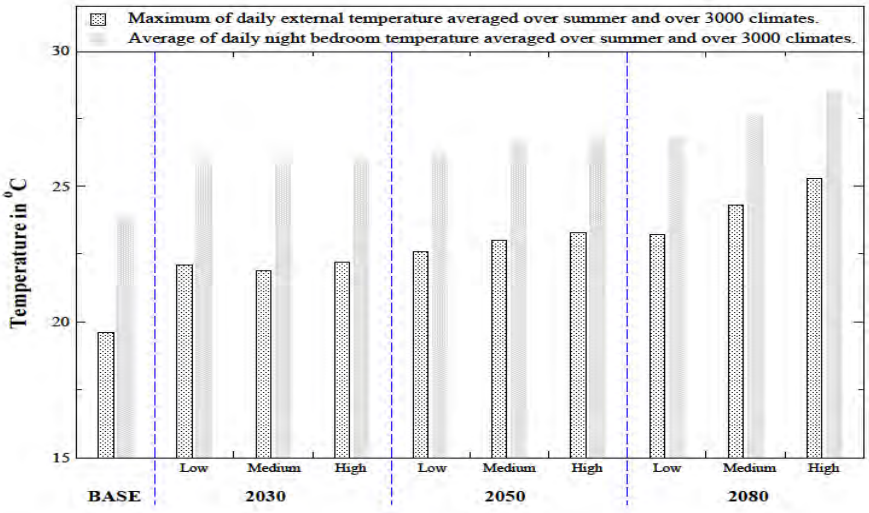

Fig. 3. Averaged daily maximum external temperature and average night bedroom temperature. Averaged over summer period and over 3000 climate years for three future time periods (2030s, 2050s, 2080s), three emission scenarios (Low, Medium, High) and baseline(1960-1990). Location: London

Finally, Fig. 3 shows the average maximum daily external temperature and corresponding average night bedroom temperature across three future time periods considered in the paper, alongside three carbon emission scenarios and the baseline period. For each scenario the average daily measurements for internal and external temperature parameters are firstly calculated over the May to October period and then over all 3000 climate years. The average of maximum daily external temperature in medium emission scenario rises to approximately 22 °C (2030s), 23 °C (2050s), and 24 °C (2080s) from 19 °C (baseline period). Average night

bedroom temperature in medium emission scenario approximately rises to 26 ^{o}C (2030s), 27 ^{o}C (2050s), and 28 ^{o}C (2080s) from 24 ^{o}C (baseline period).

3.2. Heat wave and Overheating Analysis

This subsection presents a complete analysis of summer heat wave duration and its impact on consequent overheating duration defined in criterion 1 and 2. The result has been presented across three future time periods (2030s, 2050s, and 2080s), three emission scenarios (upper panel), and the baseline period.

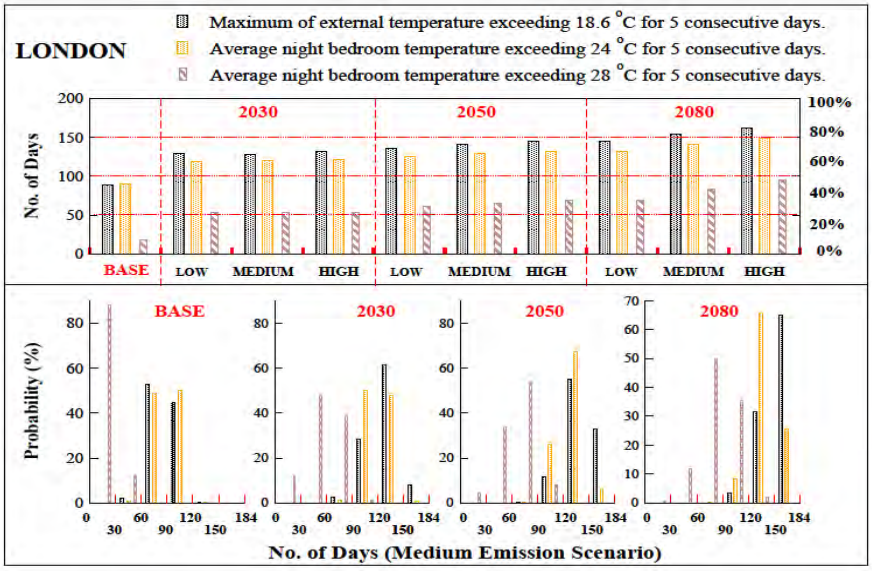

Fig. 4. Summer heat wave duration and overheating criterion 1 and 2 measured and compared. Dotted black bar: summer heat wave duration, gray (yellow online) dotted bars: overheating criterion 1, and gray (brown online) filled with slanted lines: overheating criterion 2.

In Fig. 4 the upper panel quantifies averaged (taken over 3000 climates) summer heat wave duration, overheating duration (defined in criterion 1 and 2) across all scenarios, in terms of total number of days during the identified period (May to October) along the left hand side of the *x* - axis, and in % of the May - October period along the right hand side of the *x* - axis. Dot filled black bars measure the averaged summer heat wave duration, while gray (yellow online) dotted bars measure the average duration of overheating defined under criterion 1 and gray (brown online) bars filled with slanted lines represents the average duration of overheating defined under criterion 2. Heat-wave duration and overheating duration defined in criterion 1 show similar trends in different future scenarios and, in particular, for medium emission scenario appears to rise by approximately 20 % (2030s), 30 % (2050s), and 40% (2080s) of total period in relation to baseline period. Overheating duration defined in criterion 2 increased by 15 % (2030s), 20 % (2050s), and 30 % (2080s) of total period in relation to baseline period.

Fig. 4 lower panel displays variation in summer heat wave duration, overheating duration (defined in criterion 1 and 2) across medium scenario for baseline, 2030s, 2050s and 2080s, distributed along total number of days during the period (May to October) for London - medium emission scenario. For a total of more than 90 % central probability over 3000 climates, summer heat wave duration and overheating duration defined in criterion 1 could shift from 60 - 120 days in the baseline period to 90 - 120 days in 2030s, to 90 - 184 days in 2050s, and to 120 - 184 days in 2080s. Overheating duration defined in criterion 2 could shift

from 30 - 60 days in baseline period to 30 - 90 days in 2030s, to 60 - 90 days in 2050s, and to 90 - 120 days in 2080s.

4. Discussion and Conclusions

This study presents an application of the simple statistical model which forms part of a methodology proposed by the Low Carbon Futures project to integrate future climate projections into building design and simulation. The statistical model presented in the form of a simple linear predictor has been used to describe the influence of climate change on the pattern of extreme heat events and its impact on the indoor comfort temperatures for a simple domestic building case study. Heat-wave duration and overheating duration defined under two distinct temperature based criteria in section 2.2 have been used as appropriate measures.

The results presented in Section 3.1 clearly illustrate the impact of climate change on the daily external and internal temperature profiles by means of 3D (color online) plots for given probabilistic climate projections. The average of maximum daily external temperature in the medium emission scenario appears to increases to 22 ^{o}C - 24 ^{o}C (2030s to 2080s) from 19 ^{o}C (baseline period), whereas average night bedroom temperature could reach 26 ^{o}C - 28 ^{o}C (2030s to 2080s) from 24 ^{o}C (baseline period).

In section 3.2 the summer heat-wave duration and overheating duration defined in criterion 1 appears to display a similar trend and up to a 20 % - 40% rise in total overheating period (2030s to 2080s) in relation to baseline period has been observed, whereas for the overheating duration defined in criterion 2 a 15% - 30% rise has been noticed. Outputs displayed in probabilistic format clearly show an increase in the total number of heat-wave duration days and overheating duration days defined in criteria 1 and 2.

Notably, the statistical model employed for overheating analyses has been demonstrated to replicate the outputs of ESP-r at an hourly scale within a single degree centigrade. The work presented in this paper could be used to develop methodologies for sustainable building design which could achieve a more acceptable level of thermal comfort in extreme climates. The effects of various adaptation techniques could be assessed to offset the predicted risk of overheating and in combating the influence of extreme events. Moreover, a range of possible climates, location and building variants could be investigated following the proposed methodology.

References

[1] IPCC, IPCC Fourth Assessment Report: Climate Change, 2007. Online at: http://www.ipcc.ch/publications and data/publications and data reports.htm

[2] J. Murphy et al., UK Climate Change Projections science report: Climate Change Projections., Technical report, Meteorological Office Hadley Centre, Exeter, UK, 2009.

[3] G. J. Jenkins, J. M. Murphy, D. M. H. Sexton, J. A. Lowe, P. Jones, and C. G. Kilsby, UK Climate Projections: Briefing report, Met Office Hadley Centre, Exeter, UK (2009). Online at: http://ukclimateprojections.defra.gov.uk/images/stories/briefing_pdfs/UKCP09_Briefing.pdf

[4] D. R. Easterling, G. A. Meehl, C. Parmesan, S. A. Changnon, T. R. Karl, and L. O. Mearns, Science 289, 2000, pp. 2068 – 2074.

[5] L. S. Kalkstein, and J. S. Greene, Environ. Health Perspect. 105, 1997, pp. 84 – 93.

[6] G. R. Walther, E. Post, P. Convey, A. Menzel, C. Parmesan, T. J. C. Beebee, J. M. Fromentin, O. Hoegh-Guldberg, and F. Bairlein, Nature 416, 2002, pp. 389 – 395.

[7] A. T. DeGaetano, Int. J. Biometeorol. 49, 2005, pp. 345 – 353.

[8] P. P. Marra, S. Griffing, C. Caffrey, A. M. Kilpatrick, R. McLean, C. Brand, E. Saito, A. P. Dupuis, L. Kramer, and R. Novak, Bioscience 54, 2004, pp. 393 – 402.

[9] Hadley centre coupled ocean atmosphere global climate model is known as HadCM3.

[10] 2010 — How Warm Was This Summer? NASA Goddard Institute for Space Studies (GISS), 28 September 2010. See also How Warm Was Summer 2010?, Research News (30 Sep 2010) from NASA GISS. Online at: http://data.giss.nasa.gov/gistemp/

[11] J. Hansen, R. Ruedy, M. Sato, and K. Lo, Global Surface temperature Change, NASA Goddard Institute for Space Studies, New York, New York, USA. Online at: http://data.giss.nasa.gov/gistemp/paper/gistemp2010_draft0803.pdf

[12] LCF, Low Carbon Future Project, 2009. Online: http://www.ukcip-arcc.org.uk/index.php?option=com contenttask=viewid=589Itemid=542

[13] S. Patidar, D. P. Jenkins, G. J. Gibson, P. F. G. Banfill, Statistical techniques to emulate dynamic building simulations for overheating analyses in future probabilistic climates, Journal of Building Performance Simulation, 1-14, iFirst article, 2011.

[14] D. P. Jenkins, S. Patidar, G. J. Gibson, P. F. G. Banfill, Incorporating future probabilistic climate projections into dynamic building simulation, Energy and Buildings, in correspondence.

[15] J. Clarke, N. Kelly, and D. Tang, A review of ESP-rs exible Solution Approach and its Application to Prospective Technical Domain Developments V1, In: Advances in Building Energy Research. UK: Earthscan, 2007, chap. 11.

[16] ARCC, Adaptation and Resilience in a Changing Climate, 2009. Homepage: http://www.ukcip-arcc.org.uk/

[17] P. D. Jones et al., UK Climate Projections science report: Projections of future daily climate for the UK from the Weather Generator, 2009. Homepage: http://ukclimateprojections.defra.gov.uk

[18] A. Peacock, D. Jenkins, and D. Kane, Investigating the potential of overheating in UK dwellings as a consequence of extant climate change. Energy Policy, 38 (7), 2010, pp. 3277 - 3288.

[19] http://www.metoffice.gov.uk/weather/uk/heathealth/

[20] P. J. Robinson, On the Definition of a Heat Wave, Journal of Applied Meteorology (American Meteorological Society) 40 (4), April 2001, pp. 762–775.

[21] M. Perry, A spatial analysis of trends in the UK climate since 1914 using gridded datasets. Climate Memorandum No. 21, Met Office, Exeter, 2006, pp. 29.

Incorporating Climate Change Projections into Building design: A Qualitative Study

Mehreen Gul*, Gill Menzies, Phil Banfill

Urban Energy Research Group, School of Built Environment, Heriot-Watt University, Edinburgh, UK
** Corresponding author. Tel: +44 1314514637, E-mail: M.Gul@hw.ac.uk*

Abstract: The UK climate of the future cannot be predicted with certainty and this is reflected in the current UK Climate Projections (UKCP09), which are probabilistic in nature. It is anticipated that the conventional approaches to building design will not adequately represent the effects of future warming and therefore guidance is required to overcome future overheating of a building by making it thermally more comfortable. The study presented here relates to a qualitative investigation and aims to draw out the needs and preferences of building design professionals to develop an easy to use formulation for adequately sizing Heating, Ventilation and Air-Conditioning (HVAC) plants. It will serve as an interface between professional building services engineers and the research team working on probabilistic weather data and a building simulation package. This investigation deploys a qualitative research approach of *Methodological triangulation*, which refers to the use of more than one method for gathering data. Herein, the three strands of research that will be used are the questionnaire, semi structured interviews and focus groups. This work is ongoing and the analysis is due for completion in 2012. This paper focuses mainly on some of the initial findings of the qualitative approaches mentioned above for domestic buildings only.

Keywords: *Qualitative investigation, Future climates, Focus groups*

1. Introduction

In the absence of formalised design requirements that take account of climate change, there is a need for pragmatic guidance on pro active design measures to ensure that the construction of new, and the refurbishment of older buildings avoids unacceptable problems or failures in the future. There has been growing concern that the trend towards hotter drier summers will lead to a reduction in the quality of the internal environment within buildings. Potentially this could lead to a wide range of health problems for occupants, and a significant deterioration in comfort conditions. In particular there is a concern that the overheating of buildings during the summer months could become an issue within the UK. [1]

The UK climate of the future cannot be predicted with certainty and this is reflected in the current UK Climate Projections (UKCP09) [2], which are probabilistic in nature. It is anticipated that the conventional approaches to building design will not adequately represent the effects of future warming and therefore guidance is required to inform adaptation decisions i.e. the adjustments required to overcome future overheating of a building by making it thermally more comfortable.

The Low Carbon Futures Project, as part of the Adaptation and Resilience to Climate Change (ARCC) programme in the UK, integrates UKCP09 into dynamic building simulation calculations [3]. The study presented here relates to a qualitative investigation and aims to draw out the needs and preferences of building design professionals to develop an easy to use formulation for adequately sizing Heating, Ventilation and Air-Conditioning (HVAC) plants. It will serve as an interface between professional building services engineers and the research team working on probabilistic weather data and a building simulation package [4]. Interaction with building professionals will ensure that the approach taken leads to a practitioner-focused rather than an academic outcome.

This work is ongoing and the analysis is due for completion in 2012. This research output enables the project team to tailor a design tool module that might potentially be integrated with existing building simulation packages to assess the overheating risk for future climates. The project is looking at domestic and non-domestic buildings but this paper is focusing only on domestic buildings and will present the results of initial qualitative investigation.

2. Methodology

A holistic overview of the HVAC building design process was undertaken. The initial questions were constructed after reviewing steps in the design process from statement of need to the final solution. The questions are based on issues of current and future overheating assessment, climate change impact, building performance metrics, adaptation techniques and probabilistic climatic data for the future. The aim was to get feedback and advice from the user community to understand the current practice of building design process and the measures required to combat changes that may occur due to changes in the future climate.

Since the project is reliant on feed-back from user groups to tailor the outcome of this project, this investigation deploys a qualitative research approach of *Methodological triangulation*, which refers to the use of more than one method for gathering data. The use of more than one approach to the investigation of a research question enhances confidence in the ensuing findings. Since much social research is founded on the use of a single research method and as such may suffer from limitations associated with that method or from the specific application of it, triangulation offers the prospect of enhanced confidence. By and large, researchers viewed the main message of the idea of triangulation as entailing a need to employ more than one method of investigation and hence more than one type of data. Social scientists are likely to exhibit greater confidence in their findings when these are derived from more than one method of investigation. Of course, the prospect is raised that the two sets of findings may be inconsistent, but such an occurrence underlines the problem of relying on just one measure or method [5].

Herein, the three strands of research that will be used are the questionnaire, semi structured interviews and focus groups. The results of each will be 'triangulated' to provide additional confidence in the conclusions – ideally, findings in each strand will help to support findings in the others.

Questionnaires are used in a wide range of settings to gather information about the opinions and behaviour of individuals. Questionnaires are objective and gathered in a standardised way thus providing an initial indication of the trends behind the current building services design process.

Semi-structured Interviews This type of research is valuable for an in-depth examination of people's attitudes and beliefs, and will provide insight into some of the reasons behind the decisions made. These interviews confirm what is already known and can provide reliable and comparable qualitative data.

Focus Groups can provide a dimension that is simply unavailable with a traditional survey as the interaction between participants can lead to new issues being identified. The combined effort of the group will produce a wider range of information, insight, and ideas than the responses of a number of individuals when these replies are secured privately. A bandwagon effect often operates in a group interview situation, in that a comment by one individual often triggers a chain of responses from the other participants. A signature aspect of a focus group

is the objective to better understand the group dynamics that affect individuals' perceptions, information processing, and decision making. [6]

3. Results and Discussion

3.1. Questionnaire

A questionnaire was designed with the main focus on highlighting the current process of building design, importance of different design variables, factors affecting thermal comfort, overheating and adaptation methods to mitigate the climate change for future years. The questions were orientated to gauge the differences between the typical practice and the best practice for HVAC design.

Normally, to limit the population surveyed, a sample is drawn to reflect the characteristics of the total population. By using a carefully drawn sample, there is an assurance that potential respondents have been selected in a standard, scientific manner. In this research the survey population was the Building Industry. The questionnaire was distributed via the fortnightly electronic newsletter of a building services professional body to all of its members. The resulting drawn sample therefore attempts to reflect the characteristics of the total population involved in the designing, structuring and engineering of buildings.

In this instance a total number of 42 people actually responded to the survey but as expected it was a diversity of professionals consisting of Architects, Electrical/Mechanical Engineers, Technical Directors, Energy Consultants and Sustainability Engineers. Although the responses were self selected and few in number, they still appear to suggest some trends within the Building Industry. The distorting effect of differential response rates has long been recognised as a limitation on inferences drawn from questionnaires in social research. Bias may arise even where the response is 100% and it is commonly understood that even where questionnaire response is poor, correlational studies are affected only by loss of degrees of freedom or precision [7]. In instances where the response rate is low or non neutral with regard to the topic of investigation, it is held that the conclusions suffer only from an increased sample variability, rather than from a substantial problem of bias. Increasing the response rate does not necessarily improve the precision of survey results [8]

Fig. 1 shows the hypothesis that emerged from the 31 responses to one of the questions of the questionnaire. It can be seen that the most important drivers in HVAC design are those of Building Characteristics, Available Budget, Comfort Criteria and CO_2 Emissions. Weighted scoring of these responses provides a method for evaluating the priority level of an individual at a glance. Weightings with values of 4, 3, 2 and 1, corresponding to very important, important, least important and not considered, respectively, were assigned to the columns. It can be seen that the Building Characteristics and Available Budget are the top rated parameters, followed by Comfort Criteria, Life Cycle Costs and CO_2 emissions. Plant Space and Ease of Installation are the least voted parameters.

Thermal comfort in a room is determined mostly on the basis of room air temperature, followed by external temperature and occupant activity. When asked about the incorporation of summer conditions of future climates into the design process, 77% of the professionals admitted including it, but only 33% implemented any measures to overcome future summer overheating. It emerged that adaptation is not always a part of the designing process but in some instances where it is, window opening, moveable internal blinds, air-conditioning and occupant control are highly regarded. It is also seen that beyond meeting Building Regulations and the requirement of Energy Performance Certificates, Good Practice Guides

and Building Research Establishment Environmental Assessment Method (BREEAM) are gaining priority.

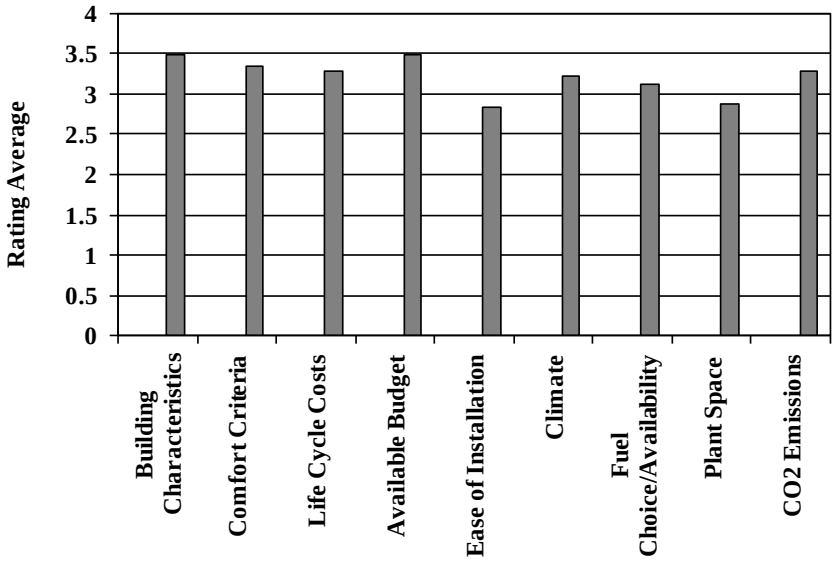

Fig. 1. Most important drivers in HVAC design

3.2. Semi-structured Conversation

The project team plans to hold at least 18 semi structured interviews, 6 of which will be undertaken for domestic and 12 for the non domestic sector (6 for offices and 6 for schools). The first round of these interviews will take place in early 2011.

There have been 2 Focus Groups held so far (see Section 3.3) where opportunities to speak to participants were fully utilized. Each Focus Group had 6 participants comprising of architects, building surveyors, building services engineers, property managers, environmmental consultants and sustainability officers. Prior to commencing the actual Focus Group sessions, a semi structured discussion ensued when an initial task was set where the participants were provided with a list of 9 factors (same as shown in Fig. 1) from which to choose, in their opinion, the 3 most important drivers for HVAC design. On selection, the participants were asked to provide the reasoning behind their choices based on their experiences.

The results of these semi structured conversations are included in this section. The generic message was that there are obvious design features that could and should be optimised to ensure efficient HVAC systems. These include Building Characteristics such as location and the orientation of buildings on a site, thermal insulation levels, glazing type, the use of shading and the use of exposed thermal mass in the structure to moderate temperature extremes. Some of the comments are quoted below.

> *''The main one that stands out probably is the Building Characteristics - absolutely getting the fabric of the building right whether that's working on an existing building or a brand new building''*

> *''HVAC design- design it out as far as possible so Building Characteristics''* (is the most important factor)''

The design process seems to rely heavily on the Available Budget as some respondents agree

that money is usually the driving force behind the decisions made and other issues are only secondary.

> *''If we have all the money in the world we could do everything but we can't - so Available Budget restricts it all''*

> *''Available Budget, I spend all of my day discussing designs with different developers to minimise spend on budget''*

> *''Available budget because there is precious little of it''*

Most of the professionals agree on CO_2 emissions to be the most important driver as it is seen as a significant problem currently and in the future. Different councils have different CO_2 emissions criteria and designers have to follow it by choosing fuels source that will produce minimal emissions. Some people are of the view that buildings are for people and whichever way the buildings are designed, comfort should be the main priority.

> *''CO_2 emissions because it seems to be a significant problem we are going to have in the future''*

> *''As the designers we have responsibility towards a cut in carbon emissions because the way we use buildings accounts for nearly half of all are national emission."*

> *''Comfort Criteria - we are designers and we are designing to know the person and always take that into account whether it's an office building or an individual's requirement''*

> *''Comfort is becoming very important in the long term especially with questions over what the future climate is doing''*

3.3. Focus Groups

There will be 6 focus groups throughout the UK, 2 for the domestic and 4 for the non domestic sector (schools and offices). To date, 2 Focus Groups on overheating in the domestic sector have been held as explained in section 3.2. Focus Groups were conducted in Edinburgh and in London to ascertain the differences in regional and climatic variations that would have an impact on the attitudes and experience of the participants. There is no magic number and more is not necessarily better, although holding 2 focus groups with similar group characteristics may place the results on firmer ground in relation to the patterning of the data. This is because it would suggest that the differences observed are not just a feature of a one-off group, but are likely to be related to the different characteristics of participants reflected in the selection [9]. A total of 6 research questions were explored in detail in these sessions but only some of the main themes that emerged are included in this paper and are as follows:

There is general agreement that the UK is in a comparatively good position as far as overheating in dwellings due to climate change is concerned. From the quotes given below one can observe the difference in trends due to regional variation. It is clear that there is little or no concern of overheating in Edinburgh (Scotland) whereas, although not regarded as an important issue in London (South England) it is nevertheless borne in mind that with suitable measures, this problem can be prevented.

"Currently, Overheating is not necessarily seen as a problem as we do not tend to install air conditioning in to domestic buildings as a norm'' (Edinburgh Focus Group)

''The UK is really in a privileged position as far as Overheating is concerned, with suitable interventions one can get both cooling in the summer and heating in the winter''(London Focus Group)

No significant attention is being paid to future overheating in the domestic sector. Strategic decisions from the outset are essential. Getting the fabric of the building absolutely right for both existing buildings and brand new buildings is imperative thus dealing with what you can within the building characteristics/fabric and then looking at what you need to add in to the building to overcome any overheating problems. Typical comments are:

''Building Characteristics top of my list because we are trying to make (these) strategic decisions from the outset''

''Building Characteristics obviously dictate whether you need HVAC for the start, whether you have to work from where you are or where you want to be"

"You have to get more mass into buildings to try and soak it up and redistribute it at times of the day when it's more beneficial''

''Some house builders have kind of set parameters for a fabric designed solution for reducing carbon and energy output"

''Building Characteristics - that's the most important - it's about reducing mechanical ventilation in the building - to maximise the way that natural ventilation can work well and also simply without being overly complex''

For normal domestic developments the envelope design is deemed critical and construction elements seem more of a concern to future climate than overheating. Improvements in windows are required as double glazed windows still let in and let out substantial heat. By moving to a proper standard triple glazed passive house window, conditions can be maintained where no matter the external temperature, internal conditions can remain stable. Experience dictates that the main driver in people to overcome overheating will be legislation. A full impact will only be achieved if stipulated in Building Regulations.

''Until we have to do it we won't do it, the money is not there and nobody is going to spend over the top"

***''**We are driven by legislation in terms of what criteria we have to actually meet and our question is whether legislation is actually accurate where it's driving us to''*

''If there is no legislation saying that you have got to do it at the moment you just have to use the latest national calculation methodology software and that's got a bit of overheating and that's all people will do''
''Every time we build one of these buildings we are almost building a little experiment based on legislation''

There is a fundamental need to inform the user. Building Regulations can change and

buildings can become more and more efficient but it is imperative to also educate in order to change user habits. Habit means that thermostats are set at the same level even though a reduction of a couple of degrees would also be perfectly acceptable.

> *''Our behaviours have got to change- The barrier is actually the values of our society and the literacy of our society to the changing climate as much as it is about regulations''*

> *''We can change the Building Regulations and buildings can become more and more efficient but people don't change their habits so how much of this energy is going into the building fabric needlessly?''*

> *''We are technical people, we come up with technical solutions and we are forgetting that there are people living in these places who may not understand''*

All participants agree that the weather will get warmer in the future, which although alarming is ignored, as it is not considered an issue at the moment. Some participants said that they preferred to keep their 'heads in the sand' in the hope that it can be avoided until it is no longer their problem. The prevalent feeling is that probability is the only way forward to deal with future predictions otherwise people will want proof. If a tool is to be provided, that specifies the overheating risk of a building, as part of an overheating analysis based on probabilistic climate projections, it needs to be really simple and understandable.

> *''There is no intrinsic value to creating a better building or a more energy efficient building at this moment in time''*

> *"Yes it's going to get warmer but not in my lifetime so I don't need to bother about it - it's my children's problem they can deal with it"*

> *''Climate Change and Overheating is actually quite difficult at the moment to calculate anything on but the construction element is even worse - how can we design better buildings and better details''*

> *''The Probability aspect is probably the only way that you can model it - you have to have those variables and perhaps some kind of benchmarks.*

> *''The Tool needs to be a form where you can add it to the way you model the building as it stands''*

4. Conclusions

The Low Carbon Futures project relies on feedback from the Building Design Community to design a tool that can predict the risk of future overheating in buildings. This paper presented the initial findings of a qualitative investigation performed to gain insights into some of the decision making process. An important aspect of this study was to get the feedback of the Building Industry, surrounding aspects of HVAC design. As with any other branch of science, the validity and reliability of the measurement tools, needs to be rigorously tested to ensure that the data collected is meaningful. Depth of qualitative information may be difficult to analyse for example, deciding what is relevant and what is not. This investigation has therefore adopted the triangulation approach to analyse the resulting data from 3 modes: A questionnaire, semi- structured conversations and focus groups.

The Questionnaire results have suggested that the Building Characteristics and Available Budget are the top rated parameters, followed by Comfort Criteria, Life Cycle Costs and CO_2 emissions. Semi-structured Conversation with 12 experienced professionals indicated that the reduction of CO_2 emissions is the lead factor as it is a regulatory requirement. The majority agreed that many problems could be solved if a building is designed properly taking into account Building Characteristics. Available Budget and Comfort Criteria also play a key role in this aspect. Analysis of the Focus Group discussions revealed that the initial decision needs to be made on the building characteristics and then what is to be added in to the building to design the HVAC system needs to be addressed. There is a need to get the fabric of the building absolutely right whether that is working on an existing building or a brand new one.

The Triangulation methodology adopted herein seemed successful in validating the suggested hypothesis from the questionnaire by confirming it with the findings of the focus groups and the semi structured conversation. Since this is an initial analysis, these issues will be fully explored and on a larger scale with the semi- structured interviews taking place in early 2011 and with more focus groups.

After the initial questionnaire and focus groups there is a strong suggestion that currently overheating is not considered as a critical element when designing or refurbishing new and existing domestic buildings. However, the use of probabilistic climate information has been heard with interest inferring that a probabilistic approach may be the way forward to tackle the unpredictable nature of the weather in the coming years. The unanimous belief was that until the building industry is forced to consider climate change they will not do it. It is also accepted that a tool, based on probabilistic predictions, that is a simple add on to existing techniques will be well-received.

References

[1] Good Building Guide 63 (GBG 63), Climate change: Impact on building design and construction. BRE press 2004, pp. 1-6

[2] P.D. Jones et al., UK Climate Projections science report: Projections of future daily climate for the UK from the Weather Generator, available from http://ukclimateprojections.defra.gov.uk

[3] Adaptation and Resilience in a Changing Climate Network (ACN), Programme website http://www.ukcip-arcc.org.uk/content/view/605/519/

[4] S. Patidar, D.P. Jenkins, G. Gibson, and P.F.G. Banfill, Statistical techniques to emulate dynamic building simulations for overheating analyses in future probabilistic climates, Journal of Building Performance Simulation, In Press, 2010

[5] A. Bryman, Quantity and Quality in Social Research. Routledge, 1988, pp. 131-134

[6] D. W.Stewart, P.N. Shamdasani and D.W.Rook, Focus groups Theory and Practice, 2nd Edition, Sage, 2007, pp. 1-16

[7] R. J. Bowden, Self-Selection Biases in Correlational Studies Based on Questionnaires, Psychometrika 51, 2, 2010, 1986, pp. 313-325

[8] W. Jones and J. Lang, Sample composition bias and response bias in a mail survey: A comparison of inducement methods. *Journal of Marketing Research* 17, 1980 pp. 69-76

[9] R.Barbour, Doing Focus groups, First Edition, Sage, 2007, pp. 57-60

Towards a unifying visualization modelling platform for supporting climate change conscious urban neighbourhood design

Amr Elwan[1,2], Chengzhi Peng[1], Mohammad Fahmy [2]

[1] *School of Architecture, University of Sheffield, Sheffield, UK*
[2] *Department of Architecture, Military Technical College, Cairo, Egypt*
** Corresponding author. Tel: +447578409402, Fax: +441142220315, E-mail: a.elwan@sheffield.ac.uk*

Abstract: Urban physical environments will face up to the challenges posed by global climate change. Various software packages for urban environmental simulation have been created to aid predictions of design performance under climate change conditions as understood today. However, the outputs from these simulation packages present great difficulties for planners, architects and urban designers working in urban neighbourhood projects. Furthermore, designers lack proper tools to bring the outdoor and indoor simulation results together to form an integrated picture at the urban neighbourhood level. It is vital that designers are enabled to achieve such a holistic understanding of their design consequences simply because those indoor and outdoor environments are constantly interconnected with each other. This paper presents this pilot study on setting up an environmental visualization methodology of global climate change at a local scale and how it can be applied to a real urban neighbourhood development project proposed for a site in the City of Cairo, Egypt. The result shows an initial step of addressing the urgent need for a practical visualization modelling platform accessible to urban designers, architects, and decision makers towards sustainable urban forms.

Keywords: *Urban neighbourhood, Outdoor-indoor climate coupling, Sustainable urban neighborhood developments.*

1. Introduction

Urban climatology is an interdisciplinary field related to urban form design. Its complexities have prevented applying climate knowledge within the urban planning process and practice (Oke 1984; Eliasson 2000; Ali-Toudert, Djenane et al. 2005; Oke 2006; Ali-Toudert and Mayer 2007b; Fahmy and Sharples 2008b; Fahmy 2010a).Recently the challenges posed by global climate change have attracted intense research attention world-wide (McEVOY 2007; Levermore 2008; Fahmy 2010a). Due to the long shelf-life of carbon dioxide in the atmosphere, much of the climate change over the coming decades has already been determined by historic emissions (Hulme, Lu et al. 2002). Additionally statistics show that urban environments caused 75% of pollution and 20 percent of carbon dioxide emissions is caused by transport which constitutes 50% of global warming (Barton 1995 and Levermore 2008). Scientists believe that greenhouse gas concentration is increasing global warming(Radhi 2009).Climate change, and increasing urbanisation will mean that, for the rest of this century, urban thermal comfort will become an increasingly important issue for many city residents. The increased use of air conditioning is not available as a long term solution as it will, not only discharge more waste heat into the urban environment, but will also add to CO2 emissions (Fahmy and Sharples 2010b).

Oke (1999) highlighted the meteorological locations and their importance on urban microclimate, this means a weather data files (WDF) of typical meteorological years is measured at weather stations. WDF is used for indoor and outdoor thermal performance simulations by many models either in their EPW, WEA, EPS-r formats to provide hourly data of the whole year or a STAT format to provide an averaged hourly data of the months (DOE, 2009; Radhi, 2009 and Fahmy et al., 2009). This hourly WDF contains the different measured hourly meteorology for a specific location extracted from 30 years ago. WDF represents meteorological parameters e.g. dry bulb temperature, wet bulb temperature, relative humidity,

Specific humidity, direct normal radiation, diffuse horizontal radiation, and global horizontal radiation illuminance.

The intergovernmental panel for climate change (IPCC) has recently drawn attention to the significant warming of capital cities across the world. Understanding the influence of the emissions on air quality motivates the planners to use near-term scenarios. *"Near-term adaptation and mitigation analyses can be matched to conventional planning time scales, can explore opportunities and constraints given institutional and technological inertia, and can play an important role in integrating climate change considerations into other areas of management and policy."(IPCC 2007).* There are several methods capable of creating near-term scenarios of climate change. One of these methods is weather data morphing methodology which manipulates historical weather data for climate scenarios. This will be provided by Climate Change World Weather File Generator, which generates future WDF for 2050(IPCC 2010).

In this research, ENVI-met 3.1 simulation software is used to relocate the measured EnergyPlus Weather (EPW), and generate an accurate WDF. Furthermore, ENVI-met 3.1 takes into consideration the influence of urban neighbourhood elements e.g. buildings, soil, vegetation, and trees. Finally, the generated WDF is used in CC World Weather Gen Tool and ECOTECT 2011. Simulation method is important to visualize the effect of outdoor thermal environment on indoor environment(He, Hoyano et al. 2009). Therefore this paper aims to assess the potential of this methodology in a pilot study, which supports climate change conscious urban neighbourhood design.

1.1. Methodology

The outdoor assessment of urban form is carried out by using the numerical model ENVI-met, which simulates the microclimatic changes within urban environments. The relationship between buildings and urban climate can be understood through the connection between indoor and outdoor thermal, comfort which have shared issues (coupling methodology)(Ali-Toudert and Mayer 2006). The relationship between buildings and urban climate can be understood through the numerical coupling methodology. that connects between indoor and outdoor thermal performances (Fahmy et al., 2009).

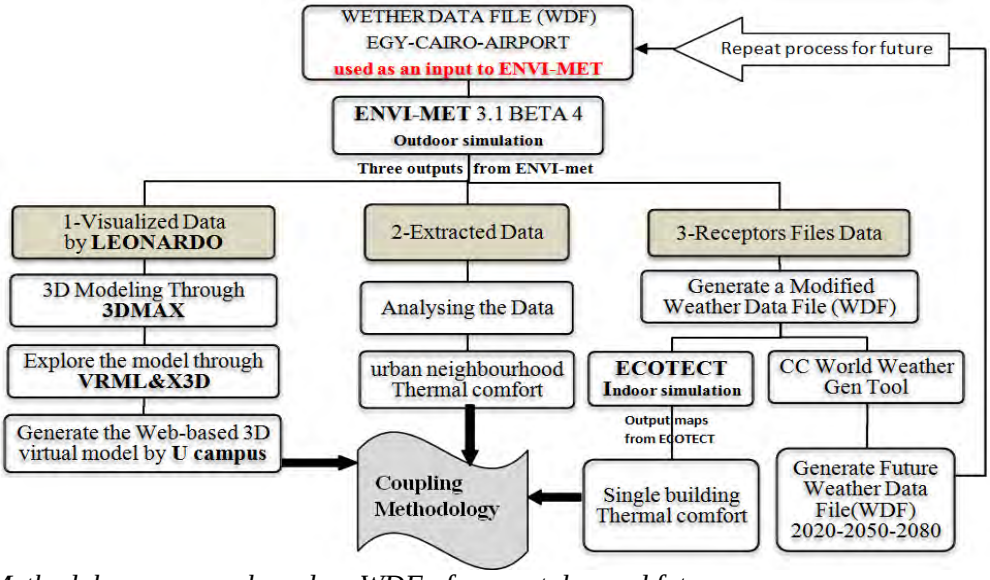

Fig.1. Methodology process based on WDF of present day and future.

The methodology has been carried out in four stages (Fig.1): Firstly, the outdoor simulation of an urban neighbourhood by numerical modeling to obtain present day outdoor meteorological

data which in turn affects the neighbourhood indoor conditions. ENVI-met 3.1 BETA4 is used to generate fine-tuned meteorological parameters at different heights of a building unit by placing snapshot receptors around the unit to obtain the near walls present day climate conditions for the building. Secondly, for the indoor simulation and thermal analyses of the prototypes residential clusters, ECOTECT 2011 is used for its computability with the various used software packages. ECOTECT uses EnergyPlus as a core for the calculation of thermal interactions in a specific location using EnergyPlus Weather data file, EPW. Cairo's EPW file is compiled from about 30 years of meteorological measurements in Cairo International Airport weather station, which ENVI-met results were added to the urban settings effects and represented in a new EPW file, fig.1.Thirdly, given the outdoor-indoor coupled simulations performed on a common set of meteorological parameters. We can plot (a) outdoor ground contoured maps for thermal comfort extracted from ENVI-met, and (b) multiple indoor thermal profiles along the building unit compartments using ECOTECT. Finally, a Web-based 3D virtual model of the entire urban neighbourhood is built to insert both the ENVI-met outdoor mapping and ECOTECT indoor profiling results. Viewers are thus able to perceive the combined results from (a) and (b) via interactive navigation through the 3D virtual urban neighbourhood. These simulations software can be used to calculate and assess comparative environmental impacts by 3D master planning of urban form. This can be applied to present and future weather by generating morphed data to be used with building performance simulation. Eventually, for an executable regeneration policy, such 3D illustrations can be accessed over the Web to support both policy and decision makers for further investigations to avoid the negative impact due to the future global warming by upgrading and regenerating urban forms. For the preparation of a morphed weather data files in the Energy Plus format, CCWorldWeatherGen1.4 will be used and the previous steps for the new future weather data file will be repeated. (CCWorldWeatherGen 2010).

2. Case study description

Due to the expected large area of a selected case study, field work including measurements is not a suitable method of assessment for the existing situation. Particularly, the simulation process will be repeated many times with different conditions. The selected Case study is in a new compound development at the east of the existing old city in Cairo. The new development is an ongoing project held by DAMAK Company, fig.2. The master plan contains repeated prototypes which consist of 3 floors. Four single semidetached building units in different locations in the neighbourhood were chosen, *Table1.*

Table1. Detailed model description of the case study.

Parameter	Detailed model(1,2)	Detailed model (3,4)
Total area	540 m2	500 m2
No. of floor	3 floors	3 floors
Ext. walls	0.25m brick 20 mm plaster inside	0.25m brick 20 mm plaster inside
Int.walls	0.25m brick 20 mm plaster inside	0.25m brick 20 mm plaster inside
Floor height	3.2m	3.2m
Orientation	North to south	East to west
Roof	20 tiles 20 mortar 50 sand 150 mm concert	20 tiles 20 mortar 50 sand 150 mm concert
Glazing	6 mm single glass	6 mm single glass
Thermal zones	Multi zones	Multi zones

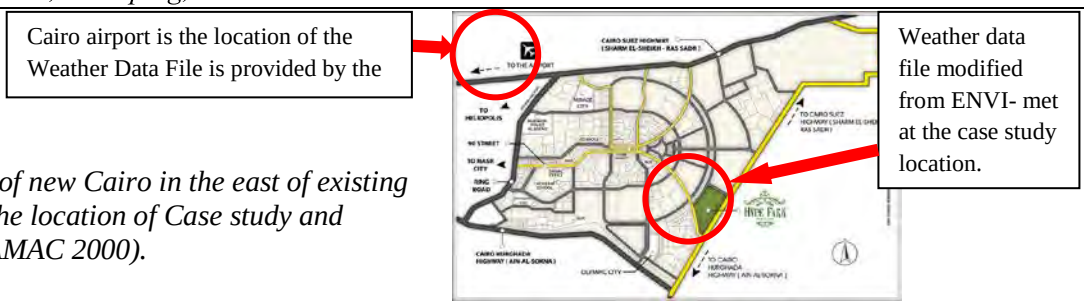

Fig.2.map of new Cairo in the east of existing old town, the location of Case study and airport(DAMAC 2000).

3. Results and analyses

Scenarios use simple models to measure the existing climate projections. This gives comparable results to the full three dimensional climate models. There are limitations of these scenarios; Firstly, the scenarios should not be considered forecasts or predictions, but representative scenarios. Secondly, these scenarios support scientific research to test their implication for adaptation and mitigation. Thirdly, there are uncertainties about using future scenarios particularly for emissions profiles. There are new techniques are developed for translating emissions and uncertainty analyses.(IPCC 2007)In this respect the morphing methodology used in CC World Weather Gen, which might include uncertainties due to wind information unchanged, but other modified meteorological parameter in the new WDF provide an acceptable level of knowledge (McEvoy 2007). Another sort of uncertainties can be expected through the applied software cycle by feeding the tool output to another with a converted file extension between them. However, there was no other way to check such methodology, because all models in literature visualize separately both outdoor and indoor simulation. In addition, architects, and planners need to communicate this software process for climate knowledge. This might height the gap between outdoor and indoor invironmental simulation software.

3.1. Outdoor simulation

The three dimensional model ENVI-met 3.1 BETA4 was chosen to simulate comfort quantities and the meteorological factors within an urban microclimate model. Our three dimensional model ENVI-met requires a few input parameters which are entered to a configuration file. Whenever the simulation starts to calculate the meteorological factors e.g.

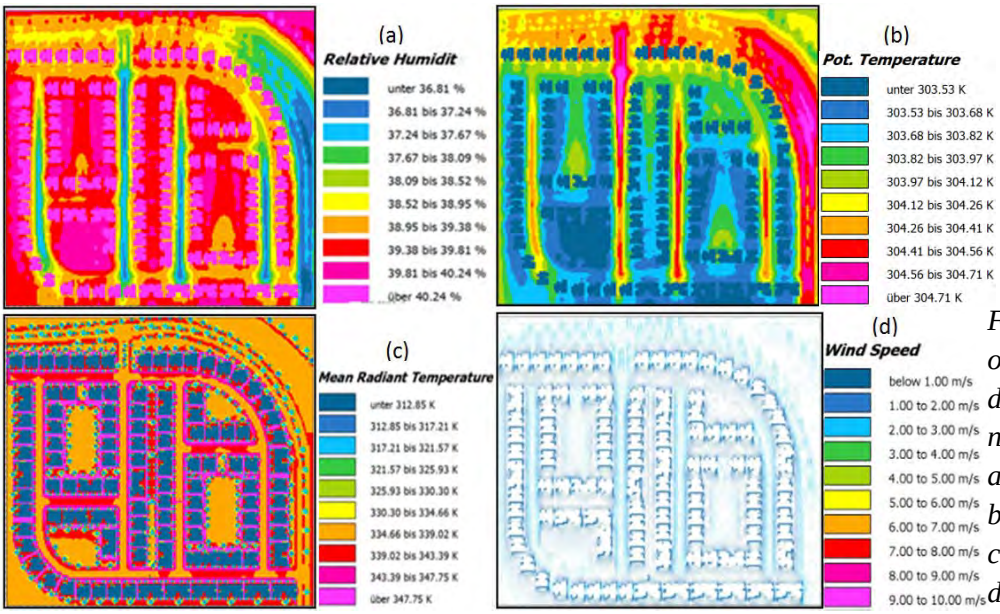

Fig.3.Visualization of metrological data of urban neighborhood: a. Relative humid. b. air temperature c. Tmrt d. wind speed.

wind speed and direction, air and surface temperature, air humidity, short- wave and long-wave radiation fluxes, in addition to the mean radiant temperature which is needed for comfort analyses. The Simulation date was on 1st of June, because it is the typical summer day and started at peak time from10:00 to 1600. After the simulation finished by 3D numerical model ENVI-met 3.1 Beta 4, we had three outputs: firstly, the maps which illustrate the different metrological factors by colors; secondly, receptors file which are used to generate an accurate WDF instead of the one provided by the USDOE, which was measured at the Cairo Airport, about 30 km away from the study site; and finally, extracted data for every hour of the simulation, fig.3.

As can see in Fig.3, there is a higher temperature at outer and inner roads. Wind speed at the outer roads is higher than the inner roads because wind direction is blocked by the buildings. Additionally, specific and relative humidity are lower inside the neighbourhood. This will lead to a lower mean radiant temperature. Eventually all the previous conditions will affect pedestrians' thermal comfort. The comparison among the meteorological data influences the thermal comfort of the urban neighbourhood, therefore air temperature, specific humidity, wind speed, relative humidity and mean radiant temperature are the parameters which control the urban neighbourhood thermal comfort.

3.2. Indoor simulation

Four housing units in different locations of the neighbourhood were selected and the closed thermal zones of every model inside ECOTECT 2011 built. The provided weather data file by ENVI-met used into the simulation. Eventually, the detailed model built by 3D MAX in separated floors and the resulted thermal maps by ECOTECT attached into the model, fig.4.

3.3. Coupling outdoor and indoor

Outdoor and indoor simulations are held and followed by 3DMAX to collect the different results in a rendered thematic model with a detailed terrain and elements of microclimate, (Fig.4). Then the models were grouped into different categories. E.g. group 1 contains the urban terrain and separated floors of the detailed modes, group 2 for the ENVI-met outdoor simulations and group 3 for ECOTECT indoor simulations. Finally, a Web-based 3D virtual model of the entire urban neighbourhood was built through VRML, X3D and made available on the web via the uCampus platform (Peng and Blundell Jones 2004).

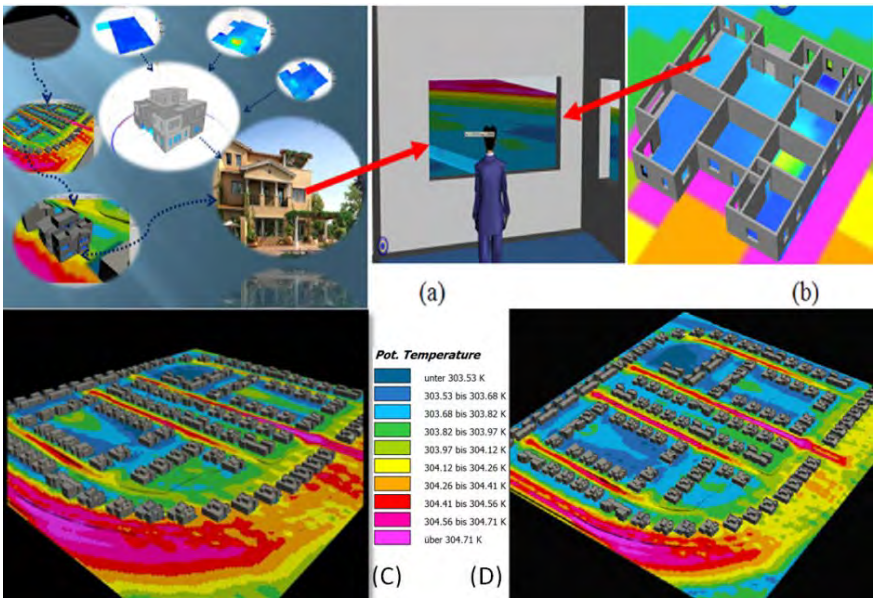

Fig.4 Bring outdoor and indoor simulation together (a) & (b) illustrate the 3D virtual model.(c)Air temperature predicted by the morphed 2050 scenario and (d) Air Temperature of present day.(c) and (d) illustrate the difference in temperature, not only at inner roads, but also at all spatial urban canyons, due to the increase in air temperature in the 2050.

Following the work of Fahmy et al., (Fahmy, Trabolsi et al. 2009), as ENVI-met does not have the capability to simulate indoor climate (it just deals with it as a heat sink through steady state conduction), ECOTECT 2011(AUTODESK 2010) was used to investigate the means of indoor climate conditions for the case study. ECOTECT has built a comprehensive 3D interface over EnergyPlus v3.1 (USDOE 2009), as an architectural dynamic modelling platform has simulated indoor thermal interactions. The meteorological factors (air temperature, wet bulb temperature, relative humidity, global radiation, short-wave direct and diffuse radiations and wind speed) for all site outdoor grids were added in their cells in a comma separated Value (CSV) file extension. This allows easy editing of the climate hourly data in an Egyptian Typical Meteorological Year (ETMY2) weather data format which can be used for Egypt, (USDOE 2009). In this study, WDF was used basically as an energy plus format, EPW, and EnergyPlus converter tool, which was used for conversion after writing new hourly data in the (CSV) file.

4. Generating Future Weather Data File (WDF)

A numerically air Temperature map (T_a) was plotted as an example of the 3D thematic maps, which was based on the morphed WDF for 2050 scenario and present day, fig.4. Climate conditions scenarios was through the weather data morphing methodology that was provided by CC World Weather Gen Tool which WDF 2020-2050-2080 e.g. WDF Of 2050, fig.5.

18	Date	HH:MM	Datasour	DryBulb {	DewPoin	RelHum {	Atmos Pr	ExtHorz
3653	01/06/2050	10:00	'?'?'?'?'	24.2	15	56	101502	1117
3654	01/06/2050	11:00	'?'?'?'?'	26.2	13.8	46	101491	1248
3655	01/06/2050	12:00	'?'?'?'?'	28.4	13.2	39	101470	1311
3656	01/06/2050	13:00	'?'?'?'?'	29.2	11.4	33	101429	1301
3657	01/06/2050	14:00	'?'?'?'?'	31.2	11.7	30	101378	1220
3658	01/06/2050	15:00	'?'?'?'?'	32	11.3	28	101337	1073
3659	01/06/2050	16:00	'?'?'?'?'	31.1	12.1	31	101317	869
3660	01/06/2050	17:00	'?'?'?'?'	32.2	12.5	30	101306	624

Fig.5. part of the weather data morphing (01/06/2050) contained meteorological factors e.g. dry bulb temperature, Dew point, Relative humidity, Atmospheric pressure

5. Implications for present and future urban developments

In a hot climate country like Egypt many planning projects have been produced and executed to cope only with population growth (Ali 2003). Particularly in Cairo, the overwhelming population growth rate did not allow the chance for full environmental studies for both the built and the natural environment, whereas buildings and open spaces have to be adequately climate responsive. Through the methodology, which visualizes the coupled outdoor-indoor climate condition, the construction market stockholders can have an idea about the whole thermal performance and energy consumption, Fig.6.

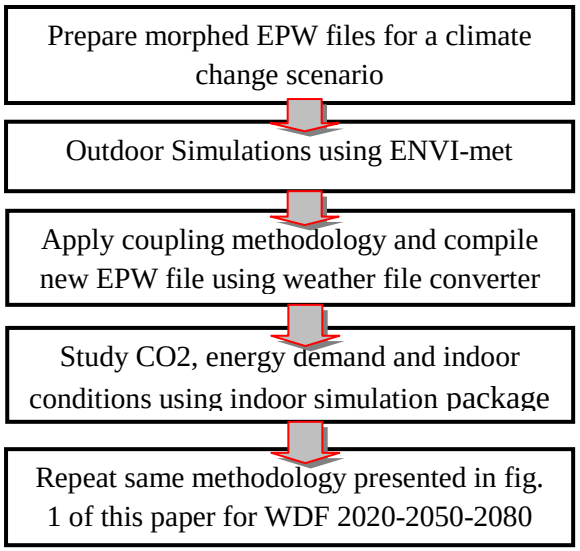

Fig.6: Climate change based outdoor-indoor coupled 3-D visualization methodology modified after Fahmy (Fahmy 2010), p-175.

6. Conclusion and future studies

This study has not developed a tool, but has carried out the process manually. This paper could lead to new software which enables architects and planners to realize the relationship between outdoor and indoor conditions. This methodology identifies the gaps between simulation software, and how a new system can be developed to connect these results. Therefore, comparison between different design alternatives would become possible, as will measuring thermal comfort efficiency of the urban neighbourhood.

This paper has investigated an approach of the combination between micro climate scale using ENVI-met and building scale using ECOTECT, and illustrated the importance of the interaction between outdoor – indoor thermal comfort. 3D virtual modeling supported planners, companies and civil society. Firstly, for visualizing the numerical calculation results; secondly, for developing outdoor – indoor coupling methodology, and understanding the comparison between present and future meteorological data; and thirdly, realizing the climate change conscious urban neighbourhood design.

Further research should draw attention to the prevailing wind due to the simulation for the typical summer day of the hot arid conditions in Cairo, which is noticed that the wind direction is blocked by some buildings, and consequently the canopies' air temperature increased and affected pedestrians' thermal comfort. Therefore future studies should focus on improving the spatial distribution of wind velocity by changing building shapes & tree lines and using green roads techniques.

References

[1] Ali-Toudert, F., M. Djenane, et al. (2005). "Outdoor thermal comfort in the old desert city of Beni-Isguen, Algeria." Climate Research 28(3): 243-256.

[2] Ali-Toudert , F. and H. Mayer (2006). "Numerical study on the effects of aspect ratio and orientation of an urban street canyon on outdoor thermal comfort in hot and dry climate." Building and Environment 41(2): 94-108.

[3] Ali-Toudert, F. and H. Mayer (2007b). "Effects of asymmetry, galleries, overhanging fac¸ades and vegetation on thermal comfort in urban street canyons." Solar Energy 81(6): 742–754.

[4] Ali, E. (2003). "Evaluation of the Egyptian Experiment in Establishment the new Towns in the Desert Areas." Journal of Engineering Sciences, Assiut University of Egypt 31(1).

[5] AUTODESK. (2010). "ECOTECT2011 [Available Online] http://www.autodesk.co.uk/adsk/servlet/mform?validate=no&siteID=452932&id=14205163 " Retrieved 19/4/2010.

[6] Barton, H. (1995). "(1995) Sustainable Settlements: A Guide for Planners, Designers and Developers, Government Management Board, University of West of England, Bristol."

[7] CCWorldWeatherGen. (2010). "Climate Change World Weather File Generator." V1.4. Retrieved 25-5, 2010.

[8] DAMAC (2000). Hyde Park. Adobe reader. H. e. Brochure. New Cairo.

[9] Eliasson, I. (2000). "The use of climate knowledge in urban planning." Landscape and urban planning 48(1-2): 31-44.

[10] Fahmy, M. (2010a). Interactive urban form design of local climate scale in hot semi-arid zone. School of Architecture. Sheffield, University of Sheffield. PhD.

[11] Fahmy, M. and S. Sharples (2008b). "The need for an urban climatology applied design model, [Online]. Available at: http://www.urban-climate.org/IAUC028.pdf." The online newsletter of the International Assocciation for Urban Climatology 2008(28): 15-16.

[12] Fahmy, M. and S. Sharples (2010b). "Urban form adaptation towards minimizing climate change effects in Cairo, Egypt. Accepted Manuscript." Building Services Engineering Research and Technology.

[13] Fahmy, M., A. Trabolsi, et al. (2009). Dual stage simulations to study microclimate thermal effect on comfort levels in a multi family residential building. 11th International Building Performance Simulation Association Conference University of Strathclyde in Glasgow, 27-30 July.

[14] He, J., A. Hoyano, et al. (2009). "A numerical simulation tool for predicting the impact of outdoor thermal environment on building energy performance." Applied Energy 86(9): 1596-1605.

[15] Hulme, M., X. Lu, et al. (2002). Climate change scenarios for the United Kingdom; The UKCIP02 scientific report. UK Climate Impacts Programme (UKCIP), Oxford (United Kingdom); Funded by the Department for Environment, Food and Rural Affairs. See m02/35481 for the briefing report.

[16] IPCC. (2007). "TOWARDS NEW SCENARIOS FOR ANALYSIS OF EMISSIONS, CLIMATE CHANGE, IMPACTS, AND RESPONSE STRATEGIES http://www.ipcc-data.org/docs/ar5scenarios/IPCC_Final_Draft_Meeting_Report_3May08.pdf."

[17] IPCC. (2010). "HadCM3 climate scenario data download page, www.ipcc-data.org/sres/hadcm3_download.html." Retrieved 25-5, 2010.

[18] Levermore, G. J. (2008). "A review of the IPCC Assessment Report Four, Part 2: Mitigation options for residential and commercial buildings." Building Service Engineering 29(4): 363-374.

[19] McEVOY, D. (2007). "Climate Change and Cities." Built Environment 33(1): 5-9.

[20] Oke, T. R. (1984). "Towards a prescription for the greater use of climatic principles in settlement planning." Energy and Buildings 7(1): 1-10.

[21] Oke, T. R. (2006). "Towards better scientific communication in urban climate." Theoretical and Applied Climatology 84(1-3): 179-190.

[22] Peng, C. and P. Blundell Jones (2004). "Reconstructing urban contexts online for interactive urban designs." Design Studies 25(2): 175-192.

[23] Radhi, H. (2009). "Evaluating the potential impact of global warming on the UAE residential buildings - A contribution to reduce the CO2 emissions." Building and Environment 44(12): 2451-2462.

[24] USDOE. (2009). "Egypt weather data [Available Online], http://apps1.eere.energy.gov/buildings/energyplus/cfm/weather_data3.cfm." Retrieved 18/7/2009.

[25] USDOE. (2009). "EnergyPlus Energy Simulation Software, [Available Online], www.apps1.eere.energy.gov/buildings/energyplus/cfm/reg_form.cfm." Retrieved 15/1/2009.

Influence of Indirect Land Use Change on the GHG Balance of Biofuels – A Review of Methods and Impacts

Elisa Dunkelberg[1,*], Matthias Finkbeiner[2], Bernd Hirschl[1]

[1] *Institute for Ecological Economy Research, Berlin, Germany*
[2] *Technische Universitaet Berlin, Berlin, Germany*
** Corresponding author. Tel: +49 30 88459436, Fax: +49 308825439, E-mail: elisa.dunkelberg@ioew.de*

Abstract: The greenhouse gas (GHG) balance or carbon footprint of biofuels, generally calculated by life cycle assessments (LCA), is heavily influenced by the modeling of land use changes (LUC). This includes direct land use changes (DLUC) and indirect land use changes (ILUC). Various methodical approaches for the integration of ILUC in LCA have recently evolved. In this study several approaches for calculating ILUC and the effects on GHG balance are compared. These are economic modeling, deterministic modeling and regional modeling. Papers published on this topic since 2007, when the ILUC debate began, are reviewed considering the following main criteria: methodological approach, uncertainties of assumptions, and the level of the GHG emissions due to ILUC. The results show that the existing approaches lead to strongly divergent results. This is due to uncertainties about relevant assumptions, e.g. the methods of linking commodity prices to ILUC, assumptions about yields, soil carbon contents, and the effect of by-products. These uncertainties and other methodological inconsistencies, e.g. the allocation issue with respect to displacing vs. displaced crops, imply that further research is needed and that current methods are not robust enough for adoption in regulation.

Keywords: *Biofuels, Greenhouse-gas balance, Life cycle assessment, Indirect land use change, EU policy*

1. Introduction

The worldwide expansion of biofuel production is being driven by several forces; these include, first and foremost, rising oil prices, promotion of a secure energy supply, and rural development [1]. In the European Union (EU), the reduction of GHG emissions in the mobility sector has been another important factor, leading to national policy objectives designed to increase the biofuels share ([1, 2]). To ensure that biofuels achieve a significant reduction in GHG emissions, the Renewable Energy Directive (RED) indicates that a life cycle GHG emissions reduction of roughly 35% as compared to fossil fuels is necessary; otherwise, biofuels will not be counted towards attainment of the quota. By 2017, this increases to a 50% reduction vs. fossil fuels [3]. Other regulations, e.g. the US Energy Independence and Security Act (EISA) of 2007, include similar reduction targets [4]. These objectives are met by most of the biofuels if LUC are not considered [5]. In 2007, however, in the context of increasing food prices, LUC linked to biofuel expansion became a topic of public discussion; the same year, EISA directed the US government to develop a LCA for biofuels that includes DLUC and ILUC [6]. The 2009 RED similarly directs the European Commission (EC) to investigate "the inclusion of a factor for indirect land-use changes in the calculation of greenhouse gas emissions" [3]. As a consequence of such political pressures, but also a growing interest in research into LUC issues, a number of ILUC studies have recently been published (e.g. [5, 7-16]).

Biofuel production-related DLUC occur when a previous land use especially a natural habitat is converted to bioenergy crop production. The conversion of grassland, tropical rain forest or peat bogs into agricultural land will generally lead to a release of additional carbon dioxide over several years or even decades [17]; these GHG emissions are often referred to as the "carbon debt" of biofuels. Depending on the previous land use, the time needed to repay this carbon debt through annual savings in GHG emissions vs. fossil fuels can range between zero and 423 yr [17]. Feedstock cultivation on degraded lands with low carbon contents, on the

other hand, can lead to a sequestration of carbon dioxide (e.g. [5, 18]). According to the IPCC [19], emissions due to LUC are generally allocated across the yields of 20 yr when calculating the emission factor for DLUC; however, since carbon contents depend not only on land use but also on tillage methods (e.g. [7,20,21]), soil texture, and hydrological and climatic conditions [22], the use of default emission factors, such as those provided by the EC, is quite imprecise − there is a lack, in particular, of reliable data on GHG balances for biofuels cultivated on degraded land [23].

ILUC occur when biofuel feedstock cultivation replaces other crops and, consequently, natural habitats are then converted to arable land to meet the demand for the displaced commodities [8]. Inclusion of ILUC in GHG balances is more difficult than with DLUC because of the high system complexity: ILUC are tied to global market dynamics. Some scientists assume that if a crop is displaced, the prices for this crop will increase and farmers will react by creating new arable land [24]; however, because of increasing global market prices, ILUC can occur anywhere in the world – not only in the country where biofuels are being produced ([8, 9]); in such situations, measuring these effects at the regional level is not sufficient. Likewise, national regulations, e.g. customs, subsidies or trade restrictions, also influence prices and trade flows and thus ILUC [25]; hence, a consideration of global prices alone is also not sufficient. Moreover, biofuel production is a multi-product system: by-products, such as dried distillers' grains with solubles, also accrue; these can substitute for fodder crops and thus reduce total land demand ([26-28]). Furthermore, forces other than agricultural expansion, such as timber harvest and infrastructure development (e.g. road building), also drive LUC [7]. ILUC-specific methodologies are thus needed. Currently three basic approaches to quantify ILUC exist: economic models, i.e. partial or general equilibrium models, that provide for calculation of ILUC (e.g. [10,11]); deterministic or descriptive-causal models, which attempt to estimate ILUC based on a set of simplified assumptions (e.g. [5]); regional models that try to take into account regional influences on ILUC [25].

Purpose of this work is to present a systematic overview of the body of literature in the area of ILUC research and to assess its influence on the GHG balance of biofuels. Therefore in the present article, these different approaches for calculating ILUC and the effects on GHG balance are described and compared.

2. Methodology

For this purpose the relevant literature (since 2007) relating to this topic was identified and evaluated; some grey literature was also considered when appropriate. The following three main criteria for evaluation were considered: methodological approach, uncertainties of assumptions, and the level of the GHG emissions due to ILUC. For the purpose of comparing the various approaches, some conversions were necessary; in these cases, conversion values (e.g. carbon contents) were taken from the original literature. The study further addresses the question and extent of ILUC integration into EU policy and poses questions for further research and development. A clear response to the question of the extent to which ILUC influence the GHG balance is not offered, but the study does address their relevance; the advantages and disadvantages of the various methodological approaches are also indicated.

3. Results

3.1. Economic modeling of ILUC

Both partial-equilibrium models (e.g. FAPRI, AGLINK, IMPACT, CAPRI) and general-equilibrium models (e.g. GTAP, LEITAP) are used to project ILUC [12]. Partial-equilibrium

models are based on linear relationships between prices, demand, and production in the agricultural market, whereas general-equilibrium models model the whole world economy (e.g. interactions of the agricultural sector with chemical industries) [12]. In general, economic modeling of ILUC follows three main steps. First, the economic model is given a so-called biofuel shock or policy shock, i.e. biofuel production is increased; the model projects the effects of nationally increased biofuel production on global commodity markets and on additional land requirements. In this step, the model also provides indications as to the countries in which additional land will need to be converted. In the second step, LUC are then mapped to specific land-cover types (e.g. grassland, forest), based on historical patterns of LUC. Finally, biophysical models are used to project the GHG emissions from land use conversion. The size of the shock allows GHG emissions to be attributed to a specific quantity of biofuels. Nearly all studies calculating ILUC by means of economic modeling found that ILUC significantly influence the GHG balance of, at a minimum, first-generation biofuels ([10-13]). Current investigations indicate that second-generation biofuels could lead to a negative ILUC effect [29]. Since the various models used different shocks respectively, it has not been possible to compare results for recent years; therefore, at the direction of the EC, modelers calculated the crop area changes for specific biofuels scenarios [12]. The results show that the range of crop area changes is quite high: for the EU biodiesel scenario, for example, the values range between 242 and 1928 kha $Mtoe^{-1}$ (see Table 1) [12] .

Table 1. Minimum and maximum values of LUC calculated with different economic models (source: authors, based on [12])

Scenario	Minimum		Maximum	
	(kha $Mtoe^{-1}$)	Model	(kha $Mtoe^{-1}$)	Model
EU biodiesel scenario	242	AGLINK	1928	LEITAP
EU ethanol scenario	223	IMPACT	743	LEITAP
US ethanol scenario	107	IMPACT	863	LEITAP
Palm oil scenario	103	GTAP	425	LEITAP

These deviations are caused by assumptions about input data made at each stage of the modeling. Many assumptions are uncertain and therefore differ among the models [9]. First, the extent to which farmers will react to rising prices by increasing yields through irrigation or fertilization is uncertain [24]; whether extra emissions due to the use of additional fertilizers are accounted for is also uncertain [12]; moreover, feedstock yields vary among the models, particularly in expansion areas [12]; the extent to which reductions in food consumption will take place as a consequence of increasing food or fodder prices is also unknown. Likewise, the share of additional crops saved by by-products differs among the models; one reason for this are differences in the methods of calculation: in GTAP and LEITAP, by-products are accounted for by substitution on the basis of relative prices; other models, such as CAPRI, account for them through physical replacement ratios [12]. Additionally, controversy exists about the extent to which production is shifted from countries with high yields to relatively less developed countries with lower yields [12] and about the share of forest and grassland conversions [9]; and, finally, as mentioned previously, emission factors related to LUC are also uncertain. To characterize ranges for the GHG emissions of different scenarios, we multiplied the ILUC values in kha $Mtoe^{-1}$ taken from Edwards. et al. [12] (see table 1) and carbon dioxide emission factors using three different values for soil C emissions: 40 tC ha^{-1} as an average value and 10 and 95 tC ha^{-1} as lower and upper values (cf. [11, 12]). Fig. 1 shows that the range for the EU biodiesel scenario, in particular, is quite large, whereas those of the EU and US ethanol scenarios as well as that for palm oil are narrower. Results for the EU ethanol scenario range between 14 and 309 g CO_2 MJ^{-1} due to

LUC. Since the default carbon footprint of fossil fuels is set at 83.8 g CO_{2e} MJ^{-1} in RED, it can be assumed that this scenario and likewise the EU biodiesel scenario will not lead to a 35% GHG reduction in comparison to fossil fuels.

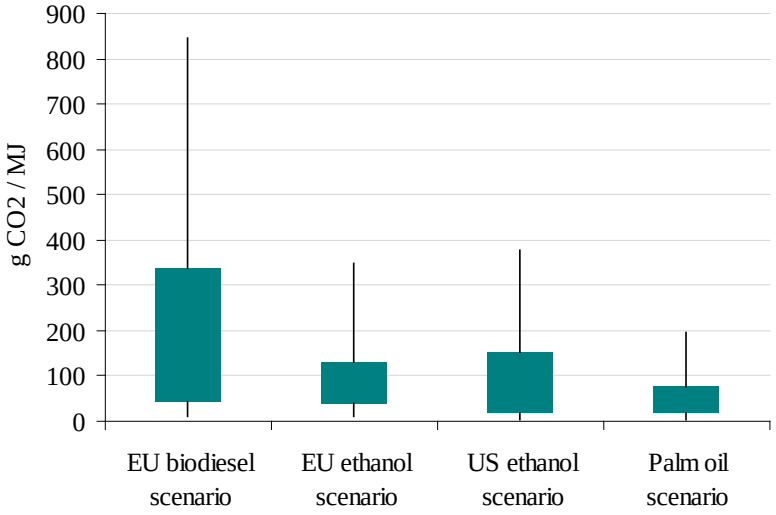

Fig. 1. Range of CO_2 emissions due to LUC calculated on basis of results of various economic models Maximum and minimum LUC values resulting from economic models in ha $Mtoe^{-1}$ [see Table 1] were multiplied with typical C emission factors 40 tC ha^{-1}[error bars: 10 tC ha^{-1}, 95 tC ha^{-1}] – authors' calculations, based on Edwards et al. [12].

3.2. Deterministic modeling of ILUC

The second main approach is called deterministic or descriptive-causal modeling. These models are simplified calculations based on explicit assumptions and are usually realized with a spreadsheet calculator. In general, these models use cause-and-effect logic to describe system behavior. One example of this approach is the ILUC factor developed by the Institute for Applied Energy, in Germany [5]. A crucial assumption in this model is that ILUC can be estimated by looking at the exported products relevant for the bioenergy sector, e.g. soy, corn (maize) and palm oil. Calculations are based on 2005 product exports, but for the purpose of simplification, only key regions, such as Argentina, Brazil, the EU, Indonesia, Malaysia, and the USA, are considered; these countries are responsible for more than 80% by mass of the global trade in the respective commodities [5]. Using the mass of commodities traded divided by the respective country-specific yields, the area needed to produce these products was calculated. From the sum of all land use for agricultural exports, each country's proportionate share could be derived – the "world mix." Next, additionally needed areas were combined with country-specific assumptions about the specific DLUC associated with the production of the export commodities. Following the application of conversion factors from IPCC, the interim results were then weighted according to each country's share of the "world mix," resulting in an ILUC factor of 13.5 t CO_2 $ha^{-1}a^{-1}$ [5]. This means that 1 ha of bioenergy feedstock production displaces 1 ha of previous production. The authors suggest three different levels of ILUC (25%, 50%, and 75% of the theoretical ILUC factor), as they anticipate yield increases and assume that a share of the expansion occurs on degraded lands [5]. Fig. 2 breaks down the level of CO_2 emissions by type of biofuel, country of production, and prior land use. The high level of GHG emissions when ILUC are included means that most biofuels will not achieve the GHG reductions called for in the RED [5]. Compared to the results of economic modeling (see Fig. 1), the results for CO_2 emissions due to DLUC, plus

the differing ILUC factors calculated with this approach, are low for biodiesel but in the same range for ethanol if calculated with 40 tC ha^{-1}.

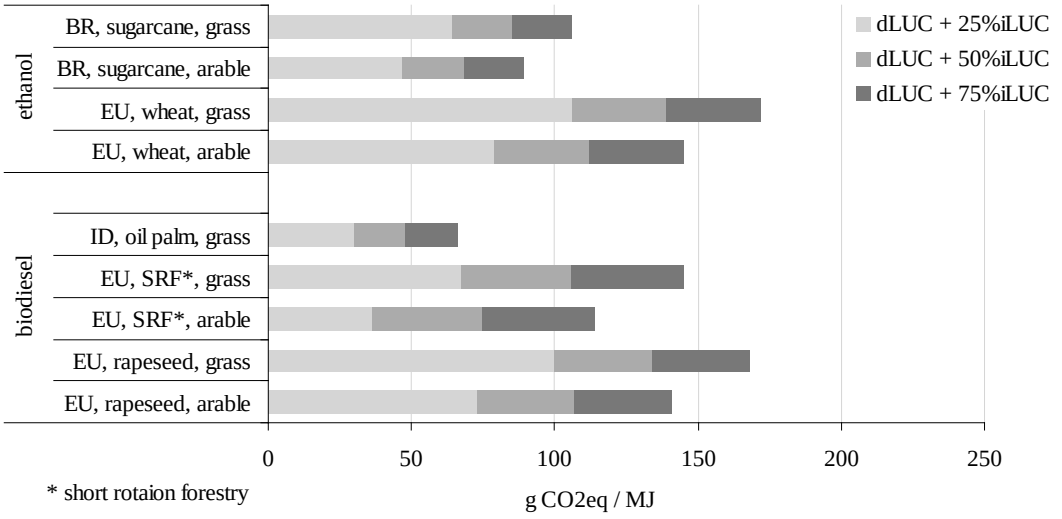

Fig. 2. CO_2 emissions calculated on basis of a deterministic model (figures from Fritsche et al. [5]).

Another deterministic model, developed by Plevin et al. [9], attempts to characterize a robust range of ILUC. For this purpose, the authors include four main parameters in a reduced-form model: net displacement factor (NDF) (ha converted land / ha biofuels), average emission factor (Mg CO_{2e} ha^{-1}), production period (yr) and fuel yield (MJ $ha^{-1}yr^{-1}$). Setting an upper and lower value for these parameters, based on the literature, the ILUC emission factor for US corn ethanol ranges between 10 and 340 g CO_{2e} MJ^{-1}, which is similar to the range as calculated according to Edwards et al. [12] (see Fig. 1). The results suggest that the NDF accounts for the major part of the variance in the ILUC factor; it includes the effects mentioned above, e.g. price-induced yield increases, relative productivity of land converted to cropping, price-induced reductions in food consumption, and by-product substitutions [9].

3.3. Regional modeling of ILUC

In Germany, another method has been discussed: regional modeling. This approach was developed, first, in response to criticism that other models do not properly consider the effects of state regulation on the global agricultural market; these can take the form of subsidies, customs duties, and trade restrictions (bans on import/export, etc.). Second, the deterministic model of Fritsche et al. [5] is limited to LUC due to product exports ([5,25]) and thus does not consider ILUC effects due to domestic trade, which, according to Lahl [25], must be included as internal trade is quantitatively more important than global trade. Lahl [25] suggests the following method for regional modeling: first, all LUC in a country and for a specific period must be ascertained. Country-specific CO_2 emissions (E^RLUC) are then calculated for the respective carbon stocks in vegetation and soil, before and after conversion. In order to calculate the share of the various biofuels in total emissions, the change in biofuel production is divided by the change in agricultural production in total and multiplied by E^RLUC. Next, the portion of total emissions due to DLUC is subtracted, and finally, the remaining emissions are allocated to the "originator," which can be separate farms or regions. In some cases a correction factor for by-products or transnational effects must be included. To determine whether transnational effects are relevant for a specific country, one should look for a drop in agricultural import levels for recent years and an absolute value of the reduction in agricultural imports higher than the absolute value of the increase of agricultural exports [25].

An application of this model is not yet known. A method of economic modeling that combines regional aspects with economic modeling was applied to the biofuels sector in Brazil [10]. Methodologically, a land-use change model was linked with a partial equilibrium model of the agricultural sector economy and a dynamic global vegetation model. Using these models, it was determined that in Brazil ILUC influence the GHG balance of biofuels much more than DLUC [10].

4. Discussion and Conclusions

LUC are of central importance for the GHG balance of biofuels. For the purpose of GHG mitigation, the EC is directed to consider inclusion of an ILUC factor in the calculation of GHG emissions of biofuels. Currently, three main approaches, economic modeling, deterministic modeling and regional modeling, exist for calculating ILUC. The results of these methods vary greatly – by a factor of more then ten, but nearly all methods indicate that ILUC increase GHG emissions significantly. With respect to the relevance of ILUC, they are thus unambiguous and call into question the viability of biofuels as a climate protection instrument. Many of the results suggest that most of the currently available biofuels will not reach the GHG reduction targets of the RED after inclusion of ILUC. The effect of biofuel specific ILUC factors may be critical with respect to their attainment of the mandated 35% reduction in GHG emissions vs. fossil fuels; this in turn is decisive for whether a specific biofuel is to be included in the intended biofuels share of total fuel consumption; thus care needs to be taken with the development of such a factor.

The deterministic model from Fritsche et al. [5] indicates that oil palm biodiesel and sugarcane ethanol are accompanied by lower ILUC effects than biodiesel produced from rapeseed and ethanol from wheat and corn. Results from economic models exist for only a few biofuel scenarios; thus it is not yet known whether deterministic and economic models will lead to corresponding results for specific biofuels. Characteristic of all ILUC modeling is that input data and assumptions are often uncertain. Some uncertainties are present in all of the methodologies, in particular, assumptions about CO_2 emission factors for various LUC; feedstock yields, particularly in expansion areas; extra emissions due to fertilizing to increase yields; and the share of extra crops replaced by by-products. In some models, by-products are accounted for by substitution on the basis of relative prices; other models account for them through physical replacement ratios [12]. It is possible to set default values, e.g. CO_2 emission factors, or calculation types, e.g. for the consideration of by-products as in RED [3]; this would lessen the deviation between the outcomes of the different models but also limit possible results. Additional uncertainties exist specific to the type of model. For economic and deterministic models, this includes assumptions about the extent to which production is shifted from countries with high yields to relatively less developed countries with lower yields, the share of forest, grassland and wetland that will be converted, and the levels of reductions in food consumption that occur as a consequence of increasing food or fodder prices. Furthermore, economic models do not take into account market distortions due to national policy [25]. Missing or dubious land-use rights in specific countries may also affect ILUC. This is not taken into account in economic and deterministic modeling. For the deterministic model from Fritsche et al. [5], the main question is whether it is sufficient to calculate ILUC on the basis of exported products or whether internal trade should also be included. Regional modeling can probably provide more precise information about real ILUC effects in specific countries; it can also be a suitable method if countries or farms that allow ILUC are to be sanctioned. However, availability of regional data is a precondition for this method and applications of the regional methods remain largely unknown. Each of the current models thus has its pros and cons.

Before establishing a specific method for calculating ILUC or setting default ILUC factors via regulatory policy, these methods should first be improved and applied to various scenarios and regions. Information and data about ILUC effects in specific regions, especially, are still lacking and need to be further explored. Some theoretical considerations are also necessary before ILUC should be accounted for in policy regulation: From the point of view of LCA, a precondition for the comparison of two products, e.g. biofuels and fossil fuels, are consistent boundaries for both systems; therefore, when calculating GHG balances including ILUC, other indirect effects arising from the production and use of biofuels and fossil fuels, e.g. price-induced increases or decreases in fuel consumption (cf. [30]), should be analyzed and similarly included. Furthermore, in most of the current methods the product previously cultivated does not receive any of the GHG emissions due to DLUC if it is displaced; once again, from the point of view of LCA, this is questionable because all environmental impacts should be allocated on all accruing products in the systems being analyzed.

References

[1] E. van Thuijl and E. Deurwaarder, European biofuel policies in retrospect, Energy Research Centre of the Netherlands, 2006.

[2] CRS, EU biofuels policy and agriculture: an overview - CRS Report for Congress, 2006.

[3] 2009/28/EC, Directive 2009/28/EC of the European Parliament and of the Council of 23 April 2009 on the promotion of the use of energy from renewable sources and amending and subsequently repealing Directives 2001/77/EC and 2003/30/EC, 2009.

[4] USEPA, Renewable Fuel Standard Program (RFS2) Regulatory Impact Analysis. US Environmental Protection Agency, 2010.

[5] U. Fritsche, K. Hennenberg, and K. Huenecke, The “iLUC factor” as a means to hedge risks of GHG emissions from indirect land use change, Darmstadt: Oeko-Institut, 2010.

[6] D. Morris, Ethanol and Land Use Changes. Policy Brief, 2008.

[7] H. Kim, S. Kim, and B. Dale, Biofuels, land use change, and greenhouse gas emissions: some unexplored variables, Environmental Science & Technology 43, 2009, pp. 961-967.

[8] E. Gnansounou, L. Panichelli, A. Dauriat, and J. Villegas, Accounting for indirect land-use changes in GHG balances of biofuels: Review of current approaches, 2008.

[9] R. Plevin, M. O’Hare, A. Jones, M. Torn, and H. Ginss, Greenhouse gas emissions from biofuels indirect land use change are uncertain but may be much greater than previously estimated, Environmental Science and Technology 44, 2010, pp. 8015-8021.

[10] D. Lapola, R. Schaldach, J. Alcamo, A. Bondeau, J. Koch, C. Koelking, and J. Priess, Indirect land-use changes can overcome carbon savings from biofuels in Brazil, Proceedings of the National Academy of Sciences 107, 2010, pp. 3388-3393.

[11] R. Searchinger, R. Heimlich, R. Houghton, F. Dong, A. Elobeid, J. Fabiosa, S. Tokgoz, D. Hayes, and T. Yu, Use of U.S. Croplands for biofuels increased greenhouse gases through land-use change, Science 319, 2008, pp. 1238-1240.

[12] R. Edwards, D. Mulligan, and L. Marelli, Indirect land use change from increased biofuels demand, European Commission, Joint Research Institute, 2010.

[13] J. Melillo, J. Reilly, D. Kicklighter, A. Gurgel, T. Cronin, S. Paltsev, B. Felzer, X. Wang, A. Sokolov, and C. Schlosser, Indirect emissions from biofuels: how important?, Science 326, 2009, pp. 1397-1399.

[14] W. Lywood, Indirect effects of biofuels, Renewable Fuels Agency, 2008.

[15] A. Liska and R. Perrin, Indirect land use emissions in the life cycle of biofuels: regulations vs. science, Biofuels, Bioproducts and Biorefining 3, 2009, pp. 318-328.

[16] J. Kløverpris, K. Baltzer, and P. Nielsen, Life cycle inventory modeling of land use induced by crop consumption. Part 2: Example of wheat consumption in Brazil, China, Denmark and the USA, Int. Journal of Life Cycle Assessment 15, 2010, pp. 90-103.

[17] L. Fargione, J. Hill, S. Polasky, and P. Hawthorne, Land clearing and the biofuel dept, Science 319, 2008, pp. 1235-1238.

[18] B. Wicke, V. Dornburg, M. Junginger, and A. Faaij, Wicke B, Dornburg V, Junginger M, Faaij A. Different palm oil production systems for energy purposes and their greenhouse gas implications, Biomass and Bioenergy 32, 2008, pp. 1322-37.

[19] IPCC, Good Practice Guidance for LULUCF, 2003.

[20] N. La Scala, A. Lopes, K. Spokas, D. Bolonhezi, D. Archer, and D. Reicosky, Short-term temporal changes of soil carbon losses after tillage described by a first-order decay model, Soil and Tillage Research 99, 2008, pp. 108-118.

[21] D. Reicosky, W. Dugasb, and H. Torbert, Tillage-induced soil carbon dioxide loss from different cropping systems, Soil and Tillage Research 41, 1997, pp. 105-118.

[22] F. Scheffer and P. Schachtschabel, eds., Lehrbuch der Bodenkunde, Heidelberg, Germany: Spektrum Akademischer Verlag, 2002.

[23] E. Menichetti and M. Otto, Energy balance and greenhouse gas emissions of biofuels from a life-cycle perspective, Biofuels: Environmental Consequences and Interactions with Changing Land Use, R. Howarth and S. Bringezu, eds., International Biofuels Project Rapid Assessment, 2009, pp. 81-109.

[24] RFA, Indirect effects of biofuels. Study by the Renewable Fuels Agency, 2008.

[25] U. Lahl, iLUC und Biokraftstoffe in der Analyse - Regionale Quantifizierung klimaschädlicher Landnutzungsänderungen und Optionen zu deren Bekämpfung, Oyten.

[26] J. Fabiosa, Land-use credits to corn ethanol: accounting for distillers dried grains with solubles as a feed substitute in swine rations. Working Paper 09-WP 489, Center for Agricultural and Rural Development. IOWA State University, 2009.

[27] W. Lywood, J. Pinkney, and S. Cockerill, Impact of protein concentrate coproducts on net land requirement for European biofuel production, GCB Bioenergy 1, 2009, pp. 346-359.

[28] E. Özdemir, M. Härdtlein, and L. Eltrop, Land substitution effects of biofuel side products and implications on the land area requirement for EU 2020 biofuel targets, Energy Policy 37, 2009, pp. 2986-2996.

[29] P. Havlik, U. Schneider, E. Schmid, H. Böttcher, S. Fritz, R. Skalsky, K. Aoki, S. De Cara, G. Kindermann, F. Kraxner, S. Leduc, I. Mc Callum, A. Mosnier, T. Sauer, and M. Obersteiner, Global land-use implications of first and second generation biofuel targets, Energy Policy. Article in press, 2010.

[30] D. Rajagopal, G. Hochman, and D. Zilberman, Indirect fuel use change (IFUC) and the lifecycle environmental impact of biofuel policies, Energy Policy 39, 2011, pp. 228-233.

Climate change mitigation through increased biomass production and substitution: A case study in north-central Sweden

Bishnu Chandra Poudel[1,*], Roger Sathre[1], Leif Gustavsson[1,2], Johan Bergh[1,3]

[1] *Ecotechnology, Mid Sweden University, Östersund, Sweden*
[2] *Linnaeus University, Växjö, Sweden*
[3] *Southern Swedish Forest Research Centre, Swedish University of Agricultural Sciences, Alnarp, Sweden*
** Corresponding author. Tel: +4663165535, E-mail: bishnu.poudel@miun.se*

Abstract: In this study, we perform an integrated analysis to calculate the potential increases in forest biomass production and substitution as an effect of climate change and intensive management. We use the BIOMASS model to simulate change in Net Primary Production due to climate change. Then we estimate the development of forest biomass growth and harvest by using the HUGIN model, the change in soil carbon stock by the use of the Q-model, and the biomass substitution benefits by the use of an energy and material substitution model. Our results show that an average regional temperature rise of 4 °C could increase annual whole tree forest biomass production by 32% and harvest by 29% over the next 100 years. Intensive forest management including climate effect could increase whole tree biomass production by 58% and harvest by 47%. A total net reduction in carbon emissions of up to 89 Tg C and 182 Tg C over 100 years is possible due to climate change effect only and due to climate change plus intensive forestry, respectively. The carbon stock in standing biomass, forest soils and wood products all increase, but the carbon stock changes are less significant than the substitution benefits.

Keywords: *Forest biomass, Carbon, Bioenergy, Construction material, Intensive forestry*

1. Introduction

Increasing atmospheric concentration of greenhouse gases (GHGs) increase earth's surface temperature [1]. The Intergovernmental Panel on Climate Change (IPCC) [2] affirms that the temperature increase will be greater in the higher latitudes. The regional climate model by the Swedish Meteorological and Hydrological Institute (SMHI) [3] based on IPCC B2 scenario projects a 4 °C average temperature increase in north-central Sweden in the next 100 years.

The increasing temperature has significant impact on physical systems. It provides a longer growing season for the trees and favorable conditions for photosynthesis that stimulates Net Primary Production (NPP) [4]. Thus, an increased temperature is expected to produce more biomass in the boreal forests [5]. Although the boreal forest is considered as less productive due to low soil temperature and low nitrogen availability [6], production can further be increased by adding nutrients, by species change, and by changes in management practices [7, 8]. As a result, there will likely be larger harvest levels available in future.

The increased forest biomass can be used as a substitute for fossil fuels and carbon intensive materials to reduce carbon emissions through several mechanisms [9]. Using biomass to substitute for fossil fuels directly avoids fossil carbon emissions, except to the extent that fossil fuels are used to operate the biomass system [10]. Using biomass to substitute for carbon-intensive materials may reduce carbon emissions by lowering fossil energy use during the manufacture of products, by avoiding industrial processes emissions, by increasing carbon stocks in wood materials, by using biomass residues to replace fossil fuels, and possibly by carbon sequestration or emissions from wood products deposited in landfills [11, 12].

This paper describes an integrated assessment of the potential forest biomass increase as an effect of climate change and intensive forestry practices in north-central Sweden, and

potential climate change mitigation with increased biomass use. Using five scenarios for forest production and two scenarios for biomass utilization, we estimate the increased biomass production, its harvest level, and carbon benefits from the substitution of non-wood materials and fossil fuels. We also estimate the carbon stock changes in standing biomass, soil, and wood products, and finally quantify the overall carbon balance for each scenario.

2. Methodology

2.1. Study area

This study considers Jämtland and Västernorrland, two counties in north-central Sweden. The area lies from 61° 33' to 65° 07' N latitude and from 12° 09' to 19° 18' E longitude. The forest land area is about 3.5 and 1.9 million ha, respectively. Of this area, productive forests[1] excluding protected areas cover about 2.6 million ha and 1.7 million ha, respectively [13].

2.2. Climate change

IPCC Special Report on Emission Scenarios (SRES) [14] describes potential GHG emissions pathways during the 21st century based on the main driving forces of GHG emissions, considering their underlying uncertainties. Our regional climate scenarios are based on the IPCC B2 global scenario, corresponding to moderate emissions of GHGs leading to an atmospheric CO_2 concentration of 572 ppm by the year 2085, with model RCA3 (The Rossby Centre's regional Atmospheric model) that uses a grid of approximately 50 km x 50 km. The RCA3 model uses global driving variables from the general circulation model ECHAM4/OPYC3 [15] covering the period of 1961-2100. Climate projections for north-central Sweden are for an increase in average annual temperature of 4 °C by 2100 [16].

2.3. Scenarios

We compare forest biomass production in a *Reference* scenario that assumes the current forest management practices without any climate change effect, and four scenarios that include climate change effect: *Current*, *Environment*, *Production*, and *Maximum*, (Table 1).

Table 1. Overview of scenarios analyzed in this study.

Scenario	Climate	Forest management goals	Biomass use
Reference	No change	Reference (current management)	Stem wood or whole tree
Current	Change	Current management	Stem wood or whole tree
Environment	Change	Fulfill environmental goals	Stem wood or whole tree
Production	Change	Increase biomass production	Stem wood or whole tree
Maximum	Change	Maximize biomass production	Stem wood or whole tree

The Current scenario assumes a continuation of current forest management practices. The Environment scenario assumes the fulfillment of additional environmental goals, e.g. 8% of total forest land is set aside for reserves, and 14% of total forest land is given special environmental care. The Production scenario uses additional silvicultural practices, e.g. improved genetic material plantation, soil scarification, selection of tree species, increased traditional fertilization and a balanced nutrient supply [8]. The Maximum scenario uses silvicultural practices to maximize the production by replacing of Scots pine with lodge-pole

[1] Non-productive forests are defined as forests with production capacity less than 1 m^3 per ha and year.

pine (*Pinus contorta*) and by adding balanced nutrient supply in young stands of lodge-pole pine and Norway spruce. The effect of a lower and higher precipitation is considered in the scenarios and had no significant effect on production in northern Sweden [4]. The scenarios are described in more detail in [17].

2.4. Forest production modeling

The process-based growth model BIOMASS describes the processes of radiation absorption, canopy photosynthesis, phenology, allocation of photosynthates among plant organs, litter-fall, and stand water balance in a tree [18]. BIOMASS uses Swedish National Forest Inventory (NFI) database and current temperature for *Reference* scenario and increased temperature based on RCA3 climate model (see Section 2.2) for the estimation of NPP. Values of daily precipitation are used in NPP simulations. The parameterization is valid for mesic soils, and the effects of water deficits would be more pronounced on drier sites [7]. Water deficits seem to be at a low level in simulations, since extremely dry summers didn't occur in the data set, which could lead to substantial losses in production. Output data on NPP from the BIOMASS are used to determine the growth functions in the HUGIN model [5, 17] an empirical model for long-term forecasts of timber yield and harvest level [19]. It uses sample plots from NFI, defining initial conditions for the model in order to describe the forest conditions during the development of young stands, their establishment, and the sivicultural treatments. The growth simulators in HUGIN are valid for all forest land in Sweden, for all types of stands, with a wide range of management alternatives [19].

2.5. Soil carbon modeling

The Q-model describes changes in soil carbon stock based on litter inputs, soil temperature, and the decomposition of litter fractions [20]. It uses old carbon in the soil, litter inputs from standing trees, thinnings and harvests, and soil carbon from fine roots. The decomposition in response to temperature is calculated as in Ågren et al. [21] and Bosatta and Ågren [20]. For more details see [5].

2.6. Biomass use modeling

The harvested biomass in thinnings and final fellings is assumed to substitute non-wood materials and fossil fuels. In the "stem wood" option we assume that 95% of coniferous stem wood (>20 cm diameter) is harvested and used as construction material to replace reinforced concrete [5, 11, 17]. The small stems and processing residues of coniferous trees, and all deciduous stem wood, is used as biofuel. In the "whole tree" option, in addition to stem wood use, 75% of branches and tops, 25% of needles, and 50% of stumps are harvested and used as biofuel [5, 11, 17]. Biofuel is assumed to replace coal in stationary plants.

2.7. Forest operations and fertilization

We account for emissions from fossil fuels used for forest management activities including stand establishment, thinnings, final harvest of round wood, and forwarding and transport of round wood to mills [22]. GHG emissions associated with production and use of fertilizers include CO_2, N_2O and CH_4 and are converted to CO_2 equivalent using global warming potentials (GWP) over a 100-year time horizon [1]. Primary energy use and GHG emissions for the production of Skog-CAN fertilizer (27-0-0) and Opti-Crop fertilizer (24-4-5) are based on Davis and Haglund [23]. The amount of fossil fuel used for fertilizer application by helicopter is based on Mead and Pimentel [24].

3. Results and discussions

3.1. Forest biomass production and harvest

Figure 1 shows the annual forest biomass production and harvest in all scenarios at the end of the study period. The annual whole tree biomass production in the *Reference* scenario is 12.8 Tg year^{-1} at the end of the study period compared to 11.0 Tg year^{-1} in the beginning of the study, a 17% increase during the 100-year period. The corresponding increases for the *Current, Environment, Production and Maximum* scenarios are 49%, 40%, 53%, and 75%, respectively. Thus biomass production increases in the *Current, Environment, Production and Maximum* scenarios are respectively 32%, 23%, 36% and 58% greater compared to the *Reference* scenario increase. The whole tree harvest in the *Current* scenario increases by 31% more and in the *Maximum* scenario by 50% more than the *Reference* scenario. The increase in stem wood biomass production for the *Maximum* scenario is 57% greater and the harvest is 54% greater compared to the *Reference* scenario.

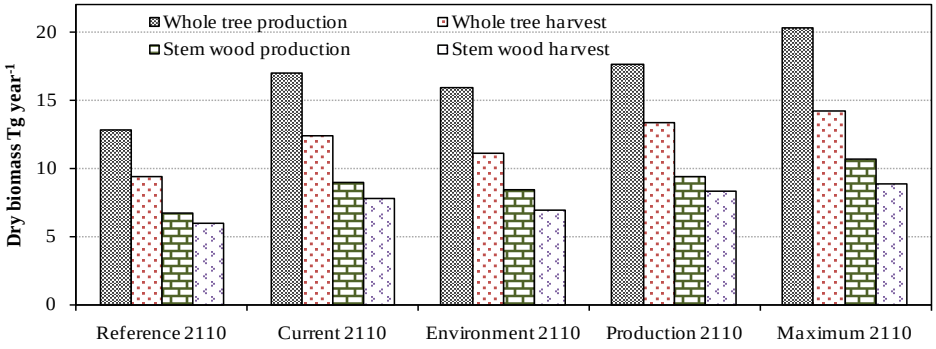

Fig. 1. Annual forest biomass production and harvest (Tg year^{-1}) in all scenarios at the end of the study period in Jämtland and Västernorrland.

Figure 2 shows the cumulative biomass harvest for all products in different scenarios during the 100 year. Stem wood is the largest fraction, while stumps are the second largest. The stump values might be slightly overestimated because of the Marklund's revised function [25] that estimates stump biomass based on spruce stumps which likely overestimates the deciduous tree stumps [5].

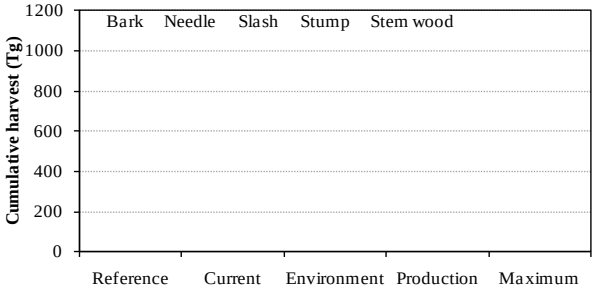

Fig. 2. Cumulative biomass harvest (Tg dry matter) for all products in the different scenarios during 100-years in Jämtland and Västersorrland.

The increased production in the *Current* scenario is caused by climate change, while in the other scenarios are the results of climate change plus intensive forestry practices such as species change, fertilization, and intensive silvicultural action [5].

3.2. Carbon stock in standing biomass, forest soils, and wood products

Annual carbon stocks in living tree biomass, soil and harvested wood products with whole tree harvest increase in all scenarios (Fig. 3). *Maximum* scenario has the largest carbon stock in forest biomass, followed in descending order by *Environment*, *Production*, *Current* and *Reference* scenarios. *Maximum* scenario has the largest soil carbon stock, followed by the *Reference* and *Production* scenarios. Caron stock increases slowly in the *Environment* and *Current* scenario after 30 years compared to the other scenarios (Fig. 3). Wood product carbon stock is also largest in *Maximum* scenario, followed by the *Production* and *Current* scenarios, while *Environment* and *Reference* have smaller. The larger carbon stock is due to larger volume of stem wood harvested and used as building materials, however, after the life span of buildings, the carbon stock may stabilize due to the demolition of old buildings [17].

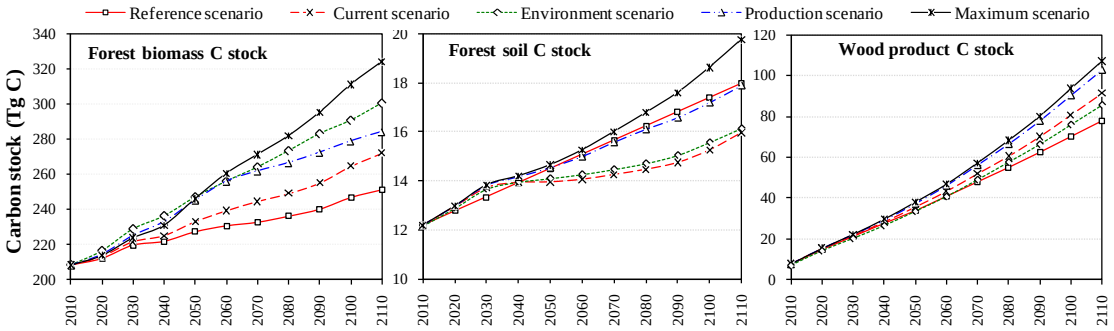

Fig. 3. Annual carbon stocks (Tg C) in living forest biomass, forest soil, and wood products in the different scenarios during 100-years in Jämtland and Västernorrland. Note differences in scale.

Table 2. Average annual avoided carbon emissions due to forest biomass use (Tg C y^{-1}) during each 10-year period for Jämtland and Västernorrland.

	2010-2019	2020-2029	2030-2039	2040-2049	2050-2059	2060-2069	2070-2079	2080-2089	2090-2099	2100-2109
Reference Scenario										
Stem wood	3.8	3.7	3.6	3.7	3.9	3.9	3.9	4.0	4.0	4.2
Whole tree	4.9	4.7	4.8	4.8	5.1	5.1	5.0	5.1	5.1	5.4
Current Scenario										
Stem wood	3.9	3.8	3.8	3.9	4.3	4.4	4.7	4.7	5.1	5.6
Whole tree	5.0	4.9	5.0	5.1	5.6	5.7	6.1	6.1	6.5	7.1
Environment Scenario										
Stem wood	3.6	3.6	3.6	3.7	4.0	4.1	4.3	4.5	4.8	5.0
Whole tree	4.6	4.6	4.7	4.9	5.2	5.3	5.5	5.7	6.1	6.4
Production Scenario										
Stem wood	3.9	3.8	4.0	4.2	4.6	5.0	5.3	5.4	5.8	6.2
Whole tree	4.9	5.0	5.2	5.5	6.0	6.4	6.7	6.8	7.3	7.8
Maximum Scenario										
Stem wood	3.9	3.9	4.1	4.3	4.7	5.0	5.5	5.7	6.0	6.6
Whole tree	5.0	5.0	5.4	5.6	6.0	6.4	7.0	7.2	7.6	8.4

3.3. Biomass substitution

Biomass substitution is largest in Maximum scenario (Table 2). The cumulative avoided carbon emission due to use of stem wood and whole tree biomass for Maximum scenario is 497 and 635 Tg C, respectively. As Maximum and Production scenarios have larger harvests,

they will give larger substitution benefits. When compared to the Reference scenario, Maximum and Production scenarios give 136 Tg C and 116 Tg C greater benefits, while Environment and Current scenario have comparatively smaller substitution benefits.

3.4. Carbon balance

Cumulative avoided carbon emission over 100 years for all scenarios with the use of whole tree biomass is shown in Figure 4. Biomass substitution is the largest contributor to the carbon balance. The avoided carbon emission due to biomass substitution with recovered harvest slash and stumps is greater than the reduced increase in soil carbon stock in the forest due to harvest of whole tree biomass. The total avoided emissions in the Maximum and Production scenarios are 182 Tg C and 117 Tg C greater than in the Reference scenario over the 100-year period for whole tree biomass use. The corresponding numbers for the Environment and Current scenarios are 31 and 48 Tg C, respectively.

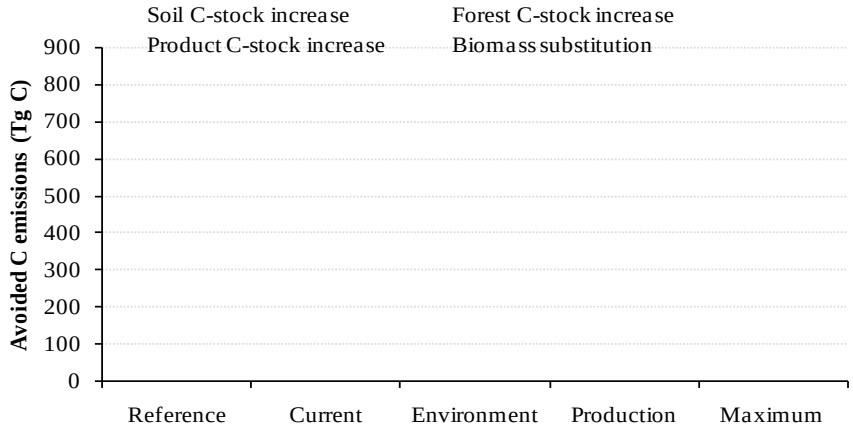

Fig. 4.Cumulative avoided carbon emissions (Tg C) over 100- years for all scenarios with whole tree biomass use for Jämtland and Västernorrland.

4. Conclusions

Climate change may substantially increase the production of biomass in boreal forests. The production can be further increased by intensive forestry practices. The increased forest biomass, if used to substitute for fossil fuels and carbon intensive materials, can avoid carbon emissions, thus contributing to climate change mitigation. This is a negative feedback on climate change. The substitution potential depends on the amount and type of forest biomass harvest. Thus, larger biomass harvests create greater substitution potential.

In this study, significant uncertainties can be observed. Net increase of greenhouse gases, driving the temperature change, depends on several factors as the development of the global population, economic growth, and on mitigation actions to be taken. The results may vary somewhat with differences in the temperature and other corresponding variables. Regional temperature increases may differ from our assumptions. Fire risk, pathogens and insect damage which may cause tree mortalities are not accounted in our study. The HUGIN model overestimates biomass in deciduous living mature trees and stumps. HUGIN does not have a function to calculate self thinning in living deciduous trees, which may lead to an overestimation of biomass in *Environment* scenario. Nevertheless, although these uncertainties may alter the exact values that we have calculated, it appears that our general conclusions are robust.

Acknowledgement
We gratefully acknowledge the support of European Union, County Administrative Board of Jämtland, Sveaskog AB, SCA Forest Products, Norrskog/SÅTAB, Jämtkraft AB. We also thank two anonymous reviewers for their comments.

References

[1] IPCC, Climate Change: The Physical Science Basis. Contribution of Working Group I to the Fourth Assessment Report of the Intergovernmental Panel on Climate Change, ed. S. Solomon, et al. 2007: Cambridge University Press, United Kingdom and New York, USA.

[2] IPCC, The Scientific Basis: Contribution of Working Group I to the Third Assessment Report of the Intergovernmental Panel on Climate Change. 2001, New York , USA: Cambridge University Press.

[3] SMHI. Climatic data, Swedish Meteorological and Hydrological Institute. 2009 [cited 2009 2, August]; Available from: http://www.smhi.se/cmp/jsp/polopoly.jsp?d=8785&l=sv.

[4] Bergh, J., U. Nilsson, B. Kjartansson, and M. Karlsson, Impact of climate change on the productivity of Silver birch, Norway spruce and Scots pine stands in Sweden with economic implications for timber production., Eco.Bulletins, 53(15), 2010: pp. 185-195.

[5] Poudel, B.C., R. Sathre, L. Gustavsson, J. Bergh, A. Lundström, and R. Hyvönen, Effects of climate change on biomass production and substitution in north-central Sweden, Manuscript, 2010.

[6] Tamm, C.O., Nitrogen in terrestrial ecosystems, Ecological Studies, (81) 1991: pp. 1-115.

[7] Bergh, J., U. Nilsson, B. Kjartansson, and M. Karlsson, Impact of climate change on the productivity of Silver birch, Norway spruce and Scots pine stands in Sweden with economic implications for timber production., Ecological Bulletins, 53(15), 2010: pp. 185-195.

[8] Skogsstyrelsen, Skogliga konsekvensanalyser – SKA-VB 08 in Swedish Forest Agency Rapport. 2008, Skogsstyrelsen, Sweden.

[9] Schlamadinger, B., M. Apps, F. Bohlin, L. Gustavsson, G. Jungmeier, G. Marland, K. Pingoud, and I. Savolainen, Towards a standard methodology for greenhouse gas balances of bioenergy systems in comparison with fossil energy systems, Biomass and Bioenergy, 13(6), 1997: pp. 359-375.

[10] Hall, D.O. and J.I. House, Trees and biomass energy: Carbon storage and/or fossil fuel substitution?, Biomass and Bioenergy, 6(1-2), 1994: pp. 11-30.

[11] Gustavsson, L., K. Pingoud, and R. Sathre, Carbon dioxide balance of wood substitution: comparing concrete- and wood-framed buildings, Mitigation and Adaptation Strategies for Global Change, 11(3), 2006: pp. 667-691.

[12] IPCC, Climate Change: Mitigation of Climate Change. Contribution of Working Group III to the Fourth Assessment Report of the Intergovernmental Panel on Climate Change. 2007: Cambridge University Press, United Kingdom and New York, USA.

[13] Skogsstyrelsen. Forestry Statistics, Swedish Forest Agency. 2009 [cited 2009 2, August]; Available from: http://www.svo.se/episerver4/default.aspx?id=38515

[14] IPCC, Special Report on Emissions Scenarios, in Emission Scenarios. Special Report of Working Group III of the Intergovernmental Panel on Climate Change. 2000, Cambridge University Press, UK.

[15] Kjellström, E., L. Bärring, S. Gollvik, U. Hansson, C. Jones, P. Samuelsson, M. Rummukainen, A. Ullerstig, Willén, and K. Wyser, A 140-year simulation of European climate with the new version of the Rossby Centre regional atmospheric climate model (RCA3), in SMHI Reports in Meteorology and Climatology, No. 108. 2006, SMHI: Norrköping, Sverige. pp. 54.

[16] SMHI. Climatic data, Swedish Meteorological and Hydrological Institute. 2009 [cited 2009, August, 2]; Available from: http://www.smhi.se/cmp/jsp/polopoly.jsp?d=8785&l=sv.

[17] Poudel, B.C., R. Sathre, L. Gustavsson, J. Bergh, A. Lundström, and R. Hyvönen, Potential effects of intensive forestry on biomass production and substitution in north-central Sweden, Manuscript, 2010.

[18] McMurtrie, R.E., D.A. Rook, and F.M. Kelliher, Modelling the yield of Pinus radiata on a site limited by water and nitrogen, Forest Ecology and Management, 30(1-4), 1990: pp. 381-413.

[19] Lundström, A. and U. Söderberg. Outline of the Hugin system for longterm forecasts of timber yields and possible cut. In Large-Scale Forestry Scenario Models: experiences and requirements. 1996: EFI proceeding.pp. 63-77

[20] Bosatta, E. and G.I. Ågren, Theoretical analyses of carbon and nutrient dynamics in soil profiles, Soil Biology and Biochemistry, 28(10-11), 1996: pp. 1523-1531.

[21] Ågren, G., R. Hyvönen, and T. Nilsson, Are Swedish forest soils sinks or sources for CO_2—model analyses based on forest inventory data, Biogeochemistry, 82(3), 2007: pp. 217-227.

[22] Berg, S. and E.-L. Lindholm, Energy use and environmental impacts of forest operations in Sweden, Journal of Cleaner Production, 13(1), 2005: pp. 33-42.

[23] Davis, J. and C. Haglund, Life cycle inventory (LCI) of fertiliser production - Fertiliser products used in Sweden and Western Europe, in SIK Report No. 654, SIK. 1999, The Swedish Institute for Food and Biotechnology Göteborg, Sweden.

[24] Mead, D.J. and D. Pimentel, Use of energy analyses in silvicultural decision-making, Biomass and Bioenergy, 30(4), 2006: pp. 357-362.

[25] Pettersson, H. and G. Ståhl, Functions for belowground biomass of Pinus sylvestris, Picea abies, Betula pendula and Betula pubescens in Sweden, Scandinavian Journal of Forest Research, (21) 2006: pp. 84-93.

Influence of biofuels production on the climate change

Carlos A. Cardona[1,*], Monica J. Valencia[1], Julian A. Quintero[1]

[1] *Universidad Nacional de Colombia, Manizales, Colombia*
** Corresponding author. Tel: +0578879300, Ext50199, Fax:+0578879300, Ext 501199, E-mail: ccardonaal@unal.edu.co*

Abstract: This work technically analyzes the biodiesel production from palm, bioethanol production from sugar cane and biotechnological hydrogen productions as well as the GHG emissions associated with the feedstocks production and processing. For this purpose modeling and simulation was used in combination with ASPEN PLUS software and Ecoinvent database for GHG calculations derived from material and energy balances obtained by process simulation. Different critical stages were simulated and analyzed: fertilizers production and use, biofuel production and pesticide production. Results indicated the importance of considering different stages and how these inclusions or exclusions affect GHG balances. For instance, fossil fuel used for industrial stage in bioethanol production increase GHG emissions eighteen-fold. According to this work, bioethanol from sugar cane was the system with largest emissions while biodiesel from palm oil had lowest emissions.

Keywords: *Green House Gas emissions, Climate change, Biodiesel, Bioethanol, Biohydrogen.*

1. Introduction

Current energy situation has reached a critical point according to different points of view: economical, social and environmental aspects [1]. It is necessary to find substitutes for conventional fuels in order to avoid environmental and social adverse effects derived from its non-renewability [2-6]. Usually, the best alternative to conventional fuels should be a substance with high calorific value, availability, easy production, transport and use. However, last is also limited by several social and environmental policies which can frustrate the possibilities to find quick and satisfactory solutions [6-7].

In the last decades it has been found as possible solution the development of biofuels as replacement for fossil fuels [8,9]. The biofuels are produced from different types of biomass and they are subject of exhaust investigations [5,8]. Today, biofuels are considered to be bioethanol, biobutanol, biodiesel, biogas and biohydrogen [9].

Bioethanol and biodiesel have been thoroughly investigated worldwide and a proof of this is the industrial plants available in America, Asia and Europe [7]. Bioethanol is produced by fermentation of sugars, starch crops or lignocellulosic materials [10]. Biodiesel is produced by extraction and methyl or ethyl- transesterification of oils contained in oleagineous plants or waste oils [4,8]. Regardless development level reached for these fuels it is suggested, but not unequivocally proven, the connection to global warming because GHG emissions with their production and use, specifically in agricultural stage [1-3,5,8,11,12]. Scientists hold unprecedented debate relating to assessment of environmental aspects in biofuels production. Many studies have been made, but their results have not helped to provide strong response and quantitative information about relationship between biofuels production and use and climate change using global warming potential [2,5,8].

Hydrogen is an energy source of recent consideration although it is a very important industrial material and its heating value and clean combustion are already well known [13-15]. Extensive investigation for this fuel use is a relatively new issue [16,17]. Different researchers focus new goals in finding biological pathways for competitive hydrogen production [16,18]. Currently, there is no a known biohydrogen production technology competitive compared to

other fuels[19-22]. The present work analyses for biohydrogen case the environmental assessment for dark fermentation technology.

2. Methodology

Biofuel assessment was carried out through quantification of GHG emissions associated with biofuel production. Input information is listed in table 1. Figure 1 shows generic process flowsheet for biofuels analysis. Analysis was separated in two parts:

- Agricultural stage: This phase contains all GHG emissions associated with biomass growth. It was assumed that the respiration process during the growth of biomass absorbs CO_2 emissions from biofuel combustion. Considered N-fertilizer was ammonium nitrate, P-fertilizer was triple superphosphate and K-fertilizer was potassium chloride. The used pesticide was carbofuran. During the mechanical harvest, the fuel used was diesel. 1.325% N-fertilizer was emitted as N_2O to the atmosphere [5].
- Industrial stage: Where biomass is converted to biofuel. GHG emissions were calculated from mass and energy balances of the biofuel production from biomass using Aspen Plus ® and Matlab® Softwares following rigorous models and synthesis procedures as described in [31,32]. Production rates were based mostly on Colombian biofuels production.

The functional unit was megajoule of energy per biofuel produced. Comparisons between studies are made using the work with lowest GHG emissions for each biofuel. Below are described the systems studied.

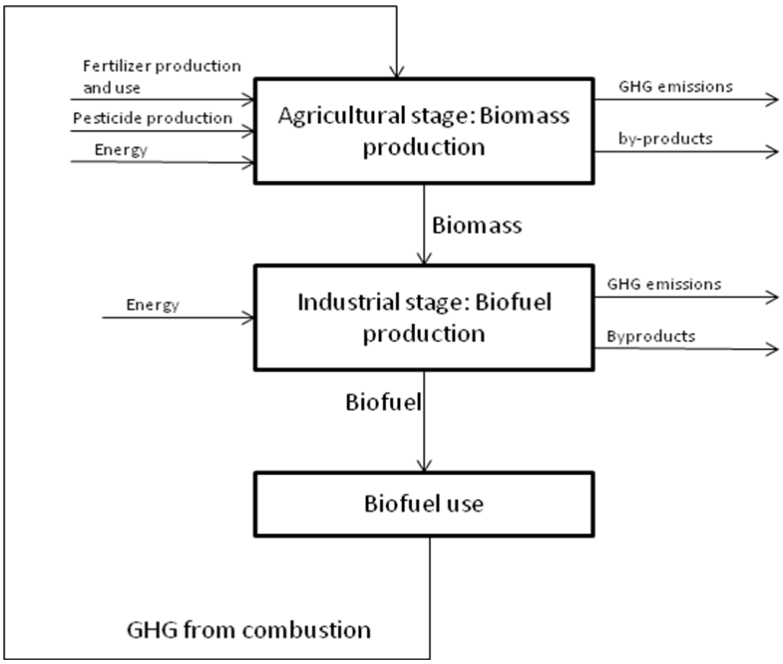

Fig 1. Process included in this work for all biofuels studied

2.1. Bioethanol from sugarcane

Information for agricultural stage was obtained from Ecoinvent database [33], which includes emissions from: fertilizer production, fertilizer use, pesticide uses, harvesting, 20% mechanical harvest. Industrial stage phase was simulated using Aspen Plus® software. Conversion technologies were fermentation, distillation and dehydration with molecular sieves.

Table 2. Values used in this study

Parameter	*Value*	*Reference*
Production rate (L/yr). Bioethanol from sugarcane	*52,800,000*	
Production rate (L/yr). Biodiesel from palm	*33,400,000*	
Production rate (L/yr). Biohydrogen from molasses	*9,504,000*	
N-P-K fertilizer. Palm. (kg/Ha)	*41.2-147.8-804*	*[23]*
Pesticide. Palm. (kg/Ha)	*1.2*	*[23]*
Factor emissions for N-fertilizer ($KgCO_2e/KgN$)	*8.66*	*[24]*
Factor emissions for P-fertilizer ($KgCO_2e/KgP_2O_5$)	*2.1*	*[24]*
Factor emissions for K-fertilizer ($KgCO_2e/KgK_2O$)	*0.90*	*[24]*
Factor emissions for pesticide ($KgCO_2e/Kg$)	*12.98*	*[24]*
Factor emissions for agricultural stage. Sugarcane. ($KgCO_2e/Kgsugarcane$)	*0.028*	*[24]*
Factor emissions for electricity ($KgCO_2e/Kwh$)	*0.306*	*[25]*
Isothermal compression efficiency (biohydrogen) (%)	*65*	*[20]*
Recuperation percentage of biofuel (%)	*99*	
Compression pressure (biohydrogen) (atm)	*200*	
Maximum hydrogen production rate (ml H_2/h)	*13.7*	*[26]*
Lag-time (h)	*4.04*	*[26]*

2.2. Biodiesel from palm

GHG emissions in agricultural stage were considered for: fertilizer production and use, pesticide production and manual harvest. Location of the production plant was considered close to the field. Industrial phase was simulated using Aspen Plus ® S oftware and the conversion technology included oil extraction followed by transesterification with methanol, neutralization and distillation.

2.3. Biohydrogen from molasses

Agricultural phase was considered to be the same as sugarcane case. Molasses were obtained as co-product from sugar industry. Information required was taken from Ecoinvent database. Biohydrogen was produced by dark-fermentation using mixed culture for their production. Data for industrial phase was calculated using Matlab® software and the emissions corresponded to fermentation, separation and compression steps.

3. Results and Discussion

Figure 2 summarizes GHG emissions associated to biofuel production for each feedstock. According to the Figure 2, biodiesel from palm was the system with the lowest GHG emissions for all stages, while bioethanol from sugar cane showed the biggest GHG emissions in its industrial phase. The total GHG emissions for bioethanol were eight-fold related to biodiesel and total GHG emissions for biohydrogen is twice bigger that biodiesel.

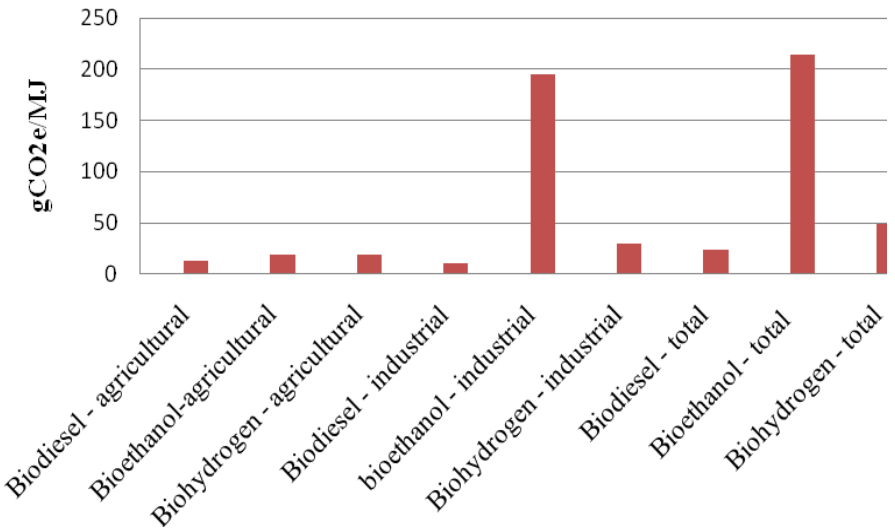

Fig. 2. GHG emissions for each system studied

Figure 3 shows emissions from different works. Macedo et al [27] and Smeets et al. [28] calculated emissions for bioethanol from sugarcane in Brazil; Yee et al [29] calculated emissions for biodiesel from palm in Malaysia and de Souza et al [23] studied biodiesel from palm oil in Brazil; Manish and Banerjee [30] estimated emissions for biohydrogen from sugarcane juice in India. In figure 3 differences between all studies are observed, even in works considering the same biofuel production. Taking as basis work for the bioethanol comparisons the one of Smeets et al. [28], GHG emissions obtained by Macedo et al [27] were almost twice bigger while for this work were eighteen-fold bigger. Based on de Souza et al [23] work for the Biodiesel comparisons, GHG emissions obtained by Yee et al [29] were more than twice bigger while for this work was one-third bigger. GHG emissions for biohydrogen in this work were eleven-fold bigger than that obtained by Manish and Banerjee [30]. Below, the obtained results are discussed in detail for each biofuel.

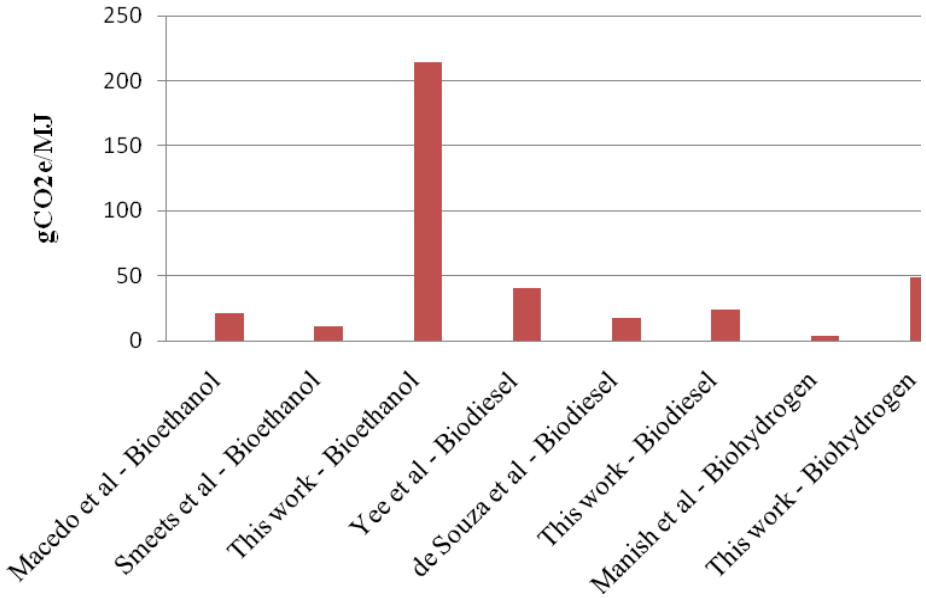

Fig. 3. GHG emissions for different studies

3.1. Bioethanol

Smeets et al. [28] study, Macedo et al. [27] study and this work differ in GHG emissions values. Smeets et al. [28] study reported lowest GHG emissions but in this paper were obtained the highest emissions. Macedo et al. [27] is considered a rigorous analysis for agricultural stage and took into account sugarcane burning. However, these authors assumed a self-sustainable plant, which implied zero GHG emissions for industrial stage. This assumption led to obtain low values in this stage.

In the case of Smeets et al. [28] study, it was similar to the Macedo et al [27] study. They assumed a global approach for bioethanol impact and their results were similar to that of Macedo et al [27]. In this work, emissions of industrial phase are bigger because alcoholic fermentation generates large amount of CO_2. Comparison of these works is significant because were made in Brazil and Colombia, countries with similar conditions. Macedo et al. [27] study reported twice GHG emissions and this work report eighteen fold GHG emissions compared to Smeets et al. study. Industrial stage proves to be very significant because of CO_2 emissions from fermentation. The CO_2 release is a problem to be stated seriously specially when land use change applied (and biomass per hectare is reduced).

3.2. Biodiesel

Yee et al. [29] study is very complete. They considered for agricultural stage: planning, nursery establishment, site preparation, field establishing, field maintenance, harvesting, and collection and replanting; milling stage: Fresh Fruit Bunches extraction, stripping and oil extraction. For industrial phase: oil conversion with methanol.

De Souza et al. [23] considered for agricultural stage: Fertilizer, pesticides, transport and manual harvest. For industrial phase: electricity and diesel use, methanol and catalyst; co-products are used for energy cogeneration.

De Souza et al. [23] study showed the lowest emissions while Yee et al. [29] reported the biggest. In this work were obtained intermediate values for emissions. Yee et al. [29] study, considered the largest secondary processes and, therefore, highest GHG emissions were obtained. Nevertheless, Yee et al [29] study was made for Malaysia while de Souza et al. [23] study was performed for Brazil. Using Colombian conditions then is more significant to compare de Souza work with the developed in this work. Taking as reference de Souza et al [23] study, Yee et al. [29] obtained 132% larger GHG emissions and this work reports 35% larger GHG emissions. Differences between De Souza et al. [23] study and these works are due to cogeneration and waste uses. Last, because these aspects change energy balance, and therefore, emissions values and rates.

3.3. Biohydrogen

GHG emissions for this work were around tenfold bigger than that obtained by Manish and Banarjee [30] because they considered exclusively industrial aspects and the input was sugarcane without any reflection of agricultural phase.

3.4. Final analysis

Agricultural stage generates significant GHG emissions because nitrous oxide and methane are emitted into the atmosphere and these gases have a Global Warming Potential (GWP) of 300 and 15 times more than carbon dioxide, respectively. Methane and nitrous oxide come from fertilizers and pesticides application, explaining the importance of their application rate

in biofuels environmental assessment. Moreover, fertilizer production methods are essential for environmental evaluation. This fact explains high emissions factors (table 1) for fertilizer production using conventional technologies.

GHG emissions for biodiesel production were greater for agricultural stage while industrial stage emissions were greater for hydrogen and bioethanol production. This is due to fermentation emissions that strongly influenced the obtained values. Carbon substrate is inadequate, almost from environmental point of view, and traditional biochemical pathways promote high emission levels.

4. Conclusions

Results indicate that the most efficient system, in terms of GHG emission balances, was biodiesel production from palm oil while the system with highest emissions was the bioethanol production. Alcoholic and acetic fermentation proved to be of great influence on emissions balances and demonstrating a number of restrictions if compared to other studies. According to results presented in this paper, bioethanol from sugarcane contribute more to climate change that biohydrogen from sugarcane and biodiesel from palm oil.

References

[1] A. Demirbas, Political, economic and environmental impacts of biofuel: A Review, Applied Energy 86, 2009; pp. S108-117.

[2] D. Larson, A review of life-cycle analysis studies on l iquid biofuel systems for the transport sector, Energy Sustainable Development, X, 2006, pp. 109-126.

[3] S.C Davis, K.J. Andenson-Texeira, E.H. De Lucia, Life cycle analysis and the ecology of biofuel, Trends in Plant Science 14, 2009, pp. 140-146.

[4] R. Hoefnagels, E. Smeets, A Faaij, Greenhouse gas footprints of different biofuel production systems, Renewable and Sustainable Energy Reviews 14, 2010, pp. 1661 - 1694.

[5] F. Cherubini, N.D Bird, A Crowie, G. Jungmeier, B Schlamandinger, S. Woess-Gallasch, Energy and Greenhouse gas-based LCA of biofuel and bioenergy systems: Key issues, ranges and recommendations, Resources, Conservation and Recycling 53, 2009, pp. 197-208.

[6] A. Zidanšek, R. Blinc, A Jeglič, S Kabashi, S. Bekteshi, I. Šlaus, Climate change, biofuel and sustainable future, International Journal of Hydrogen Energy 34, 2009, pp. 6980 - 6983.

[7] E.A. Kaditi, Bioenergy policies in a global context, Journal of Clean Production 17, 2009, pp. 4-8.

[8] P. Borjeson, L.M Tufvesson, Agricultural crop-based biofuel – resource efficiency and environmental performance including direct land use change, Journal of Clean Production, 2010, submitted for publication.

[9] A. Demirbas, Biofuels sources, biofuel policy, biofuel economy and global projections, Energy Conversion and Management 49, 2008, pp. 2106-2116.

[10] M.I. Montoya, J.A Quintero, O.J Sánchez, C.A. Cardona, Evaluación del impacto ambiental del proceso de obtención de alcohol carburante utilizando el algoritmo de

reducción de residuos, Revista Facultad de Ingeniería de la Universidad de Antioquia 36, 2006, pp. 85-95.

[11] H.V. Blottnitz, M.A. Curran, A review of assessment conducted on bioethanol as a transportation fuel from a net energy, greenhouse gas, and environmental life cycle perspective, Journal of Clean Production 15, 2007, pp. 607-619.

[12] S Kim, B.E Dale, Life cycle assessment of various cropping systems utilized for production biofuels: Bioethanol and biodiesel, Biomass and Bioenergy 29, 2005, pp. 426-439.

[13] R. Kothari, D. Buddhi, R.L. Sawhnet, Comparison of environmental and economic aspects of various hydrogen production methods, Renewable and Sustainable Energy Reviews 12, 2008, pp. 2008.

[14] X. Deng, H. Wang, H. Huang, M. Ouyang, Hydrogen flow chart in China, International Journal of Hydrogen Energy 35, 2010, pp. 6475-6481.

[15] M. Balat, M. Balat, Political, economic and environmental impacts of biomass-based hydrogen, International Journal of Hydrogen Energy 34, 2009, pp. 3589-3606.

[16] S.M Kotay, D. Das, Biohydrogen as a renewable energy source – Prospects and potentials, International Journal of Hydrogen Energy 33, 2008, pp. 258-263.

[17] C.J. Winter, Hydrogen energy – Abundant, efficient, clean: A debate over the energy-system-of-change, International Journal of Hydrogen Energy 34, 2009, pp. S1-S52.

[18] D. Das, T.N. Veziroglu, Advances in biological hydrogen production process, International Journal of Hydrogen Energy 33, 2008, pp. 6046-6057.

[19] L.B. Bentner, J. Peccia, J.B. Zimmerman, Challenges in developing biohydrogen as a sustainable energy source: Implications for a research agenda, Environmental Science & Technology 44, 2010, pp. 2243-2254.

[20] M. Granovskii, I. Dincer, M.A. Rosen, Environmental and economic aspects of hydrogen production and utilization in fuel cell vehicles, Journal of Power Sources 157, 2006, pp. 411-421.

[21] D.B. Levin, R. Chahine. Challenges for renewable hydrogen production from biomass. International Journal of Hydrogen Energy 35, 2010, pp. 2243-2254.

[22] M. Ball. M. Wietschel, The future of hydrogen – Opportunities and challenges, International journal of Hydrogen Energy 34, 2009, 615-627.

[23] S.P. de Souza, S. Pacca, M.T. de Ávila, J.L.B. Borges, Greenhouse gas emissions and energy balance of palm oil biofuel. Renewable Energy 35, 2010, pp. 2552-2561.

[24] Ecoinvent, 2006, Swiss Center for Life Cycle Interventories. Switzerland.

[25] Misterio de Minas y energía, Cálculo del factor de emisión de CO_2 del sistema eléctrico interconectado colombiano. 2008.

[26] W.H. Chen, S.Y. Chen, S.K. Khanal, S. Sung, Kinetic study of biological hydrogen production by anaerobic fermentation, International Journal of Hydrogen Production 31, 2006, pp. 2170-2178.

[27] I.C. Macedo, M.R. Lima, J.E. Ramos, Assessment of greenhouse gas emissions in the production and use of fuel ethanol in Brazil, Government of the State of São Paulo, Brazil, 2004.

[28] E. Smeets, M. Junginger, A. Faaij, A. Walter, P. Dolzan, W, Turkenburg., The sustainability of Brazilian ethanol – An assessment of the possibilities of certified production, Biomass and Bioenergy 32, 2008, pp. 781-813.

[29] K.F. Yee, K.T. Tan, A.Z. Abhullah, K.T. Lee, Life cycle assessment of palm biodiesel: Revealing facts and benefits for sustainability, Applied Energy 86, 2009, pp. S189-S196.

[30] S. Manish, R. Banerjee, Comparison of biohydrogen production processes, International Journal of Hydrogen Energy 33, 2008, pp. 279-286.

[31] C.A. Cardona Alzate, Oscar Julian Sanchez Toro, Luis Fernando Gutierrez Mosquera, "Process synthesis for fuel ethanol production" United States of America, 2009. ed: CRC Press Taylor & Francis Group, ISBN: 978-1-4398-1597-7, v. 1, p. 390.

[32] L.F. Gutierrez Mosquera, O.J. Sanchez Toro, C.A Cardona Alzate, "Process integration possibilities for biodiesel production from palm oil using ethanol obtained from lignocellulosic residues of oil palm industry". England, Bioresource Technology ISSN: 0960-8524 ed: Elsevier. v.100 2009p.1227 – 1237.

[33] Frischknecht R., Jungbluth N., Althaus H.-J., Doka G., Dones R., Hischier R., Hellweg S., Nemecek T., Rebitzer G. and Spielmann M. Overview and Methodology. Final report Ecoinvent data v2.0, No. 1. 2007. S wiss Centre for Life Cycle Inventories, Dübendorf, CH.

Impact of Climate Change on Wheat Production for Ethanol in Southern Saskatchewan, Canada

Hong Wang[1,*], Yong He[1,2], Budong Qian[3], Brian McConkey[1], Herb Cutforth[1], Tom McCaig[1], Grant McLeod[1], Robert Zentner[1], Con Campbell[3], Ron DePauw[1], Reynald Lemke[4], Kelsey Brandt[1], Tingting Liu[1,5], Xiaobo Qin[1,6], Gerrit Hoogenboom[7], Jeffrey White[8], Tony Hunt[9]

[1]*Semiarid Prairie Agricultural Research Centre, Agriculture and Agri-Food Canada, Box 1030, Swift Current, Saskatchewan, S9H 3X2, Canada*
[2]*Department of Soil and Water Sciences, Resources and Environmental Sciences College, China Agricultural University, Beijing, 100094, China*
[3]*Eastern Cereal and Oilseed Research Centre, Agriculture and Agri-Food Canada, Ottawa, Ontario, Canada*
[4]*Saskatoon Research Centre, Agriculture and Agri-Food Canada, Saskatoon, Saskatchewan, Canada*
[5]*Renmin University of China, Beijing, 100872, China*
[6]*Institute of Agro-Environment and Sustainable Development, Chinese Academy of Agriculture Sciences/The Key Laboratory for Agro-Environment and Climate Change, Ministry of Agriculture, Beijing, 100081, China*
[7]*Washington State University, 24106 North Bunn Road, Prosser, Washington 99350-8694, USA*
[8]*USDA ARS, ALARC, 21881 N Cardon Lane, Maricopa, AZ 85138, USA*
[9]*University of Guelph, Canada*
** Corresponding author. Tel: +1 3067787288, Fax: +1 3067783188, E-mail: hong.wang@agr.gc.ca*

Abstract: This study assessed the impact of climate change on wheat production for ethanol in southern Saskatchewan, Canada. The DSSAT-CSM model was used to simulate biomass and grain yield under three climate change scenarios (IPCC SRES A1B, A2 and B1) in the 2050s. Synthetic 300-yr weather data were generated by the AAFC stochastic weather generator for the baseline period (1961-1990) and scenarios. Compared to the baseline, all three scenarios increase precipitation every month except July and August and June (A2 only), when less rains are projected. Annual air temperature is increased by 3.2, 3.6 and 2.7 ^{o}C for A1B, A2 and B1, respectively. The model predicted increases in biomass by 28, 12 and 16% without the direct effect of CO_2 and 74, 55 and 41% with combined effect (climate and CO_2) for A1B, A2 and B1, respectively. Similar increases were found for yield. However, the occurrence of heat shock (>32^{o}C) will increase during grain filling under climate change conditions and could cause severe yield reduction, which is not simulated by DSSAT-CSM; therefore, the yield could be overestimated. Several measures such as early seeding must be taken to avoid heat damage and take the advantage of projected increase in precipitation.

Keywords: *Climate change, Wheat, Bioenergy crop, Heat shock, Seeding date*

1. Introduction

Because of the shortage of fossil fuels and the negative impact of fossil fuel consumption on global climate and environment, the production of bioenergy crops as an alternative to traditional fossil fuels has become much more attractive to the world. Approximately 44% of Canada's agricultural land is located in the province of Saskatchewan and the major (close to 40%) crop is wheat (*Triticum aestivum* L.), which is a potential bioenergy crop. No matter what measures are taken, global climate change will continue. Since the process of substituting energy crops for fossil fuels would occur gradually over several decades, climate change will affect its production. The objective of this study was to use the DSSAT-CSM model to assess the impact of climate change on the production of wheat as a bioenergy crop grown in southern Saskatchewan.

2. Methodology

2.1. Site Condition

The site selected for this study was located on a gently sloping Swinton silt loam (Typic Haploboroll) at the Semiarid Prairie Agricultural Research Centre, Swift Current, in southern Saskatchewan. Daily maximum and minimum air temperatures and precipitation were obtained from the weather station located on the research site. Daily solar radiation was calculated using the Mountain Climate Simulator [1]. Soil property inputs for DSSAT-CSM (organic carbon, total nitrogen, clay and silt in percent, cation exchange capacity, pH, soil lower, drained upper and saturated points, saturated hydraulic conductivity, and bulk density) were observed on the site. The management used for simulation was a continuous wheat rotation under no-till with a seeding depth of 5 cm. Nitrogen fertilizer was assumed to be applied at a rate of 100 kg ha^{-1} at planting time. Seeding dates were predicted with the model developed by Bootsma and De Jong [2], and subsequently modified by McGinn et al. [3].

2.2. The DSSAT-CSM Model

The Decision Support System for Agrotechnology Transfer-Cropping System Model (DSSAT-CSM), a widely used process-based modeling package [4], was selected for simulating the wheat production system. This model simulated wheat yield and biomass generally well in western Canada [5-7]. The wheat module of DSSAT-CSM (v4.0) was modified to improve the prediction of seedling emergence rate [8-9] and leaf appearance rate [10]. The spring wheat cultivar Biggar (Canada Prairie Spring Wheat class) was used for modeling because this wheat class has higher starch content and lower protein concentration in comparison to bread wheat class and is recognized as a viable feedstock for ethanol [11]. Genetic coefficients of Biggar were calibrated with the data collected by Jame and Cutforth [12] and tested using data from the New Rotation experiment at Swift Current [13]. In order to predict the long-term effect we used the Sequence Analysis of DSSAT to run the model.

2.3. Climate Change Baseline and Scenarios

Weather data during the period of 1961-1990 were treated as baseline climate. Climate change scenarios in 2050s (2040-2069) were projected by the third generation global climate model developed at Canadian Centre for Climate Modelling and Analysis (CGCM3) with the forcing of three greenhouse gas (GHG) emission scenarios (i.e., IPCC SRES A1B, A2 and B1) [14]. Synthetic 300-yr weather data were generated by the AAFC Stochastic Weather Generator (AAFC-WG) for the baseline period and each scenario [15]. These generated data were used to predict the climate effect on wheat production with the DSSAT model. Qian et al. [16] found that simulations of crop models with 30-yr observed and the 300-yr synthetic weather data generated by AAFC-WG with parameters calibrated from the same 30-yr observed data, in general, do not show significant differences, with regard to timing of biomass accumulation, crop maturity date, as well as final biomass and grain yield at maturity. The simulations were run with and without direct effects of increased atmospheric CO_2 levels. The CO_2 levels were 550 ppm for A1B and A2 and 450 ppm for B1 [14]. The hourly air temperature was calculated using the subroutine HTEMP of DSSAT-CSM [17].

2.4. Data Analysis

Statistical analyses were done by SAS [18]. Means, lower and upper limits of the 95% confidence interval and standard deviation of synthetic air temperature and precipitation were calculated and compared among baseline and climate change scenarios by PROC MEANS. Predicted and calculated variables were compared between scenarios with PROC MIXED [19].

3. Results

3.1. Climate Change Baseline and Scenarios

3.1.1. Precipitation

All the climate change scenarios increased annual precipitation compared to the baseline period (331 mm, Fig. 1). The most significant increase is scenario A1B (55 mm), followed by A2 (39 mm) and B1 (37 mm). All three scenarios increase precipitation every month except July and August and June (A2 only), when less rains are projected. Scenario A2 was similar to A1B in terms of precipitation distribution except that it was markedly (10 mm) less than A1B in June. Precipitation for scenario B1 was generally slightly less than that of A1B, except in July and August when B1 had more rain than A1B.

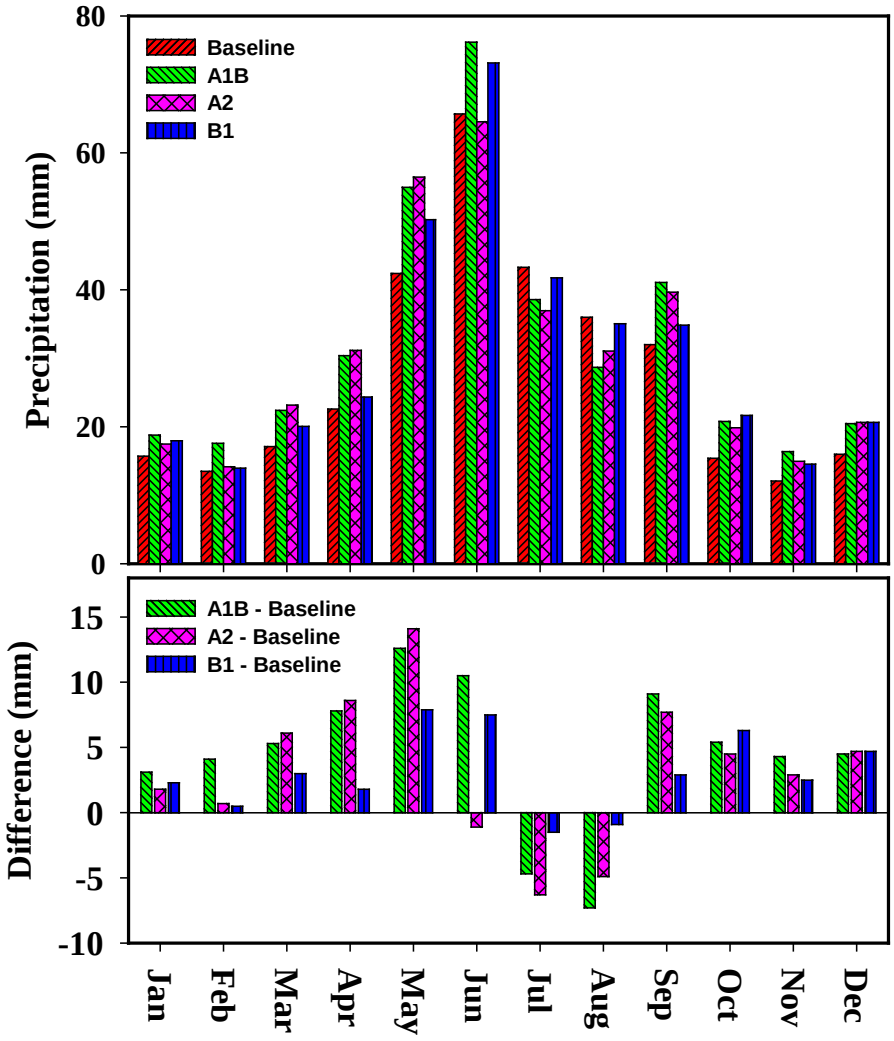

Fig. 1. Monthly precipitation under baseline and three scenarios and difference between baseline and scenarios.

3.1.2. Air temperature

Air temperature in all climate scenarios was increased compared to the baseline climate (Fig. 2). Scenarios A1B, A2 and B1 had 3.2, 3.6 and 2.7 ^{0}C higher annual mean air temperatures than the baseline, respectively. The highest differences in temperature occurred in the winter, followed by summer, and relatively small differences occurred in the spring and fall. Scenario

A2 had the highest temperature in most of the days of the year. The change in pattern and difference between scenarios in daily maximum and minimum air temperatures were similar to that in daily mean temperature (data not shown).

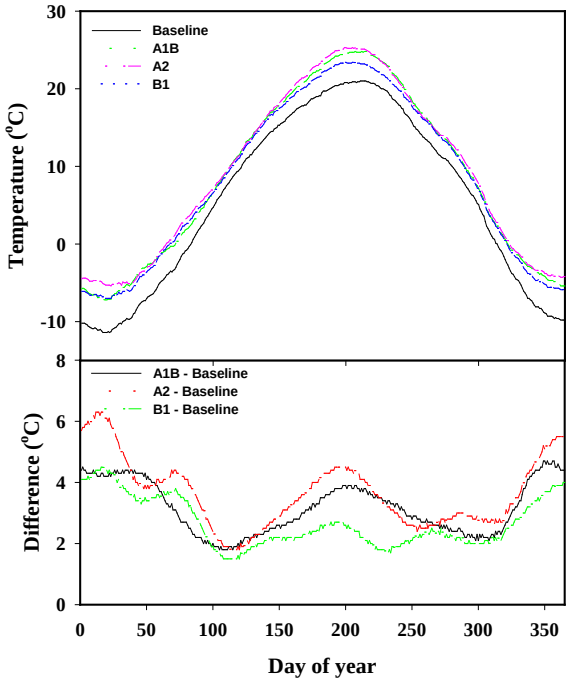

Fig. 2. Daily mean air temperature under baseline and three scenarios and difference between baseline and scenarios.

3.2. Phasic Development

The predicted seeding dates under all climate change scenarios are six days earlier than the prediction under the baseline climate (Day 124, May 10) (Table 1). Because of the earlier seeding and higher temperatures, predicted dates of anthesis and maturity averaged nine and 13 d earlier than simulations based on the baseline climate, respectively. The vegetative (from emergence to anthesis) and grain filling stages were shortened by 2-3 and 3-5d, respectively. The total time to maturity was shortened by 6-9 d. Among the three climate scenarios, the scenario that reduced days to plant maturity the most was scenario A2, which is associated with its higher temperature.

Table 1. Effects of climate change on phasic development of wheat

	Day of year			Duration (days)			
Scenario	Seeding	Anthesis	Maturity	Seeding to emergence	Emergence to anthesis	Grain filling	Seeding to Maturity
Baseline	123.5a[z]	185.2a	218.4a	11.3a	50.4a	33.1a	94.8a
A1B	118.0b	176.7bc	205.5c	10.9ab	47.9c	28.7c	87.5c
A2	117.8b	175.7c	203.8d	10.7b	47.1d	28.1d	86.0d
B1	118.1b	177.5b	207.5b	10.9ab	48.6b	30.0b	89.4b

[z] Within columns and depth, values followed by the same letter are not significantly different at the 0.05 level of probability.

3.3. Biomass and Grain Yield

Without the direct effect of CO_2, the model predicted that all three climate change scenarios significantly increases biomass production compared to the baseline (Table 2), with A1B

increasing the most (28%) followed by B1 (16%) and A2 (12%). The combined effect (climate and CO_2) increased biomass production much more, with A1B increasing the most (74%) and A2 (55%) and B1 (41%) being similar. Increased CO_2 concentrations of 220 and 120 ppm resulted in increased biomass production of 43-45% and 25%, respectively. The effect of the climate change scenarios on grain yield shows the same trend as biomass with a slightly higher increase rate.

Table 2. Effects of climate change on biomass and grain production of wheat.

Scenario	CO2 ppm	Biomass kg ha-1	Grain Yield kg ha-1
Baseline	330	5039f[z]	2467f
A1B	330	6463d	3167d
A1B	550	8753a	4349a
A2	330	5651e	2834e
A2	550	7813b	3978b
B1	330	5856e	2880e
B1	450	7104c	3520c

[z] Within columns and depth, values followed by the same letter are not significantly different at the 0.05 level of probability.

4. Discussion and Conclusions

The estimated increase in yield under climate change is consistent with the study by Arthur [20] who predicted an increase in wheat yield under four climate change scenarios in Saskatchewan. However, caution must be exercised when interpreting the model-simulated results as the effect of heat stress on wheat growth is not well described by the model. Heat stress occurs often in wheat on the Canadian Prairies especially during reproductive growth, which has markedly negative impacts on yield [21]. At the grain growth stage (anthesis to maturity), heat stress is divided into two types according to Wardlaw et al. [22]: chronic stress (20–32°C) and heat shock (>32°C). Chronic stress involves a progressive decrease in kernel weight with increasing temperature because the increase of grain filling rate associated with the increase of temperature does not compensate enough for the reduction of grain filling duration [23]. In southern Saskatchewan, McCaig [21] found that the cumulative maximum daily air temperature >20°C during and after anthesis was negatively correlated with the yield of wheat. Heat shock can inhibit pollen growth, cause sterility and abortive grain, trigger premature senescence, inhibit kernel development and cause significant reduction in yield [24-25].

The occurrence of chronic stress increased for all the climate change scenarios compared to baseline (data not shown). Significant and more obvious increase of heat shock incidence was found for all scenarios (Table 3). Under the baseline climate, heat shock (>32 ^{o}C) occurred for only 30 hours during the first 20 days of grain filling. Heat shock occurred for 73, 87 and 56 hours during this same period under climate change scenarios A1B, A2 and B1, respectively, which are 1.8-2.9 times of that under the baseline climate. Note that if daily temperature is used, increases of heat shock are significant, but not as tremendous as calculated by using hourly results. This means that under climate change conditions heat shock will occur longer in a day than under the baseline climate. It is obvious that heat shock will damage the kernel development and reduce grain yield if the future cultivars are not improved in heat shock resistance. This is not predicted by the model because the DSSAT-CSM model, like many other models, does not simulate the yield loss caused by heat shock [26]. Therefore, grain yield, and probably biomass, is likely overestimated.

Table 3. Effects of climate change on duration of air temperature surpassing 32 ^{o}C during the first 20 days of grain filling.

Scenario	Day	Hour
Baseline	5.0d[z]	30.1d
A1B	9.3b	72.8b
A2	10.9a	87.3a
B1	7.6c	55.5c

[z] Within columns and depth, values followed by the same letter are not significantly different at the 0.05 level of probability.

Adaptation measures must be taken in regards to the high temperature under climate change. One possible strategy is early seeding. This would allow wheat to mature earlier, avoiding heat shock which will mostly occur in July. The prediction of seeding dates in this paper (Table 1) was calculated by an empirical model [3] which is based on observations from 1956 to 1984 [2]. In recent years, the adoption of no-till and stubble mulch tillage systems allows seeding even earlier. Therefore, if this technique is used in the 2050's the seeding dates could be significantly earlier than the predicted dates. Early seeding of wheat on the Canadian Prairies may have other advantages, such as reducing the application of herbicides for weed control [27], and could possibly reduce the incidence of some insects and diseases and improve the timeliness of planting operations in the spring. Dormant-seeding in the fall or winter is another method to be considered. This is already practiced by some farmers and some research has been conducted [28].

Two other strategies to cope with the heat stress are breeding heat resistant cultivars [29] and adopting improved tillage methods. The surface residue and standing stubble in a no-till and stubble mulch system act as insulation and impede the exchange rate of thermal energy between the soil and atmosphere. The slightly higher soil moisture under this system can also help buffer the extremes in daily soil temperatures and reduce near-surface root heat stress. Merrill et al. [30] and Wang et al [25] observed that no-till mitigated heat stress of wheat and improved growth and yield.

Although the projected increase of air temperature, especially the increase of heat shock, may cause yield loss, all three climate change scenarios projected an increase in precipitation. Proper management methods are needed to capitalize on this advantage. Fortunately, one of the strategies is also to seed wheat early which allows wheat to take advantage of the wetter spring while avoiding the drier period in July [31-32].

References

[1] P.E. Thornton, H. Hasenauer, M.A. White, Simultaneous estimation of daily solar radiation and humidity from observed temperature and precipitation: an application over complex terrain in Austria, Agricultural and Forest Meteorology 104, 2000, pp. 255–271.

[2] A. Bootsma, R. De Jong, Estimates of seeding dates of spring wheat on the Canadian Prairies from climate data, Canadian Journal of Plant Science 68, 1988, pp. 513–517.

[3] S.M. McGinn, A. Touré, O.O. Akinremi, D.J. Major, A.G. Barr, Agroclimate and crop response to climate change in Alberta, Canada, Outlook On Agriculture 28(1), 1999, pp. 19–28.

[4] J.W. Jones, G. Hoogenboom, C.H. Porter, K.J. Boote, W.D. Batchelor, L.A. Hunt, P.W. Wilkens, U. Singh, A.J. Gijsman, J.L. Ritchie, The DSSAT cropping system model, European Journal of Agronomy 18, 2003, pp. 235–265.

[5] A.P. Moulin, H.J. Beckie, Evaluation of the CERES and EPIC models for predicting spring wheat grain yield, Canadian Journal of Plant Science 73, 1993, pp. 713–719.

[6] A.C. Chipanshi, E.A. Ripley, R.G. Lawford, Large–scale simulation of wheat yields in a semi–arid environment using a crop–growth model, Agricultural Systems 59, 1999, pp. 57–66.

[7] H. Wang, G.N. Flerchinger, R. Lemke, K. Brandt, T. Goddard, C. Sprout, Improving SHAW long–term soil moisture prediction for continuous wheat rotations, Alberta, Canada, Canadian Journal of Plant Science 90, 2010, pp. 37–53.

[8] H. Wang, H. Cutforth, T. McCaig, G. McLeod, K. Brandt, R. Lemke, T. Goddard, C. Sprout, Predicting the time to 50% seedling emergence in wheat using a Beta model, NJAS – Wageningen Journal of Life Sciences 57, 2009, pp. 65–71.

[9] H. Wang, H. Cutforth, P.R. Bullock, R.M. DePauw, T. McCaig, G. McLeod, K. Brandt, G.J. Finlay, Testing a nonlinear model for simulating the time of seedling emergence of wheat, Canadian Biosystems Engineering 51, 2009, pp. 4.1–4.6.

[10] H. Wang, H.W. Cutforth, R. DePauw, T. McCaig, G. McLeod, K. Brandt, X. Qin, Modeling leaf appearance rate for Canada Western Red Spring wheat cultivars, Canadian Journal of Plant Science 90, 2010, pp. 399–402.

[11] K. Sosulski, F. Sosulski, Wheat as a feedstock for fuel ethanol, Applied Biochemistry and Biotechnology 45(6), 1994, pp. 169–180.

[12] Y.W. Jame, H.W. Cutforth, Simulating the effects of temperature and seeding depth on germination and emergence of spring wheat, Agricultural and Forest Meteorology 124, 2004, pp. 207–218.

[13] R.P. Zentner, C.A. Campbell, F. Selles, B.G. McConkey, P.G. Jefferson, R. Lemke, Cropping frequency, wheat classes and flexible rotations: Effects on production, nitrogen economy, and water use in a Brown Chernozem, Canadian Journal of Plant Science 83, 2003. pp. 667–680.

[14] N. Nakicenovic, R. Swart, Emissions Scenarios IPCC Special Report, 2000. Nebojsa Nakicenovic and Rob Swart (Eds.) – Cambridge University Press, UK, 2000, pp. 570.

[15] B.D. Qian, S. Gameda, H. Hayhoe, R. De Jong, A. Bootsma, Comparison of LARS–WG and AAFC–WG stochastic weather generators for diverse Canadian climates, Climate Research 26, 2004, pp. 175–191.

[16] B.D. Qian, R. De Jong, J.Y. Yang, H. Wang, S. Gameda, Comparing the simulation of climate impacts on crop yields with observed and synthetic weather data, 2010. 2010 AGU Fall Meeting. 13–17 December, San Francisco, California, USA.

[17] W.J. Parton, J.A. Logan, A model for diurnal variation in soil and air temperature, Agricultural Meteorology 23, 1981, 205-216.

[18] SAS Institute, Inc., SAS procedures guide. Version 8. SAS Institute, Inc., Cary, NC, USA, 1999.

[19] I.P. Little, The relationship between soil pH measurements in calcium chloride and water suspensions, Australian Journal of Soil Research 30, 1992, pp. 587–92.

[20] L.M. Arthur, The implication of climate change for agriculture in the prairie provinces, Climate Change Digest 88-01. 1988, Downsview, ON. Atmospheric Environment Service.

[21] T.N. McCaig, Temperature and precipitation effects on durum wheat grown in southern Saskatchewan for fifty years, Canadian Journal of Plant Science 77, 1997, pp. 215–223.

[22] I.F. Wardlaw, C. Blumenthal, O. Larroque, C.W. Wrigley, Contrasting effects of chronic heat stress and heat shock on kernel weight and flour quality in wheat,Functional Plant Biology 29, 2002, pp. 25–34.

[23] I.F. Wardlaw, C.W. Wrigley, Heat tolerance in temperate cereals: An overview, Australian Journal of Plant Physiology 21, 1994, pp. 695–703.

[24] P.J. Stone, M.E. Nicolas, The effect of duration of heat stress during grain filling on two wheat varieties differing in heat tolerance: grain growth and fractional protein accumulation, Australian Journal of Plant Physiology 25, 1998, pp. 13–20.

[25] H. Wang, R. Lemke, T. Goddard, C. Sprout. Tillage and root heat stress in wheat in Central Alberta, Canadian Journal of Soil Science 87, 2007, pp. 3–10.

[26] T.R. Wheeler, P.Q. Craufurd, R.H. Ellis, J.R. Porter, P.V. Vara Prasad, Temperature variability and the yield of annual crops, Agriculture, Ecosystems & Environment 82, 2000, pp. 159–167.

[27] K.N. Harker, G.W. Clayton, R.E. Blackshaw, J.T. O'Donovan, E.N. Johnson, Y. Gan, F.A. Holm, K.L. Sapsford, R.B. Irvine, R.C. Van Acker, Glyphosate–resistant wheat persistence in western Canadian cropping systems, Weed Science: November 2005, Vol. 53, No. 6, 2005, pp. 846–859.

[28] R.O. Ashley, D. Barondeau, H. Peterson, J. Larson, B. Rettinger, A survey of dormant–seeded Hard Red Spring Wheat fields in Southwest North Dakota, 2001. Annual Report. Dickinson Research Extension Center, http://www.ag.ndsu.nodak.edu/dickinso/

[29] M.A. Semenov, N.G. Halford, Identifying target traits and molecular mechanisms for wheat breeding under a changing climate, Journal of Experimental Botany 60(10), 2009, pp. 2791–2804.

[30] S.D. Merrill, A.L. Black, A. Bauer, Conservation tillage effects root growth of dryland spring wheat under drought, Soil Science Society of America Journal 60, 1996, pp. 575–583.

[31] H.W. Cutforth, B.G. McConkey, R.J. Woodvine, D.G. Smith, P.G. Jefferson, O.O. Akinremi, Climate change in the semiarid prairie of southwestern Saskatchewan: Late winter–early spring, Canadian Journal of Plant Science 79: 1999, 343–350.

[32] H. Harricharan and J. McKinlay, Frost Seeding - A Cheaper Alternative. 2010. Ministry of Agriculture, Food and Rural Affairs. Government of Ontario, Canada. http://www.omafra.gov.on.ca/english/crops/facts/98-071.htm.

Thermodynamic and dynamic investigation for CO_2 storage in deep saline aquifers

Xiaoyan Ji[1,*], Yuanhui Ji[1], Chongwei Xiao[2]

[1] *Division of Energy Engineering, Luleå University of Technology, Luleå, Sweden*
[2] *Petroleum Recovery Research Center, New Mexico Institute of Mining and Technology, New Mexico, USA*
** Corresponding author. Tel: +46 920492837, Fax: +46 920491074, E-mail: xiaoyan.ji@ltu.se*

Abstract: Thermodynamic and dynamic investigations are needed to study the sequestration capacity, CO_2 leakage, and environmental impacts. The results of the phase equilibrium and densities for CO_2-sequestration related subsystems obtained from the proposed thermodynamic model on the basis of statistical associating fluid theory equation of state were summarized. Based on the equilibrium thermodynamics, preliminary kinetics results were also illustrated with chemical potential gradient as the driving force. The proposed thermodynamic model is promising to represent phase equilibrium and thermodynamic properties for CO_2-sequestration related systems, i.e. CO_2-(H_2S)-H_2O-ions (such as Na^+, K^+, Ca^{2+}, Mg^{2+}, Cl^-, CO_3^{2-}), and the implementation of thermodynamic model into kinetics model to adjust the non-ideality of species is vital because of the high pressure for the investigation of the sequestration process.

Keywords: *Carbon sequestration, CO_2 storage, Thermodynamics, Dynamics, CO_2 diffusion*

1. Introduction

Storage of CO_2 in deep saline aquifers is one way to limit the buildup of greenhouse gases in the atmosphere. Large-scale injection of CO_2 into saline aquifers will induce a variety of coupled physical and chemical processes including multiphase fluid flow, solute transport, and chemical reactions between fluids and formation minerals. Thermodynamic and dynamic investigations are needed to study the sequestration capacity, CO_2 leakage, and environmental impacts. Co-injection of CO_2 and H_2S (from flue gases and natural gas fields) may substantially reduce the capture and sequestration costs, and the effect of H_2S on bot h thermodynamic and dynamic models is also needed.

In thermodynamics, experimental solubility data for the CO_2 in water and aqueous NaCl solution and for the H_2S in water and aqueous NaCl solutions have been determined in a wide temperature and pressure range[1, 2]. However, only few experiments are for CO_2 solubility in brines[3]. For more complicated system, there is no available experimental data. Density is also essential to reservoir/aquifer simulation applications. The dissolution of CO_2 in aqueous solutions under most reservoir, aquifer, or deep-ocean conditions results in an increase in the density of the solution, which can induce a natural convection[3-5]. Meanwhile, the properties of the H_2O-rich phase are also strongly dependent on de nsity, which varies greatly with temperature, pressure, CO_2 concentration and salinity[6]. However, the experimental data of density for the related system are much less than those of the solubility data[7, 8].

Meanwhile, thermodynamic models have been proposed to represent the CO_2 or H_2S solubility in H_2O or aqueous NaCl solutions. The models proposed by Spycher et al.[9] and Duan et al.[2] for CO_2+H_2O and CO_2+H_2O+salt are examples of a γ-ϕ approach, where an equation of state (EOS) is used to describe the non-ideality in the CO_2-rich phase and Henry's law or an activity model is used to describe the non-ideality in the H_2O-rich phase. The inherent disadvantage of this approach is that it does not allow for estimating the density of the H_2O-rich phase. This is not an issue in a ϕ-ϕ approach, where an EOS is used for both phases. The ϕ-ϕ approach has been applied to the CO_2+H_2O+NaCl[1], H_2S+H_2O[10-14]

systems. However, to the best of our knowledge, the ϕ-ϕ approach has never been used to describe the phase equilibrium and density for other or more complicated systems.

Dynamic models were investigated on the basis of the available thermodynamic models, and sometimes the effect of ions on the CO_2 solubility is neglected[15]. Moreover, the empirical models with the concentration difference as the driving force were used to represent the dynamic process[3], such as gas dissolution, diffusion, mineral dissolution and precipitation. All these assumptions will bring uncertainty of the simulation results. It is crucial to develop a both reliable thermodynamic model and theory-based dynamic (kinetics) model in order to provide a reliable prediction for CO_2 storage in deep saline aquifers.

We have been working on the related studies for several years and obtained promising results[8, 16-21]. Thermodynamic study is on the basis of statistical associating fluid theory (SAFT) EOS, and preliminary kinetics investigation is based on the non-equilibrium thermodynamics with chemical potential gradient as driving force. In this work, our work on the thermodynamic and dynamic models is summarized, and then perspective is given.

2. Modeling

The thermodynamic properties are represented using SAFT EOS in which the dimensionless residual Helmholtz energy is defined as:

$$\tilde{a}^{res} = \tilde{a}^{seg} + \tilde{a}^{assoc} + \tilde{a}^{chain} + \tilde{a}^{ion} \qquad (1)$$

where the superscripts refer to terms accounting for the residual, segment, association, chain, and ionic interactions, respectively. The model was proposed as SAFT1-RPM first, and then improved to SAFT2. The detailed description for both SAFT1-RPM and SAFT2 was in references[8, 16-20].

In model, each component is modeled as one kind of segments with parameters, i.e. segment number m, segment volume v^{oo}, segment energy u/K, and the reduced range of the potential well λ. For molecule with association interactions, there are two additional parameters, i.e. the well depth of the association site-site potential ε, and the parameter related to the volume available for bonding κ. For ions, there is one additional parameter, effective diameter d. The mixing rules are followed those in our previous work[8, 16-19, 20].

To describe the CO_2 diffusion in water or brine, non-equilibrium thermodynamic model was used in which the chemical potential gradient was used as the driving force with the following equation:

$$\frac{\partial f_i(x,t)}{\partial t} = D_{eff} \frac{\partial^2 f_i(x,t)}{\partial x^2} \qquad (2)$$

where x is the position in m, t is the time in s, f is the fugacity of a component that is calculated with SAFT EOS, and D_{eff} is the effective diffusion constant that is a combination of a molecule diffusion and natural convection. The detail description was in reference[21].

3. Results and perspective

To represent properties of CO_2-(H_2S)-H_2O-ions (such as Na^+, K^+, Ca^{2+}, Mg^{2+}, Cl^-, CO_3^{2-}) up to high pressures, research has been carried out for several years for different subsystems.

3.1. Phase equilibrium and properties for CO_2-H_2O-NaCl system

Phase equilibrium and thermodynamic properties of CO_2-H_2O and CO_2-H_2O-NaCl system are very important for the CO_2 sequestration, and then they were investigated firstly with the SAFT1-PRM model[8] in which CO_2 was modeled as a molecule with three association sites, two sites of type O and one site of type C. H_2O was modeled as a molecule with four association sites, two sites of type O and two sites of type H. The salt was modeled as a molecule composed of two charged, but non-associating, spherical segments, of which one represents the cation and one represents the anion. For the CO_2-H_2O system, only one type of cross association was assigned, i.e., between site of type O in CO_2 and site of type H in H_2O. Using temperature-dependent parameters, SAFT1-RPM is found to represent the density and equilibrium data for the CO_2-H_2O system, including the minimum H_2O concentration in the CO_2-rich phase in the composition (y)- pressure (P) diagram, as shown in Fig. 1 (a) at 308.15 K. For CO_2-H_2O-NaCl system, an additional binary interaction constant was used, the same for both CO_2-Na^+ and CO_2-Cl^- pairs, which was needed to correct the short-range interactions. SAFT1-RPM is also found to represent the equilibrium and density data for the CO_2-H_2O-NaCl system. As shown in Fig. 1 (b), the CO_2 solubility decreases with increasing salt concentration (molality, m, mol/kgH_2O), salt-out effect, and the model captures not only the pressure effect on the CO_2 solubility but also the salting-out effect.

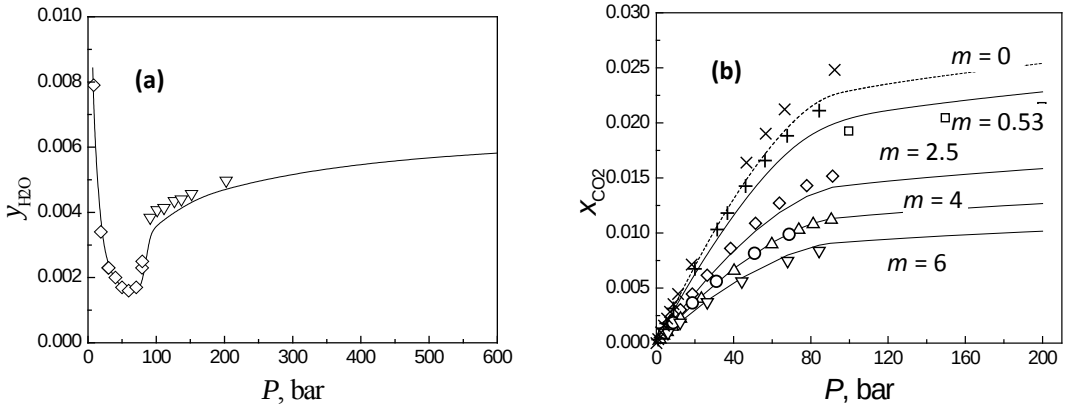

Fig. 1. (a) Mole fractions of H_2O in CO_2-rich phase (y_{H2O}) for CO_2-H_2O at 308.15 K at different pressures (P). Experimental data[22-24]; —, calculated. (b) Mole fractions of CO_2 in H_2O-rich phase (x_{CO2}) for CO_2-H_2O-NaCl at 313.15 K, different pressures (P), and salt concentration (molality, m). Experimental data[23, 25-27] : —, calculated (m = 0.5292, 2.5, 4.0 and 5.999). ···; calculated (m = 0).

3.2. CO_2 diffusion in brines

Numerous investigations on the mass transfer of CO_2 in high-pressure water or brines have been pursued to simulate the CO_2 geological and ocean disposal processes. It has been showed that the dissolution of CO_2 in brines increases the density, and then induces the density-driven natural convection, which then significantly accelerates the diffusion of CO_2 in the brine. Yang and Gu[3] investigated experimentally the CO_2 dissolution in brine at elevated pressures and described the mass transfer of CO_2 in brine using a modified diffusion equation with an effective diffusion coefficient. The effective diffusion coefficients are two orders of magnitude larger than the molecular diffusivity of CO_2 in water, which implies that the density-driven natural convection greatly accelerates the mass transfer of CO_2 in brines.

Since the salinity of brines is low for the experimental data of Yang and Gu[3], the main components are Na^+ and Cl^-, it is reasonable to assume that the brine is the aqueous solution of NaCl[21]. Based on this assumption, the CO_2 equilibrium concentration was calculated with SAFT1-RPM and compared with those measured experimentally with good agreement, as shown in Fig. 2 (a). Moreover, the mass transfer of CO_2 in brines was investigated further by chemical potential gradient model based on non-equilibrium thermodynamics[21]. Fig. 2 (b) illustrates the CO_2 concentration distribution at 300.15 K calculated with the non-equilibrium thermodynamics and those obtained from the modified Fick's second law. The difference in the concentration distribution reveals the importance to combine the thermodynamic model with kinetics model.

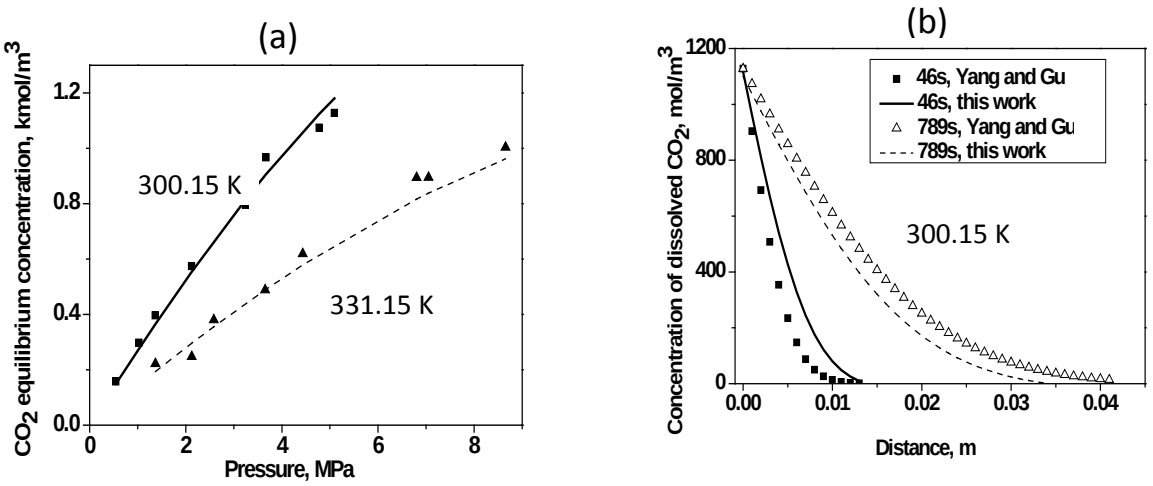

Fig. 2. (a): Equilibrium concentration of CO_2 in brine, symbols: experimental data[3], curves: prediction. (b): CO_2 concentration distribution. Curves: calculation with chemical potential gradient as driving force. Symbols: calculation with concentration difference as driving force[3].

3.3. Properties for aqueous electrolyte solutions

Properties of brines are different from different sources, and it is not always reasonable to assume it be aqueous NaCl solution when the effect of other ions is considerable. Generally, the components in brines include Na^+, K^+, Ca^{2+}, Mg^{2+}, Cl^-, CO_3^{2-}. Meanwhile, ions of Li^+, Br^-, I^-, NO_3^-, HCO_3^-, and SO_4^{2-} play important roles in other industries. Thus, the properties of such aqueous electrolyte solutions were studied. In SAFT1-RPM, except the diameter, the parameters for electrolytes are ion-based. Later, the ion-based SAFT EOS was proposed and called ion-based SAFT2[19, 20].

To represent the properties of aqueous single-salt solutions in the temperature, pressure, and concentration ranges of 298.15 to 473.15 K, 1.013 to 1000 bar, and 0 to 6 mol/kgH_2O in ionic strength, respectively, the short-range interaction between cation and anion was needed to capture the effect of pressure on the properties of electrolyte solutions. A set of parameters at 298.15 K for 5 cations (Li^+, Na^+, K^+, Ca^{2+}, Mg^{2+}) and 7 anions (Cl^-, Br^-, I^-, NO_3^-, HCO_3^-, SO_4^{2-}, CO_3^{2-}) was obtained from the fitting of the experimental mean ionic activity coefficients and liquid densities of 26 aqueous single-salt solutions. An additional set of ion-specific coefficients used in the temperature-dependent parameter expressions for 5 cations (Li^+, Na^+, K^+, Ca^{2+}, Mg^{2+}) and 5 anions (Cl^-, Br^-, HCO_3^-, SO_4^{2-}, CO_3^{2-}) was obtained from the fitting of the experimental mean ionic activity coefficients and liquid densities of 15 aqueous single-salt solutions at low pressures and temperatures up to 473.15 K.

For the properties of aqueous multiple-salt solutions at ambient and elevated temperatures and pressures, the short-range interactions between two different cations were allowed to obtain better representations of the solution properties. The adjustable parameter used in the mixing rule for the segment energy was fitted to the experimental osmotic coefficients of two-salt solutions containing one common anion at various temperatures and low pressures. The predictions of the osmotic coefficients, densities, and activity coefficients of multiple-salt solutions including brine/seawater are found to agree with experimental data. Fig. 3 illustrates the comparison of the density calculated with model and reference data[28] for aqueous NaCl solutions and experimental data for brines[29].

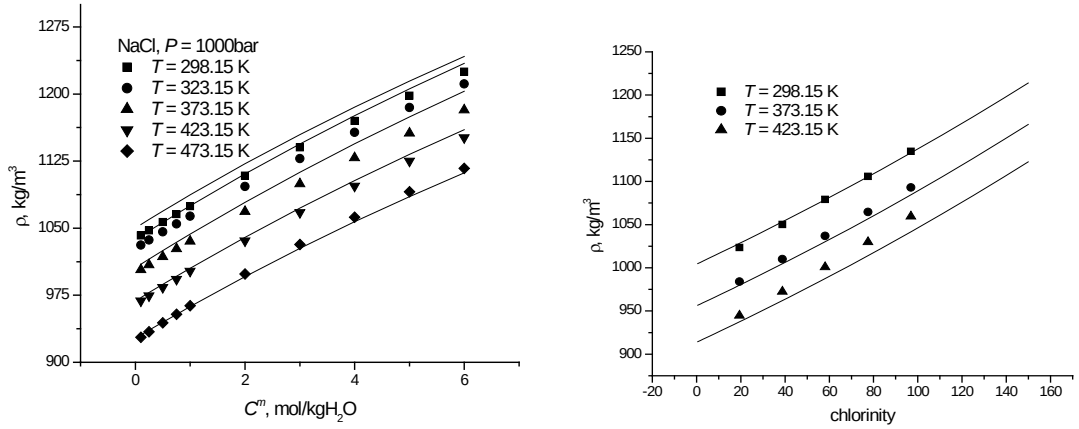

Fig. 3. Density (ρ) for aqueous NaCl solutions and brines. Symbols: experimental data[28, 29]; —, calculation.

3.4. Phase equilibrium for H_2S-H_2O system

CO_2 capture is a former step of CO_2 sequestration. Research reveals that the cost for CO_2 capture is two thirds of the totally cost for CO_2 capture and storage. How to cut the cost for CO_2 capture is one of the main barriers. Generally, H_2S is another main component in flue gases and natural gas fields, the co-injection of H_2S and CO_2 will substantially reduce the capture and sequestration costs, while it will also affect the sequestration capacity and the sequestration process (from solubility to transfer to reaction with rocks). This leads to the significance of the study of the thermodynamics and kinetics for H_2S-CO_2 related sequestration systems.

Thus, the phase equilibrium of the binary system of H_2S-H_2O was represented using ion-based SAFT2[14] in which H_2S was modelled as a molecule with four association sites, i.e., two sites of type S and one site of type H, and sites of the same type did not associate with each other. The parameters of H_2S were fitted to its vapor pressure and saturated liquid density. Cross association between the association site H in H_2S and the site O in H_2O was allowed, and two temperature-dependent parameters were used to describe this cross association. A temperature-dependent binary interaction parameter was used to correct the cross dispersive energy for this binary system. Cross parameters were fitted to mole fractions both in H_2S-rich/vapor and H_2O rich phases[30]. The model is found to represent the phase equilibria from 273 to 630 K and at pressure up to 200 bar[14]. Fig. 4 shows the equilibrium compositions. At 310.93 and 366.48 K, the vapor phase changes to H_2S-rich liquid phase when the pressure increases up to a certain value, while at higher temperatures of 422.04K and 477.49K, no H_2S-rich liquid phase exists in the investigated pressure range. This observation is represented with the model.

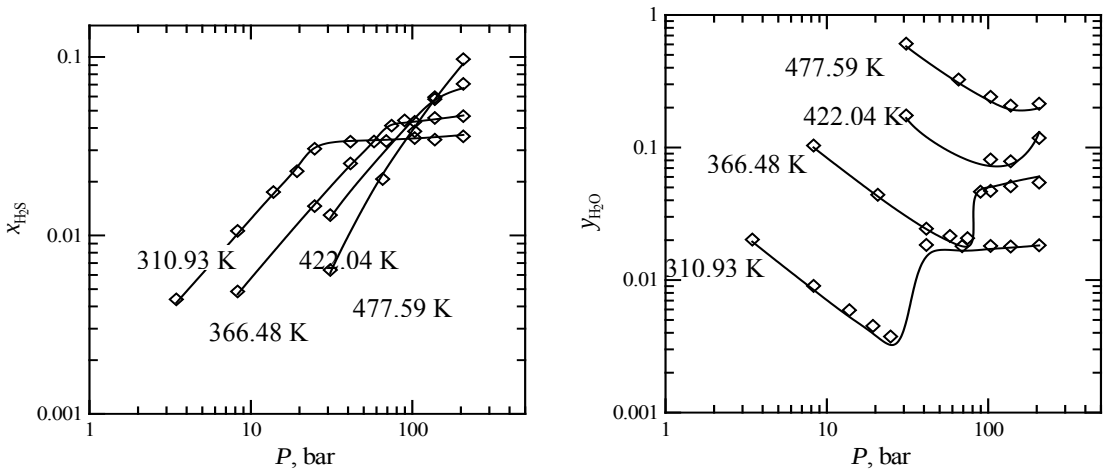

Fig. 4. Mole fractions of H_2S in H_2O-rich phase (x_{H2S}) and mole fractions of H_2O in H_2S-rich/vapor phase (y_{H2O}) for H_2S-H_2O system. ◇: experimental data[14]; —, calculation.

3.5. Perspectives

To represent properties of CO_2-(H_2S)-H_2O-ions (such as Na^+, K^+, Ca^{2+}, Mg^{2+}, Cl^-, CO_3^{2-}), the phase equilibrium and thermodynamic properties for CO_2-H_2S, H_2S-H_2O-NaCl, H_2S-brines, CO_2-brines system are needed to investigated further. In kinetics, the preliminary result reveals the importance of the combination of thermodynamic model with mass transfer model. While the improvement itself relates both the thermodynamic model and the description of the CO_2 sequestration process of solubility, dissolution, transfer, and reaction with rocks. The implementation of the thermodynamic model into the process model to provide reliable long-term prediction pertaining to geochemical carbon sequestration, such as sequestration capacity, CO_2 leakage, and environmental impacts, is another main part of the further work.

4. Conclusions

Storage of CO_2 in deep saline aquifers is one way to limit the buildup of greenhouse gases in the atmosphere, and the co-injection of CO_2 and H_2S may substantially reduce the capture and sequestration costs, and the effect of H_2S on both thermodynamic and dynamic models is also needed to study the sequestration capacity, CO_2 leakage, and environmental impacts. Based on SAFT EOS, the phase equilibrium and densities for H_2S-CO_2-sequestration related subsystems have been investigated and summarized. Meanwhile, using non-equilibrium thermodynamics in which the chemical potential difference as the driving force, preliminary kinetics results were illustrated. The proposed thermodynamic model is promising to represent phase equilibrium and thermodynamic properties for CO_2-sequestration related systems, i.e. CO_2-(H_2S)-H_2O-ions (such as Na^+, K^+, Ca^{2+}, Mg^{2+}, Cl^-, CO_3^{2-}), and it is necessary to implement the reliable thermodynamic model into kinetics model to adjust the non-ideality of species because of the high pressure to investigate the sequestration process.

Acknowledgment

X. Ji and Y. Ji thank the Swedish Research Council for the financial support.

References

[1] Y. H. Ji, X. Y. Ji, X. Feng, C. Liu, L. H. Lu, X. H. Lu, Progress in the study on the phase equilibria of the CO_2-H_2O and CO_2-H_2O-NaCl systems. Chinese Journal of Chemical Engineering 15(3), 2007, pp. 439-448

[2] Z. H. Duan, R. Sun, R. Liu, C. Zhu, Accurate thermodynamic model for the calculation of H_2S solubility in pure water and brines. Energy & Fuels 21(4), 2007, pp. 2056-2065

[3] C. D. Yang, Y. G. Gu, Accelerated mass transfer of CO_2 in reservoir brine due to density-driven natural convection at high pressures and elevated temperatures. Industrial & Engineering Chemistry Research 45(8), 2006, pp. 2430-2436

[4] J. J. Adams, S. Bachu, Equations of state for basin geofluids: algorithm review and intercomparison for brines. Geofluids, 2, 2002, pp. 257–271

[5] A. Riaz, M. A. Hesse, H. Tchelepi, F. M. Orr Jr., Onset of convection in a gravitationally unstable, diffusive boundary layer in porous media. J. Fluid Mech., 548, 2006, pp. 87 – 111

[6] V. Vilarrasa, D. Bolster, M. Dentz, S. Olivella, J. Carrera, Effects of CO_2 compressibility on CO_2 storage in deep saline aquifers. Transp. Porous Media, 85, 2010, pp. 619-639

[7] J. J. Adams, S. Bachu, Equations of state for basin geofluids: algorithm review and intercomparison for brines. Geofluids, 2, 2002, pp. 257–271

[8] X. Y. Ji, S. P. Tan, H. Adidharma, M. Radosz, SAFT1-RPM approximation extended to phase equilibria and densities of CO_2-H_2O and CO_2-H_2O-NaCl systems. Industrial & Engineering Chemistry Research 44(22), 2005, pp. 8419-8427

[9] N. Spycher, K. Pruess, J. Ennis-King, CO_2-H_2O mixtures in the geological sequestration of CO_2. I. Assessment and calculation of mutual solubilities from 12 to 100 degrees C and up to 600 bar. Geochimica et Cosmochimica Acta 67(16), 2003, pp. 3015-3031

[10] Z. D. Li, A. Firoozabadi, Cubic-Plus-Association Equation of State for Water-Containing Mixtures: Is "Cross Association" Necessary? AIChE Journal 55(7), 2009, pp. 1803-1813

[11] E. Perfetti, R. Thiery, J. Dubessy, Equation of state taking into account dipolar interactions and association by hydrogen bonding: II - Modelling liquid-vapour equilibria in the H_2O-H_2S, H_2O-CH_4 and H_2O-CO_2 systems. Chemical Geology 251(1-4), 2008, pp. 50-57

[12] M. C. dos Ramos, C. McCabe, Modeling the phase behavior, excess enthalpies and Henry's constants of the H_2O + H_2S binary mixture using the SAFT-VR plus D approach. Fluid Phase Equilibria 290(1-2), 2010, pp. 137-147

[13] X. H. Tang, J. Gross, Modeling the phase equilibria of hydrogen sulfide and carbon dioxide in mixture with hydrocarbons and water using the PCP-SAFT equation of state. Fluid Phase Equilibria 293(1), 2010, pp. 11-21

[14] X. Y. Ji, C. Zhu, Modelling of phase equilibria in the H_2S-H_2O system with statistical associating fluid theory. Energy & Fuels 24, 2010, pp. 6208-6213

[15] B. McPherson, W. S. Han, B. S. Cole, Two equations of state assembled for basic analysis of multiphase CO_2 flow and in deep sedimentary basin conditions. Computers & Geosciences 34(5), 2008, pp. 427-444

[16] S. P. Tan, X. Y. Ji, H. Adidharma, M. Radosz, Statistical associating fluid theory coupled with restrictive primitive model extended to bivalent ions. SAFT2: 1. Single salt plus water solutions. J. Phys. Chem. B 110(33), 2006, pp. 16694-16699

[17] X. Y. Ji, S. P. Tan, H. Adidharma, M. Radosz, Statistical associating fluid theory coupled with restrictive primitive model extended to bivalent ions. SAFT2: 2. Brine/seawater properties predicted. J. Phys. Chem. B 110(33), 2006, pp. 16700-16706

[18] X. Y. Ji, H. Adidharma, Ion-based SAFT2 to represent aqueous single- and multiple-salt solutions at 298.15 K. Ind. Eng. Chem. Res. 45(22), 2006, pp. 7719-7728

[19] X. Y. Ji, H. Adidharma, Ion-based statistical associating fluid theory (SAFT2) to represent aqueous single-salt solutions at temperatures and pressures up to 473.15 K and 1000 bar. Ind. Eng. Chem. Res. 46(13), 2007, pp. 4667-4677

[20] X. Y. Ji, H. Adidharma, Ion-based SAFT2 to represent aqueous multiple-salt solutions at ambient and elevated temperatures and pressures. Chemical Engineering Science 63(1), 2008, pp. 131-140

[21] Y. H. Ji, X. Y. Ji, X. H. Lu, Modeling Mass Transfer of CO_2 in Brine at High Pressures by Chemical Potential Gradient. Fluid Phase Equilibria, submitted 2010

[22] A. Valtz, A. Chapoy, C. Coquelet, P. Paricaud, D. Richon, Vapour-liquid equilibria in the carbon dioxide-water system, measurement and modelling from 278.2 to 318.2K. Fluid Phase Equilibria 226, 2004, pp. 333-344

[23] R. Wiebe, V. L. Gaddy, The solubility of carbon dioxide in water at various temperatures from 12° to 40° and at pressures to 500 atmospheres. Critical phenomena. J. Am. Chem. Soc. 62, 1940, pp. 815-817

[24] M. B. King, A. Mubarak, J. D. Kim, T. R. Bott, The mutual solubilities of water with supercritical and liquid carbon dioxide. Journal of Supercritical Fluids 5(4), 1992, pp. 296-302

[25] J. Kiepe, S. Horstmann, K. Fischer, J. Gmehling, Experimental Determination and Prediction of Gas Solubility Data for CO_2 + H_2O Mixtures Containing NaCl or KCl at Temperatures between 313 and 393 K and Pressures up to 10 MPa. Industrial & Engineering Chemistry Research 41(17), 2002, pp. 4393-4398.

[26] S. Bando, F. Takemura, M. Nishio, E. Hihara, M. Akai, Solubility of CO_2 in Aqueous Solutions of NaCl at (30 to 60) °C and (10 to 20) MPa. Journal of Chemical and Engineering Data 48(3), 2003, pp. 576-579

[27] B. Rumpf, H. Nicolaisen, C. Ocal, G. Maurer, Solubility of carbon dioxide in aqueous solutions of sodium chloride: experimental results and correlation. Journal of Solution Chemistry 23(3), 1994, pp. 431-48

[28] K. S. Pitzer, J. C. Peiper, R. H. Busey, Thermodynamic properties of aqueous sodium chloride solutions. J. Phys. Chem. Ref. Data 13, 1984, pp. 1-102

[29] B. M. Fabuss, A. Korosi, A. Huq, Densities of binary and ternary aqueous solutions of NaCl, Na_2SO_4, and $MgSO_4$, of sea waters, and sea water concentrates. J. Chem. Eng. Data 11, 1966, pp. 325-31

[30] P. C. Gillespie, G. M. Wilson, Vapor-Liquid and Liquid-Liquid Equilibria: Water-Methane, Water-Carbon Dioxide, Water-Hydrogen Sulfide, Water-nPentane, Water-Methane-nPenatne, RR-48; Utah, 1982

Mineral sequestration for CCS in Finland and abroad

Ron Zevenhoven[1,*], Johan Fagerlund[1]

[1] *Åbo Akademi University, Thermal and Flow Engineering Laboratory, Åbo/Turku, Finland*
** Corresponding author. Tel: +358 2 2153323, Fax: +358 2 2154792 E-mail: ron.zevenhoven@abo.fi*

Abstract: The long-term storage of CO_2 using mineral sequestration is becoming increasingly interesting in many regions, especially where CO_2 underground sequestration is considered impossible or unfeasible. Despite the recognised and documented advantages of CO_2 mineral sequestration, twenty years of R&D work did not yet result in mature, economically viable technology that can be applied on a large scale. Lacking other CCS options while having access to large resources of suitable rock material, a route for carbonation of magnesium silicate mineral is currently being optimised in Finland. It involves the production of magnesium hydroxide, $Mg(OH)_2$ from the mineral followed by carbonation of this in a pressurised fluidised bed reactor. Although the $Mg(OH)_2$ production requires energy the consequent carbonation step is exothermic and the overall process could still be rendered energy neutral. Significant amounts of iron oxides are obtained as by-products. Carbonation levels of ~50% of several 100 μm diameter $Mg(OH)_2$ particles were obtained within 10 minutes at pressures > 20 bar and temperatures up to 500ºC. This paper reports on the latest developments of the work, addressing also process energy efficiency. Also, the large-scale application of this in Finland and at the locations of project partners abroad is briefly addressed.

Keywords: *Carbon dioxide sequestration, Mineral carbonation*

1. Introduction

The long-term storage of CO_2 using mineral sequestration is becoming of increased interest in many regions, especially where CO_2 underground sequestration is not possible or considered unfeasible. At many locations worldwide very large deposits of suitable mineral, usually magnesium silicates (serpentine, olivine) but sometime also calcium silicates (wollastonite) are available. Examples for this are Finland, East-coast Australia, Portugal and regions at the west coast of the USA and Canada. Despite the recognised and documented advantages of CO_2 mineral sequestration (very large capacity, no post-storage monitoring needed, exothermic overall process chemistry) the development work is still in the laboratory demonstration scale: twenty years of R&D work did not yet result in mature technology that can be applied on a large scale in an economically viable way [1,2,3]. Motivated by the slow deployment of large scale underground storage of CO_2 or simply the availability of large amounts of suitable mineral, progress on mineral sequestration is being steadily made and reported from an increasing number of research teams and projects worldwide. Also, increasingly realistic understanding of usable storage capacity for underground sequestration is changing the relative positioning of different CCS methods [4]. As a result, CO_2 mineral sequestration shows a clear trend towards scale-up and commercialisation, as is further illustrated by a significant number of patents awarded quite recently [5,6]. In addition, the issue of what to do with the solid product material has resulted in developments in CO_2 mineral sequestration towards both low value (land reclamation) and high value (pharmaceutics) applications.

Development work in Finland, where the exothermic carbonation chemistry is the reason for focussing on high temperature, gas/solid carbonation at elevated pressures involves cooperation with a growing list of international partners, such as in the Baltic states Estonia and Lithuania but also in the Netherlands, Portugal, UK and more recently also Canada and Singapore. The route for carbonation of magnesium silicate mineral as currently being optimised at Åbo Akademi University (ÅA) in Finland involves the production of magnesium

hydroxide, $Mg(OH)_2$ from the mineral followed by carbonation of this in a pressurised fluidised bed (PFB) reactor. Although the $Mg(OH)_2$ production step requires energy the consequent carbonation step is exothermic and the overall process could still be rendered energy neutral (or even negative). This energy recovery distinguishes the method from other routes for CO_2 mineralisation. In addition, significant amounts of iron oxides are obtained as by-products [7]. Carbonation levels of ~50% of several 100 µm diameter $Mg(OH)_2$ particles where obtained within 10 minutes at pressures > 20 bar and temperatures up to 500 ºC [8-11]. The production of $Mg(OH)_2$ currently requires more heat than is generated by its carbonation, but nonetheless this route shows similar or better energy economics (0.9 - 1.2 vs. 1.0 - 2.3 kWh/kg CO_2 fixed) than the more straightforward route that is widely considered as "state of the art", i.e., direct mineral carbonation of superheated aqueous suspensions under high CO_2 pressure [12, 1 (p. 326)]. The route via $Mg(OH)_2$ also shows (much) faster carbonation kinetics than the conventional process, especially for larger particles – see below for more detail and results. One important benefit of the stepwise approach is that oxides of iron and calcium are obtained as separate by-products, such that magnesite ($MgCO_3$) is the unique carbonation product. The main mineral contaminant (iron oxide) thus extracted is sufficiently abundant to be of interest to the iron- and steelmaking industry [13].

This paper reports on the latest results of the development work where the carbonation of several rock types are compared, addressing the production of $Mg(OH)_2$ and the rate and final level of $Mg(OH)_2$ carbonation, and process energy efficiency. Also, the application of this for large-scale CO_2 mineral sequestration in Finland and at the locations of our project partners abroad will be addressed. This includes the use of the (by-) products of the process which can be used for land reclamation (as is an objective in Singapore), heat storage, or iron- and steelmaking. Finding such uses or markets for the solid products and by-products is essential.

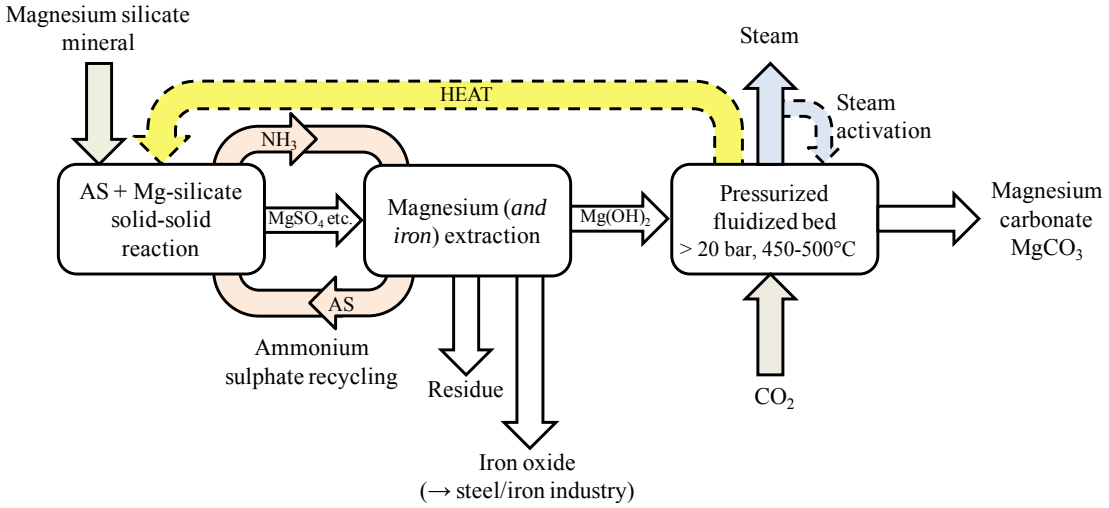

Fig. 1. A schematic illustration of the mineral carbonation process under development at ÅA

2. Process description: serpentinite carbonation via $MgSO_4$ and $Mg(OH)_2$

The staged process under development at ÅA is schematically given in Fig. 1. As raw material, serpentinite rock rich in serpentine ($Mg_3Si_2O_5(OH)_4$) is considered (being abundant in Finland), although most carbonation tests have been made using a commercial $Mg(OH)_2$ sample. Besides this, tests were made with magnesium silicate-based rock material from Lithuania, Portugal, Australia and other locations [14,15]. Table 1 lists selected composition data for some of the materials studied.

Table 1. Composition of some of the magnesium silicate rock samples being studied

Rock	MgO (% wt)	CaO (% wt)	Fe_2O_3 * (% wt)	SiO_2 (% wt)	Al_2O_3 (% wt)	Others (% wt)
Hitura, FI	38.1	0.5	14.8	47.6	10.0	6.2
Vammala, FI	14.5	5.6	12.5	49.5	8.8	9.1
Varena, LT	31.4	1.2	17.6	34.0	0.5	15.3
Braganca, PT	35.8	< 0.1	8.2	41.9	1.2	12.9
Great Serpentine Belt, AU	49.0	< 0.1	6.9	41.9	1.8	0.4

* Calculated, presumably a mixture of FeO and Fe_2O_3, i.e. Fe_3O_4.

2.1. $Mg(OH)_2$ production

In the first process step, (preheated) serpentinite rock is thermally treated with ammonium sulphate (AS) at 400 – 500 °C and atmospheric pressure for 10 – 60 minutes. A significant amount of the magnesium, Mg, in the rock is thus converted to sulphate, $MgSO_4$, which is highly soluble in water. Unfortunately, $MgSO_4$ cannot be directly converted with CO_2 to $MgCO_3$, but in an aqueous solution it can be converted to $Mg(OH)_2$. After cooling, the solid from the reaction with AS is slurried in water, leaving behind unreacted mineral and insoluble reaction products, e.g., silica. The pH of the filtrate solution is raised to 8 – 9, precipitating iron and calcium (from the mineral, see Table 1) as FeOOH and $Ca(OH)_2$, respectively, while increasing the pH further to 10 – 11 precipitates $Mg(OH)_2$. For the Finnish Hitura mineral, the preferable conditions for extraction of Mg (and Fe) to $MgSO_4$ (and $FeSO_4$) are temperatures 400 – 440 °C, for 30 – 60 minutes at S/AS = 0.5 – 0.7 kg/kg, with 60 – 66 % extraction of Mg. Lower temperatures and longer reaction times give a higher (relative) extraction of iron. Ammonia vapour, NH_3, released during the thermal step is collected and used to give the necessary pH increases for precipitation. It is thereafter recovered for regeneration of the AS salt downstream, using heat from another process step. Nonetheless, the recovery of solid ammonium sulphate from the aqueous form incurs a not insubstantial energy penalty.

2.2. $Mg(OH)_2$ carbonation

The $Mg(OH)_2$ produced as described above is converted into $MgCO_3$ in a pressurised fluidised bed (PFB) reactor at pressures > 20 bar and temperatures 450 – 600 °C. Results on conversion levels obtained under varying conditions (temperature, pressure, water content of the gas, time, fluidisation velocity) are reported elsewhere [9-11] for both the synthetic, commercial $Mg(OH)_2$ material and $Mg(OH)_2$ produced from Finnish or Lithuanian serpentinites. A few tests were made under supercritical CO_2 conditions (pressure > 74 bar) which showed significantly lower conversion levels and rates, suggesting that little benefit should be expected from operating at such pressure levels. It was found that the $Mg(OH)_2$ materials produced from the serpentinites are much more reactive (as a result of a ~10× larger specific surface of ~45 m^2/g vs. ~5 m^2/g), giving conversion levels of 50 % within 15 minutes for ~300 μm particles. The product gas from the carbonator is a hot, pressurised mixture of CO_2 and H_2O, the solids obtained will be partly recycled for further carbonation conversion. Unfortunately, although the carbonation reaction is rapid it levels off at a carbonation level of 50-55 % for the synthetic, commercial $Mg(OH)_2$ which may be the result of calcination of $Mg(OH)_2$ to MgO. However, it is noted that in order for $Mg(OH)_2$ to carbonate, dehydroxylation (i.e. calcination) has to occur. Apparently, carbonation takes place at a slower rate than dehydroxylation, resulting in a partially calcined and carbonated product. The amount of $Mg(OH)_2$, MgO and $MgCO_3$ in samples after test is plotted in Fig. 2 as a function of temperature for ~ twenty experiments (CO_2 pressure range 20 – 58 bar) with varying experiment time, fluidisation velocity, particle size, etc.

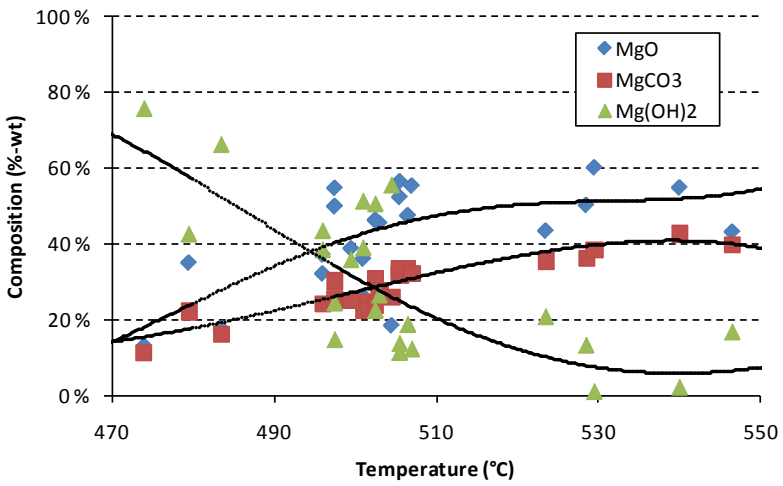

Fig. 2. Composition of Mg-species as a function of temperature for various experimental conditions using a PFB reactor [11].

2.3. Process (energy) efficiency

One of the features of CO_2 mineralisation using magnesium silicates is that the overall chemical reaction is exothermic. However, the direct carbonation of magnesium silicates is too slow, too energy demanding, or otherwise economically unviable, although work on improving the rate of processes based on pressurised aqueous solutions is still ongoing at several locations [3,6]. For the process route presented above an analysis was made of the heat requirement of the thermal treatment of Finnish Hitura (nickel mine tailing) serpentinite (see Table 1) with ammonium sulphate and the heat generated by carbonation of the resulting $Mg(OH)_2$. This showed that producing $Mg(OH)_2$, at 400 – 500 °C will require 4× more heat than what is obtained, at 450 – 550 °C, from carbonating it. Although ~1.2 MJ/kg CO_2 can be recovered as reaction heat the overall heat input requirements add up to 4 – 5 MJ/kg CO_2, consuming 3 – 4 ton rock per ton CO_2 [16]. An improved design using pinch analysis to optimise the heat exchanger network of the process, followed by process simulation with Aspen Plus® and exergy analysis (of the process heat input and outputs) reduces this to ~3 MJ/kg CO_2 heat input requirements while consuming ~3.1 ton rock per ton CO_2. The regeneration of ammonium sulphate (AS), which is obtained as aqueous solution after $Mg(OH)_2$ precipitation (while powdered, dry AS is used in the thermal treatment of serpentinite) puts a high energy penalty on the process [16].

It has been reported [17] that AS crystallisation from an aqueous solution can be accomplished at ~90 °C against a moderate heat input of ~120 kW/m^3 (residence time 95 minutes in a 0.97 m^3 DTB crystalliser). Nonetheless, a less energy consuming alternative for the AS recovery must be found and the solid/solid extraction must be improved, not only for energetic reasons, but also to recover more by-products thereby reducing the amount of solid residue. The rather high solubility of magnesium sulphate and ammonium sulphate in water should allow the use of minimal amounts of water in the precipitation steps towards $Mg(OH)_2$. Further improvement is obtained by optimising the different temperatures in the three aqueous precipitation steps. A variety of process refinements that lead to better energy efficiency, extraction from serpentinite, and AS recovery, was recently reported by Romão et al. [14] A recent study by Björklöf [18] applies mechanical vapour recompression (MVR) for the recovery of AS salt, making use of pinch analysis combined with chemical exergy analysis (in a spreadsheet calculation). The outcome of the study gives an energy penalty of 5.54 MJ/kg CO_2 fixed, expressed as exergy (using conservative data for the magnesium

sulphate solubility in water). Fig. 3 gives a so-called Grassmann diagram that clearly points out the exergy destruction in the various stages. Similar to Romão et al. [14,16] the energy penalty of the process (as exergy losses) was identified to arise primarily from 1) the AS recovery from dilute aqueous solutions, 2) the magnesium extraction using AS, and 3) the cooling of hot extraction products to aqueous solution temperature.

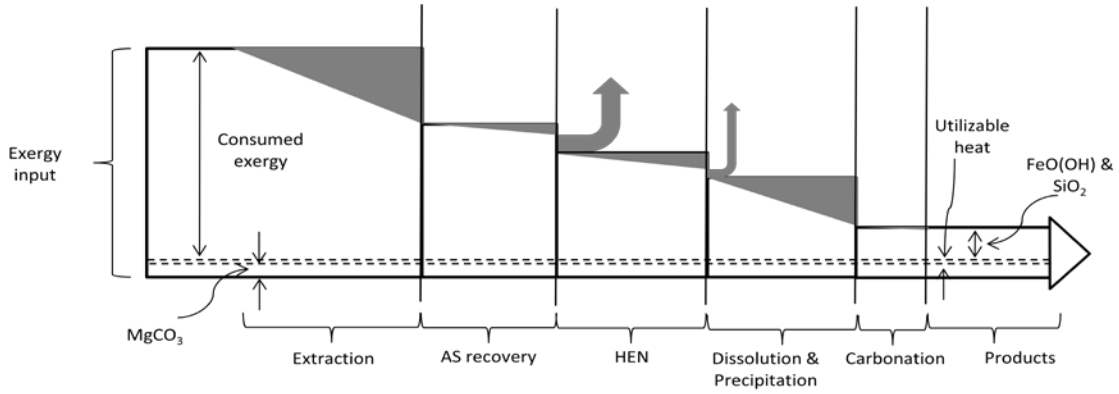

Fig. 3. A Grassmann diagram of the staged ÅA process. The gray triangles represent exergy destruction in the various process steps and the arrows represent exergy losses. At the far right, the products consist of the chemical exergies of the products and the recoverable heat from the carbonation step. [18]

2.4. Magnesium extraction and carbonation efficiency, ammonium sulphate recovery

Besides carbonation efficiencies for $Mg(OH)_2$ in the PFB levelling off at 50-55 % (for a synthetic, commercial sample) also the extraction of magnesium from serpentinite needs improvement, with extraction efficiencies obtained so far seldom exceeding 60% of the Mg content of the rock. For this, development work commences at ÅA, aiming at using a rotary kiln for the magnesium extraction, instead of using a fixed bed ("heap") for the conversion because this requires higher temperatures than necessary to compensate for heat and mass transfer limitations. The excess temperature leads to irreversible loss of the AS salt as SO_2 and N_2O. Detailed chemical reaction and solid product analysis suggest that temperatures should not exceed 400 °C. The possibility of losses of AS, e.g., occluded within the solid residue of unreacted serpentinite, silica etc., or in the $Mg(OH)_2$ fed to the carbonator (probably as NH_4^+ & SO_4^{2-} ions) was addressed by Björklöf [18]. Analysis showed that the solid residue contained < 0.1 %-wt nitrogen and < 0.9 %-wt sulphur which corresponds to ~ 0.15 % and ~ 1.5 %, respectively, of the incoming AS. For the $Mg(OH)_2$ the nitrogen – and sulphur contents were 0.1 %-wt and 0.8 %-wt, respectively.

3. Implementation of the results in Finland and abroad

Finland, like many countries in the EU, has commitments with respect to greenhouse gas emissions under the Kyoto Protocol and a continuation of the use of fossil fuels may be difficult without also implementing a CCS method. In Finland, the following schemes can be considered – see also Fig. 4 for industry sector integration:

- CO_2 from large-scale producers in Central / Northern Finland can be fixed using the vast resources of serpentinite-containing rock (estimated CCS capacity 2.5 – 3.5 Gt CO_2 [19]). One example is Ruukki's iron- and steelmaking plant at Raahe, which is ~110 km from the nickel mine at Hitura where large amounts of mine tailings are deposited. At the same time, large amounts of iron oxide by-products will be obtained from the rock, ready for use at the iron- and steelmaking plant. And, the slag by-products, most importantly steel

converter slag, may be carbonated to yield valuable calcium carbonates of PCC (precipitated calcium carbonate) quality [20].

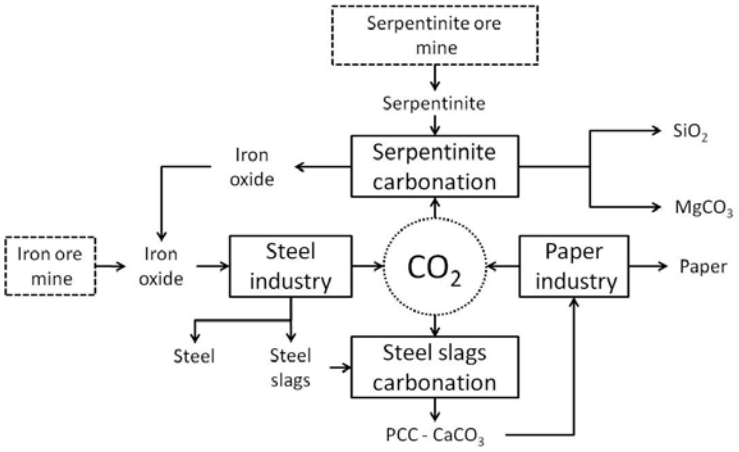

Fig. 4. Integrated processing for magnesium silicate carbonation, iron- and steelmaking and steel slag carbonation [13]

- With most CO_2 produced in Southern Finland, lower-grade minerals than found in Central/Northern Finland must be made use of. At several locations in South / South-west Finland rock with an MgO content of 10-15 %-wt were found, offering potential for source-sink combinations such as
  * Vammala serpentinite for use at the coal-fired plant at Meri-Pori (distance ~ 90 km)
  * Suomusjärvi serpentinite for use at a lime kiln in Parainen (distance ~ 90 km) or at a power plant in Naantali (distance ~ 95 km)

Also abroad the technology can be made use of, for example our cooperation with:

- Lithuania, where significant and suitable (although maybe located somewhat deep) serpentinite were found in the Varena region in the South-east of the country [15]
- In Portugal, suitable rock was located at several locations within the country [14], offering good opportunities for CO_2 mineralisation while also the option of (on-shore) underground sequestration is being investigated [21]
- Singapore, where CCS is combined with land reclamation during the next decade, using rock material that is imported from the region, for example from Australia [22]

In most of the cases, except the last mentioned obviously, CO_2 would be transported to the mineral site. On the other hand, like fossil fuels, metal ores or other raw material also rock transport can be feasible, with the advantage that the carbonation process can operate directly on the CO_2-containing gases. This removes the CO_2 capture step from the CCS chain.

4. Conclusions

The performance and efficiency (with respect to energy and chemicals recovery) of a staged process for serpentinite carbonation as under development at ÅA was described and assessed. It involves the production of magnesium hydroxide, $Mg(OH)_2$ from the mineral using ammonium sulphate, AS (which is later recovered) followed by carbonation of this in a pressurised fluidised bed (PFB) reactor. The process can be considered to be a variety of a process route patented by Pundsack in 1967 [23], which is based on extraction of magnesium from serpentine using an aqueous solution of ammonium bisulphate (ABS). The ÅA route for serpentinite carbonation, instead, uses AS in a high temperature step for magnesium

extraction that proceeds much faster than that with ABS in an aqueous solution (<< 1 h vs. >> 1 h) whilst also the reaction heat release from the carbonation is taken advantage of in the gas/solid reactor. However, recovery of solid ammonium sulphate from the aqueous form incurs a not insubstantial energy penalty. Thus, there seems to be a need to develop an alternative route to $Mg(OH)_2$ that bypasses the aqueous stage, and/or a route in which $MgSO_4$ is carbonated directly, e.g., using ammonium (bi)carbonate produced from CO_2 absorption in (aqueous) ammonia in an upstream scrubbing stage. Ammonium sulphate is a cheap and abundant reagent for extracting magnesium from serpentinite, but its performance must be evaluated under milder conditions as predicted by thermodynamics. The other technical issue linked with its use is the containment of NH_3 in the system.

Ammonium salts, i.e., (bi-)carbonate and (bi-) sulphate, could play an important role for extracting magnesium from rock material and as reactants produced from scrubbing CO_2 from process gases with chilled aqueous ammonia solutions – see for example [24]. An important benefit of the CO_2 mineral sequestration routes that look most promising for scale-up and large-scale application is that the expensive and potentially problematic CO_2 capture stage can be removed from the CCS chain. This is one of the drivers of current interest for CO_2 mineral sequestration. It is also considered for the ÅA process route, although the gas/solid carbonation will require CO_2 partial pressures > 20 ba r. On the other hand, scrubbing CO_2 from a power plant flue gas will introduce water and other species (and potential contaminants) into the process loop, eventually contaminating the sorbent.

Acknowledgements

This work was supported by the Academy of Finland program “Sustainable Energy” (2008 – 2011), with further support from KH Renlund Foundation (2007 - 2009). Thomas Björklöf, Experience Nduagu and Joel Songok of ÅA, Inês Romão of the University of Coimbra, Portugal and Dr. James Highfield of ICES/A*Star, Singapore are acknowledged for valuable comments and contributions.

References

[1] IPCC. Special Report on Carbon Dioxide Capture and Storage. Metz, B., Davidson, O., de Coninck, H.C., Loos, M., Meyer, L.A. (Eds.) Cambridge University Press, 2005.

[2] Lackner, K S. A guide to CO_2 sequestration. Science 300, 2003, pp. 677-1678.

[3] Zevenhoven, R., Fagerlund, J. Mineralisation of CO_2 Chapter 16 in: Developments and innovation in CCS technology M. Maroto-Valer (Ed.), Woodhead Publishing Ltd., Cambridge (UK), 2010, pp 433-462

[4] IEA. Carbon capture and storage – Progress and next steps. IEA/CSLF Report to the Muskoka 2010 G8 Summit. IEA, Paris, 2010, 39 pp.

[5] Delgado Torróntegui, M. Assessing the mineral carbonation science and technology M.Sc. Thesis ETH Zürich, Switzerland, 2010

[6] Zevenhoven, R., Fagerlund, J., Songok, J.K. CO_2 mineral sequestration – developments towards large-scale application. Greenhouse Gases: Science and Technology, 2011, *accepted / in press* doi: 10.1002/ghg3.007

[7] Nduagu, E. Mineral carbonation: preparation of magnesium hydroxide [$Mg(OH)_2$] from serpentinite rock, M.Sc. Thesis, Åbo Akademi University, Finland, 2008

[8] Fagerlund, J. Teir, S. Nduagu, E., Zevenhoven, R. Carbonation of magnesium silicate mineral using a pressurized gas/solid process. Energia Procedia 1, 2009, pp. 4907-4914.

[9] Fagerlund, J., Nduagu, E., Romão, I., Zevenhoven, R. A stepwise process for carbon dioxide sequestration using magnesium silicates. Front. Chem. Eng. China 4(2), 2010, pp. 133-141.

[10] Fagerlund, J., Nduagu, E. Zevenhoven, R. Recent developments on the carbonation of serpentinite- derived $Mg(OH)_2$ using a pressurised fluidised bed. Presented at GHGT-10, Amsterdam (the Netherlands) September 19-23, 2010. (Energia Procedia 2011)

[11] Fagerlund, J., Nduagu, E., Romão, I. & Zevenhoven, R. CO_2 fixation using magnesium silicate minerals. Part 1: Process description and performance. Energy – the Int. J. (special edition ECOS2010), *submitted (October 2010)*

[12] Gerdemann, S.J., O'Connor, W.K., Dahlin, D.C., Penner, L.R., Rush, H. Ex Situ Aqueous Mineral Carbonation Environ. Sci. Technol. 41, 2007, pp. 2587-2593

[13] Zevenhoven, R., Fagerlund, J., Nduagu, E., Romão. I. Mineralisation of CO_2 and recovery of iron using serpentinite rock. Proceedings of R´09, Davos (Switzerland), Sept. 14-16, 2009 (paper 149)

[14] Romão, I., Gando Ferreira, L. M., Fagerlund, J., Zevenhoven, R. CO_2 sequestration with Portuguese serpentinite. in: Proceedings of ACEME10, Turku (Finland) Nov. 29 - Dec.1, 2010, p. 77-87

[15] Stasiulaitiene I., Fagerlund J., Nduagu E., Denafas G., Zevenhoven R. Carbonation of serpentinite rock from Lithuania and Finland. Presented at GHGT-10, Amsterdam (the Netherlands) September 19-23, 2010. (Energia Procedia 2011)

[16] Romão, I., Nduagu, E., Fagerlund, J., Gando-Ferreira, L. M. & Zevenhoven, R. CO_2 Fixation Using Magnesium Silicate Minerals. Part 2: Energy Efficiency and Integration with iron-and steelmaking. Energy – the Int. J. (special edition ECOS2010), *submitted (October 2010)*

[17] O'Meadhra, R., and van Rosmalen, G.M. Scale-up of ammonium sulphate crystallization in a DTB Crystallizer. Chem. Eng. Sci. 51(16), 1996, pp. 3943-3950

[18] Björklöf, T. An energy efficiency study of carbon dioxide mineralization. M.Sc. Thesis, Åbo Akademi University, Finland, 2010

[19] Teir, S. Fixation of carbon dioxide by producing carbonations from minerals and steelmaking slags. PhD (Eng) thesis, Helsinki Univ, of Technol., Espoo Finland, 2008

[20] IEA, Carbon capture and storage: a key carbon abatement option. IEA, Paris, France, 2008. pp. 189-190

[21] Eloneva, S. Reduction of CO_2 emissions by mineral carbonation: steelmaking slags as raw material with a pure calcium carbonate end product. PhD (Eng) thesis, Aalto Univ. School of Sci and Technol., Espoo Finland, 2010

[22] Khoo, H.H., Sharatt, P.N., Bu, J., Borgna, A., Yeo, T.Y., Khor, T.Y., Björklöf, T.G., Zevenhoven, R. Carbon capture and mineralization in Singapore: preliminary environmental impacts and costs via LCA. Sci. Total Environ., *submitted (July 2010)*

[23] Pundsack, F.L., Recovery of silica, iron oxide and magnesium carbonate from the treatment of serpentine with ammonium bisulphate. U.S. Patent 3,338,667, 1967

[24] Hunwick, R.J., System, apparatus and method for carbon dioxide. World patent WO2008101293(A1), Australian patent AU2008000232, 2008

CO_2 capture in oil refineries – an evaluation of different heat integration possibilities for heat supply to the post-combustion process

Daniella Johansson[1,*], Per-Åke Franck [2], Thore Berntsson[1]

[1] *Heat and Power Technology, Chalmers University of Technology, Gothenburg, Sweden*
[2] *CIT Industriell Energi AB, Gothenburg, Sweden*
** Corresponding author. Tel: +46 317723008 Fax: +46 317721152, E-mail:Daniella.johansson@chalmers.se*

Abstract: This paper estimates the costs of CO_2 post-combustion capture for two refineries by comparing different alternatives for supplying the heat needed for the regeneration of the absorbent. The cost of capture ranges from 30 to 472 €/ tCO_2 avoided, depending on technology choice for heat supply and energy penalty for the CO_2 separation. In this study, it is concluded that process integration leads to a reduction in avoidance costs. However, the avoidance cost depends greatly on which system perspective is considered, i.e. whether CO_2 emission changes outside the refinery are included or not.

Keywords: *Carbon capture and storage, Post combustion, Oil refinery, Process integration*

1. Introduction

The oil refining industry generates large amounts of CO_2 emissions. Today and in the future, harder regulations (e.g. the EU ETS system and the Renewable Energy Directive) both on CO_2 emissions from the refinery process and on the refinery products will give new incentives for the oil refining industry to act towards CO_2 mitigation measures. However, the process structure of a refinery implies that even a perfect, energy-efficient refinery will continue to emit significant amounts of CO_2. Carbon Capture and Storage (CCS) is an alternative that can further reduce CO_2 emissions from the oil refining process. The interest in CCS has grown over the past years, among researchers as well as companies. Different capture technologies are possible: post-combustion, oxy-fuel combustion, chemical looping and pre-combustion. However, post-combustion is the most studied technology and is chosen in this paper as a promising technology since it does not require any extensive rebuilding of the existing refinery. Several previous studies have evaluated the costs for CCS at refineries [1-3], but none has been found that has investigated the costs with different heat supply options in combination with future energy market scenarios. Therefore, the aim of this paper is to examine how the avoidance costs for CO_2 in refineries are affected by different heat integration possibilities and future energy market scenarios.

In this paper, the CO_2 avoidance cost for post-combustion carbon capture, with mono-ethanolamine (MEA), is evaluated at two case refineries in the Skagerrak region. The oil refining industry is rather complex and therefore often offers opportunities for process integration which can facilitate substantial cost reductions for the heat supply. In this paper, possibilities to use excess heat from the main process to supply heat to the desorption unit, with or without the need of a heat pump, are evaluated as well as integration of a Natural Gas Combined Cycle (NGCC), a natural gas boiler and a biomass boiler. Also combinations of these alternatives are evaluated which is described in Section 2.1.

2. Studied systems and alternatives with related assumptions

The first case refinery is a hydroskimming refinery (Refinery no. 1) with a crude oil capacity of 6 Mt/y and ca. 0.5 Mt CO_2. The second is a complex refinery (Refinery no.2) with a crude oil capacity of 11.4 Mt/y and ca. 1.9 Mt CO_2. CO_2 emissions from the oil refining process originate from several sources. Only the largest CO_2 emission sources (89% of the total CO_2

emissions) have been selected for capture, resulting in 2 sources (totally 0.45 Mt CO_2/y) for Refinery no.1, and 4 sources (totally 1.7 Mt CO_2/y) for Refinery no. 2.

In this analysis the desorption column in the CO_2 capture unit has a working temperature of 120°C. After capture, the CO_2 is compressed to a pressure of ca. 75 bar with an absorber efficiency of 0.85. In order to generate the absorbent (MEA), large quantities of energy are needed. There are uncertainties regarding the heat demand needed per CO_2 emission captured, and therefore, to handle this discrepancy, two levels of desorption heat demand in the desorption are used, 2800 kJ/kg CO_2 and 4700 kJ/kg CO_2. The heat demand needed for desorption can be satisfied in different ways, and the alternatives used in this paper are described in more detail below. Key figures for the different alternatives are found in Table 1.

2.1. Process integration, utilization of excess heat (EH)

In this alternative the excess heat available above 129°C (EH) has been investigated in order to produce steam for the desorption unit. Two cases are used in Refinery no. 1. First, all excess heat is assumed to be available, presented as EH[1]&HP in Table 1. In the alternative with low heating demand (2800kJ/kgCO_2) enough heat above 129°C is available. However, in the alternative with high heating demand (4700kJ/kg CO_2) a heat pump must be used for supplying the additional heat needed. Second, due to contract regulations the amount of excess heat delivered to the current district heating network is assumed to be reserved. In this case only remaining excess heat is available for heat supply, and additional heat is supplied by a NGCC (EH[2]&NGCC), Biomass boiler (EH[2]&BB) or a Natural gas boiler (EH[2]&NB). Hence, the latter alternatives are a combination of excess heat above 129° (heat left after district heat delivery) and NGCC, BB and NB.

The prerequisites for Refinery no. 2 are different. The current district heat delivery is only a few percent of the excess heat, compared to over 50 percent for the first refinery. According to this fact, the alternative where the current level of district heat is reserved is not examined in Refinery no.2. On the other hand Refinery no.2 has the opportunity to increase the capacity of the current boilers. When evaluating Refinery no.2, the excess heat above 129°C is not enough to cover the whole heating demand for any of the levels of heating demands. Here, several alternatives to supply the additional energy needed are explored. First, a heat pump is used to supply the extra energy, presented as EH[1]&HP. Second, the capacity of the current steam boiler is increased (SP) and a biomass boiler, a natural gas boiler or a NGCC is used to supply the rest of the steam needed, presented as EH[3]&BB, EH[3]&NB and EH[3]&NGCC respectively. In both alternatives the available excess heat above 129°C has been used.

2.2. Heat pump (HP)

The heat pump uses heat available above 90°C at the refinery to produce LP steam (2.3 bar). The configuration is shown in Fig. 1. It is assumed that the temperature drop of available heat, related to the collection of heat from process streams, is 5°C. The heat pump is a semi-open cycle Mechanical Vapour Recompressor (MVR) using water vapour as working fluid [4].

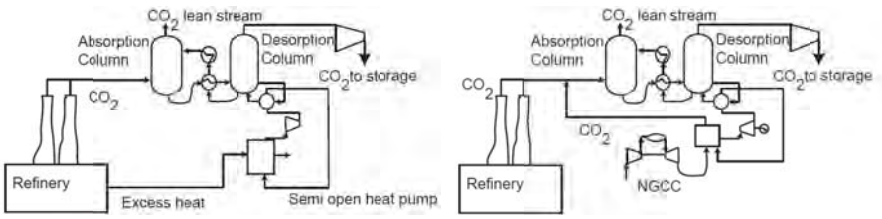

Figs. 1 & 2. The design of the capture unit using a HP (Fig. 1) or a NGCC (Fig. 2) for heat supply.

2.3. Natural gas combined cycle (NGCC)

The NGCC alternative is designed so that the heat recovery steam generator (HRSG) produces enough HP steam (80 bar) to cover the demand of LP steam (2.3 bar) needed for capturing CO_2 generated from both the refinery process and the NGCC; see Fig. 2.

2.4. Biomass and natural gas boilers (BB and NB)

In the biomass boiler alternative, a boiler (with efficiency 0.9) is installed. The boiler produces HP steam (80 bar) that is expanded in a back-pressure steam turbine to produce LP steam (2.3 bar). The boiler capacity is adjusted to produce enough LP steam to cover the heat demand for CO_2 capture from both the current process and the biomass boiler; see Fig 3. The natural gas boiler follows the design of the biomass boiler, except from the efficiency (0.94).

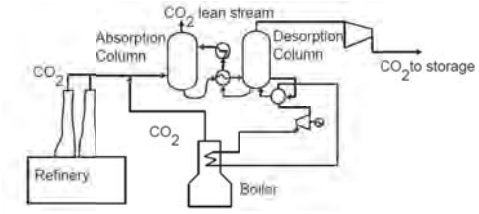

Fig. 3. The design of the capture unit using a biomass boiler or a natural gas boiler for heat supply.

Table .1 Key figures for the case refineries and the studied alternatives. Numbers within parentheses indicate figures for the high desorption heating demand (4700 kJ/kg CO_2). Ref. indicates the current figures for the refinery. In the current refinery (ref.) excess heat used refers to district heat delivery.

Refinery no.1	**Ref.**	**EH[1] &HP**	**NGCC**	**BB**	**NB**	**EH[2]& NGCC**	**EH[2] & BB**	**EH[2] NB**
Natural gas (MW)	19	19 (19)	178 (458)	19 (19)	86 (153)	142 (397)	19 (19)	70 (134)
Biomass (MW)	-	-	-	86 (195)	-	-	58 (195)	-
Excess heat used (MW)	120	37 (62)	-	-	-	129	129	129
CO_2 captured (t/h)	48	48	75 (123)	73 (114)	59 (71)	84 (113)	65 (105)	56 (67)
Electricity import (MW)	21	29 (30)	-39 (-157)	15 (-8)	16 (3)	-21 (-132)	19(-3)	19 (6)
Refinery no.2	**Ref.**	**EH[1] & HP**	**EH[3]& NGCC**	**EH[3] &BB**	**EH[3] &NB**	**NGCC**	**BB**	**NB**
Natural gas (MW)	-	-	118(843)	67 (67)	88 (304)	470(1420)	67(67)	236 (480)
Biomass (MW)	-	-	-	28 (400)	-	-	218 (697)	-
ΔSP[1] (t/h)	-	-	80	80	80	80	80	80
Excess heat used (MW)	27	136 (227)	82	82	82	-	-	-
CO_2 captured (tone/h)	174	174 (174)	195(319)	194 (303)	189 (226)	255 (418)	250 (391)	215 (257)
Electricity import (MW)	654	683 (704)	650(331)	668 (596)	668 (623)	637 (586)	631 (539)	638 (587)

[1,] Increased capacity of the current boiler

3. Methodology

The main methodology in this work is to combine knowledge from process integration in the refinery industry with knowledge about the CCS technology (similar methodology is used in [5]). The methodology and data collection are described by the following steps:

- The potential for steam savings and usage of excess heat from the refinery process are investigated using Pinch analysis. A thorough description of the methodology can be found in several editions; one of the most recently updated is [6]. Heat exchanger cost calculations for collection of excess heat are taken from [7], and used also for calculations for collection of excess heat streams for heat pumping.
  The data regarding the CO_2 capture unit are taken from previous studies of the MEA absorption process [3, 5, 8, 9]. The cost for the capture plant (excluding costs for the energy plant) has originally been taken from studies by Tel-tek [8] and adjusted to fit the refineries studied by using cost information in [9].
- The SGT-800 is assumed to be representative for gas turbines and data are taken from [10]. The size of the gas turbine is scaled to fit the applications studied in this paper, and economic scaling is based on price levels for different NGCC sizes in [11].
- The heat pump is designed using the software IEA Annex 21[4]. Using the chemical engineering plant cost index from 2010, updated investment cost is provided by the software.
- Economic data for the biomass boiler case are taken from [12], including installation and engineering costs, and data for the natural gas boiler are taken from [5].
- To include costs for installation and engineering, the budget prices for all equipment are scaled using a factor 2 (in cases when this is not already included), which is a mean value from [11] and [13]. For the heat exchangers, however, a factor of 3.5 is used [7]. Data for economic calculations for the steam turbines are taken from [14].
- Finally, to evaluate the costs for the different cases, future energy market scenarios are used. The scenarios are based on an energy market model adapted for evaluation of long-term investments in the process industry; a thorough description is found in [15].

3.1. Pinch analysis at the refineries

The pinch analysis only includes streams that are not already integrated (i.e. streams that are heated and cooled with utility, e.g. air). It shows that a significant amount of excess heat is available at Refinery no.1. Theoretical, 54 MW is available above 129°C, and 53 between 90° & 129°C. In the case when the current excess heat used for district heating delivery is inaccessible (EH[2]) the available excess heat is less: 9 MW above 129°C, and 15 MW between 90°C & 129°C. In Refinery no.2 the result shows a theoretically potential of 82 MW available excess heat above 129°C and 145 MW between 90°C & 129°C.

3.2. Economic calculations

In order to evaluate the above-described alternatives, the cost of each avoided tonne of CO_2 emitted is calculated from both a company and a society point of view, in Eqs. (1-5).

$$C_{avoided,company} = \frac{C_{annual}}{CO_{2\_avoided,company}} \quad \textbf{or} \quad C_{avoided,society} = \frac{C_{annual}}{CO_{2,\_avoided,society}} \quad [€/\text{tonne } CO_2] \quad (1,2)$$

$$CO_{2\ \text{avoided, company}} = CO_{2\ \text{before capture}} - CO_{2\ \text{after capture}} \quad (3)$$

$$CO_{2\ \text{avoided, society}} = CO_{2\ \text{before capture}} - CO_{2\ \text{after capture}} + CO_{2\ \text{reduced by replacing electricity production}} \quad (4)$$

$$\text{Where: } C_{annual} = \Delta C_{inv} + \Delta C_{running\ costs} + \Delta E * p_e + \Delta F * p_f - \Delta n_{biomass} * p_{Co2}\ [€/year] \quad (5)$$

ΔC_{inv} = Annualised investment costs (including installation costs)

$\Delta C_{running\ costs}$ = Annual change in running costs except for energy (e.g.MEA costs)

ΔE= Annual change in electricity

ΔF= Annual change in fuel use

$\Delta n_{biomass}$ = Annual captured CO_2 from biomass (from BB)

p_{Co2} = Price of CO_2 permits

p_f = Fuel price

p_e= Electricity price

The avoided amount from a society point of view also includes the CO_2 emissions saved from replacing marginal electricity production, as shown in Fig. 4. In all calculations an annuity factor of 0.1 and operation time of 8000h are used. All costs are calculated in 2010 prices levels. In this paper, CO_2 emissions generated from biomass are evaluated as not included in the EU ETS system. However, since capturing CO_2 emissions from the biomass boiler leads to a reduction of CO_2, and since alternative use of biomass – for example combustion for heat and power production – would otherwise release this CO_2, revenues related to the price of the CO_2 emissions (p_{CO2}) are allocated to the captured CO_2 emissions from the biomass.

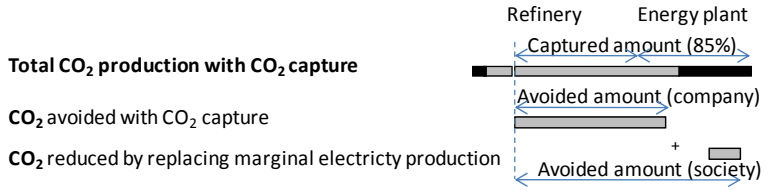

Fig. 4. Description of the avoided amount of CO_2.

3.3. Future energy market scenario

The performance of the CO_2 capture investments is evaluated by using consistent energy market scenarios based on the tool ENPAC [15]. The scenario data are shown in Table 2.

Table 2. Energy market parameters for the different scenario

Scenario	1	2	3	4	5	6	7	8
Fossil fuel price	Low	Low	Low	Low	High	High	High	High
CO_2-price [€/tCO2]	15	27	45	85	15	27	45	85
RES-E support[1] [€/MWh_{el}]	20	20	20	20	20	20	20	20
El price [€/MWh-el]]	56	66	81	87	62	72	87	95
CO_2 from el [kg/MWh_{el}]	679	679	679	129	679	679	679	129
Marginal technology for electricity production	Coal	Coal	Coal CCS	Coal CCS	Coal	Coal	Coal	Coal, CCS
Price of biomass [€/MWh_{fuel}]	26	31	39	56	29	34	42	60
Natural gas price [€/MWh_{fuel}]	33	33	33	33	51	51	51	51

[1]Premium paid to producers of renewable electricity from combustible renewable

By using a number of different scenarios that outline possible cornerstones of the future energy market, robust investments can be identified and the climate benefit can be evaluated. Since CO_2 capture is a technology under development and will most likely not be implemented before 2030, scenarios for 2030 are used. This case consists of eight scenarios which are a result of combining two levels of fossil fuel and four levels of CO_2 prices.

4. Results

The results of the calculated avoidance costs are presented in Figs. 5 and 6, together with the price of the CO_2 emission certificates. The CO_2 price can be viewed as an estimate of the possible income from performing these measures at the refinery.

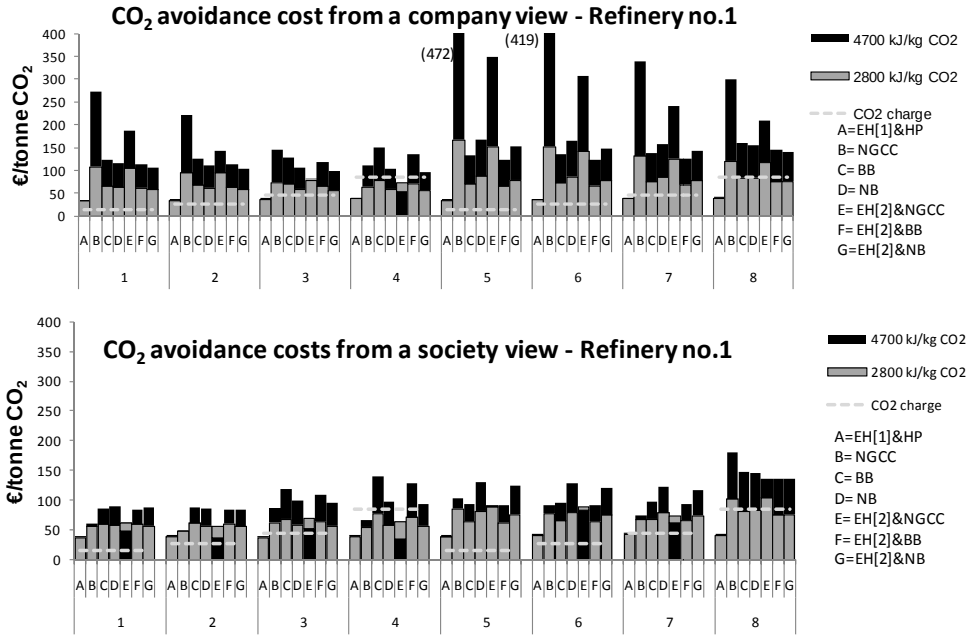

Fig. 5. The avoidance costs (from a company and a society view) for the different alternatives in Refinery no.1. Black bars lower than grey bars indicate that the high heating demand causes lower avoidance costs. Only one bar indicates that the avoidance costs for the two energy levels are similar.

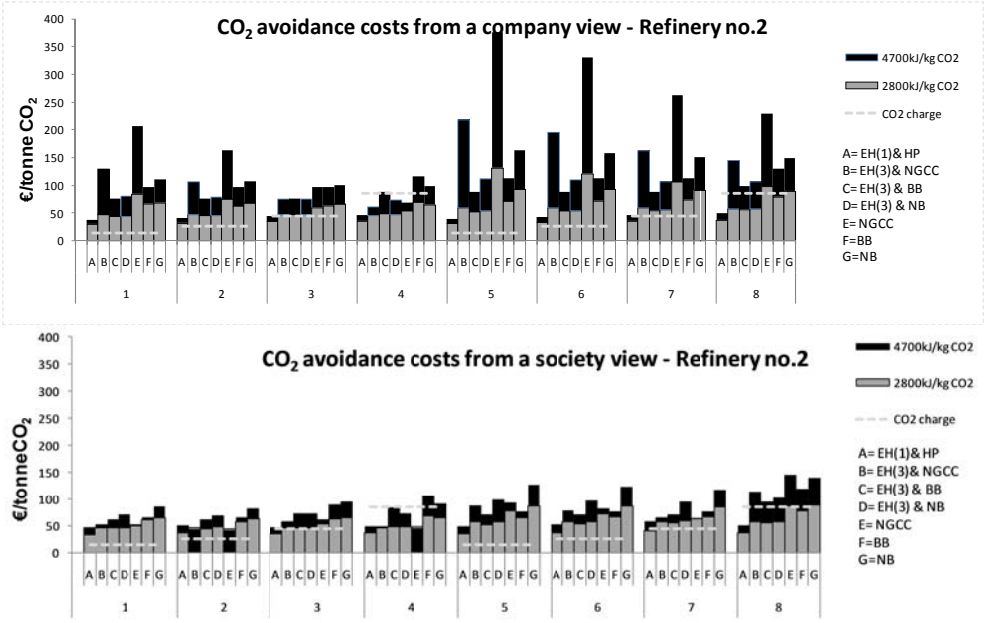

Fig. 6. The avoidance costs (from a company and a society view) for the different alternatives in Refinery no.2. Black bars lower than grey bars indicate that the high heating demand causes lower avoidance costs. Only one bar indicates that the avoidance costs for the two energy levels are similar.

The avoidance costs from a company view are for both refineries, in most scenarios, lowest for the alternatives using excess heat and heat pump. The avoidance costs for these

alternatives are also robust with respect to changes in scenario data, which is due to the relatively small amount of electricity used and the fact that no additional fuel is necessary. Figs. 5 and 6 show that only if the price of CO_2 emissions will become high (85 €/tCO_2), and if excess heat is used to supply the heat demand, could investing in a capture unit be a robust and promising alternative. If the fossil fuel price is low at this level of CO_2 price, several more alternatives could be promising. Moreover, the results from Refinery no. 2 show lower avoidance costs for almost all alternatives compared to Refinery no.1. This can be explained by cheaper investment costs (in relative terms) and the fact that Refinery no. 2 has the opportunity to increase the capacity of current boiler.

When evaluating the costs from a society view, meaning that CO_2 changes outside the refinery are considered, most alternatives will have much lower avoidance costs compared to the results from a company view; see Figs. 5 and 6. The largest impact can be seen for the NGCC alternative. The large generation of electricity from the NGCC implies large CO_2 savings from marginal production of electricity, especially in Scenarios 1, 2, 5, 6 and 7 when marginal electricity producers are coal power plants without CCS. The benefits from including the reduction of CO_2 emissions from electricity production result in a lower avoidance cost for the high heating demand in almost all cases for the NGCC alternatives. The NGCC alternatives (in both refineries) with high heating demand (4700kJ/kg CO_2) have the lowest avoidance costs.

5. Conclusions and discussion

The main conclusion from this study is that process integration of the capture process at the refinery, i.e. use of excess heat and heat pumping, can significantly reduce the avoidance costs for CO_2 capture at a refinery and be a robust and promising alternative at high CO_2 price levels. However, the avoidance cost depends greatly on which system perspective is considered, i.e. including CO_2 changes in marginal electricity production or not. The alternatives with NGCC could be competitive if high heating demand is needed in combination with a high CO_2 price and low fossil fuel prices (an unlikely combination).

Previous research by [1], [2] and [3] examining CO_2 capture at refineries reported capture costs in the range 50-120 €/tCO_2. This study's estimates range between 30 and 472 €/ tCO_2 avoided. However, the previous studies have all used natural gas CHP to supply the extra energy needed, and in this study that alternative ranges from 45 to 168 € /tCO_2 avoided. It should be noted that the estimated costs in other studies arise from different assumptions and the costs can be calculated per CO_2 captured or CO_2 avoided (as in this study and in [1] and [3]). First, different values for the desorption heat are used in the different studies: 2800 kJ/kg CO_2 in [3] , 4700 kJ/kg CO_2 [2] and undefined in [1]. Second, the values for the different costs (e.g. investments and fuel) also arise from different assumptions. In this study, for example, fuel and electricity costs are calculated from future energy market scenarios. Moreover, in this study the transport costs are not included: however, studies by [16] indicate that the costs for transport and storage are around 15-25 €/t CO_2.

Before CCS becomes a commercial technology, a lot can occur with the available excess heat levels and demands at a refinery. This is to be investigated in more detail in other studies. Finally, to improve the cost estimations of the post-combustion capture process, future work would also include a comparison of the avoidance costs for other absorbents, e.g. ammonia.

Acknowledgement

This work has been carried out within the Energy Systems Programme, which is primarily financed by the Swedish Energy Agency, and within the project *CCS in the Skagerrak/ Kattegat region*, which is an intraregional CCS project partly funded by the EU. The work has also been co-financed by Preem AB. Finally, the authors would also like to thank Preem AB for valuable inputs.

References

[1] MT. HO, GW. Allison, DE. Wiley, Comparison of MEA capture cost for low CO2 emissions sources in Australia, International Journal of Green Gas Control.2011;5(1), pp. 49-60

[2] Tel-Tek, CO_2 capture from industrial facilities, Tel-Tek, 2009, Tel-Tek Porsgrunn, Norway, 2009

[3] J. Van Straelen, F. Geuzebroke, N. Goodchild, L. Mahony, CO2 capture for refineries, a practical approach. Energy Procedia. 2009, pp.179-185

[4] IEA Annex 21, Industrial heat pump screening program, IEA Heat Pump Centre c/o SP Technical Research Institute of Sweden, 1997

[5] E. Hektor, Post-Combustion CO_2 Capture in Kraft Pulp and Paper Mills – Technical, Economic and System Aspects, PhD thesis, Chalmers University of Technology, Sweden, 2008

[6] Kemp I, Pinch Analysis & Process Integration – A user guide on process integration for the efficient use of energy, 2nd ed., Butterworth-Heinemann, Oxford, UK, 2007

[7] R. Sinnot, G. Towler, Chemical engineering design, 5th ed., Elsevier Ltd, 2009

[8] Personal communication with Stefan Nyström and Christina Simonsson, Refinery Development, Preem AB, 2010-12-08

[9] Sherif A, Integration of a Carbon Capture process in a chemical industry – Case study of a steam cracking plant, Master Thesis, Chalmers University of Technology, Gothenburg, Sweden, 2010

[10] Siemens SGT-800 brochure, available online 2010-12-3:http://www.energy.siemens.com

[11] Gas Turbine World Handbook, Performance Spec, 2007

[12] E. Pihl, Integrating biomass in existing natural gas-fired power plants – a techno-economic assessment, Lic. Thesis, Chalmers University of Technology, Sweden, 2010

[13] J. Strömberg, P.Å Franck, T. Berntsson, Learning from experiences with Gas-Turbine-Based CHP in Industry, CADDET Analyses Series No.9, 1993

[14] E. Axelsson, Energy Export Opportunities from Kraft Pulp and Paper Mills and Resulting Reductions in Global CO2 Emissions, PhD thesis, Chalmers University of Technology, Sweden, 2008

[15] E. Axelsson, S. Harvey, Scenario assessing profitability and carbon balances of energy investments in industry, The AGS report: 2010: EU1, 2010

[16] McKinsey & Company, Carbon Capture & Storage: Assessing the Economics, 2008

BECCS in South Korea – An Analysis of Negative Emissions Potential for Bioenergy as a Mitigation Tool

Florian Kraxner[1,*], Kentaro Aoki[1], Sylvain Leduc[1], Georg Kindermann[1], Jue Yang[2], Yoshiki Yamagata[2], Kwang Il Tak[3], Michael Obersteiner[1]

[1] *Forestry Program, International Institute for Applied Systems Analysis (IIASA), Laxenburg, Austria*
[2] *Center for Global Environmental Research (CGER), National Institute for Environmental Studies (NIES), Tsukuba, Japan*
[3] *Forestry Department, Kookmin University, Seoul, Republic of Korea*

** Corresponding author. Tel: +43 2236 807 233, Fax: +43 2236 807 299, E-mail: kraxner@iiasa.ac.at*

Abstract: The objective of this study is to analyze the in-situ BECCS capacity for green field bioenergy plants in South Korea. A technical assessment is used to support a policy discussion on the suitability of this mitigation tool. We first examined the technical potential of bioenergy production from domestic forest biomass. For this exercise, in a first step, the biophysical Global Forestry Model G4M was applied in order to estimate the biomass availability. In a second step, the biomass results from the forestry model were used as input data for an engineering model (BeWhere) for optimized scaling and locating of coupled heat and power plants (CHP). The obtained geographically explicit locations and capacities for forest-based bioenergy plants were then overlaid with a geological suitability map for carbon storage. From this, a theoretical potential for in-situ BECCS was derived. Results indicated that, given the abundant forest cover in South Korea, there is a substantial potential for bioenergy production which could contribute to substituting emissions from fossil fuels and to meeting the targets of the country's commitments under any climate change mitigation agreement. However, there seems to be only limited potential for direct in-situ carbon storage in South Korea.

Keywords: *BECCS, Bioenergy, Carbon Capture and Storage, Biomass modeling, Energy policy*

1. Introduction

An active debate in the scientific community is revolving around the possibility of using bioenergy in combination with carbon capture and storage (BECCS), which could remove CO_2 from the atmosphere in order to contribute substantially to achieving low levels of concentration. In the Fourth Assessment Report of the Intergovernmental Panel on Climate Change (IPCC), BECCS is considered "a potential rapid-response prevention strategy for abrupt climate change" and is consequently considered as one of the options to comply with the targets agreed in the Kyoto Protocol [1]. During the last decade it was demonstrated by e.g. [2-4] that terrestrial ecosystems when combined with the use of biomass energy can offer a permanent carbon sink by capturing carbon from biomass conversion facilities and permanently storing carbon in geological formations. However, compared to CCS (Carbon Capture and Storage) combined with conventional fossil fuel systems, very little information can be found in scientific literature so far for both the technical and potential application of BECCS. Moreover, apart from engineering papers presented at e.g. special BECCS conferences such as [5] on Europe, there is - according to our knowledge - to date no literature available that features geographic explicit BECCS applications, especially not for non-European countries.

Although the land base of Korea is small, as much as 64% of the country is forested. Due to a highly efficient and rapid national reforestation program in the 1970s, a majority of the forests in Korea has now reached age classes of 30 and 40 years, which require intensive care in terms of thinning and pruning. By-products from these silvicultural activities can generate a significant amount of raw material to produce e.g. wood pellets and wood chips. Korea

appears further to be an interesting study area for bioenergy, since the country's forestry regained importance both from an ecological as well as from an economical point of view only recently. While trying to build up a bioenergy sector for both energy security and contributing to reduce CO_2 emissions in order to comply with climate change mitigations efforts, sustainable forest management is seen as a key for mobilizing forest biomass for energetic use or direct carbon sequestration. Consequently, ambitious policies and plans for bioenergy production were introduced by the country's government (e.g. "Low Carbon – Green Growth" initiative by the National Energy Plan [6]). However, the lack of forestry infrastructure such as adequate forest roads - for important management activities like harvesting or replanting - causes still too high costs for biomass and related energy production [e.g. 7]. Moreover, this alternative energy sector is facing strong competition from e.g. lower cost fossil and nuclear energy sectors. Hence, being able to better quantify the sustainable bioenergy potential in these countries by identifying economically and biophysically optimized locations for new bioenergy plants and adding value to this information by selecting those locations with promising in-situ combination with CCS technology, policy makers in Korea would be able to develop and support improved and better targeted policies in the area of energy, climate and environment while being supportive to various co-benefits such as rural development, (re-) activation of sustainable forest management etc. The aim of the technical part of our manuscript was threefold. First, to help identifying - in a geographically explicit manner - the available biomass from forest for bioenergy production under sustainable management conditions in South Korea; second, to indicate the optimal size and location of green-field forest biomass-based bioenergy CHP (Coupled Heat and Power technology) plants; and third, to identify the amount and capacity of in-situ BECCS units in South Korea.

2. Method

There are various systems for CCS, such as underground geological storage, ocean storage, mineral carbonation, or industrial use. In this study, we considered the CCS System (with post combustion capture technology) for the underground geological storage into a certain geological formation in the on-shore earth's subsurface. Additionally, we were especially aiming at direct "in-situ" storage. The storage happens in direct vicinity to the combustion units (CHP plants) in order to minimize transport costs and complications. Further we assumed that the total amount of CO_2 - emissions generated at a BECCS unit will be captured and stored in-situ. A technical assessment was used to support a policy discussion on the suitability of this mitigation tool. We first examined the technical potential of bioenergy production from domestic forest biomass. For this exercise, in a first step, the biophysical global forestry model G4M [8] was applied in order to estimate the biomass availability. In a second step, the biomass results from the forestry model were used as input data for the engineering model BeWhere [9] for optimized scaling and locating of CHP plants. The obtained geographically explicit locations and capacities for forest-based bioenergy plants were consequently overlaid with a geological suitability map for carbon storage. From this, a theoretical potential for "in-situ" BECCS was derived.

2.1. The Global Forest Model (G4M)

The Global Forest Model (G4M) from IIASA was used to calculate the growing stock and the sustainable biomass extraction rate. G4M, as described by [8], has been developed in order to predict wood increment and stocking biomass in forests. As input parameter it uses yield power which is achieved through the net primary productivity (NPP) for a specific region. This NPP can be supplied by existing NPP-maps [e.g. 10] or – for higher accuracy – estimated with the help of driver information of soil, temperature and precipitation. The

model can be used like common yield tables to estimate the increment for a specific rotation time. It can further be used to estimate the increment– related optimal rotation time and to provide information on how much biomass can be harvested under a certain rotation time and how much biomass is stocking in the forest. G4M also supplies information on the harvesting losses like needles, leaves and branches which typically remain in the forests under sustainable management. Further, other economic parameters such as harvesting costs - depending on tree size and slope - can be calculated.

2.2. The BeWhere Model

The BeWhere Model - a spatially explicit optimization model, depicting the supply chain of bioenergy industries - was used for the in-situ BECCS assessment [9]. The model, developed at IIASA, considers industries competing for wood resources. On the supply side, forest wood harvests, sawmill co-products (SCP) and wood imports serve as biomass resources for possible new bioenergy plants. Wood demand of pulp-and-paper mills, of existing bioenergy plants and of private households is considered on the demand side The model assumes that the existing wood demand has to be fulfilled, allowing new plants to be built only if there is enough surplus of wood available. The model is spatially explicit and the transportation of wood from biomass supply to demand spots is considered either by truck, train or boat. The model selects optimal locations of green-field bioenergy plants by minimizing the costs of biomass supply, biomass transport and energy distribution. Full costs and emissions at the optimal locations were calculated such that we were able to indicate the BECCS potential for the country under investigation. Spatial distribution of forestry yields was estimated and provided by the G4M, as well as the harvesting costs (as a function of tree size depending on site quality and rotation time) and the slope steepness were provided by the same model.

3. Results

There were 3 complementary main sets of results derived from this study and indicated at country level: 1) the sustainably available biomass potential for harvest together with the national heat demand as a main prerequisite for the installation of green-field CHP plants; 2) the geological suitability for CS (Carbon Storage); and 3) the identified locations for BECCS units together with their individual bioenergy production capacity as well as their carbon capture and storage capacity. All presented geographically explicit data sets were compiled at a 0.25-deg (degree grid cell) resolution (25 x 25 km). We used a conversion factor of 0.5 to estimate dry matter biomass (ton dry matter, tdm) from stem volume irrespective to the tree species. The defined forest harvesting scenarios were based on the amount of extracted biomass, while the baseline for harvesting was considered under a sustainable forest management regime, assuming that the average annual harvesting rate is substantially lower than the annual allowable cut. We further assumed that only stem biomass was extracted from the forest stands and that 100% of the extracted biomass was used for energy production. Following conversion factor for the national currency was applied for economic calculations of harvesting, transport and energy (heat) costs: 1 Korean Won = 0.000908987 USD (2008).

3.1. Biomass availability and energy demand

For our analysis, we assigned a managed forest area of 4,852,330 ha (about 78 % of total South Korean forest area) for biomass extraction dedicated to energy production. This forest area was modeled as an aggregated forest cover map based on GLC 2000 [11], the Relative Human Influence concept for each terrestrial biome [12], a classification of pristine and non-pristine forest [13] and protected area [14]. We excluded the forest area where the Relative Human Influence was less than 50 % and where protected areas designated by IUCN

Categories I – VI were located. For the geographical distribution of the actual growing stock we calculated 555,363,300 m^3 (protected area excluded), which was achieved with the help of the global biomass map [15] which was harmonized with FAO statistics of 2005 [13], while the official national statistics of South Korea reported a total growing stock of 506,376,806 m3 for 2005 [16]. Derived from Korean forest statistics in 2008, we limited the biomass extracted annually for energy production to 0.36 % of the total growing stock (sustainable forest management criteria), amounting 999,653 tdm/year (on average 1.62 tdm/ha-year) - see Fig. 1 for the spatial distribution. Further information for our economic optimization process with respect to costs (wood chip and stumpage price, harvesting and extraction costs) were derived from various Korean resources and adapted to local slope conditions for harvesting operations with different technologies.

In South Korea, the total heat energy consumption was 625,915 GJ/year in 2008 [6]. As input for the energy demand calculations, we geographically weighted the heat demand with the population for 2005 at 0.25 degree resolution and assumed that the average heat demand per person was 0.0127 GJ/person (Fig. 1). The average energy prices for Korea in 2008 were adapted from the national statistics.

The demand-supply optimization routines of the BeWhere model also consider transportation costs (truck, train, ship - derived from [17]), as well as the existing road and railway networks for South Korea which were taken from vmap0 [18], also considering different travel speeds.

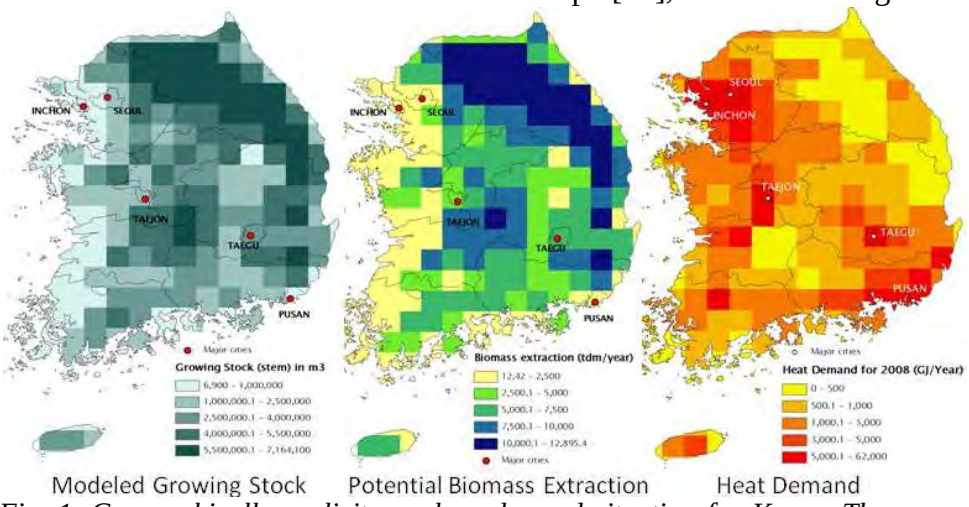

Fig. 1. Geographically explicit supply – demand situation for Korea. The map on the left hand side indicates the modeled spatial distribution of the growing Stock (m^3) in Korean forests (biomass supply). The highest growing stock could be identified in the north-east and the center of Korea (dark pixels). The map in the center indicates the modeled potential biomass extraction rate (tdm/year) - under sustainable conditions - from Korean forests (biomass supply). Highest biomass extraction rates could be achieved also in the north-east and center of the country. The map on the right hand side indicates the modeled spatial distribution of the heat demand (GJ/year). Highest demand was identified around the large urbanized areas (e.g. Seoul) in the western and south-eastern part of the country.

3.2. Identification of geological suitability for C - storage

The geological CS facility can be installed only under specific conditions such as geological characteristics (e.g. tectonic activity, sediment type, geothermal and hydrodynamic regimes) and maturity of infrastructure to build CCS units. In general, sedimentary basins are the sites with the highest potential for geological CS. Suitable sites for geological CO_2 storage can be found on: 1) basins formed in mid-continent locations, 2) basins formed near the edge of stable continental plates, 3) basins behind mountains formed by plate collision such as European

basins immediately north of the Alps and Carpathians, 4) fold belts, and 5) some of the highs [e.g. 1]. Other geological formations such as shield areas (e.g. Scandinavia) or tectonically active areas (e.g. Japan) are less suitable for geological CO_2 storage. However, the suitability for geological CS depends to a great extent on their local conditions. We identified mostly basins as potentially suitable locations for geological in-situ CS in South Korea. The geological map shown in Fig. 2 was mainly based on the studies by [19] and [20]. The location for CO_2 injection can be different from the site of the bioenergy plants where CO_2 emissions occur. In the case of South Korea mainly the geological Gyeongsang Basin located in the south-east of the country could be identified to be potentially suitable for in-situ CS.

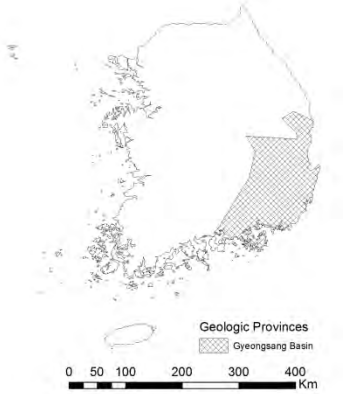

Fig. 2 Potential locations (Geologic Province) suitable for geological CO2 storage in South Korea (on-shore only). Source: modified after [19] and [20].

3.3. Potential in-situ BECCS units identified for South Korea

To identify the optimal locations for green-field bioenergy plants, three different sizes of CHP plants are considered (5, 20, and 70 MW). We assumed that diversification with respect to plant size would on the one hand result in a better distribution of plants within the country, which increases usually also the co-benefits of bioenergy plants. On the other hand we expected to identify more bioenergy plants suitable for in-situ CS. Within each scenario (plant capacity) the aim was to meet the target for the maximum sustainable biomass extraction (about 1 M tdm/year).

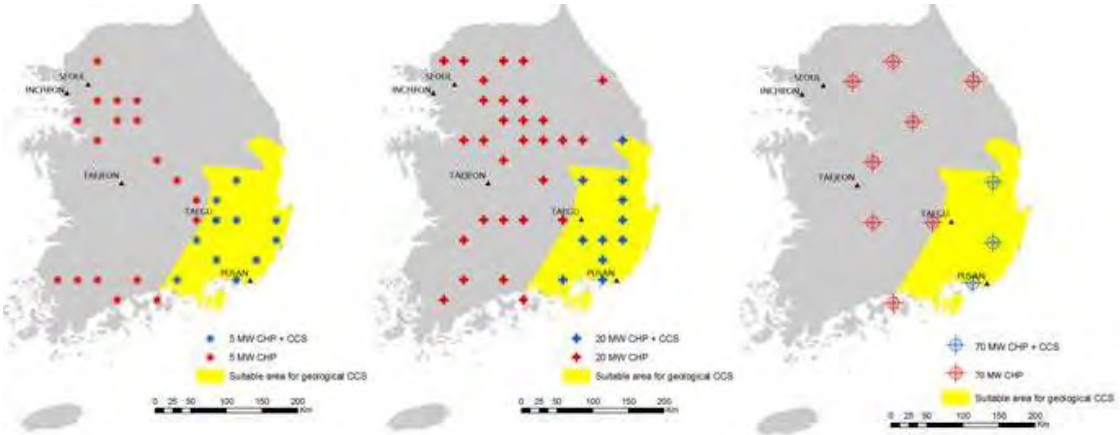

Fig. 3. Three different scenarios (from left to right 5; 20; 70 MW) for optimized green-field biomass plant locations in South Korea. The geographic explicit location of bioenergy plants without CCS is indicated in red color and the BECCS unit locations are indicated in blue color on light yellow background (geologically suitable formation for CS).

For this study we defined in-situ CS suitability such that the bioenergy plant needs to be located within a 0.5 degree grid cell (about 55 x 55 km) of the suitable geologic province in

order to directly inject CO2 underneath a plant or at any place up to a maximum of 25 km radius distance (e.g. with the help of a short pipeline).

Based on these assumptions, Fig. 3 shows the optimized location in a geographically explicit manner by plant size. Table 1 indicates the optimized amount of green field bioenergy plants for Korea, listed by plants with and without in-situ CS suitability, divided into the different plant capacity categories.

Table 1. Energy produced, emissions substituted and CCS Capacity by forest biomass CHP plants with/without BECCS system under a sustainable forest biomass production regime.

Plant size Technology	5 MW **NO** CCS	20 MW **NO** CCS	70 MW **NO** CCS	5 MW CCS	20 MW CCS	70 MW CCS
Plant #	18	29	8	11	11	3
Biomass used (tdm/year)	117,000	716,300	712,400	71,500	271,700	267,150
Heat produced (GJ/year)	1,190,475	7,288,353	7,248,670	727,513	2,764,548	2,718,251
El. produced (GJ/year)	757,575	4,638,043	4,612,790	462,963	1,759,258	1,729,796
Subst. emissions (tCO_2/year)	215,516	627,050	625,036	131,704	237,847	234,389
CCS Capacity (tCO2/year)	***0***	***0***	***0***	***131,704***	***237,847***	***234,389***

We could identify a maximum of 40 green-field bioenergy plants under the 20 MW-scenario of which 11 plants were located on geologically suitable ground in order to meet the criteria for BECCS units. Under the 5 MW scenario, 29 bioenergy plants were optimally distributed over the country, among which also 11 plants qualified as BECCS plants. Under the 70 MW scenario a total of 11 bioenergy plants were computed of which 3 met the criteria for BECCS units. In the best case (20 MW scenario), the "BECCS-effect" (emissions accounted as negative) could reach a potential capacity of some 238,000 tons of CO_2 to be directly stored permanently belowground per year and to be accounted as negative emissions.

4. Discussion and Conclusions

Our BECCS exercise offers several new insights to the bioenergy sector in South Korea and provides crucial information for policy support and design. First of all, it is important to note that even under our rather conservative assumptions – especially with respect to sustainable biomass extraction - we still could theoretically produce some 10% of the present heat demand (being equivalent to a 20 times increment of the present bioenergy share for heat production in Korea [21]), and 1.3% of the total electricity produced in South Korea (15 times the present bioenergy share for electricity production [21]). These results indicate a substantial potential of bioenergy growth in South Korea – especially given the present policies and targets of the National Energy Plan to e.g. increase the bioenergy share in total energy production from 0.2% (2007) to 3.4% by 2030 [6].

Among the 3 different scenarios (plant capacities), the 20 MW scenario turned out to offer the best country-wide coverage with its 40 green-field bioenergy facilities, which consequently could provide direct and indirect co-benefits such as driving the green economy, i.e. providing job opportunities both at the facility and in the biomass production. Another major benefit of growth in the bioenergy sector would be the resulting investments in forest and forest management primarily by small-scale forest owners, e.g. in forest infrastructure. These benefits are based on the assumption that forest biomass would see a price increase, which justifies investments into forest infrastructure (to harvest the biomass more easily) which lowers harvesting costs and increases competitiveness.

Although the suitable geological formations for in-situ CS in South Korea are limited to about 1/5 of the country area (the Gyeongsang Basin), with the help of this study we could show that there is a theoretical potential for 3 (70 MW plants) to 11 (5 / 20 MW plants) green-field BECCS plants with in-situ CS. Based on our assumptions, the BECCS-effect might amount to 130,000 – 240,000 tons CO_2 per year in addition to a similar amount of substituted fossil fuel emissions. This means that about 3-4% of the total demand for heat energy in South Korea could be produced in BECCS plants with in-situ CS. As a consequence, 3-4% of the fossil fuel emissions could be substituted and additionally accounted as negative because they would be actively removed from the atmosphere by BECCS plants. This BECCS effect comes additionally to the biomass co-benefits discussed earlier and could be used as a key issue for future policy design and decision makers.

However, the BECCS effect - and with it a crucial lever for climate, environment and rural development policies - could certainly be substantially increased and strengthened. An important caveat to bear in mind is that with our study we only could point out the theoretical potential without considering the costs of the actual CCS process. If bioenergy plants with higher capacities would be applied, costs could be substantially decreased (scale effect or poly-production). Further, although the suitable geological formations for geological CCS appearing in South Korea are limited (e.g. earthquake and volcanic activity), there are wide off-shore prospective areas in this region (e.g. East Sea). Using further capacity for CS (non in-situ), basically all substituted emission from bioenergy production could additionally be stored and accounted as negative. The use of a (trans-national) CO_2-pipeline could actually boost the BECCS effect and lower the costs, but further research needs to be done in this field. Also the joint use of off-shore CS together with e.g. Japan would substantially increase BECCS capacity, which requires similar research to be extended to South East Asia, potentially using a higher data resolution than 0.25-deg.

We conclude that policy targeted bioenergy-based re-activation of forest management in South Korea would evoke a real win-win-situation. First, bioenergy production and BECCS would directly contribute to meet ambitious climate change mitigation targets. Second, the forest ecosystem would benefit from sustainable management (including thinning etc.) e.g. in terms of improved forest health, stand stability and lower exposure to threatening hazards like wind throw or pests. Third, the forest owners - and with them the forest sector industry - would benefit from an increased value of the forest property, from better prized forest products, as well as from a higher quality of the grown timber and competitive harvesting conditions as a consequence of investment into forest infrastructure. And last not least, society would benefit through e.g. an improved protective function (from e.g. flooding, landslides, avalanches etc.) and an increased recreational value of the forest.

References

[1] IPCC, Special Report on Carbon Dioxide Capture and Storage. ISBN-13 978-0-521-86643-9. Cambridge University Press, 2005.

[2] M. Obersteiner, C. Azar, P. Kauppi, K. Möllersten, J. Moreira, S. Nilsson, P. Read, K. Riahi, B. Schlamadinger, Y. Yamagata, J. Yan, J-P. van Ypersele, Managing climate risk, Science 294(5543), 2001, pp. 786–787.

[3] F. Kraxner, S. Nilsson, M. Obersteiner, Negative emissions from BioEnergy use, carbon capture and sequestration (BECS)—the case of biomass production by sustainable forest management from semi-natural temperate forests, Biomass and Bioenergy 24, 2003, pp. 285–296.

[4] C. Azar, K. Lindgren, M. Obersteiner, K. Riahi, D.P. van Vuuren,· K.M.G.J. den Elzen, K. Möllersten,·E.D. Larson, The feasibility of low CO_2 concentration targets and the role of bio-energy with carbon capture and storage (BECCS). Climatic Change 100, 2010, pp. 195–202.

[5] F. Kraxner, G. Kindermann, S. Leduc, K. Aoki, M. Obersteiner, Bioenergy Use for Negative Emissions – Potentials for Carbon Capture and Storage (BECCS) from a Global Forest Model Combined with Optimized Siting and Scaling of Bioenergy Plants in Europe. Paper presented at the First International Workshop on Biomass & Carbon Capture and Storage October 2010, University of Orléans, France, 2010.

[6] Korea Energy Management Corporation, 2010, available at: http://www.kemco.or.kr/new_eng/main/main.asp

[7] F. Kraxner, J. Yang, Y. Yamagata, Attitudes towards forest, biomass and certification – A case study approach to integrate public opinion in Japan. Bioresource Technology, 100(17), 2009, pp. 4058–4061.

[8] G. Kindermann, M. Obersteiner, B. Sohngen, J. Sathaye, K. Andrasko, E. Rametsteiner, B. Schlamadinger, S. Wunder, R. Beach, Global cost estimates of reducing carbon emissions through avoided deforestation, PNAS 105(30), 2008, pp. 10302-10307.

[9] S. Leduc, E. Schmid, M. Obersteiner, K. Riahi, Methanol production by gasification using a geographically explicit model. Biomass and Bioenergy, 33(5), 2009, pp. 745-751.

[10] S.W. Running, Terrestrial remote sensing science and algorithms planned for EOS/MODIS. International Journal of Remote Sensing 15, 1994, pp. 3587-3620.

[11] JRC Global Land Cover 2000 version 1. Database. Joint Research Centre, European Commission, 2000, http://bioval.jrc.ec.europa.eu/products/glc2000/products.php

[12] WCS-CIESIN, Last of the Wild Data Version 2, 2005 (LWP-2): Global Human Footprint data set (HF), 2005, http://sedac.ciesin.columbia.edu/wildareas/downloads.jsp#infl

[13] FAO Global Forest Resources Assessment 2005. FAO Forestry Paper 147. Food and Agriculture Organization of the United Nations, Rome, 2005.

[14] UNEP-WCMC, World Database on Protected Areas (WDPA), United Nations Environment Programme World Conservation Monitoring Centre, 2009.

[15] G. Kindermann, I. McCallum, S. Fritz, M. Obersteiner, A global forest growing stock, biomass and carbon map based on FAO statistics. Silva Fennica 42(3), 2008, pp. 387-396.

[16] Korea Forest Service, Statistical Yearbook of Forestry 2009. Korea Forest Service, Daejeon, 2009.

[17] P. Börjesson, L. Gustavsson, Regional Production and Utilization of Biomass in Sweden. Energy 21, 1996, pp. 747-764.

[18] National Imagery and Mapping Agency, World roads (VMAP0) Fairfax, VA: National Imagery and Mapping Agency, 1997

[19] J.B. Bradshaw, T. Dance, Mapping geological storage prospectivity of CO_2 for the world sedimentary basins and regional source to sink matching, GHGT-7, September 5–9, 2004, Vancouver, Canada, v.I, pp. 583-592.

[20] USGS, U.S. Geological Survey World Petroleum Assessment 2000 - Description and Results, DDS-60. United States Geological Survey, 2001.

[21] IEA, International Energy Agency, Country Statistics, 2008, available at: http://www.iea.org

What are the rules for biofuel carbon accounting?

Eric P Johnson[1,*]

[1] *Atlantic Consulting, Gattikon, Switzerland*
** Corresponding author. Tel: +41 44 772 1079, E-mail: ejohnson@ecosite.co.uk*

Abstract: Most quantitative assessments of biomass fuels or biofuels assume that bioenergy is inherently carbon neutral, that biogenic emissions of carbon dioxide should be excluded from a carbon footprint. This 'carbon neutral' assumption makes an enormous difference in carbon accounts and in the policies that those accounts would suggest. For instance, if harvested logs burnt as fuel are considered carbon neutral, their carbon footprint is far lower than that of natural gas. However, if the logs' biogenic carbon emissions are counted, then their carbon footprint is much higher than gas's. Moreover, this can lead to absurd conclusions. If carbon neutrality is presumed, it makes no difference to a carbon footprint if a forest is standing or if it has been chopped down for fuel wood. Since the mid-1990s, some researchers have contradicted the 'carbon neutral' assumption, and their view that biogenic emissions should be counted has begun to attract significant attention of policy makers. This paper reviews the history and current state of biogenic-carbon accounting rules, including the ISO/CEN rules being developed under the EU Renewable Energy Directive. Without taking sides, it will define the debate for researchers and policy-makers, reflect on its significance and suggest possible means of resolution.

Keywords: *biofuels, carbon accounting, carbon neutral*

1. Introduction: The premise of carbon neutral

In the fields of life-cycle assessment and carbon footprinting, biofuels traditionally have been considered as inherently carbon neutral: biogenic emissions of carbon dioxide are excluded from the inventory or footprint. Two landmark studies in the field, (Argonne Labs GREET) and (Joint Research Centre of the EU Commission, EUCAR et al. 2008) take this position as given, and many other studies follow their leads.

More recently, however, some researchers have begun to question this approach. Probably the best-known are (Searchinger, Hamburg et al. 2009), but the issue had already been raised by others, namely (Rabl, Benoist et al. 2007) and (Johnson 2009). More recently (Manomet Center for Conservation Sciences 2010) published a large report that questioned the 'carbon-neutral-assumption'. The International Energy Agency's (IEA) Bioenergy Task 38 group, 'Greenhouse Gas Balances of Biomass and Bioenergy Systems', has also raised questions[1], particularly from (Berntsen and Peters 2010) and (Cowie 2010).

Some regulators appear to be taking these questions seriously. The (Manomet Center for Conservation Sciences 2010) report was commissioned by and adopted by the US Commonwealth of Massachusetts with respect to its regulation of biomass-fueled power plants. Presumably Task 38 is being taken seriously by IEA member governments, and at the United Nations level, the idea of that REDD (Reducing Emissions from Deforestation and Forest Degradation) is generally desirable seems to be undisputed.

Furthermore, the issue has come into the domain of standards organizations. Technical Committee 383 at CEN is working on norms in this area, as is ISO Project Committee 248 (of which the author is a member).

[1] See a March 2010 conference record at http://ieabioenergy-task38.org/workshops/brussels2010/

And what is the question? Primarily it is this: should biofuels be considered inherently carbon neutral? The first-generation position was yes (although it was more an assumption than an answer to a question); the emerging position is at minimum not an automatic yes, but a definitive second-generation answer is yet to be determined fully.

The importance of this question, in environmental terms, is very high. Biofuels are clearly the main solution proposed by governments to the twin problems of climate change and energy security. Non-bio, non-fossil energies – such as solar, tidal and wind – are and will for the medium term be marginal contributors, whereas biofuels are aimed at taking, for instance, a 20% share of the EU energy mix by 2020. If these biofuels turn out to be, relative to conventional fossil fuels, carbon negative rather than positive, then their subsidies will not only have cost billions[2], they will also have worsened rather than mitigated global warming!

This paper is meant to elaborate the issue from the perspective of carbon footprinting. After a brief statement of method, it presents results, i.e. characterization of the 'carbon neutral' question from six different methodological perspectives. It concludes with findings and suggestions for further study.

2. Method

The author has reviewed the literature as well as the political and the standards documentation, and then refracted these in the light of carbon-footprint methods.

3. Results: how the 'carbon neutral' question can be categorised

Using the method of carbon footprinting or life-cycle assessment, the question of biofuel carbon neutrality can be characterized in six ways, which are described in the following six subsections.

3.1. Boundary of the system

In impact analyses such as life-cycle assessment or carbon footprinting, for a full life-cycle the ideal boundary is 'cradle-to-grave', i.e. from the environment to the environment. As the ISO standard for life cycle assessment (ISO 2006, section 5.2.3) expresses it: "Ideally, the product system should be modelled in such a manner that inputs and outputs at its boundary are elementary flows." In other words, the life-cycle boundary begins and ends with human intervention. Purely natural processes – biogenic as opposed to anthropogenic – are not included.

Growing of crops, say as feedstock for fuel, is of course an anthropogenic activity. Fields of rapeseed, soybeans or wheat do not spring up on their own. The carbon released in creating and maintaining such fields (so-called 'land-use change' emissions), as well as the carbon emitting in cropping them, is included in current assessments; however, the carbon taken in during a growing season is netted out against the carbon emitted in combustion. And this seems consistent with the boundary definition above.

But what about a natural forest? If human activity was not needed to create it, why should its carbon emitted in combustion – clearly a human activity – be netted against carbon taken from the atmosphere to create the trees? This seems inconsistent with the human/nature

[2] OECD countries' annual subsidy of biofuels in 2007 was estimated at about $15 billion.

boundary applied to other assessments. To be consistent, human harvesting of natural forests should not be netted against their biogenic creation. (Plantations are a different matter; they are created by humans.) This would be consistent with how harvest of other natural resources – say, oil or limestone – is treated in LCA and footprints. Harvest of these is not netted against their creation.

3.2. Temporal definition of the system

In common usage, the terms biofuels and renewables are actually misnomers. Surely conventional oil and gas, which are derived from long-dead plants and animals – are biofuels? And solar power, as astrophysicists tell us, is not renewable. The sun is does not recycle its hydrogen, and in some millions of years will burn itself out. These observations are more than just amusing. They point out the temporal boundaries placed implicitly on LCAs and carbon footprints. To be careful in carbon accounting, analyses should recognize such temporal boundaries explicitly.

Also, researchers should consider the theoretical basis for granting carbon credits to biofuels, yet not doing so to fossil-biofuels. At present this appears to be done out of intuition – not out of thought-through reasoning. The reasoning should be developed, or the practice should be ended.

People often justify 'carbon neutrality' of biofuels by saying: 'the tree will grow back'. If it grows back in 10 minutes, fine. But what if if grows back in 10 years, or 100 years? Surely there is an inflection point (and it could be calculated) as to when the grow-back timing changes from favourable to unfavourable.

3.3. Shadow/alternative/counterfactual scenarios

If we had not grown a crop to be used as fuel, what would have happened to the carbon balance then?

This idea of a 'shadow' or alternative scenario, sometimes called 'the counterfactual', is not present in most studies of biofuels. In a 2008 survey of over 100 publications by 56 researchers about solid biomass fuels (Johnson 2009), not one of them postulated a shadow scenario. After extensive work on liquid biofuels over the past eight years, the author is aware of only two researchers who have applied it in this area: (Joint Research Centre of the EU Commission, EUCAR et al. 2006) and (Heinen and Johnson 2008).

Broader research by (Manomet Center for Conservation Sciences 2010) and IEA Task 38 suggest that shadow scenarios should be standard, not the exception. Moreover, the idea of REDD (Reducing Emissions from Deforestation and Forest Degradation) in the UNFCCC and the idea of 'additionality' in the Clean Development Mechanism (CDM) and elsewhere, both suggest that counterfactuals should be customary.

3.4. Allocation

There are two open issues here. One is allocating carbon burden to crop components by weight. This has led to the dubious practice of assigning the majority of a grain footprint to the straw that is grown along with the grain. Dubious yes, but it has been applied in numerous studies for the German government, only a few years ago, that the government then promoted.

The other is the allocation of CO_2 capture, i.e. the removal of carbon dioxide from the atmosphere by photosynthesis. Why is the captured CO_2 always allocated to a biofuel? Why

cannot a fossil fuel take that carbon credit? Or should the credit be shared proportionately between the two? The answers here are not immediately obvious, but even more obvious is that the questions appear not to be asked in most studies – and yet they should be.

3.5. Marginal/consequential modelling

Simply put, current practice presumes that every additional unit of biogenic CO_2 emitted is recycled to the biosphere via photosynthesis – from the earth to the earth. By contrast, every additional unit of fossil CO_2 emitted stays in the atmosphere, creating more heat.

Yet as pointed out in the allocation discussion, this cannot make sense: carbon dioxide is carbon dioxide. Also, the ability of the biosphere to capture carbon can and does change, depending particularly on forest conditions and water-saturation levels. Once again, the answers here are not immediately obvious, but the questions should be addressed.

3.6. Additionality and subtractionality

The idea of additionality may be useful in creating accurate accounts of forest carbon. If a forest is planted on previously non-forested land, with the express intent of using the harvested trees as biofuel, then this might properly be considered as carbon neutral. Indeed, it probably is carbon negative: although carbon is being harvested, on a net basis, more carbon might be returned to the soil and the vegetation above.

Likewise, what about 'subtractionality'? If trees are being harvested for fuel that otherwise would have remained standing, their carbon surely should be removed from the forest's carbon stock, and debited against the footprint. The case for this has been made by (Rabl, Benoist et al. 2007), (Johnson 2009) and (Searchinger, Hamburg et al. 2009), but the term subtractionality – you first heard it here.

4. Discussion and conclusions

This paper has raised more questions than it has answered – and that is its intent. Without addressing these questions, carbon accounting will continue to be wildly inaccurate. And 'wildly' is no overstatement: the current discussion in CEN and ISO[3] of biofuel standards demonstrates how divergent current opinion is on these issues.

Getting more convergent opinion is important, and not just for the reputation of LCA and carbon footprint analysts, who often are cursed with the epithet of 'you can get any answer you want'. More convergence will be critical to investors, policy makers and the general public. If we really believe that reducing carbon emissions is critical to our future, the questions raised in this paper are worth serious exploration.

To conclude, there might be a simple principle to guide further research: *efficiency is the key*. The source of carbon is surely less important than the efficiency by which it is used. Moreover, efficiency also drives economics; efficient fuels generate the most consumer demand. Efficiency can and should guide the evaluation of future fuels, and the rules of carbon accounting should be constructed to promote this.

Put another way, the key to reducing atmospheric concentrations of carbon is to put less carbon up there in the first place and to keep more of it down here on the ground. We should

[3] The author is a delegate and part of the ongoing discussions.

be more worried about how much net carbon is being emitted, and less worried about which kind of carbon, i.e. biogenic or fossil, is being emitted. If we use this simple concept as our guide, I think we will make much greater progress toward solving this great problem.

References

[1] Argonne Labs GREET, Greenhouse Gases, Regulated Emissions, and Energy Use in Transportation, Version 1.8c.

[2] Joint Research Centre of the EU Commission, EUCAR, et al. (2008). Well-to-Wheels analysis of future automotive fuels and powertrains in the European context.

[3] Searchinger, T. D., S. P. Hamburg, et al. (2009). "Fixing a critical climate accounting error." Science 326 (23 October 2009): 527-528.

[4] Rabl, A., A. Benoist, et al. (2007). "How to Account for CO_2 Emissions from Biomass in an LCA." International Journal of LCA 12(5): 281.

[5] Johnson, E. (2009). "Goodbye to carbon neutral: getting biomass footprints right. ." Environmental Impact Assessment Review.

[6] Manomet Center for Conservation Sciences (2010). Massachusetts Biomass Sustainability and Carbon Policy Study: Report to the Commonwealth of Massachusetts Department of Energy Resources. Brunswick, Maine.

[7] Berntsen, T. and G. P. Peters (2010). CO_2 perturbation and associated global warming potentials following emissions from biofuel based on wood. Greenhouse gas emissions from bioenergy systems: impacts of timing, issues of responsibility Brussels.

[8] Cowie, A. (2010). Is bioenergy really carbon neutral? Greenhouse gas emissions from bioenergy systems: impacts of timing, issues of responsibility Brussels.

[9] ISO (2006). ISO 14040: Environmental management — Life cycle assessment — Principles and framework.

[10] Heinen, R. and E. Johnson (2008). "Carbon footprints of biofuels & petrofuels." Industrial Biotechnology 4(3): 257-261.

Coupling mass transfer with mineral reactions to investigate CO_2 sequestration in saline aquifers with non-equilibrium thermodynamics

Yuanhui Ji[1,*], Xiaoyan Ji[1], Xiaohua Lu[2], Yongming Tu[3,4]

[1] *Division of Energy Engineering, Luleå University of Technology, 971 87 Luleå, Sweden*
[2] *State Key Laboratory of Materials-Oriented Chemical Engineering, Nanjing University of Technology, 210009, Nanjing, P. R. China*
[3] *Key Laboratory of Concrete and Prestressed Concrete Structures of Ministry of Education, Southeast University, 210096, Nanjing, P. R. China*
[4] *Division of Structural Design and Bridges,Royal Institute of Technology (KTH),10044 Stockholm, Sweden*
** Corresponding author. Tel: +46 920491271, Fax: +46 920491074, E-mail: yuanhui.ji@ltu.se*

Abstract: The coupling behaviors of mass transfer of aqueous CO_2 with mineral reactions of aqueous CO_2 with rock anorthite are investigated by chemical potential gradient and concentration gradient models, respectively. SAFT1-RPM is used to calculate the fugacity of CO_2 in brine. The effective diffusion coefficients of CO_2 are obtained based on the experimental kinetic data reported in literature. The calculation results by the two models and for two cases (mass transfer only and coupling mass transfer with mineral reaction) are compared. The results show that there are considerable discrepancies for the concentration distribution with distance by the concentration gradient and chemical potential gradient models, which implies the importance of consideration of the non-ideality. And the concentrations of aqueous CO_2 at different distances by the concentration gradient model are higher and further than that by the chemical potential gradient model. The mineral reaction plays a considerable role for the CO_2 geological sequestration when the time scale reaches 10 years for the anorthite case.

Keywords: *CO_2 geological sequestration, Non-equilibrium thermodynamics, Chemical potential gradient, Mass transfer, Geochemical reaction*

1. Introduction

Geological sequestration of anthropogenic CO_2 is a promising carbon mitigation strategy[1, 2], which includes the injection of CO_2 into deep saline aquifers, depleted oil and gas reservoirs, and deep coal seams[2, 3], and the storage in deep saline aquifers seems to have the largest potential capacity[3, 4, 5]. The four main CO_2 sequestration mechanisms in deep saline aquifers proposed are solubility trapping; capillary trapping; hydrodynamic trapping and mineral trapping[1, 2]. In order to study the long-term behaviors of CO_2 in formations, and to estimate the possible CO_2 leakage risk, it is necessary to investigate the dissolution of CO_2 in brine, the mass transfer of dissolved CO_2 and the coupling behaviors of mass transfer with the mineral reactions of aqueous CO_2 with rocks over a wide range of spatial and temporal scales[1, 3, 6-8].

Phase equilibria of CO_2 in water and brines have been widely studied[9-12]. The molecular-based statistical associating fluid theory (SAFT) equation of state (EOS) is a promising model for systems up to high pressures, which represents the density and phase equilibrium for CO_2-H_2O from 285 to 473 K and up to 600 bar, and for CO_2-H_2O-NaCl from 298 to 373 K and up to 200 bar[10, 13]. For the kinetics research, numerous investigations on the mass transfer of CO_2 in high-pressure water or brines have been conducted to simulate CO_2 geological or ocean disposal processes[5, 14-16]. Yang and Gu[5] studied CO_2 dissolution in brine at elevated pressures experimentally and described the mass transfer of CO_2 in brine using Fick's Second Law with an effective diffusion coefficient considering the effect of convection, which are two orders of magnitude larger than the molecular diffusivity of CO_2 in water[5], and it implies that the density-driven natural convection greatly accelerates the mass transfer of CO_2 in brines. Generally, mass transfer flux is described with concentration gradient as the driving

force. However, in real systems, Fick's law must be amended to account for nonideal behavior. So the driving force for solute fluxes is not the concentration gradient, but the chemical potential gradient[17, 18]. Our previous work[19, 20] also reveals that it is necessary to consider the non-ideality of the complicated systems. Therefore, on the basis of the work by Yang and Gu[5], the mass transfer of CO_2 in brines is investigated by chemical potential gradient model[21] based on derivation of $\partial a_i/\partial t$ (a_i is the activity of species i). The calculated results show the importance of the consideration of the non-ideality. Moreover, path-of-reaction and kinetic modeling of CO_2-brine-mineral reactions in deep saline aquifers have been conducted[9, 22-25]. The nonisothermal reactive transport code TOUGHREACT[26, 27] were developed which introduced reactive chemistry into the multi-phase fluid and heat flow code TOUGH2[28].

In this paper, the coupling behaviors of the mass transfer of aqueous CO_2 with the typical mineral reactions of aqueous CO_2 with rocks will be investigated and analyzed by chemical potential gradient and concentration gradient models, respectively.

2. Thermodynamic model

The fugacities of the aqueous CO_2 are calculated using SAFT1-RPM EOS[13] and the details are described in literature[13].

3. Kinetics modeling

3.1. Model description

3.1.1. Mass transfer

Concentration gradient model

The flux generalized to three dimensions is described as[18, 29]

$$J_i = -D_C \nabla C_i \tag{1}$$

where, J_i is molar flux of species i; D_C is the effective diffusion coefficients in concentration gradient model; C_i is the molar concentration of species i.

Chemical potential gradient model

As described in above text, in real systems, chemical potential gradient is the driving force for solute fluxes[17, 18], and the flux generalized to three dimensions is described as[18, 29]

$$J_i = -(D_\mu C_i / RT) \nabla \mu_i \tag{2}$$

where, J_i is molar flux of species i; D_μ is the effective diffusion coefficients in chemical potential gradient model; μ_i is the chemical potential of species i and described by Eq. (3)[30].

$$\mu_i = \mu_i^0 + RT\ln(f_i / f_i^0) = \mu_i^0 + RT\ln a_i \tag{3}$$

where, μ_i^0, a_i, f_i and f_i^0 are the standard chemical potential, activity, fugacity and standard fugacity of component i, respectively. At a certain T and P, both μ_i^0 and f_i^0 are constants. In this paper, one-dimensional case is studied, and the convective molar flux by the bulk motion of the fluid is not added in Eqs. (1) and (2), but an effective diffusion coefficient considering the effect of convection is used. Combining Eq. (2) with Eq. (3), Eq. (4) can be obtained.

$$\boldsymbol{J_i = -\frac{D_\mu C_i}{RT}\nabla(RT \ln f_i) = -D_\mu C_i \nabla \ln f_i} \tag{4}$$

Diffusion coefficient determination

The effective diffusion coefficient is obtained based on the experimental kinetic data in Test 4 reported by Yang and Gu[5]. At the temperature and different pressures of Test 4, the quantitative relations of fugacities of aqueous CO_2 with their concentrations are determined from fitting according to the calculation results by SAFT1-RPM EOS[13] with a function form as $f_{CO2(aq)}=a+b\cdot C_{CO2(aq)}$ in which a and b are parameters at a certain temperature and pressure. The aqueous CO_2 concentrations at the interface are calculated with SAFT1-RPM[13] by assuming instantaneous saturation of CO_2[21]. In the work of Ref. [5], the CO_2 dissolution was performed in a PvT cell with a cross-sectional area A (7.9273×10^{-4} m^2) and brine phase height H (0.0442 m), the CO_2 pressures P_t at different time t were recorded. The number of moles of dissolved CO_2 (n_t) are determined from the gaseous pressure at different time t and the initial experimental conditions. Based on the mass balance, Eq. (5) can be obtained.

$$\int_0^x C_{CO_2(aq)} A dx = n_t \tag{5}$$

where $C_{CO2(aq)}$ ($mol\cdot m^{-3}$) is the concentration of aqueous CO_2 in brines, and A (m^2) is the contact area of gaseous CO_2 with brine and is assumed to be the cross-sectional area of the cell, and x (m) is the mass transfer distance. In the work of Yang and Gu[5], only the experimental kinetics data after 180s were used to analyze the mass-transfer process of CO_2 in the brine. In this paper, we also take the flux J and n_t after 180s.

According to the flux J and n_t at different pressures in Test 4[5] and combining Eqs. (1) with (5), the effective diffusion coefficient at respective pressures in the one-dimensional concentration gradient model can be determined directly. While for the effective diffusion coefficient in the chemical potential gradient model, a simple but effective method, direct search method, can be used, in which the initial value and step length of the effective diffusion coefficient are assumed as 1.0×10^{-9} $m^2\cdot s^{-1}$, while the maximum value is 1.0×10^{-6} $m^2\cdot s^{-1}$. The minimum, maximum values and step length of the distance x are assumed as 1.00×10^{-6}, H and 5.00×10^{-4} m. Then according to the flux J and n_t at different pressures in Test 4[5] and combining Eqs. (4) and (5), the effective diffusion coefficient at respective pressures can be determined by the numerical simulation calculation.

3.1.2. Mineral reaction rate

Mineral reaction

Mineral trapping is the fixing of CO_2 in carbonate minerals due to a series of geochemical reactions[9, 31]. It is reported that the most promising reactions for mineral trapping involve the minerals which provide divalent cations (Ca^{2+}, Mg^{2+}, Fe^{2+}) for precipitation of carbonate[9, 31]. One of the most common sedimentary-mineral sources of divalent cations is anorthite and is studied as a case in this paper. The mineral trapping takes place due to the following reactions as demonstrated by the example of anorthite dissolution:

Dissolution of CO_2 acidifies formation water through the following reaction[31].

$$CO_2(aq)+H_2O \rightleftharpoons H_2CO_3 \rightleftharpoons HCO_3^- + H^+ \rightleftharpoons CO_3^{2-} + 2H^+ \tag{6}$$

Aqueous CO_2 dissociates in water and produces carbonic acid, bicarbonate and carbonate ions, the acid attacks anorthite, leaching Ca^{2+} and neutralizing the acid through Reaction (7)[9, 31].

$$CaAl_2Si_2O_8 + 2H^+ + H_2O \rightleftharpoons Ca^{2+} + Al_2Si_2O_5(OH)_4 \tag{7}$$

The divalent cations precipitates as calcium carbonate through Reactions (8) and (9)[9, 31].

$$Ca^{2+} + HCO_3^- \rightarrow CaCO_3 + H^+ \quad (8)$$

$$Ca^{2+} + CO_3^{2-} \rightarrow CaCO_3 \quad (9)$$

In this work, Eq. (7) and the following net reaction are considered to study the mineral reaction rate.

$$Ca^{2+} + CO_2(aq) + H_2O \rightarrow CaCO_3 + 2H^+ \quad (10)$$

Mineral reaction rate

According to nonequilibrium thermodynamics, the chemical reaction rate of a single reaction is described as Eq. (11)[32],

$$\text{Rate} = R_f (1 - e^{-A/RT}) \quad (11)$$

where, R_f is the forward rate of the reaction, A is the affinity and is described as the negative of the molar Gibbs free energy change of reaction, R is the gas constant, T is the temperature. Based on Eq. (11), the general rate equation for geochemical reaction kinetics is[22, 24]:

$$\mathbf{Rate} = (1/V) \cdot \mathrm{d}n_i / \mathrm{d}t = (1/V) \cdot K \cdot A_{\min} \cdot \exp(-E_a / RT) \cdot [1 - \frac{Q}{K_{eq}}] \quad (12)$$

where, V is the volume of brines, K is the rate constant, $A_{\min}$ is the reactive surface area, E_a is the activation energy, Q is the activity product and is described through Eq. (13), and K_{eq} is the equilibrium constant.

$$Q = \frac{[H^+]}{[Ca^{2+}] \cdot f_{CO_2(aq)}} \quad (13)$$

In Eq. (13), $[H^+]$ and $[Ca^{2+}]$ are the molar concentrations of H^+ and Ca^{2+} ions, respectively.

Mineral reaction rate parameters

Anorthite is chosen for a case study. The volume of brines is assumed as 1 m^3 (approximately equals to 1 kg). The rate constant, activation energy and specific reactive surface area of the rocks used are taken from literature[23] and shown in Table 1. The water:rock ratio is fixed at 1 kg water per 15 kg of rock[24]. The gas constant is taken as 8.3145 $J \cdot mol^{-1} \cdot K^{-1}$. The effect of temperature on the mineral reaction rate is neglected and the temperature is taken as 298.15K. In the calculation of Q, $[H^+]$ and $[Ca^{2+}]$ are taken from the pH value and composition of Rose Run brines[22]. The fugacities of aqueous CO_2 are determined by SAFT1-RPM EOS[13]. According to the equilibrium constants of the following Eqs. (14) and (15), the equilibrium constant of Eq. (10) can be obtained as shown in Eq. (16).

$$CO_2(aq) + H_2O \rightarrow HCO_3^- + H^+ \quad \log K(298.15K) = -6.37 \quad (14)$$

$$CaCO_3(calcite) + H^+ \rightarrow Ca^{2+} + HCO_3^- \quad \log K(298.15K) = 1.71 \quad (15)$$

$$Ca^{2+} + CO_2(aq) + H_2O \rightarrow CaCO_3 + 2H^+ \quad \log K(298.15K) = -8.08 \quad (16)$$

Table 1. The mineral considered and its reaction rate constant (K), activation energy (Ea) and specific reactive surface area[23].

Mineral	K ($mol \cdot m^{-2} \cdot s^{-1}$)	Ea ($J \cdot mol^{-1}$)	Specific reactive surface area ($m^2 \cdot g^{-1}$)
Anorthite	7.6×10^{-10}	1.78×10^{4}	1.00×10^{-3}

3.1.3. Model of coupling mass transfer with mineral reaction

The model of coupling mass transfer with mineral reaction can be derived from the equation of continuity for species *i* in a multicomponent reacting mixture as shown in Eq. (17)[29].

$$\frac{\partial C_i}{\partial t} = -(\nabla \cdot J_i) - r_i \tag{17}$$

where, r_i is the consumption rate of *i* by reaction. According to the different flux forms of Eqs. (1) and (4) and the reaction rate form of Eq. (12), the concentration gradient and chemical potential gradient models of coupling mass transfer with mineral reaction can be obtained.

3.2. Initial and boundary conditions

The initial condition is given by Eq. (18)

$$C_i(x,t)\big|_{t=0} = \begin{cases} C_{i0} & (x=0) \\ 0 & (x>0) \end{cases} \tag{18}$$

where, C_{i0} is the aqueous CO_2 saturated concentration. The left boundary conditions are the interface concentrations of aqueous CO_2 calculated with SAFT1-RPM[13] by assuming instantaneous saturation of CO_2[21]. The right boundary condition is

$$\frac{\partial C_i(x,t)}{\partial x}\Big|_{x=x_R} = 0 \quad (t>0) \tag{19}$$

where, x_R represents the distance between the right boundary and the interface.

3.3. Numerical solution

The partial differential equations are solved numerically using the built-in "pdepe" in the MATLAB program, which solves initial-boundary value problems for systems of parabolic and elliptic partial differential equations. The diffusion coefficient is taken the value calculated in this paper at 7.5322 MPa and the other experimental conditions of Test 4[5].

4. Results and Discussions

4.1. Effective diffusion coefficient

The effective diffusion coefficients at different pressures and other experimental conditions of Test 4[5] are calculated and shown in Fig. 1. Fig. 1 shows that the effective diffusion coefficients by both concentration gradient and chemical potential gradient models are close to each other and decrease with increasing pressure. Moreover, the effective diffusion coefficients calculated in this paper are close to that in our previous work by the chemical potential gradient model based on the derivation of $\partial a_i/\partial t$[21].

4.2. Concentration distribution by concentration and chemical potential gradient models

The concentration distribution of aqueous CO_2 with distance at 10 and 20 years through the concentration gradient and chemical potential gradient models coupling mass transfer with mineral reaction is shown in Fig. 2. From Fig. 2, there are considerable discrepancies for the concentration distribution with distance by the two models, which implies the importance of the consideration of non-ideality. The concentrations of aqueous CO_2 by the concentration gradient model are higher and further than that by the chemical potential gradient.

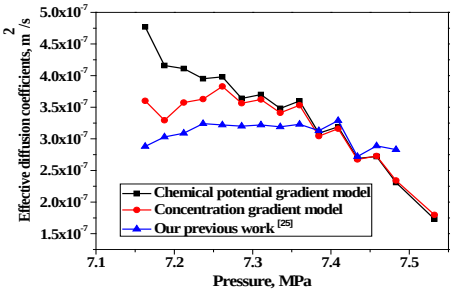

Fig. 1. Calculated effective diffusion coefficients at different pressures

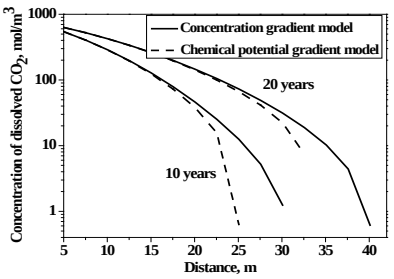

Fig. 2. Concentration distribution with distance for coupling mass transfer with mineral reaction.

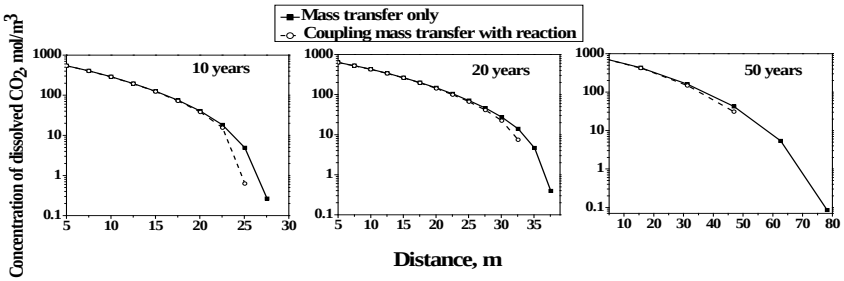

Fig. 3. C alculated concentration distribution with distance at different time scales in which two different cases are considered (1) mass transfer only; (2) coupling mass transfer with mineral reaction.

4.3. Concentration distribution by chemical potential gradient model for two cases: mass transfer only and coupling mass transfer with mineral reaction.

The concentration distribution of aqueous CO_2 with distance at 10, 20, 50 years by the chemical potential gradient model for two cases (mass transfer only and coupling mass transfer with mineral reaction) is shown in Fig. 3. From Fig. 3, for the anorthite case, it is observed that the mineral reaction plays a considerable role for the geological sequestration when the time scale reaches 10 years. Moreover, our results show that the mineral reaction does not bring obvious effect on the concentration distribution of aqueous CO_2 for time scale less than 10 years, and when the time scale is 1000 years, the aqueous CO_2 by the mass transfer can be completely reacted by the model rock anorthite due to the neglection of the effects of hydrodynamics and gravity. In future work, more types of rocks and the effects of hydrodynamics and gravity should be considered.

5. Conclusions

In this paper, the coupling behaviors of the mass transfer of aqueous CO_2 with the mineral reactions of aqueous CO_2 with model rock anorthite are investigated by chemical potential gradient and concentration gradient models, respectively. The effective diffusion coefficients of CO_2 are obtained based on the experimental kinetic data reported in literature. The results

show that there are considerable discrepancies for the concentration distribution with distance by the concentration gradient and chemical potential gradient models, which implies the importance of the consideration of the non-ideality. And the concentrations of aqueous CO_2 at different distances by the concentration gradient model are higher and further than that by the chemical potential gradient. The mineral reaction plays a considerable role for the geological sequestration when the time scale reaches 10 years for the anorthite case.

Acknowledgment

The authors thank Luleå University of Technology, the Swedish Research Council, the National Basic Research Program of China (2009CB226103), the National Natural Science Foundation of China (50808039) and the Natural Science Foundation of Jiangsu Province, China (BK2009138) for the financial supports.

References

[1] D. P. Schrag, Preparing to capture carbon, Science 315, 2007, pp. 812-813.

[2] A. Firoozabadi, P. Cheng, Prospects for subsurface CO_2 sequestration, AIChE J. 56, 2010, pp. 1398-1405.

[3] R. G. Jr. Bruant, A. J. Guswa, et al. Safe storage of CO_2 in deep saline aquifers, Environ. Sci. Technol. 36(11), 2002, pp. 240A-245A.

[4] S. Bachu, J. J. Adams, Sequestration of CO_2 in geological media in response to climate change: capacity of deep saline aquifers to sequester CO_2 in solution, Energy Convers. Manage. 44, 2003, pp. 3151-3175.

[5] C. Yang, Y. Gu, Accelerated mass transfer of CO_2 in reservoir brine due to density-driven natural convection at high pressures and elevated temperatures, Ind. Eng. Chem. Res. 45, 2006, pp. 2430-2436.

[6] S. M. V. Gilfillan, B. S. Lollar, et al. Solubility trapping in formation water as dominant CO_2 sink in natural gas fields, Nature 458, 2009, pp. 614 -618.

[7] D. W. Keith, J. A. Giardina, et al. Regulating the underground injection of CO_2, Environ. Sci. Technol. 39, 2005, pp. 499A-505A.

[8] C. M. Oldenburg, Transport in geologic CO_2 storage systems, Transp. Porous Med. 82, 2010, pp. 1-2.

[9] B. Zerai, CO_2 sequestration in saline aquifer: geochemical modeling, reactive transport simulation and single-phase flow experiment. Doctoral Dissertation, January, 2006.

[10] Y. H. Ji, X. Y. Ji, et al. Progress in the study on the phase equilibria of the CO_2-H_2O and CO_2-H_2O-NaCl systems. Chin. J. Chem. Eng., 15(3), 2007, pp. 439-448.

[11] N. A. Darwish, N. Hilal, A simple model for the prediction of CO_2 solubility in H_2O-NaCl system at geological sequestration conditions, Desalination 260, 2010, pp. 114-118.

[12] N. N. Akinfiev, L. W. Diamond, Thermodynamic model of aqueous CO_2-H_2O-NaCl solutions from 22 to 100 degrees C and from 0.1 to 100 MPa, Fluid Phase Equilibria 295, 2010, pp. 104-124.

[13] X. Y. Ji, S. P. Tan, et al. SAFT1-RPM approximation extended to phase equilibria and densities of CO_2-H_2O and CO_2-H_2O-NaCl systems. Ind. Eng. Chem. Res. 44, 2005, pp. 8419-8427.

[14] B. Arendt, D. Dittmar, R. Eggers, Interaction of interfacial convection and mass transfer effects in the system CO_2-water, Int. J. Heat Mass Transfer 47, 2004, pp. 3649-3657.

[15] R. Farajzadeh, H. Salimi, et al. Numerical simulation of density-driven natural convection in porous media with application for CO_2 injection projects, Int. J. Heat Mass Transfer 50, 2007, pp. 5054-5064.

[16] R. Farajzadeh, P. L. J. Zitha, J. Bruining, Enhanced mass transfer of CO_2 into water: experiment and modeling, Ind. Eng. Chem. Res. 48, 2009, pp. 6423-6431.

[17] N. Kocherginsky, Y. K. Zhang, Role of standard chemical potential in transport through anisotropic media and asymmetrical membranes, J. Phys. Chem. B 107, 2003, pp. 7830-7837.

[18] G. A. Truskey, F. Yuan, D. F. Katz., Transport phenomena in biological systems. Prentice Hall, 2009.

[19] C. Liu, Y. Ji, et al. Thermodynamic analysis for synthesis of advanced materials. Molecular Thermodynamics of Complex Systems, Struct Bond 131, 2009, pp. 193-270.

[20] Y. H. Ji, X. Y. Ji, et al. Modelling of mass transfer coupling with crystallization kinetics in microscale, Chem. Eng. Sci. 65(9), 2010, pp. 2649-2655.

[21] Y. H. Ji, X. Y. Ji, X. H. Lu, Modeling mass transfer of CO_2 in brine at high pressures by chemical potential gradient, Fluid Phase Equilibria 2010 submitted.

[22] B. Zerai, B. Z. Saylor, G. Matisoff, Computer simulation of CO_2 trapped through mineral precipitation in the Rose Run Sandstone, Ohio, Applied Geochemistry 21, 2006, pp. 223-240.

[23] F. Gherardi, T. Xu, K. Pruess, Numerical modeling of self-limiting and self-enhancing caprock alteration induced by CO_2 storage in a depleted gas reservoir, Chemical Geology 244, 2007, pp. 103-129.

[24] R. T. Wilkin, D. C. Digiulio, Geochemical impacts to groundwater from geologic carbon sequestration: controls on pH and inorganic carbon concentrations from reaction path and kinetic modeling, Environ. Sci. Technol. 44, 2010, pp. 4821-4827.

[25] T. Xu, Y. K. Kharaka, et al. Reactive transport modeling to study changes in water chemistry induced by CO_2 injection at the Frio-I Brine Pilot, Chemical Geology 271, 2010, pp. 153-164.

[26] T. Xu, K. Pruess, Modeling multiphase non-isothermal fluid flow and reactive geochemical transport in variably saturated fractured rocks: 1. Methodology. Am. J. Sci. 301, 2001, pp. 16-33.

[27] T. Xu, E. L. Sonnenthal, et al. TOURGHREACT: a simulation program for non-isothermal multiphase reactive geochemical transport in variably saturated geologic media. Comp. Geosci. 32, 2006, pp. 145-165.

[28] T. Xu, J. A. Apps, K. Pruess, Numerical simulation to study mineral trapping for CO2 disposal in deep aquifers. Appl. Geochem. 19, 2004, pp. 917 – 936.

[29] R. B. Bird, W. E. Stewart, et al. Transport Phenomena, John Wiley & Sons, Inc., 2006.

[30] J.M. Prausnitz, R.N. Lichtenthaler, E.G. de Azevedo, Molecular Thermodynamics of Fluid-phase Equilibria. Third edition, NJ, Prentice Hall PTR, 1999.

[31] J. M. Matter, P. B. Kelemen, Permanent storage of carbon dioxide in geological reservoirs by mineral carbonation, Nature Geoscience 2, 2009, pp. 837 – 841.

[32] D. Kondepudi, I. Prigogine, Modern Thermodynamics: From Heat Engines to Dissipative Structures. John Wiley & Sons, Chichester, 1998.

Clean Coal Utilization Based on Underground Coal Gasification Integrated Solid Oxide Fuel Cells and Carbon dioxide Sequestration

Prabu V*, Jayanti S

Indian Institute of Technology Madras, Chennai, India
** Corresponding author. Tel: +4422575152 E-mail: vprabu1979@yahoo.co.in*

Abstract: Underground coal gasification (UCG) is a clean coal technology which converts coal into a combustible gas *in situ* without mining and without bringing up the ash contained in the coal. Thus, the attendant problems of coal washing, ash handling and disposal can be avoided. The combustible gas mixture, consisting primarily of hydrogen, methane, carbon monoxide--all of which are fuels for an solid oxide fuel cell (SOFC) system-- and carbon dioxide, can be fed to a battery of SOFC after gas cleaning to remove hydrogen sulphide and other impurities. A large portion, typically 50%, of the chemical energy contained in the product gas can be converted into electrical energy by the SOFC. The exhaust gases from the SOFC are typically at a temperature of the order of 600 to 800 deg C. Heat energy from these will be extracted to produce steam, part of which will be used for UCG and the rest will be sent for SOFC internal reforming and shifting reactions. The exhaust gases, consisting primarily of carbon dioxide and steam, will be finally fed through a condenser and will then be sent for compression and sequestration. Thus, the overall system envisaged makes use of oxygen-fed UCG and SOFC to generate electrical energy and an exhaust gas consisting primarily of carbon dioxide and the easily condensable steam which enables CO_2 sequestration. The overall integrated system can be divided into five units namely underground coal gasification, UCG product gas purification, electrical power generation from SOFC, heat recovery system and carbon sequestration unit. An energy analysis with heat integration of all the systems for a nominal 500 MWt will be discussed.

Keywords: *Underground coal gasification, Solid oxide fuel cell, Carbon sequestration, Heat integration.*

Nomenclature

W_{ele}	electrical work ..... kJ	η	efficiency.....
F	Faraday's constant C	f	flow rate ..... $mol \cdot s^{-1}$
K	equilibrium reaction constant.....	c_p	specific heat..... kJ/kg K
p	partial pressure..... bar	E	Nernst potential V
T	mean temperature ..... K	E_o	Ideal potential at standard condition V
R	universal gas constant ..... kJ/kmol K	j	electron number.....
H	enthalpy ..... kJ	U_f	fuel utilization factor……
N_{H_2}	moles of hydrogen converted……..mol	HV	Heating value……..kJ/mol
ΔH_R	Heat of reaction……..kJ/mol	Q	excess heat……..kW

1. Introduction

Coal is the major fossil fuel in the world and 70% of electricity produced in India comes from coal. Coal is expected to be the mainstay of electricity generation in India for the next several decades. However, coal utilization is fraught with environmental problems. Given that Indian coal typically has large ash content, its mining, washing, and final utilization in pulverized coal boilers leads to significant land, water and air pollution. The ash collected from the stacks also poses a disposal problem. On top of these, there is increased awareness of the need to reduce CO_2 emissions into the atmosphere. Hence it is necessary to develop suitable technologies for coal conversion efficiently without environmental pollution.

Underground coal gasification (UCG) is a clean coal technology with *in situ* gasification having no mining problem, no ash disposal, offering economical exploitation of low grade coal. It is a clean coal technology which enables exploitation of coal reserves in an

environmental friendly manner. A large amount of work has been reported in the 1970s and 80s on UCG [1-5] and there has been renewed interest in UCG as showed by a number of publications in the last decade [6-10]. These studies have focused on coal gasification per se and not much on CO_2 sequestration. In the present paper, we describe a process by which UCG can be coupled to a solid oxide fuel cell (SOFC) system to develop an integrated power plant which makes use of the fuel gas from the UCG, generates electricity from it and leaves an exhaust gas consisting of 85% CO_2 which can therefore be readily sequestered. The layout of the proposed plant is described in Section 2 and a thermodynamic analysis of the system is discussed in Section 3.

2. Description of the coupled UCG-SOFC system

A schematic diagram of the integrated UCG-SOFC system is shown in Figure 1. The product gas from the UCG system typically has some particulate matter and impurities in the form of tar, sulphur and its compounds. These are removed as the gas passes through a cyclone separator, a gas filter unit and a tar removal unit. The hot gas from the cyclone separator exchanges heat with the clean gas coming from the tar removal system in a gas-to-gas heat exchanger. The clean fuel gas is further heated (by the hot anode side exhaust of the solid oxide fuel cell (SOFC) unit) and is mixed with steam and is fed to the anode side of the SOFC unit. The unused portion of hydrogen and carbon mono oxide (85% fuel utilization efficiency is assumed in the SOFC) is then fed to a combustor to completely convert the remaining fuel into CO_2 and steam. These gases are fed to a condenser in which most of the steam is removed and the remaining gas, consisting mostly of CO_2 is sent to the CO_2 sequestration unit. The thermal energy in the exhaust gas of the combustor is used to generate steam in the condenser unit which is used for fuel reforming in the SOFC as well as for coal gasification in the UCG gasifier. Further, the thermal energy of the hot air from the cathode code is also used to preheat the air that is supplied to the cathode so as to maintain the SOFC temperature at the design condition. In order to eliminate nitrogen from the system (so as to facilitate CO_2 sequestration), an air separation unit is used to supply oxygen in required quantity to the combustor (this is especially needed to maintain stable combustion as the anode gas from the SOFC contains only a small percentage of fuel, namely, H_2 and CO, the rest being CO_2 and steam) as well as that required for gasification in the UCG gasifier unit. The flow paths of the various streams are shown in Figure 1.

The above coupling of the UCG with an SOFC enables proper thermal integration of the various units to produce electrical energy directly from the product gas of the UCG. Moreover, the combination of UCG and SOFC is such that the integration can be done in such a way that all the CO_2 that is produced in the fuel utilization can be captured in a relatively straightforward manner without the need for an external CO_2 absorption unit as is required in normal combustion of the UCG gas. One disadvantage however is the need to clean the UCG gas to remove tar and sulphur products so that it can be used in an SOFC. The technology for the required gas cleaning already exists; the calculations described in the next section show that the gas cleaning can also be done without a significant energy penalty resulting in a combined system with a significantly higher overall thermal efficiency and little environmental pollution.

3. Thermodynamic model and analysis

The overall integrated plant consist of five units, namely, underground coal gasification, UCG product gas purification, electrical power generation from SOFC, heat recovery systems and carbon sequestration unit. An energy balance on these units has been carried out to determine

the overall utilization of energy. The UCG system is considered to be operating at atmospheric pressure and the bituminous grade coal in underground undergoes partial oxidation and gasification in presence of pure oxygen to produce calorific value synthesis gas. The electrical efficiency of SOFC fuel cell is found out based on the shifting, reforming and electrochemical reaction with reaction kinetics.

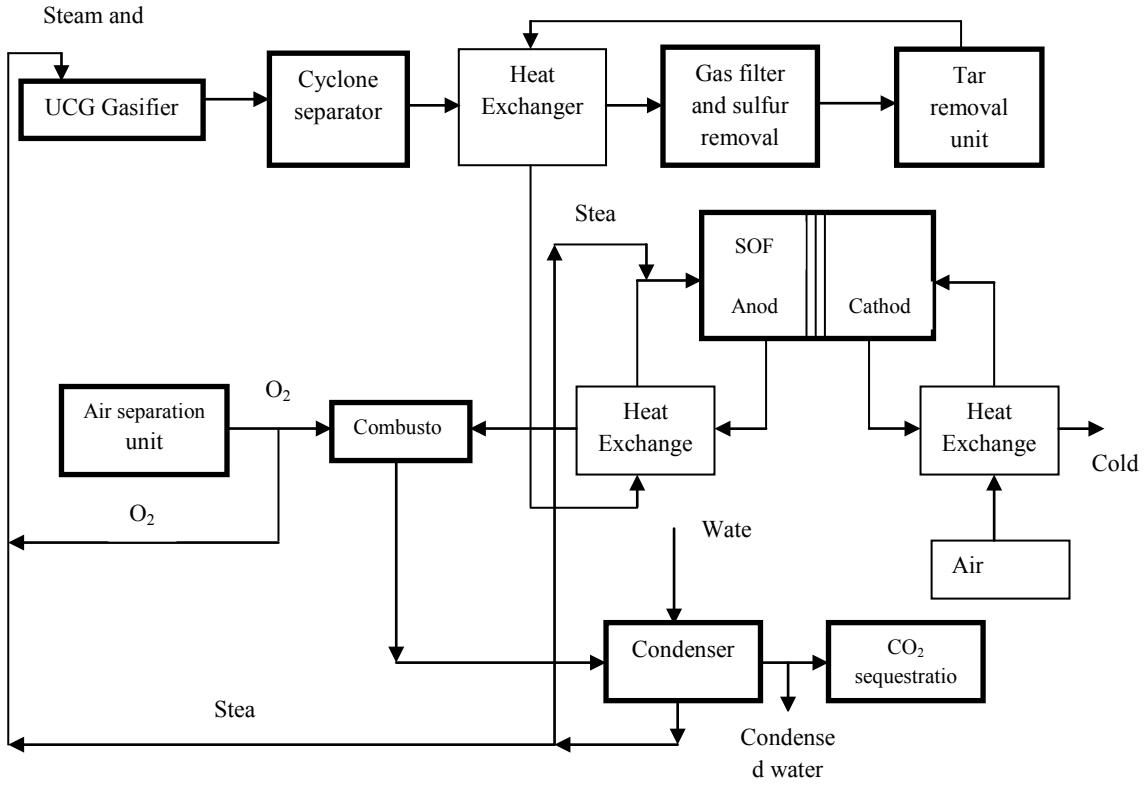

Fig.1. Schematic of the integrated underground coal gasification with solid oxide fuel cell

3.1. UCG Plant

A 500 MW of product gas generated from UCG and the flow rate of input and output stream of gases and its molar composition has taken from Lawrence Livermore national laboratory (LLNL) literature [11] and used for the basis of theoretical calculation. Table 1 represents the product gas molar composition and total product gas flow rate from UCG of 2600 mol/s.

Table 1. Product gas composition from UCG plant

Species	Mole fraction	Product gas flow rate[mol/s]
N_2	0.018	47.36
CO	0.11	289.47
CO_2	0.44	1157.89
H_2	0.37	973.68
CH_4	0.05	131.58

Heat of combustion of product gas (HV) = 190 kJ/mol
Product gas flow rate from UCG to SOFC (f_p) = 2631.58 mol/s
Total injection flow rate of steam and oxygen = 2255.63 mol/s
Injection mole fraction of oxygen = 0.47
The UCG gasifier operating temperature is assumed to about 800°C in oxyfuel mode. Pure oxygen from air separation unit and steam generated from condenser unit are injected into

injection hole and the gasified products at 650°C are collected from the production hole of UCG.

3.2. UCG product gas purification system

In UCG system, volatile matter liberated during combustion, gasification and pyrolysis zone will move along the cavity and make contact with the fresh coal. This would results in product gas enriched with tar content since there is no further thermal cracking [12]. The issue of removal of mercury, arsenic and other trace metals is not addressed here as not much is known about their formation and presence in the UCG gas. In order to utilize these product gases in SOFC for power generation, it is necessary to remove the tar and sulfur content impurities. Cyclone separator and ceramic filters are used to remove the particulate matter and alkali compounds from product gases before the tar removal. A wet electrostatic precipitator is used for tar condensation and removal. The purified gas stream is cooled to about 50° C and the enthalpy is again gained from the inlet gas stream of purification system and fed into the SOFC.

3.3. SOFC fuel cell system

The purified hot gas stream from with steam is introduced at the anode side of the SOFC. To avoid the carbon deposition in SOFC, a steam to carbon ratio of 2:1 is assumed [13]. Excess oxygen of 400% in air is supplied at the cathode side to recover the generated heat energy. The operating temperature of SOFC is assumed to be 700°C. The temperature of exit stream from anode and cathode side is same as the operating temperature of SOFC. In IRSOFC (Internal reforming SOFC), only hydrogen is assumed to undergo oxidation for electric power generation. Carbon monoxide, methane undergoes reforming and water gas shifting reactions [Eq. (1)] with steam and produces hydrogen. High operating temperature of SOFC is suitable for reforming and shifting reaction which converts the CO and other hydrocarbons to hydrogen. A fuel utilization factor of 0.85 is assumed for the fuel cell.

Reforming reaction: $CH_4 + H_2O \overset{K_{ref}}{\longleftrightarrow} CO + 3H_2$ (1)

Water gas shifting reaction: $CO + H_2O \overset{K_{shf}}{\longleftrightarrow} CO_2 + H_2$

$$K_{ref} = [CO][H_2]^3/[CH_4][H_2O] \quad (2)$$

$$K_{shf} = [H_2][CO_2]/[CO][H_2O] \quad (3)$$

where K_{ref} and K_{shf} are the equilibrium constants for reforming and shifting reaction respectively. The equilibrium constants are calculated using the temperature dependent polynomial expressions [14]. The equilibrium gas composition can be determined using Eq. (2 & 3).

3.4. Estimation of Overall Thermal Energy Conversion Efficiency

The overall thermal energy conversion efficiency (η) of the coupled UCG-SOFC process can be estimated from the thermal energy content in the UCG gas and the electrical power output from the SOFC system. The latter is estimated as follows. The cell e.m.f, E, of the SOFC is calculated for the particular concentrations of hydrogen, oxygen and steam produced (p_{H_2}, p_{O2}, p_{H_2O}) used in the cell using the Nernst equation [15]:

$$E = Eo + (RT/jF) \ln[(p_{H_2}.p_{O_2}^{1/2})/p_{H_2O}] \quad (4)$$

where Eo is the ideal potential at standard condition, j is the electron number.

The electrical power output from the SOFC is then calculated as

$$W_{ele} = EN_{H_2} jF \quad (5)$$

where N_{H2} is the number of moles of hydrogen, and F is the Faraday's constant.
The overall thermal energy conversion efficiency can now be calculated by dividing the electrical power output by the thermal energy flow rate in the UCG gas:

$$\eta = W_{ele} / (f_p \times HV) \quad (6)$$

where f_p is product gas flow rate from UCG in mol/s and HV is the heating value of the product gas from UCG.

3.5. Estimation of the air inlet temperature for the SOFC

Energy balance can be made over the SOFC fuel cell system to calculate the air inlet temperature to the cathode side [Fig.2]. Eq. (7) gives the excess energy generated in the fuel cell is taken up by the incoming air and gas stream to maintain a constant operating temperature in the cell.

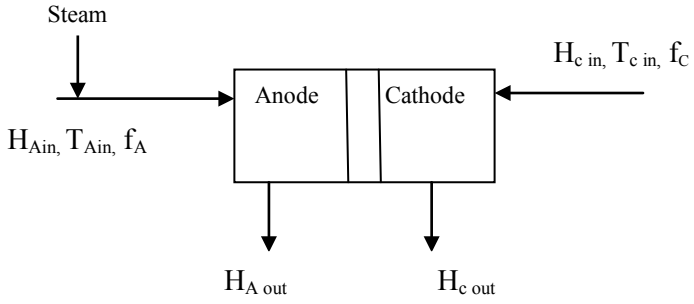

Fig.2. Schematic diagram of SOFC Model

$$\Delta H_R = W_{ele} + Q \quad (7)$$

where ΔH_R is the heat of reaction (kJ/mol), Q is the excess energy generated in the fuel cell.

$$Q = f_A \int_{T_{Ain}}^{T_{sofc}} Cp\, dT + f_C (H_{SOFC} - H_{C\ in}) \quad (8)$$

where f_A and f_c are the input flow rates of anode side gas stream and cathode side air stream respectively.
From Eq. (8), the air inlet temperature to cathode side of the fuel cell is calculated.

3.6. Heat recovery system

The outlet gas from anode and cathode of SOFC at high temperature of 700°C are utilized for the heat recovery system. The inlet gas streams of cathode and anode are heated using heat exchangers by their respective outlet gas streams. The trace quantity of unconverted gas from SOFC can be burnt in a combustor with oxygen and the hot gas from combustor has sent to the condenser. A fresh steam is generated from condenser which is then supplied to the SOFC

cathode inlet and UCG injection hole. The two heat exchangers at the inlet of SOFC system of cathode and anode and the combustor and the condenser for fresh steam generation will constitutes the heat recovery system of the integrated system.

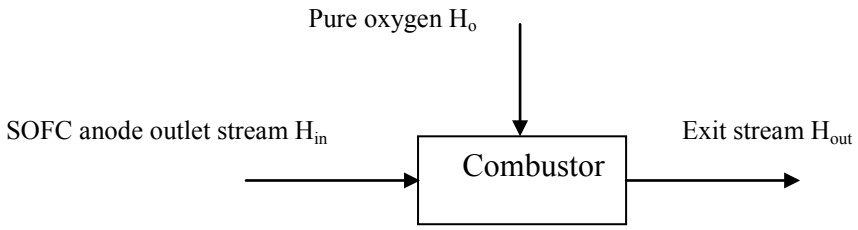

Fig.3. Schematic diagram of combustor model.

Complete combustion of remaining hydrogen, carbon monoxide and trace amount of methane are assumed in the combustor. Pure oxygen of 150% in excess of stoichiometric requirement for complete combustion is supplied to the combustor. The temperature of the exit stream from combustor (Fig.3) can be calculated from the enthalpy balance [Eq. (9)] over combustor.

$$H_{in} + H_o = H_{out} \tag{9}$$

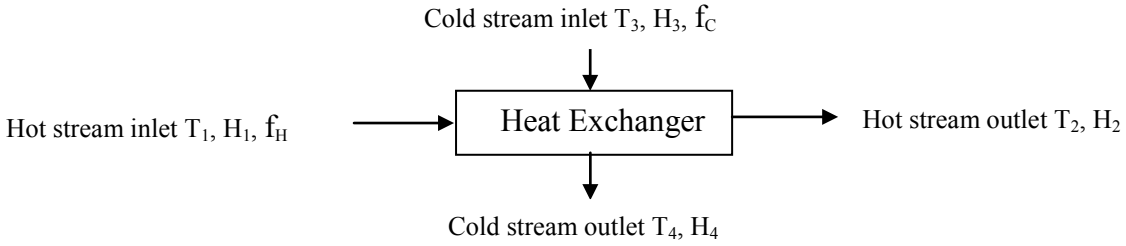

Fig.4. Schematic diagram of Heat Exchanger model

Fig.4 represents the schematic diagram of heat exchanger model. The cold stream outlet temperature can be calculated from the enthalpy balance equation [Eq. (10)].

$$f_H (H_1 - H_2) = fc \int_{T_3}^{T_4} Cp \, dT \tag{10}$$

where f_H and f_C are the flow rates of hot and cold streams respectively.

4. Results and Discussion

An overall energy balance is made for the entire thermodynamic model for the integrated system of UCG and SOFC. The steam generated from condenser at 600°C is sent to the UCG and SOFC with approximately equal proportion.

The hot product gas from the UCG plant enters the purification system at 650°C and cooled in a heat exchanger to 200°C and then it enters into the filter. Small particulate matters and condensed alkali compounds are filtered through the gas filter. Particulate free gases are then entered into the wet electrostatic precipitator to remove the tar which is enriched in the product gases. The tar free product gas are coming out from the wet ESP at about 50°C are heated to about 525°C using the exit gas stream of UCG. In order to raise the temperature of

the product gas at about 650°C to meet the SOFC operating temperature, the purified gas is heated again with the outlet gas stream of SOFC at anode side.

Table 2. SOFC inlet and outlet gas stream composition.

Species	Inlet stream mole percent	Outlet stream mole percent
N_2	1.28	1.19
CO_2	31.25	38.15
CO	7.81	1.64
CH_4	3.55	0.000044
H_2	26.28	6.52
H_2O	29.83	52.5

Table 2 represents the SOFC inlet and outlet gas composition of cathode side. In outlet gas stream, only a trace amount of methane is present and constitutes 50 mole % of steam. The electrochemical work done by the SOFC can be calculated using the Nernst equation as 312.53MW. Electrical efficiency of the SOFC cell is found as 62.5%.

The unconsumed fuel from SOFC is burnt in the combustor with pure oxygen to extract more energy and the outlet gas is purely a composition of steam and carbon dioxide. The combustion of unconsumed fuel from SOFC in the combustor can be carried out using excess oxygen.

Table 3. Combustor inlet and outlet gas stream composition

Species	Inlet stream mole percent	Outlet stream mole percent
N_2	1.08	1.125
CO_2	34.62	37.49
CO	1.49	0
CH_4	0.00004	0
H_2	5.91	0
H_2O	47.64	55.62
O_2	9.25	5.77

Table 3 shows the combustor outlet gas composition. Combustor outlet stream contains 37% of CO_2 and 55% of steam which is then sent to the condenser to extract the heat energy. All the steam can be condensed and the pure CO_2 is separated and sent to sequestration unit.

5. Conclusion

A fully integrated UCG-SOFC system is proposed to provide clean electrical energy from underground coal. The combination of UCG and SOFC is such that thermal as well as system integration of the two units can be carried out readily. A first-cut energy analysis, without including the cost of the air separation unit and the cost of compression of the CO_2 for the purposes of, say, underground sequestration, gives an overall thermal efficiency of above 60%. The combined system also utilizes fossil fuel in a clean manner without any particulate or gaseous emissions, thus providing a clean source of energy from conventional sources.

References

[1] W.R.Aiman, W.T.Fisher, Lawrence Livermore National Laboratory Insitu coal gasification Program Quarterly Progress Report. January through March 1978, UCRL 50026-78-1

[2] C.B.Thorsness, J R Creighton. Review of underground coal gasification field experiments at HOE creek. Report No.UCRL-87662-Rev.1. U.S.DOE. Livermore, CA: Lawrence Livermore National Laboratory; 1983

[3] P.N.Thompson, Gasifying coal underground. Endeavour 1978;2: 93 -97

[4] A.M.Winslow, Numerical Model of coal gasification in a packed bed. S ymbosium on combustion (international) 1977:16:503 – 513.

[5] C B Thorsness, E A Grens, A Sherwood, A one dimensional Model for Insitu coal gasification. Report No.UCRL-52523, U.S.DOE.Livermore, CA: Lawrence Livermore National Laboratory; 1978.

[6] M.S.Blinderman, D.N.Saulov, A.Y.Klimenko. Forward and reverse combustion linking in underground coal Gasification. Energy 2008; 33: 446-454.

[7] L Yang, J Liang, L Yu, Clean coal technology – Study on the pilot project experiment of underground coal gasification. Energy 2003;28:1445 – 1460

[8] L Yang, X Zhang, S Liu, W. Zhang, Field test of large-scale hydrogen manufacturing from underground coal gasification. International journal of Hydrogen Energy 2008; 33:1275 – 1285.

[9] G.Perkins, V.Sahajwalla. A Mathematical Model for the chemical reaction of a s emi-infinite block of coal in underground coal Gasification. Energy and fuels 2005;19:1679 – 1692

[10] S.Daggupati, N.Ramesh. R.N.Manadapati, S.M.Mahajani, A.Ganesh, D.K Mathur, R.K Sharma, P.Aghalayam, Laboratory studies on c ombustion cavity growth in lignite coal blocks in the context of underground coal Gasification. Energy 2010;35: 2374-2386.

[11] W.R.Aiman, M L Donohue, LLL insitu coal gasification project, Quarterly progress Report, Lawrence Livermore laboratory, Report No. UCRL 50026 -79 -3, 1979.

[12] T.Kivisaari, P Bjornbom, C Sylwan, B Jacquinot, D Jansen, A Groot, The feasibility of a coal gasifier combined with a high temperature fuel cell, Chemical Engineering Journal 100, 2004, pp 167 -180.

[13]A.O.Omosun, A.Bauen, N.P.Brandon, C.S.Adijman, D.Hart, Modelling system efficiencies and costs of two biomass-fuelled SOFC systems, Journal of power sources 131, 2004, pp 96 – 106.

[14] S.Ghosh, S.De, Thermodynamic performance study of an integrated fuel cell combined Cycle- an energy analysis, Journal of Power and Energy 217, 2002, pp 137 -147.

[15] S.Ghosh, S.De, Energy analysis of a cogeneration using coal gasification and solid oxide fuel cell, Energy 31, 2006, pp 345 – 363.

Climate Change and Water Resources for Energy Generation in Tanzania

Z. J .U. Malley[1*]

[1]*Agricultural Research Institute-Uyole P.O. Box 400, Mbeya, Tanzania*
**Corresponding author's Tel: +255252510363, Fax: +255252510065, Email: zjmalley@yahoo.co.uk*

Abstract: Tanzania is one of the low income countries, which heavily depends on hydro-power for electric energy supply to the national grid. Impacts of climate change patterns on water resources supply to dams for hydro-energy generation is now evident. In turn, this has impacted national socio-economic development in numerous ways. The objective of this work was to analyze the link of climate change to water shortages for hydro-power generation in the Mtera reservoir, which supply 50% of the hydro-power to the national grid. Literature survey, records collection and analyses and observations were research tools used. The study revealed that, 64% of increasing variability in rainfall over years in the watersheds described declining water levels in Mtera dam. This strong relationship means that climate change is main driver of water shortages for hydro-power generation. This suggests a need for national adaptation strategies to water supply shortages. Improvements in the present hydro-power sources for water recycling and/or development of micro-dams for storage of excess water need exploration. Rain-water harvesting and recycling seems important adaptation strategies to changing hydrological patterns for water supply to the hydro-energy plants in Tanzania.

K***eywords:*** *Electric energy supply, Hydro-energy plants, Increasing rainfall variability, National grid, Water supply*

1. Introduction

Climate change and variability are now becoming one of the significant development challenges due to shift in the average patterns of weather. Environmental change, manifested by climate change and variability, is no longer a mythical discourse; the scientific consensus is not only that, human activities have contributed to it significantly, but that the change is far more rapid and dangerous than thought earlier (IPCC, 2007). While climate change results from activities all over the globe, with rather unevenly spread contributions to it, it may lead to very different impacts in different countries, depending on local, regional environmental conditions and on differences in vulnerability to climate change (UNEP/Earthscan, 2002). The Millennium Ecosystem Assessment (2005) shows that, in all ecosystems of the world, the climate changes impacts are rapidly increasing, such as, on water resources, environmental services and other livelihoods capital assets for sustainable human development. In the World Summit on Sustainable Development (WSSD) held from August 26-4 September 2002 in Johannesburg, South Africa, the UN Secretary General outlined priority areas for sustainable development as water and sanitation, energy, health, agriculture and biodiversity protection and ecosystems management (WSSD, 2002).

Climate change impact on water resource supply significantly affects all aspects of sustainable socio-economic development of a country or a society, where energy sector is heavily dependent on hydropower. Current contribution of hydro-power in Tanzania to national grid is 52% and the rest is from thermal sources (Karekezi et al. 2009). There has been a concern over water supply for energy generation in Mtera reservoir. This concern is manifested at national level a decade ago by the government declaration in March 2001 that, the Great Ruaha River should return to its year-round flow characteristics by 2010. The concern comes from power shortages in early-

1990s, attributed to low water flows into the Mtera/Kidatu hydropower system from the Great Ruaha River (Lankford *et al*, 2004; Yawson, *et al*, 2003). The hydrological change in the Usangu-Mtera ecosystem has attracted number of investigations into causes of this problem, which include: Sustainable Management of the Usangu Wetlands and its Catchments (SMUWC) from 1998-2002 (Lankford *et al*, 2004); investigation into cause of the failure of the Mtera-Kidatu Reservoir system (Yawson *et al*, 2003); a study of the effects of land degradation in the uplands on land use changes in the plains (Mwalukasa, 2002); a study of the socio-economic root cause of the loss of biodiversity in the Ruaha Catchment Area (Sosovele and Ngwale, 2002). These studies agree that, there is hydrological flow change in Mtera reservoir, but there is no consistent consensus on cause of hydrological change. These studies did not attempted to directly link change in rainfall variability with water supply from Mtera reservoir. This work focuses on the hydrological flow change and how it links to changes in rainfall variability. Therefore, this paper explores the trends in variability of the Mtera reservoir mean water levels and watershed rainfall amounts and discusses linkages to energy generation for the national grid and socio-economic development. Furthermore, it recommends opportunities for harnessing in the national adaptations strategies to climate influenced hydrological flows changes.

2. Methodology

The study area is Usangu-Mtera ecosystem, which covers, south-western Tanzania's highlands watershed catchments to the Mtera reservoir, which is used to conserve water for hydro-electricity generation in Kidatu, downstream. Data collection tools from the area were survey of literature, key informants interviews, informal appraisals, questionnaire interviews and biophysical records collections and analysis.

The literature was searched from the Internet, published and grey materials of the relevant regional, national and area studies. Then a critical analysis of information gathered through literature surveys was undertaken. Key informants interviews were held with Rufiji Basin Water Office (RBWO) and the Tanzania Electricity Company (TANESCO). Informal village appraisals were conducted in six villages, which were Ikoga and Sololwambo in lower part, Yala and Matebete middle part, and Mhwela and Mabadaga in upper part of the Usangu central plain. Informal interviews were supplemented with participatory village resources mapping and on the ground observations through transect walks.

Household questionnaire interviews were held in April to December 2004, involving 266 households in six above villages. Interviews assessed climate change perceptions and its link to water problems at local level. Verification of this perceptions, were done through collection and analysis of biophysical records on rainfall and water levels in the Mtera reservoir over 22-years (1982-2003). A 22-years measurements data of Mtera reservoir water levels collected from TANESCO and rainfall data from the Agricultural Research Institute meteorological station located in the Uyole-Uporoto uplands watershed, typical of the south-western watersheds.

Analysis of the total annual rainfall amounts were summation of monthly precipitations. Monthly sum of each rainfall year starts in October of the preceding year and ends in September of the following year. The relationship was tested and linkage established between rainfall variability and water supply shortage experienced by analyses of the collected information. Quantitative data were analysed using the Statistical Package for Social Science (SPSS).

3. Results

3.1 Climate change Indicators

Local people experience strongly attested links of climate changes with respect to water resources, rainfall amount and duration, temperature, land resources degradation and land use change in the Usangu-Mtera ecosystem (SMUWC, 2002; Malley *et al*, 2007). Interview of 266 household, in area of study, about 82.6% of respondents, reiterated that rainfall amount has decreased, and a similar number (83%), reported shortened duration of rainfall in Usangu-Mtera ecosystem. These perceptions are supported by analysis of rainfall trends (Table 1).

Analysis revealed that annual rainfall amounts in the south-western watershed, is declining, though not statistically significant (p= 0.05). However, a high variability pattern of rainfall amount from year to year is evident. More frequencies of below average annual rainfall amounts were conspicuously notable, from late 1980s to 2003, which indicate increased frequency of drier-years than normal in about last 22 years.

3.2 Water supply for energy generation in Mtera

The Mtera reservoir mean annual water levels trend, over 22-years, depicts closely similar pattern to the annual rainfall amounts trend in the south-western highlands watersheds (Table 1). More frequencies of low mean annual water levels were observed from the late 1980s to 2003. This similarity in the pattern, attest a possible linkage between the annual hydrological droughts in the reservoir to the rainfall amount and pattern change in the south-western highlands watersheds.

Table 1 Trends in rainfall, water levels and their relationships in Usangu-Mtera ecosystem

Environmental variable	Direction	Method of analysis	Extent (%)	Sign.
Trends				
Rainfall quantity	Declining	PRA	-	
		Respondents perception	82.6	***
		Regression over years	6.8	Ns
Rainfall variability	Increasing	PRA	-	
		Respondents perception	83	***
Patterns of mean annual water levels in Mtera reservoir	Declining	Regression over years	5.8	Ns
Mean annual water level variability	Increasing	Regressions over years	10.2	Ns
Rainfall variability vs water levels	Positive and strong	Regression	64.2	***

Ns = not significant, * significant at P ≤0.05; ** significant at P ≤ 0.01, *** Significant at P ≤ 0.001
Source: Own analyses of field data (2004)

3.3 Climate change indicators and Mtera reservoir water supply

Regression analysis of variations in the amounts of rainfall, significantly ($p<0.001$) accounted for 64.2% of the variations in mean annual water levels in Mtera reservoir (Table1). This suggests that, the lower the annual rainfall amount in the upper catchments the lower the mean annual

water supply from the Mtera reservoir. It implies that, increasing variability in the annual rainfall amounts is a cause of increasing variability in the mean annual water supply in the Mtera reservoir for electricity generation. These direct close relationship, gives new evidence, that there is a strong causal relationship between the perceived changes in climate indicators with the changes in the hydrology of the Usangu-Mtera eco-system.

4. Discussions

Lankford *et al*, (2004), showed that SMUWC investigation found that hydrological change in the Great Ruaha River is linked to dry season abstraction for irrigation activities and environmental losses, but not to climate change. Mwalukasa (2002) showed that, there is significant degradation of the land cover in the plain and upland of the Chimala River catchments, and there is increase in land use for irrigated agriculture in the plain. According to Yawson *et al*, (2003), the failure of the Mtera/Kidatu system is due to unaccounted spillage from Mtera reservoir, caused by inefficient management of the system. These investigations did not attempt to analyse linkage of climate indicators with water supply from Mtera reservoir. Sosovele and Ngwale, (2002) and Malley *et al*., (2007) analysed rainfall trends from different stations which indicated that climate change might have played a significant role in the experienced water supply shortages. These studies supported the anecdotal evidence that, climate change plays a greater role in the observed hydrological flow change. The results of present findings, which established direct relationships between water supply change and rainfall variability further supports findings of Sosovele and Ngwale (2002) and Malley *et al* (2007) and the anecdotal evidence.

According to Karl *et al*., (1995), increase in frequency of drought or rainfall variability is linked to climate change, which is also characterised with events of short severe storms. According to U.S. National Drought Monitor (2006), hydrological drought is manifested by shortfalls in surface and sub-surface water supply, which can be detected through decline in water levels in rivers, reservoirs, lakes and aquifers. Frequency and severity of hydrological drought is discernible at a watershed or river basin scale (Wilhite and Glantz, 1985). Mbwambo (2010) reported decline in number of flowing rivers from 79 to 39 now in Kilombero basin in Morogoro, Tanzania, due to climate change. In the Usangu-Mtera ecosystem, work of Sosovele and Ngwale (2002) reported that, rivers from upper watersheds of Uporoto and Mbeya mountains, which flow into the Usangu plain, and then to the Great Ruaha River only Chimala and Mbarali still have flows, however, amount of flowing water has declined substantially. These observations are supported by SMUWC (2002) measurements of flows in the rivers, which show that dry season flows of rivers have declined. Dried and silted up perennial rivers and streams were encountered during the course of this study, in the middle and lower villages of the Usangu plain. The SMUWC (2002), indicated that the western wetlands area (about 900 km^2), experienced reduced seasonal flooding in recent years, and it seem it no longer qualifies as a wetland, only remaining indicators of its past wetlands status is vegetation and soils. Kashaigili (2005) results show that, the eastern wetland perennial swamp size has shrunk by almost 70% between 1984 and 2000. According to Yawson *et al* (2003), in 1991 and 1992, water levels in the Mtera-Kidatu reservoir system, went very low to its dead levels. This is attested by the increasing frequency of below average mean annual water levels in Mtera reservoir. Presence of these indicators in the watersheds, fans and wetlands ecosystems in Usangu, and in the Mtera reservoir, explain the link of climate change-to-water supply problem from Mtera reservoirs for hydropower generation.

4.1 Impact of climate change on energy generation and socio-economic development

According to Libiszewski (1992), socio-economic impacts of environmental change may include: (1) decrease economic production, (2) general economic decline, (3) population displacements, and (4) disruption of institutions and the social relations. In the Usangu-Mtera ecosystem, similar socio-economic impacts, linked to hydrological change are evident. To abate, water shortage problem for energy generation, pastoral communities were forcefully displaced from their livelihood resources, water sources and dry season grazing land (Edwin, *The East African,* April 9-15, 2007). This forceful displacement of pastoral people has resulted into disruptions of their social institutions and soured their relations with the state, which mean a disruption of social capital, important in development process.

Climate change impact on water supply, results into reduced hydro-power production, which causes increase in outages and load shedding. In Tanzania, in dry year of 1997, the Mtera dam water went down, due to drought causing 17% drop in hydropower generation (Karekezi *et al*, 2009). In the period, 1990-2008, the water supply problem from the Mtera reservoir led to electric power shortage, which in turn affected the national grid, because the Mtera-Kidatu system generates about 50% of the power to national grid (WWF, 2002). The electric generation failures caused the nation wide power rationing, which impacted the industrial economic production, either, through increased costs of production of goods, or through reduced level of production, due to unavailability of power during certain periods of operations. Energy shortage affected economic production, raises the costs of electricity and thus goods and socio-economic service provisions from trade, health, education and domestic sectors, which in turn affect the welfare and livelihoods of the people in different ways. The emergency response, to reduce the impacts of the national power crisis, by hiring and/or investing into expensive alternative power sources, greatly constrained the government budget for the socio-economic development activities, and has forced the nation to a debt burden (Simbeye, *The East African*, July 12-18, 2004). Furthermore, in 2006, according to analysis of Kerekezi *et al* (2009), Tanzania incurred a loss of about 1% of its GDP earnings due to drought related load shedding exercise.

4.2 Conclusion and Recommendations

4.2.1 Conclusion

Climate change and variability is evident from increasing frequency of annual rainfall amounts variability in the upper catchments of south-western highlands of the Usangu-Mtera ecosystem. Increasing frequency of hydrological drought as manifested by mean annual water supply from Mtera reservoir for energy generation has strong relationship with increasing rainfall amount variability.

4.2.2 Recommendations

- Micro-dams for rainwater harvesting to adapt to years of extreme rainfall variability would help conserve water to support the main dam if constructed on the upper side of the Mtera reservoir along the Great Ruaha River to harvest excess water and store it, when the reservoir capacity approaches its maximum (698.5m.a.s.l). The stored water would be the source for recharge of the reservoir, when its water level approaches the critical minimum level (690m.a.s.l). The restriction at Nyaluhanga is another opportunity need to be explored for storage

of water in the western wetlands, and then slowly released over time to recharge eastern wetlands and hence the Great Ruaha River.

- An investment into alternative energy sources is a commendable strategy. The use of coal in electricity generation appears available and potentially cheap alternative in Tanzania. However, in the long term, the coal burning is one of the highest emitters of a greenhouse gas, the carbon dioxide, which significantly contribute to the environmental changes, which would be environmentally un-friendly investment. This means heavy investment to this source, would seem to compromise the environmental sustainability efforts in a long-term, therefore a modest investment in coal energy plants as an emergency backups during the hydropower shortage is recommended.

- The hydro-power remains the known clean and cheapest sources of electric energy for sustainable economic development. This implies that, more careful considerations should be on improvement and maintenance of the present hydro-power sources and new ones identified and developed. The design should incorporate multiple and efficient re-use of water through recycling system as an important aspect of water management, which should be considered in planning and designs of new development in hydro-power generation plants.

Acknowledgements

The data was collected by the financial support of the International Foundation for Science (IFS) in Sweden and the United Nations University Institute of Advanced Studies (UNU/IAS) in Japan. The Ministry of Agriculture and Food Security in Tanzania made its research facilities available for the work and administered the funds at the Agricultural Research Institute-Uyole (ARI-Uyole). I wish to thank and appreciate the assistance of the Mbarali District council, the TANESCO, Regional Water Engineer-Mbeya and the Directorate of Meteorological services, Tanzania for availing the information needed to undertake the reported analysis in this work.

References

[1] IPCC, Climate Change 2007: The Physical Science Basis: Summary for Policy Makers, Paris: IPCC, WMO, 2007.

[2] UNEP/Earthscan, United Nations Environmental Program/ Earths can. Global Environmental Outlook 3. London: Earthscan, 2002.

[3] Millennium Ecosystem Assessment (MA), International scientific assessment: ecosystem changes and human well-being. www.millenniumassessment.org, 2005.

[4] World Summit on Sustainable Development (WSSD), A framework for Action on Agriculture. Johannesburg: WEHAB Working Group, 2002

[5] S. Karekezi, J. Kimani, O. Onguru, Climate Change and Energy Security in East Africa. Energy Environment and Development Network for Africa (AFREPREN/FWD), 2009 46 pp.

[6] B. Lankford, B. Koppen, T. Franks, and H. Mahoo, Entrenched views or insufficient science? Contested causes and solutions of water allocation, insights from the Great Ruaha River Basin, Tanzania. Agricultural Water Management 2004, pp 135-153.

[7] D.K. Yawson, J.J. Kashaigili, J. Kachroo, and F.W. Mtalo, Modelling the Mtera-Kidatu reservoir system to improve integrated water resources management. International Conference on Hydropower. (Arusha: Hydro Africa), 2003.

[8] SMUWC, Baseline 2001. http://www.usangu.org/baseline2001/part1-5.shtml, 2001.

[9] E.H. Mwalukasa, Effects of Land Degradations in the Uplands on Land Use Changes in the Plains: The Case Study of Chimala River Catchment in the Usangu Plains. MSc. Dissertation. Sokoine University of Agriculture, 2002.

[10] H. Sosovele, and J.J. Ngwale, Socio-economic Root Cause of the Loss of Biodiversity in the Ruaha Catchment Area. (Dar-es-salaam: WWF-Tanzania), 2002.

[11] Z.J.U. Malley, M. Taeb, T. Matsumoto, T. and H. Takeya, Environmental change and vulnerability in Usangu plain, South-western Tanzania: Implications for Sustainable Development. The International Journal of Sustainable Development and World Ecology, 2007, pp 145-159.

[12] T.R. Karl, R.W. Knight, and N. Plummer, Trends in High Frequency of Climatic Variability in the Twentieth Century. Nature, 1995, pp 217-220.

[13] U.S. National Drought Monitor, http://www.drought.unl.edu/dm/monitor.html, 2006.

[14] D.A. Wilhite, and M.H. Glantz, Understanding the drought phenomenon: the role of definitions. Water International 1985, pp 111-120.

[15] J. Mbwambo, Kilombero: Kutoka mito 79 hadi 39 ya sasa, kulikoni? (Kilombero: From 79 rivers to 39 now, what need be done?), Raia Mwema Issue No 161, November 24-30, 2010, pp 12-13.

[16] J. J. Kashaigili, Integrated Hydrological Modelling of Wetlands for Environmental Management: The Case of the Usangu Wetlands in the Great Ruaha Catchment. RIPARWIN Seminar Presentation, Mbeya Peak Hotel: Mbeya, 2005.

[17] S. Libiszewski, What is an environmental conflict? (ENCOP Occasional papers: Center for Security Studies, ETH Zurich/Swiss Peace Foundation Zurich/ Berne 1992-1995), 1992.

[18] W. Edwin, Thousands of cattle dying as Dar relocates herders from the Wetlands, The East African, 2007, April 9-15.

[20] F. Simbeye, Songas to Replace Imported Furnace Oil. The East African, July 12-18, 2004.

[21]World Wide Fund (WWF), African Rivers Initiative: Concept Paper. Living Water Programme. Iringa, WWF, 2002.

Optimal hydraulic structures profiles under uncertain seepage head

Raj Mohan Singh[1,*]

1 Motilal Nehru National Institute of Technology, Allahabad-211004, India
** Corresponding author. Tel: +91-532-2271322(O); Fax: +91-532-2545341 E-mail: rajm@mnnit.ac.in; rajm.mnnit@gmail.com*

Abstract: Most of the hydraulic structures are founded on permeable foundation. There is, however, no procedure to fix the basic barrage parameters, which are depth of sheet piles/cutoffs and the length and thickness of floor, in a cost-effective manner. Changes in hydrological and climatic factors may alter the design seepage head of the hydraulic structures. The variation in seepage head affects the downstream sheet pile depth, overall length of impervious floor, and thickness of impervious floor. The exit gradient, which is considered the most appropriate criterion to ensure safety against piping on permeable foundations, exhibits non linear variation in floor length with variation in depth of downstream sheet pile. These facts complicate the problem and increase the non linearity of the problem. However, an optimization problem may be formulated to obtain the optimum structural dimensions that minimize the cost as well as satisfy the exit gradient criteria. The optimization problem for determining an optimal section for the weirs or barrages normally consists of minimizing the construction cost, earth work, cost of sheet piling, length of impervious floor etc. The subsurface seepage flow is embedded as constraint in the optimization formulation. Uncertainty in design, and hence cost from uncertain seepage head are quantified using fuzzy numbers. Results show that an uncertainty of 15 percent in seepage will result in 22 percent of uncertainty in design represented by overall design cost. The limited evaluation show potential applicability of the proposed method.

Keywords: *Nonlinear Optimization Formulation, Genetic Algorithm, Hydraulic Structures, Barrage Design, Fuzzy Numbers, Uncertainty Characterization.*

1. Introduction

Hydraulic structures such as weirs and barrages are costly water resources projects. A safe and optimal design of hydraulic structures is always being a challenge to water resource researchers. The hydraulic structure such as barrages on alluvial soils is subjected to subsurface seepage. The seepage head causing the seepage vary with variation in flows. Design of hydraulic structures should also insure safety against seepage induced failure of the hydraulic structures.

The variation in seepage head affects the downstream sheet pile depth, overall length of impervious floor, and thickness of impervious floor. The exit gradient, which is considered the most appropriate criterion to ensure safety against seepage induced piping (Khosla, et al., 1936; Asawa, 2005) on permeable foundations, exhibits non linear variation in floor length with variation in depth of down stream sheet pile. These facts complicate the problem and increase the non linearity of the problem. However, an optimization problem may be formulated to obtain the optimum structural dimensions that minimize the cost as well as satisfy the safe exit gradient criteria.

The optimization problem for determining an optimal section for the weirs or barrages consists of minimizing the construction cost, earth work, cost of sheet piling, and length of impervious floor (Garg et al., 2002; Singh, 2007). Earlier work (Garg et al., 2002) discussed the optimal design of barrage profile for single deterministic value of seepage head. This study first solve the of nonlinear optimization formulation problem (NLOP) using genetic algorithm (GA) which gives optimal dimensions of the barrage profile that minimizes unit cost of concrete work, and earthwork and searches the barrage dimension satisfying the exit gradient criteria. The work is then extended to characterize uncertainty in design due to

uncertainty in measured value of seepage head, an important hydrogeologic parameter. Uncertainty in design, and hence cost from uncertain head value are quantified using fuzzy numbers

2. Subsurface flow

The general seepage equation under a barrage profile may be written as:

$$\frac{\partial^2 h}{\partial x^2}+\frac{\partial^2 h}{\partial y^2}+\frac{\partial^2 h}{\partial z^2}=0 \qquad (1)$$

This is well known Laplace equation for seepage of water through porous media. This equation implicitly assumes that (i) the soil is homogeneous and isotropic; (ii) the voids are completely filled with water; (iii) no consolidation or expansion of soil takes place; and (iv) flow is steady and obeys Darcy's law.

For 2-dimensional flow, the seepage equation (1) may be written as:

$$\frac{\partial^2 h}{\partial x^2}+\frac{\partial^2 h}{\partial y^2}=0 \qquad (2)$$

The need to provide adequate resistance to seepage flow represented by equation (1) both under and around a hydraulic structure may be an important determinant of its geometry (Skutch, 1997).The boundary between hydraulic structural surface and foundation soil represents a potential plane of failure.

Stability under a given hydraulic head could in theory be achieved by an almost limitless combination of vertical and horizontal contact surfaces below the structure provided that the total length of the resultant seepage path were adequately long for that head (Skutch, 1997; Leliavsky, 1979). In practical terms, the designer must decide on an appropriate balance between the length of the horizontal and vertical elements. Present work utilized Khosla's Method of independent variables (Asawa, 2005) to simulate the subsurface behavior in the optimization formulation. Method of independent variables is based on Schwarz-Christoffel transformation to solve the Laplace equation (1) which represents seepage through the subsurface media under a hydraulic structure. A composite structure is split up into a number of simple standard forms each of which has a known solution. The uplift pressures at key points corresponding to each elementary form are calculated on the assumption that each form exists independently. Finally, corrections are to be applied for thickness of floor, and interference effects of piles on each others.

3. Optimal design methodology

Minimize $C(L, d_1, d_d) = c_1(f_1) + c_2(f_2) + c_3(f_3) + c_4(f_4) + c_5(f_5)$ (4)

Subject to $$SEG \geq \frac{H}{d_d \pi \sqrt{\lambda}} \qquad (5)$$

$$L^l \leq L \leq {}^u \qquad (6)$$

$$d_1{}^l \leq d_1 \leq d_1{}^u \qquad (7)$$

$$d_d^{\,l} \le d_d \le d_d^{\,u} \quad (8)$$

$$L, d_1, d_d \ge 0 \quad (9)$$

where C (L, d_1, d_d) is objective function represents total cost of barrage per unit width (Rs/m), and is function of floor length (L), upstream sheet pile depth (d_1) and downstream sheet pile depth (d_d); f_1 is total volume of concrete in the floor per unit width for a given barrage profile and c_1 is cost of concrete floor (Rs/m^3); f_2 is the depth of upstream sheet pile below the concrete floor and c_2 is the cost of upstream sheet pile including driving (Rs/m^2); f_3 is the depth of downstream sheet pile below the concrete floor and c_3 is the cost of downstream sheet pile including driving (Rs/m^2); f_4 is the volume of soil excavated per unit width for laying concrete floor and c_4 is cost of excavation including dewatering (Rs/m^3); f_5 is the volume of soil required in filling per unit width and c_5 is cost of earth filling (Rs/m^3); SEG is safe exit gradient for a given soil formation on which the hydraulic structure is constructed and is function of downstream depth and the length of the floor; $\lambda = \frac{1}{2}[1+\sqrt{1+\alpha^2}]$; $\alpha = \frac{L}{d_d}$; L is total length of the floor; H is the seepage head ; d_1 is the upstream sheet pile depth; d_2 is downstream sheet pile depth; L^l, $d_1^{\,l}$, and $d_d^{\,l}$ is lower bound on L, d_1 and d_d respectively**;** L^u, $d_1^{\,u}$, $d_d^{\,u}$ are upper bound on L, d_1 and d_d respectively. The constraint equation (5) may be written as follows after substituting the value of λ :

$$L - d_d\left(\{2(\frac{H}{d_2\pi(SGE)})^2 - 1\}^2 - 1\right)^{1/2} \ge 0 \quad (10)$$

In the optimization formulation, for a give barrage profile and seepage head H, f_1 is computed by estimating thickness at different key locations of the floor using Khosla's method of independent variables and hence nonlinear function of length of floor (L), upstream sheet pile depth (d_1) and downstream sheet pile depth (d_2). Similarly f_4, and f_5 is nonlinear. The constraint represented by equation (10) is also nonlinear function of length of the floor and downstream sheet pile depth (d_2). Thus both objective function and constraint are nonlinear; make the problem in the category of nonlinear optimization program (NLOP) formulation, which are inherently complex. Characterization of functional parameters is available in literature (Singh, 2007; Garg et al., 2002).

3.1. Characterizing model functional parameters

For a given geometry of a barrage and seepage head H, the optimization model functional parameters f_1, f_2, f_3, f_4 and f_5 are characterized for the barrage profile shown in Fig. 1.

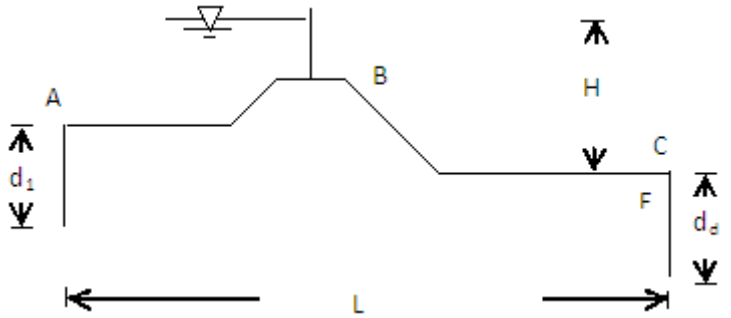

Fig. 1. Schematic of barrage parameters utilized in performance evaluation

Intermediate sheet-piles are not effective in reducing the uplift pressures and only add to the cost of in reducing the uplift pressures and only add to the cost of the barrage (Garg et al., 2002). In present work, no intermediate sheet piles are considered.

3.2. Optimization procedure using genetic algorithm

GA was originally proposed by Holland (Holland, 1975) and further developed by Goldberg (Goldberg, 1989). It is based on the principles of genetics and natural selection.GA's are applicable to a variety of optimization problems that are not well suited for standard optimization algorithms, including problems in which the objective function is discontinuous, non-differentiable, stochastic, or highly nonlinear (Haestad 2003). The GA search starts from a population of many points, rather than starting from just one point. This parallelism means that the search will not become trapped on local optima (Singh and Datta, 2006).

The optimization model represented by equations (4)-(10) and the functional parameters embedded in the optimization model are solved using Genetic Algorithm on M ATLAB platform. The basic steps employed in solution are available in Singh, 2007. Table 1 shows physical parameters obtained by conventional methods for Fig. 2.

Table 1. Physical parameters values of barrage profile

Physical parameters	Values (meters)
*L	105.37
H	7.12
*d_1	5.45
*d_2	5.9

* Decision variables to be optimized

4. Uncertainty characterization in the optimization model

Real-world problems, especially those that involve natural systems, such as soil and water, are complex and composed of many non-deterministic components having non-linear coupling. In dealing with such systems, one has to face a high degree of uncertainty and tolerate imprecision. There is a high degree of local soil variability, and imprecision in the determination of soil parameters and hydrological parameters like seepage head. Statistical techniques have been traditionally used to deal with parametric variation in model inputs, but these require substantial hydrogeologic explorations data for estimates of probability distributions. In the presence of limited, inaccurate or imprecise information, simulation with fuzzy numbers represents an alternative tool to handle parametric uncertainty. Fuzzy sets offer an alternate and simple way to address uncertainties even for limited exploration data sets. In the present work, the optimal design is first obtained assuming a deterministic value of hydrogelogic parameter, safe exit gradient, in optimization model. Uncertainty in safe exit gradient is then characterized using fuzzy numbers. The fuzzified NLOF is then solved using GA.

Uncertainty in general comes in two forms: aleatory (stochastic, random natural variability or noncognitive) and epistemic (cognitive or subjective) (Hofer et al., 2002). Recently, Srinivasan et al. (2007) identified these uncertainties in hydrogeological applications. Aleatory uncertainty refers to uncertainty that cannot be reduced by more exhaustive

measurements or by a better model. Epistemic uncertainty, on the other hand, refers to uncertainty that can be reduced (Ross et al., 2009).

One of the milestones in the evolution of these new uncertainty theories is the seminal paper by Lofti A. Zadeh (1965). He proposed a new mathematical tool in his paper and called this new mathematical tool "fuzzy sets." He proposed the concept of fuzzy algorithms in 1968 (Zadeh, 1968), and together with Bellman, proposed a new approach for decision-making in fuzzy environments in 1970 (Bellman & Zadeh, 1970). Fuzzy set theory has been recently applied in various fields for uncertainty quantification (Cho et al., 2002; Hanss, 2002; Kentel & Aral, 2004; Mauris et al., 2001).

The transformation method presented by Hanss, (2002) uses a fuzzy alpha-cut (FAC) approach based on interval arithmetic. The uncertain response reconstructed from a set of deterministic responses, combining the extrema of each interval in every possible way unlike the FAC technique where only a particular level of membership (α-level) values (Hanss & Willner, 1999) for uncertain parameters are used for simulation.

Fuzzy modeling of uncertainty for hydrogeologic parameters such as exit gradient and seepage head is based on Zadeh's extension principle (Zadeh, 1968) and transformation method (TM) (Hanss, 2002). In present study only seepage head is considered to be imprecise. Input seepage head as imprecise parameter, is represented by fuzzy numbers. The resulting output i.e. minimum cost obtained by the optimization model is also fuzzy numbers characterized by their membership functions. The reduced TM (Hanss, 2002) is used in the present study. The measure of uncertainty used is the ratio of the 0.1-level support to the value of which the membership function is equal to 1 (Abebe et al., 2000).

5. Results and discussion

Earlier (mid 19th century), weirs and barrages have been designed and constructed in India on the basis of experience using the technology available at that period of time. Some of them were based on Bligh's creep theory, which proved to be unsafe and uneconomical. Comparison of the parameters of these structures with the proposed approach is, thus, not justified. Therefore, a typical barrage profile, a spillway portion of a barrage, is chosen for illustrating the proposed approach as shown in Fig. 2. The barrage profile shown in Fig. 2 and parameters values given Table 1 is solved employing the methodology presented in this work. The optimized values of parameters for a deterministic seepage head value of 7.12m are shown in Table 2. During the process of optimization, the process of going into new generation continues until the fitness of the population converged i.e. average fitness of population almost matches with the best fitness. This criterion proves the solution to be optimized. The optimized values of parameters for a deterministic seepage head value of 7.12m are shown in Table 2.

Table 2. Optimized parameters for safe exit gradient equal to 1/8 and minimum thickness of floor as 1m

Physical parameters	Values
L	61
d_1	3.1
d_2	9.2

It also resulted in a smaller floor length and overall lower cost. It has shown a savings in the barrage cost ranging from 16.73 percent.

For characterization of uncertainty, seepage head is assumed to vary from 6.0m to 8.19m with central value of 7.12m i.e. almost 15 percent in triangular fuzzy numbers representation. The result of variation in cost is corresponding different degree of membership for seepage head shown in Fig.2. The measure of uncertainty is found to be 22 percent. Since, left and right spread from central value of exit gradient is almost 15 percent, it can be concluded that uncertainty in seepage head reflects comparatively more uncertainty) more than 15 percent) in cost.

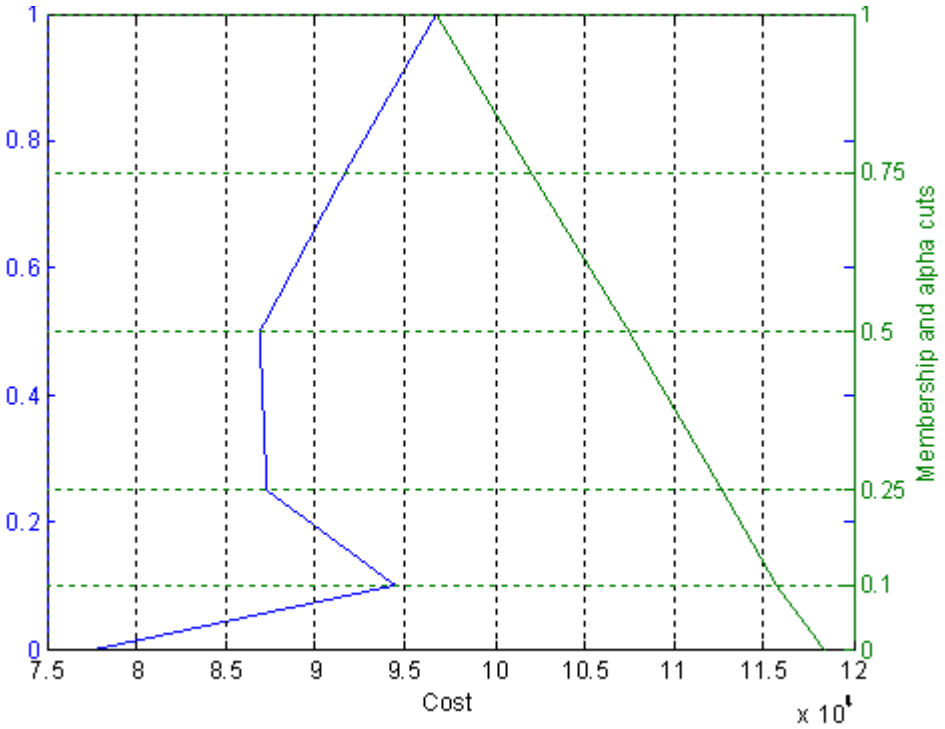

Fig.2. Costs variations corresponding to different α-cuts of seepage head

6. Conclusions

The present work also demonstrates the fuzzy based framework for uncertainty characterization in optimal cost for imprecise hydrologic parameter such as seepage head. The uncertainty in cost is found not to be directly proportional to uncertainty in seepage head. The GA based optimization approach is equally valid for optimal design of other major hydraulic structures.

References

[1] Khosla, A. N., Bose, N. K., and Taylor, E. M., Design of weirs on permeable foundations. *CBIP Publication No. 12*, Central Board of Irrigation and Power, New Delhi, 1936, Reprint 1981.

[2] Asawa, G.L. Irrigation and water resources engineering, New Age International (P) Limited Publishers, New Delhi. 2005.

[3] Garg, N.K., Bhagat, S.K., and Asthana, B.N., Optimal barrage design based on subsurface flow considerations. *Journal of Irrigation and Drainage Engineering*, Vol. 128, No. 4, 2002, 253-263.

[4] Singh. R.M., Optimal design of barrages using genetic algorithm. Proceedings of National Conference on Hydraulics & Water Resources (Hydro-2007) at SVNIT, Surat, 2007, 623-631.

[5] Skutch, J., Minor irrigation design DROP - Design manual hydraulic analysis and design of energy-dissipating structures. *TDR Project R 5830,* Report OD/TN 86, 1997.

[6] Leliavsky, S., Irrigation engineering: canals and barrages. Oxford and IBH, New Delhi, 1979.

[7] Holland, J. H., Adaptation in natural and artificial systems. University of Michigan Press, Ann Arbor, MI,1975.

[8] Goldberg, D. E., *Genetic algorithms in search, optimization and machine learning*. Kluwer Academic Publishers, Boston, MA, 1989.

[9] Haestad, M., Walski ,T. M., Chase, D. V., Savic, D. A., Grayman, W., Beckwith, S., and Koelle, E., *Advanced water distribution modeling and management.* Haestad Press, Waterbury, CT, 2003, 673-67.

[10] Singh, R. M., and Datta, B. 2006. Identification of unknown groundwater pollution sources using genetic algorithm based linked simulation optimization approach. *Journal of Hydrologic Engineering,* ASCE, Vol. 11, No.2, 101-109.

[11] Hofer, E., Kloos, M., Krzykacz-Hausmann, B., Peschke, J. and Woltereck, M., An approximate epistemic uncertainty analysis approach in the presence of epistemic and aleatory uncertainties. *Reliab. Eng. Syst. Safety*, 77(3), 2002, 229– 238.

[12] Srinivasan, G., Tartakovsky, D. M., Robinson, B. A., and Aceves, A. B., Quantification of uncertainty in geochemical reactions. Water Resour. Res. 43, 2007, W12415.

[13] Ross, J.L., Ozbek, M.M. and Pinder, G.F., Aleatoric and epistemic uncertainty in groundwater flow and transport simulation. Water Resour. Res., 45, 2009, W00B15.

[14] Zadeh, L., Fuzzy sets. *Information and Control*, 8, 1965, 338– 353.

[15] Zadeh, L. A., Fuzzy algorithms. Information and Control 12, 1968, 94-102.

[16] Bellman, R.E., Zadeh, L.A., Decision-making in a fuzzy environment. *Management Science,* 17, 1970, 141-164.

[17] Cho, H.N., Choi, H.-H., Kim, Y.B., A risk assessment methodology for incorporating uncertainties using fuzzy concepts. Reliability Engineering and System Safety 78, 2002, 173-183.

[18] Kentel, E., Aral, M.M., Probabilistic-fuzzy health risk modeling. Stochastic Environmental Research and Risk Assessment (SERRA) 18, 2004, 324-338.

[19] Mauris, G., Lasserre, V., Foulloy, L., A fuzzy approach for the expression of uncertainty in measurement. Measurement, 29, 2001, 165-177.

[20] Hanss, M., Willner, K., On using fuzzy arithmetic to solve problems with uncertain model parameters. In Proc. of the Euromech 405 Colloquium, Valenciennes, France, 1999, 85-92.

[21] Abebe, A.J., Guinot, V., Solomatine, D.P., Fuzzy alpha-cut vs. Monte Carlo techniques in assessing uncertainty in model parameters. 4th Int. Conf. Hydroinformatics, Iowa, USA, 2000.

The impact of the March 10, 2009 dust storm on meteorological parameters in central Saudi Arabia

Abdullrahman H. Maghrabi

National Centre For Mathematics and Physics, King Abdulaziz City For Science and Technology, Riyadh , Saudi Arabia
** Corresponding author. Tel: +966-501051884, Fax: +966-14813521, E-mail. amaghrabi@kacst.edu.sa*

Abstract: Dust particles play an important role in air quality and environmental health. They affect both solar and terrestrial radiation by scattering and absorption and are therefore considered to be a significant climate-forcing factor. Dust storms are natural hazards that affect daily life for an interval ranging from a few hours to a few days, and they are a very frequent phenomenon in Saudi Arabia, especially in the pre-monsoon season.
On 10th March 2009 a widespread and severe dust storm event that lasted several hours struck Riyadh (24.9 1° N, 46.41° E, 764 m) and represented one of the most intense dust storms experienced in Saudi Arabia in the last two decades. In this study, the effect of this dust storm on meteorological parameters was investigated. These parameters are relative humidity, air temperature, visibility and atmospheric pressure. Around noon local time on the event day, with the arrival of the dust plume, there were dramatic changes in weather conditions. Air temperature dropped by about 6 ^{o}C, relative humidity increased dramatically reaching a value of 33 %. The visibility deteriorated dramatically to a value of 1 m. These results also, show that the effect of this storm was associated with an increase in both atmospheric pressure and relative humidity as well as a r eduction in temperature and visibility for the two days following the storm in comparison with conditions before the storm. The impact of several other dust storms on meteorological parameters during the year of 2009 were investigated and compared to the March 10th storm. It was found that this storm had a greater effect on the meteorological variables than the other storms.

Keywords: *Dust Storm, Riyadh, Temperature, Solar Radiation*

1. Introduction

Atmospheric aerosols are linked to the climate system and to the hydrologic cycle. Depending on their composition, atmospheric aerosols can absorb solar radiation in the atmosphere, producing further cooling of the surface and warming the atmosphere. Dust particles affect both solar and terrestrial radiation and are thus considered a significant climate-forcing factor and an important parameter in radiation budget studies [1]. The net effect of atmospheric aerosols is to cool the planet by reflecting incoming solar radiation. One of the major problems associated with dust storms is the considerable reduction of visibility that limits various activities, increases traffic accidents, and may increase the occurrence of vertigo in aircraft pilots [2]. Other environmental impacts include reduced soil fertility at the source area, damage to crops, a reduction of solar radiation, and, consequently, a reduction in the efficiency of solar devices, damage to telecommunications and mechanical systems, dirt, and air pollution. In addition, aerosols have a significant impact on hum an health. Goudie[3] recently provided an up-to-date and comprehensive review on dus t storms and their significance for many fields.

The frequency of dust-storm occurrence in Saudi Arabia is at a maximum during the pre-monsoon (March–May) season, when dust aerosols are transported by south-westerly winds from the arid and semi-arid regions around the Arabian Sea.

In Saudi Arabia, dust storms are considered among the most severe environmental problems. Several investigators have studied desert dust in Saudi Arabia [4]. Most of the previous studies have used either surface or satellite observations to characterise the large-scale dust loading of the atmosphere over the Arabian Peninsula. H owever, almost nothing has been

done to study the effect of these dust storms on meteorological parameters and solar and infrared radiation in this region.

On the 10th of March 2009, a dramatic windstorm moved over Riyadh that was accompanied by a strong dust storm. This short-lived but intense dust storm caused a widespread, heavy dust load, greatly affected visibility and air quality, and caused a total airport shutdown as well as damage to buildings, vehicles, power poles and trees throughout the city of Riyadh. This storm was massive enough to be seen clearly from outer space and is considered to be one of the heaviest recorded dust storms in the last two decades. The outbreak of the dust storm was associated with a cold frontal passage that coincided with the propagation of a pre-existing synoptic-scale upper tropospheric jet stream over the northern and central parts of Saudi Arabia.

An investigation of the impact of this storm on solar and infrared radiation will be presented in another paper. This paper studies the impact of this severe storm on meteorological parameters and shows the variability of these parameters due to the storm.

2. Experimental Site and data:

The study area of Riyadh lies in the central region of the Arabian Peninsula at 24° 43 ′N; 46° 40′E, 764 m a.s.l. Riyadh is the capital of Saudi Arabia and its largest city; its population is 4500000 according to the 2005 census. It is a purely urbanised area and is one of the most polluted areas in the Kingdom because it is surrounded by industrial areas and traffic arterials, with the natural environment of the Empty-Quarter Desert lying beyond. The arid conditions prevailing at this site are responsible for large seasonal temperature differences, providing cool winters and very hot summers. The area experiences extremely low humidity, particularly in the summer. The climate of the region exhibits four dominant seasons each year: winter (December–February), pre-monsoon (March–May), monsoon (June–August), and post-monsoon (September–November). The pre-monsoon season, during which the present case study was conducted, is characterised by frequent dust storms and long dry spells.

Standard meteorological observations such as air temperature, relative humidity, and cloud information were used in the current study. These data were obtained using Riyadh Airport records provided by the Presidency of Meteorology and Environment.

3. Results and Discussion

3.1. Event Description

For the purpose of clarification the discussion of results will include the behaviour of the considered variables two days before and two days after the storm along with the event day. These will be referred as pre-event, post-event and the event day respectively.

The hourly values of four meteorological variables; relative humidity (RH), temperature (T), visibility (vis), and atmospheric pressure (P) for March 8-12, 2009, are plotted in Figure 1. As shown in Figure 1a, both T and RH reveal a diurnal cycle throughout, displaying a trend opposite to what one would expect. Visibility was in the 8-10 km range on the 8th and 9th of March and on the morning of the 10th, which is the normal maximum visibility found in Riyadh at this time of the year. The atmospheric pressure shown in Figure 1b shows a less clear diurnal cycle with some variability from one hour to the next on each day. Through most of the period from the morning of the 8th of March until the morning on the 10th, wind

directions were consistently southerly. Wind speeds increased during this period from ~10 m/s on the 8th to ~20 m/s on the 9th.

On the day of the event, before the arrival of the storm, the weather was stable; T was ~28 °C, P was 939.8 hPa, RH was 10%, and the local wind was relatively light towards the south. Around noon local time, with the arrival of the dust plume, there were dramatic changes in weather conditions. The wind swung to a northerly direction and wind speed rapidly increased to a maximum of 30 ms^{-1}.

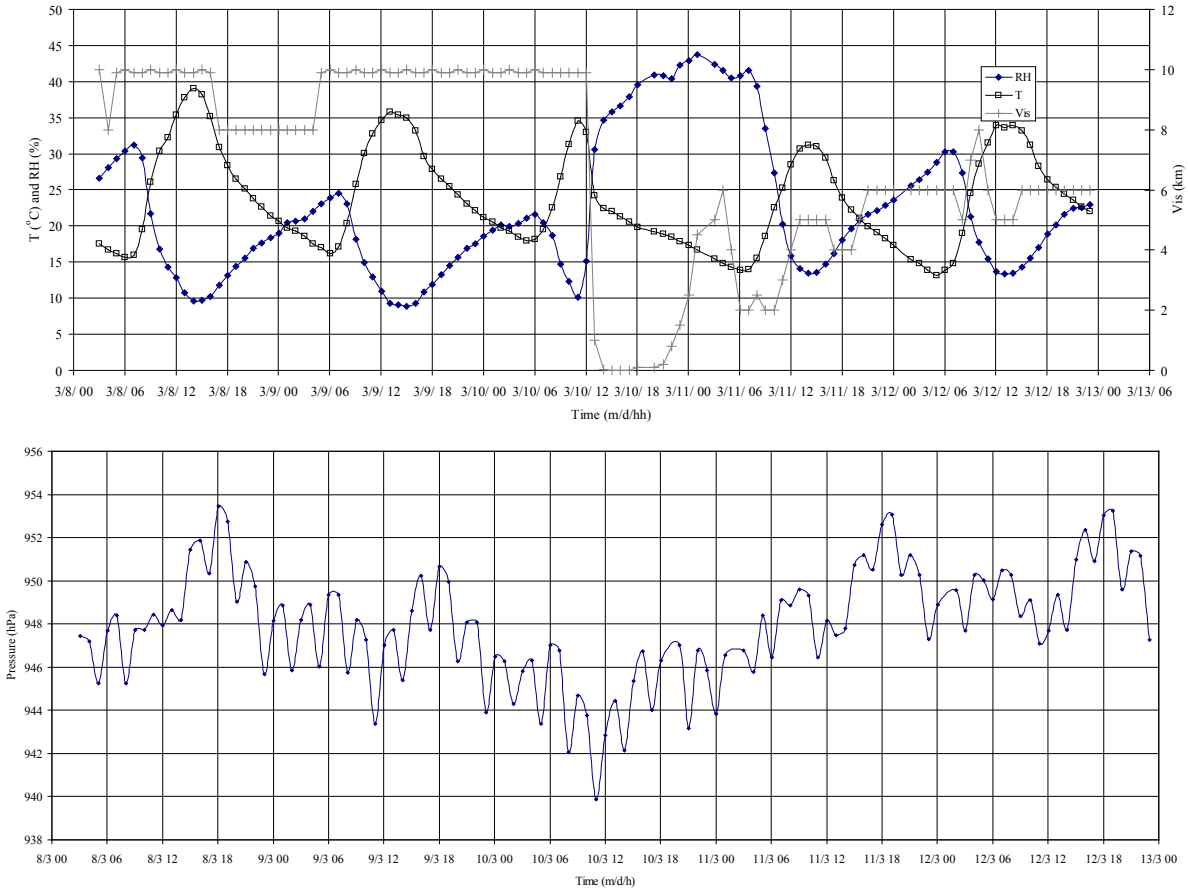

Fig. 1. Day-to-day variations of meteorological parameters (a) relative humidity ,air temperature, and visibility ;and(b) atmospheric pressure for the period from March 8th to March 12th 2009.

Because of the wind change and dust storm, T dropped by about 6 °C within an hour to reach 22 °C. The temperature continued to decrease until it reached the daily minimum of about 14 °C at 07:00 a.m. on the 11th. The air temperature then resumed its normal daily cycle, although temperatures remained cool on the 11th with a maximum of only 23 °C. It is likely that this reduction in the daytime temperature was caused by the reduced heating near the surface resulting from shortwave energy extinction by the additional aerosol loads arriving with the storm on the 10th. Relative humidity, on the other hand, increased dramatically with the arrival of the dust storm, reaching a maximum of 44 % at 01:00 on the 11th. The change in relative humidity is partly due to the cooler air temperatures but is also likely due to the moisture brought to the region by the storm. The visibility deteriorated dramatically with the arrival of the dust storm and then remained around 1 m for the 3 hours following the event. It then increased to 6 km by 03:00 on the 11th. After another decrease to ~ 2 km in the early

hours of the morning, it rose to between 5 km and 6 km and stayed around this mark for the rest of the period considered.
Several investigations on the dust storms in the Arabian Gulf and adjacent Gulf countries [5] and other places around the world [6] have reported similar variations and characteristic changes in meteorology.

3.2. Comparisons with other events

Table 1 shows a list of seven storm events during 2009. It summarises the change of the four meteorological parameters during these events. These changes represent the difference between the measured value immediately before the event and the maximum and minimum values reached immediately due to the event. In the last column, the time of maximum change occurs after the arrival of the storm is provided. Three of these events occurred in the pre-monsoon season, two in spring, one in summer and one in winter. In the last row of the table, the changes in the meteorological parameters for the 10th of March are summarised. Apart from the 18/9 event, the ranges of the changes in both atmospheric pressure and air temperature are confined between 2-4 hPa and 2-3 ^{o}C, respectively. The drop in the visibility varies between a minimum of 4 to a maximum of 8 km. The maximum changes in the relative humidity occurred on 4/6 and 18/9, followed by that on 20/5. For the events on 19/3 and 6/10, the RH dropped by -7 and -5 respectively. This drop may be due to the characteristics of the dry air mass that brought the storm to the study region. The 4/6 event is considered the strongest of the seven events. For this event, two hours after the storm, RH and atmospheric pressured increased by 10% and 3 hPa; temperature and visibility dropped by 3^{o}C and 8 km, respectively. Comparisons between the 10th of March event and the seven other storm events showed, with the exception of the atmospheric pressure, that the changes in the meteorological variables are higher for the 10th March. In addition, although the two hours after the event on the 10th are considered to be relatively short, dramatic changes occurred during this time.

Table 1 shows the difference between the meteorological variables before the storm and after the storm for the storm event in 2009. The last column is the time when maximum change occurred after the arrival of the storm

DAY/MONTH	Δ VIS (KM)	Δ T (^{O}C)	Δ P (HPA)	ΔRH (%)	TIME OF MAX. (HOURS)
20/5	4	2	3	9	2
28/5	7	3	2	7	3
4/6	8	3	3	10	2
19/3	8	3	2	-7	2
6/10	5	2	4	-5	2
28/2	6	2	3	9	3
18/9	5	4	5	10	2
10/3	**9.9**	**6**	**4**	**25**	**2**

The effect of different aerosol loads on both the spectral and broadband solar radiation components have been investigated extensively both experimentally and theoretically by several researchers. It has been found that the aerosols may reduce the solar radiation by as much as 50% [7]. Additionally, it was found that dust storms severely affect meteorological variables. Their impact on these variables is different and becomes severe in some cases,

such as the one presented in this paper. Moreover, because several models have been developed to predict the solar radiation components (e.g., global and diffuse), it is important to consider the impact of such transient and severe events and study their effects to produce the appropriate predictability.

4. Conclusion

On 10 March 2009, a severe and extensive dust storm event struck Riyadh and lasted for several hours. The impact of this event on ground–based measurements of meteorological parameters was investigated. These parameters are relative humidity, air temperature, visibility and atmospheric pressure. The analysis for the behaviour of the considered variables two days before and two days after the storm along with the event day were conducted and presented.

The investigations show significant changes in all of the measured parameters as a result of this event. Around noon local time on the event day, with the arrival of the dust plume, there were dramatic changes in weather conditions. Air temperature dropped by about 6 ^{o}C, relative humidity increased dramatically reaching a value of 33 %. The visibility deteriorated dramatically to a value of 1 m. These results also, show that the effect of this storm was associated with an increase in both atmospheric pressure and relative humidity as well as a reduction in temperature and visibility for the two days following the storm in comparison with conditions before the storm. Comparisons between this storm event and seven other reported events that occurred in the same year showed that this event was the most extreme and the most severe.

References

[1] A. Jayaraman, Lubin, D., Ramachndran, S., Ramanathan, V., Woodbridge, E., Collins W. and Zalupuri, K. S.. Direct observation of aerosol radiative forcing over the tropical Indian Ocean during the Jan.- Feb. 1996 pre-INDOEX cruise. J. Geophys. Res. 1998, 103,13827–13836.

[2] H. Kutiel, and Furman, H.,. Dust storms in the Middle East: Sources of origin and their temporal characteristics. Indoor and Built Environment, 2003, 12(6),419-426

[3] A.S., Goudie, Dust storms: Recent developments. Journal of Environmental Management, 2009,90,89-94.

[4] B. H. Alharbi, and Moied, K. 2005. Riyadh air quality report (1999-2004), King Abdulaziz City for Science and Technology, No. 279-25-ER.

[5] D. L. McNaughton, Possible connection between anomalous anticyclones and sandstorms. Weather, 1987, 42 (1),8-13.

[6] P. M., Pauley, Baker, N. L. and Barker, E. H., An Observational Study of the "Interstate 5" Dust Storm Case; Bulletin of the American Meteorological Society, 1996, 77 (4), 693-720.

[7] K.V.S., Badarinath, Kharol, S.K, , Kaskaoutis, D.G., and Kambezidis , H.D. 2007. Case study of a dust storm over Hyderabad area, India: Its impact on solar radiation using satellite data and ground measurements; Science of the Total Environment 384 :316–332.

The medium to long-term role of renewable energy sources in climate change mitigation in Portugal

Sofia Simões[1,*], Júlia Seixas [1], Patrícia Fortes[1], Luís Dias[1], João Gouveia[1], Bárbara Maurício[1]

[1] *CENSE, Departamento de Ciências e Engenharia do Ambiente, Faculdade de Ciências e Tecnologia, Universidade Nova de Lisboa, Caparica, Portugal*
** Corresponding author. Tel: +351 212948354, Fax: +351 212948354, E-mail: sgcs@fct.unl.pt*

Abstract: Portuguese policy-makers have adopted ambitious targets for RES promotion until 2020, but there are no national targets for the medium to long -term (2050) and it is not clear to what extent which RES can contribute to CC mitigation. This paper aims to assess the contribution of RES for the CC mitigation in Portugal until 2050, under cost-effectiveness criteria. The TIMES_PT linear optimization bottom-up technology model was used to generate six scenarios to 2050 combining GHG emission caps, levels of socio-economic growth and share of RES electricity. In order to meet the 2050 energy demand, the share of RES in primary energy consumption increases 4 to 6 times from 2005 and in final energy grows from 15% in 2005 to 56-59% in 2050. RES were found to be cost-effective even without a GHG cap. Regarding CC mitigation the high RES shares in final energy correspond to less 49-74% GHG emissions in 2050 compared to a baseline without cap. The role of renewable electricity is determinant to mitigate CC especially due to hydro and onshore wind. Other important deployments of RES technologies are solar water heating and heat pumps in buildings, biomass use for process heat in industry and biodiesel in transport.

Keywords: *Climate change mitigation, Renewable energy, Energy modeling, Portugal.*

1. Introduction

Renewable energy sources (RES) play a key-role in climate change (CC) mitigation. Moreover, RES have added benefits of reducing external energy dependency and fostering economic development. Acknowledging this, Portugal has been pointed worldwide as a success case for RES deployment (IEA, 2009, NYT, 2010). National CC & energy policy-makers have adopted ambitious targets for RES promotion until 2020. The National Energy Strategy for 2020 (Cabinet Resolution n. º 29/2010 of April 15) defines the following main objectives: i) reduce the external energy dependency to 74% (it was 87% in 2008); ii) ensure compliance of commitments within EU climate change policies, allowing that in 2020 60% of generated electricity is renewable based (RES-E) and 31% of final energy consumption is from RES (respectively 50% RES-E in September 2010 and 20% in 2005), and iii) achieving a reduction of 20% final energy consumption in the terms of the Energy-Climate policy package. The Portuguese National Action Plan (PNAER) within the Directive 2009/28/EC sets even more ambitious policies & measures (P&M) that will allow reaching 70% RES-E in 2020 and 10% biofuels in transport (update on PNAER by the Decree-Law nº 117/2010 of October 25). Other P&M are in place to promote RES heating and cooling and end-use energy efficiency, namely through the National Energy Efficiency Action Plan (RCM 80/2008).

Although there is high policy focus on medium-term RES promotion (2020) there are no national targets for the medium to long-term (2050). Likewise there are no quantitative estimates on avoided GHG emissions due to RES promotion, both in medium and long-term. Furthermore, there is no information on which RES (e.g. solar or waves) and which RES technologies (e.g. PV panels or biomass boilers) are the most cost-effective for Portugal. This is highly relevant to support national policy making, particularly regarding the design of incentives to promote the most cost-effective RES. This paper aims to assess the contribution of RES for the reduction of GHG emissions in Portugal until 2050 looking into detail into which technologies are most cost-effective.

2. Methodology

To assess the role of RES in CC mitigation in Portugal up to 2050, we used the TIMES_PT model to generate six scenarios combining different assumptions as presented in Table 1.

Table 1. GHG and RES scenarios for Portugal up to 2050

Scenario	GHG cap	Economic Growth[a)]	Minimum fossil electricity
C	None	Conservative	30% of total electricity
F	None	Fenix	30% of total electricity
-50C	-50% in 2050 / 1990	Conservative	30% of total electricity
-50F	-50% in 2050 / 1990	Fenix	30% of total electricity
Cefre	None	Conservative	None
Fefre	None	Fenix	None

[a)] Two socio-economic scenarios were developed for Portugal as briefly outlined below.

To assess RES contribution to CC mitigation, we consider a **GHG[1] emission cap** in the -50C and -50F scenarios starting from 2015 with +27% of the 1990 (the Kyoto target for 2010-2012 extended to 2015) and linearly more stringent until -50% of 1990 for combustion and productive processes GHG emissions in 2050. (A trend line was then generated from the 2015 to the 2050 cap to obtain intermediate emission caps for every 5 years. The -50% cap is quite severe as it roughly leads to per capita emissions of 2.04 t CO2e in 2050 whereas in 2008 Portugal had 7.4 t CO2e. The per capita EU 15 average in 2008 was 10.1 tCO2e according to EEA data.

Regarding **economic growth and demand for energy services**, two contrasting socio-economic scenarios were used: Conservative and Fenix. The Conservative scenario follows the current economic and demographic trends (1% GDP annual growth rate and population decrease); whereas the Fenix scenario has more optimistic economic and population evolution forecasts (2 to 2.26% GDP annual growth rates and more 12% inhabitants in 2050 compared to 2005). These scenarios were used to generate two demand projections for materials and energy services such as residential lighting or cement which are inputs of the TIMES_PT model. More information on the demand projections and can be found on Seixas *et al.* (2009).

Finally, in four of the six studied scenarios (C, F, -50C and -50F) we assumed a conservative requirement to assure the reliability of the power system translated as a **minimum of 30% of total generated electricity is produced by centralized fossil plants** from 2015 to 2050. In the Cefre and Fefre scenarios we removed this constraint and the system is free to adopt as much RES-E as needed according to cost-effectiveness criteria. Such approach could be associated with ensuring security of supply via expanded transmission capacity and increased electricity trade. In this paper however, we do not deal with electricity trade. We assumed that the net electricity imports are nil from 2025 onwards following the Portuguese transmission system operator expectations. If assumed otherwise the entire configuration of the electricity system would alter depending on how much electricity could be exported. However, at the moment there are absolutely no expectations on amounts of electricity traded after 2025 and any scenarios would by highly uncertain and out of the scope of this paper. Thus we have focused instead on the cost-effective assessment of maximum potential of national renewable

[1] This paper solely refers to energy related GHG emissions, i.e. from fuel combustion activities, fugitive emissions from oil, natural gas and other sources and from major industrial processes. These were approximately 81% of 2005 national emissions.

resources for the national CC mitigation considering nil electricity imports after 2025.

All these assumptions were inputted into the linear optimization bottom-up technology TIMES_PT[2] model which represents the Portuguese energy system from 2005 to 2050. The TIMES_PT is an implementation of the TIMES family of models developed by ETSAP of IEA which has been implemented at global, regional or national level (ETSAP, 2008), namely for the whole of UE (Pan European Times model from the NEEDS project) or for the countries Spain (Labriet, *et al.*, 2010), Belgium (Proost, *et al.*, 2009) or Germany (Blesl, *et al.*, 2007), among other EU countries. It considers both the supply and demand sides and disaggregates the energy demand sectors. The model is supported by a detailed database, which includes the technical and economical characteristics of the existing and future energy technologies and present and future sources of primary energy supply and their maximum technical and economic potentials (e.g. maximum available biomass or area for solar panels). TIMES_PT finds the optimum combination of energy supply and demand technologies to satisfy the demand with the lowest possible total costs. More information on the details of the model can be found in Simões *et al.* (2008) and more details on the technology and primary energy assumptions in Seixas *et al.* (2009). The learning curves for RES-E solar and wave technologies are from the IEA (IEA, 2010, IEA, 2008) which were validated by national stakeholders. Wind RES-E technologies learning curves were supplied by national experts of the National Energy and Geology Research Institute (LNEG, 2010).

Other exogenous assumptions are very briefly outlined: 1) 8% discount rate for centralized electricity generation, buses and trains; 12% for commercial, industry, decentralized electricity generation, CHP and freight transport; and 17.5% for residential, cars and motorcycles. 2) maximum of 5000 Gg CO2 carbon capture and storage potential were assumed as available since there is no data at the moment available for Portugal. More information on CCS cost data can be found at Simões *et al.* (2008); 3) no nuclear due to current policies and the purpose of this work focusing the role of RES; 4) new coal power plants without CCS not allowed due to climate policy; 5) RES targets, subsidies or feed-in tariffs not considered; 6) cost of oil barrel of 100 USD$_{2008}$ for the year 2020, 115 in 2030 and 145 in 2050.

3. Results

3.1. RES in primary energy consumption

In order to meet the 2050 energy demand, the share of RES in primary energy consumption can increase to two to three times the 2005 values in the scenarios without GHG emission cap (Figure 1) which shows the cost-effectiveness of RES. To meet the CO2 caps (-50C and -50F) RES can further increase to 4 to 6 times the 2005 values. The most competitive RES in all scenarios are wind and hydro which achieve its maximum potential in 2050. Solar, national biomass and, to a lesser scale, geothermal are also competitive but only if a GHG cap is in place. Removing the 30% fossil electricity requirement does not lead to significant changes in RES in 2020. However, in 2050 the higher RES-E share leads to higher consumption of solar especially in the Fefre scenario, where it achieves its maximum potential.
The increase in RES allows decreasing the external energy dependency from 87% in 2008 to 70-77% in 2020 and to 58-72% in 2050. The lowest values are not obtained due to the GHG

[2] The Portuguese model development was undertaken within the EU FP7 research project NEEDS (www.needs-project.org). The NEEDS RS2a research team is responsible for the model structure. The authors are responsible for some structural changes, the base-year and new technologies information and for calibration and validation of the national model.

cap but instead due to 100% RES-E. If a backup of 30% fossil electricity is removed imports of natural gas for centralized CCGT plants can be reduced already in 2020. In any case, in 2050 a new energy import paradigm appears; instead of being dependent on imported fossil fuels the energy system will import biomass, particularly biofuels for transports.

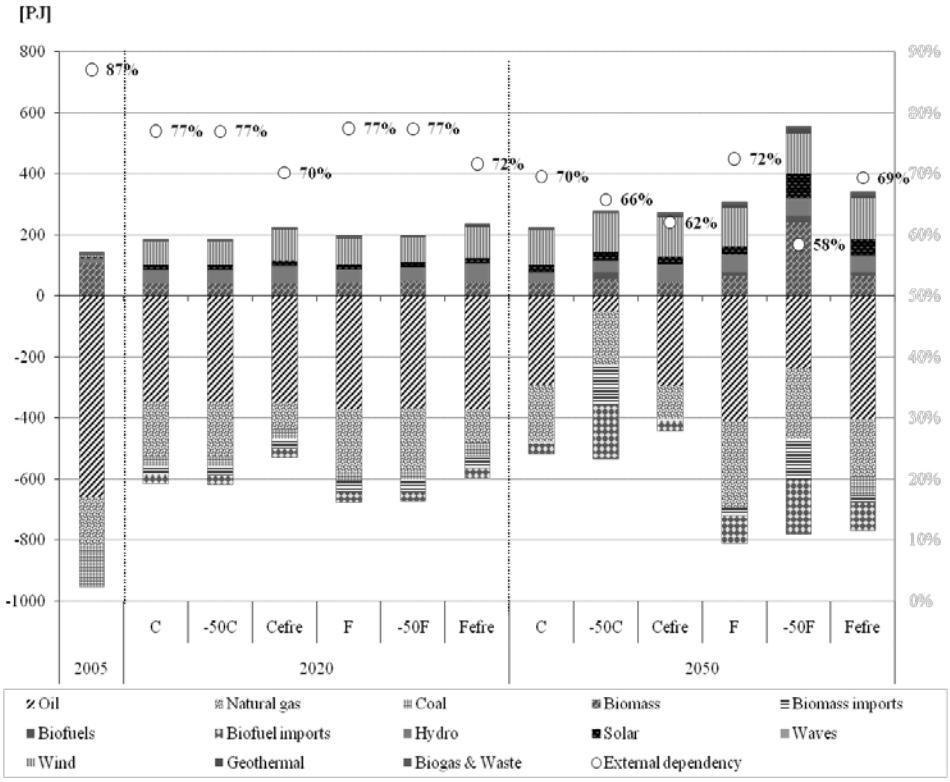

Fig. 1. Primary energy consumption in the studied scenarios, % of external energy dependency and % of RES (in the top rectangle). The lower values for 2020 are due to increase of refinery exports, decommissioning of a major coal power plant and slow recovery from 2010-2015 economic crisis.

3.2. RES in electricity generation

Until 2020 the electricity sector profile will be similar to 2009 since it will rely in recent investments both on RES (wind and hydro) and on new gas CCGT. Globally, approximately 58% of total electricity in 2020 is RES-E, in all scenarios with minimum 30% fossil electricity. In 2050 the GHG cap has a significant effect in RES-E technologies profile only in the -50F scenario since there is a higher overall demand for electricity (107.16 TWh, in comparison with 84.03 TWh in F). In -50C wind and hydro are sufficient to meet the demand. The system will firstly use all available hydro and onshore wind resources and in -50F this is followed by centralised PV, biomass and biogas CHP, and both geothermal steam turbines and hot dry rock systems. These technologies are practically negligible in 2050 in C, F, and -50C as the demand for RES-E is not high enough also due to the requirement for minimum 30% electricity from centralised fossil fuel. Without this requirement, in Cefre and Fefre, already in 2020 at least 78% of electricity will be RES-E and hydro and wind potentials will be achieved (9.7 and 6.5 GW, respectively). In 2050 74-89% electricity is RES and in Fefre large PV plants achieve the maximum potential (9.33 GW) and appears 0.50 GW of wind offshore. Both in 2020 and 2050 the gas CCGT plants will not work due to higher fuel and O&M costs.

In Cefre and Fefre there is a lower demand for electricity than in the other scenarios due to the higher contribution of efficient equipments and appliances in buildings, district heating in

commercial and biomass and insulation in the residential. This means that the 30% fossil electricity requirement hampers energy efficiency and RES use in final energy.

3.3. RES in final energy consumption

Concerning final energy consumption (FEC) in 2020, no significant changes in the energy profile are expected, even with the cap, although RES share increases from15% of total FEC in 2005 to 30-35%. In the long term (2050) it is clear that the increase in electricity is a major strategy to mitigate CC as there are endogenous energy resources used to generate RES-E, especially wind and hydro, as mentioned before. In 2050, the FEC in the F scenario is almost 70% higher than in the C leading to new technologies to meet the cap, such as H2 for transports. The share of RES in FEC in 2050 varies from 31-36% in scenarios without the GHG cap to 56-59% with the cap (Table 2). The RES share grows more due to the GHG cap in the transports (both in C and F) and industry (only in the -50F scenario) sectors.

Table 2. RES contribution in final energy consumption for the six scenarios

Sector/Scenario [PJ]	2005	2050					
		C	-50C	Cefre	F	-50F	Fefre
RES Electricity	32	159	188	203	221	300	252
RES Heath & cold	96	69	68	69	91	206	93
Residential	50	34	32	34	39	38	39
Commercial	0	11	8	10	14	13	13
Industry	45	25	27	25	39	155	41
RES in Transport	0	36	245	36	98	200	98
Final Renewable Energy (a)	128	263	501	307	410	707	442
Total Final Energy (b)	826	863	846	860	1225	1253	1224
% Renewables (a/b)	**15**	**31**	**59**	**36**	**33**	**56**	**36**

Other relevant uses of RES are solar for water and space heating in buildings, which in all scenarios, regardless of GHG cap and RES-E restrictions; achieve its maximum potential already in 2020. In 2050 with the GHG cap, solar panels are also cost-effective to generate heat for industry and the potential is also achieved. The role of biomass is reduced in buildings as electricity, solar thermal and heat pumps become more appealing. On the other hand, biomass will become more cost-effective in CHP to generate heat for industry. In transports the share of biofuels is expected to increase above 10% in 2020 in all scenarios and in 2050 up to 60-40% due to the GHG cap. Other impacts of the GHG cap in 2050 in the transport sector are to create room and need for electric vehicles and for H2 freight trucks.

4. Discussion

We found that RES technologies are highly cost–effective in the Portuguese energy system even without any CO2 cap (36-38% of PEC and 31-33% of FEC in 2050). If an ambitious CC mitigation cap is in place, the contribution of RES is even higher to 65-72% of PEC and 59-56% of FEC in 2050. If the layout of the power sector does not require centralised fossil plants, for example by ensuring security of supply via expanded transmission capacity, RES contribute with 41-44% of PEC and 36% of FEC in 2050. So, a cap on GHG emissions has a larger impact in RES contribution than a reconfiguration of the power system. Although RES play a fundamental role in CC mitigation in Portugal it should be noted that it is not possible to reduce external energy dependency below 77% in 2020 and below 50% in 2050. Further reductions are only possible with stronger efforts on energy efficiency, which were not in the

scope of this paper.

Regarding RES technologies, hydro and wind power can achieve the maximum technical and economic potential in Portugal in the medium run (2020) and contribute significantly to generated electricity. To some extent, this already occurs as in 2009 wind and hydro ensured 34% of total generated electricity. Until 2050 they can generate 60-80% of total electricity, respectively if a GHG cap is in place or if no fossil electricity backups are required. On the other hand, electricity generation technologies from solar are still in an early-phase and need extra incentives to become competitive before 2050. Nonetheless, policy support to solar technologies should be considered from a R&D perspective anticipating future technology costs reductions since Portugal already has know-how in this area and some national companies manufacture components. Electricity generation from waves and offshore wind technologies are competitive from 2035 onwards only if Portugal adopts an aggressive GHG cap or no centralised fossil backup is needed. In these conditions and considering the existing national R&D capacities and wind parts supply chain, these two technology groups should be considered by policy makers as a priority.

Besides RES electricity, solar (both for water and space heating) is highly competitive already in the medium term (2020) even without any GHG emission cap. Heat pumps are also extremely competitive but only if a cap is in place. On the other hand electric vehicles are only cost-effective in 2050 if a cap is in place and the technology evolves to supply long-distance mobility as existing cars do. Otherwise, biofuels are a cheaper alternative.

Finally, the results presented have the following main caveats: 1) learning curve for energy technologies with high uncertainty, especially for the least mature technologies; 2) high uncertainty of profile of electricity trade within the Iberian electricity market; 3) high uncertainty on the availability of endogenous and imported biomass and biofuels. Moreover, the TIMES_PT is a partial equilibrium model and thus does not model economic interactions outside the energy sector and does not consider in detail demand curves and non-rational aspects that condition investment in new technologies. All of these caveats reflect real life uncertainties which policy makers have to deal with especially when thinking of long-term policies. An approach to try to handle uncertainty is to perform sensitivity analysis which the authors did for the RES electricity technologies learning curve (solar, wind offshore and waves) and for available biofuels and biomass. For electricity trade this was no done due to lack of any indication of plausible scenarios and involved amount of work considering the scope of the paper, as mentioned in section 2. It was found that assumptions on the technology learning rate affect the share of the different RES-E technologies in the energy system but the total share of RES-E is not altered. Variations on the amounts and prices of available biomass significantly affect RES potential for CC mitigation in Portugal, as biomass and biofuels are preferable to RES-E in the industry and transport sectors, since they are more cost-effective. However, it is not in the scope of this paper to discuss and assess uncertainty in detail and thus it is not possible here to present and discuss in detail the performed sensitivity analysis, but only to draw attention to the limitations of the results, which serve to illustrate that in Portugal RES are very effective for CC mitigation goals.

5. Conclusions

This paper's objective is to assess the contribution of RES for CC mitigation in Portugal until 2050 looking into detail into which technologies are most cost-effective. We have found that the RES share in final energy consumption can increase from 15% in 2005 to 31-33% in 2050 in a baseline scenario without an emission cap. This illustrates that RES are cost-effective

regardless of the goal of CC mitigation, especially in the electricity generation sector (mostly hydropower and wind onshore technologies). To meet the GHG cap of-50% in 2050 this share can further increase to 56-59% of total final energy consumption. This represents a growth of more than 200% of 2005 values. Although the increase of energy efficiency is an alternative cost-effective strategy to CC mitigation, the GDP energy intensity in 2050 is only less 32-40% of 2005 values. This seems to suggest that RES can contribute more significantly to the emission targets than energy efficiency improvements.

Regarding GHG emission reduction, a49-74% emission reduction is achieved in 2050 for the -50% cap compared to the baseline. Electricity generation is the most relevant sector for abatement. This sector can be responsible for up to 98% of all abatement in 2050 if the constraint of a minimum of 30% total generated electricity is produced by centralized fossil plants is not present. In this situation all electricity will be renewable. In the scenarios where this minimum fossil electricity is required the electricity sector is not completely renewable and the transport sector is the most important sector for total GHG abatement (up to 57% of total GHG emission reduction in 2050 compared to baseline). In both sectors RES are the main reason for emission abatement, both hydropower and onshore wind technologies, followed to a lesser extent by solar PV and geothermal electricity generation technologies, and biofuels for individual cars and freight trucks.

References

[1] IEA. Energy Policies of IEA Countries – Portugal 2009 Review. OECD / International Energy Agency. Paris, France, 2010, pp. 131-146.

[2] J. Seixas, S. Simões, P. Fortes, L. Dias, J. Gouveia, B. Alves, B. Maurício, [New Energy Technologies: Road Map Portugal 2050, D3: Competitiveness Assessment of New Energy Technologies], Novas Tecnologias Energéticas: Road Map Portugal 2050, D3: Análise da Competitividade das Novas Tecnologias Energéticas, Portuguese Innovation Fund for Renewable Energy of the Ministry of Economy, 2010, pp. 1-88.

[3] NYT. Portugal Gives Itself a Clean-Energy Makeover, The New York Times, August 10th, 2010.pp. A1. Available at: [http://www.nytimes.com/2010/08/10/science/earth/10portugal.html?_r=2&ref=global-home]

[4] ETSAP – International Energy Agency Implementing Agreement for a Programme of Energy Technology Systems Analysis, Global Energy Systems and Common Analysis Final Report of Annex X (2005-2008), Ed. G. Goldstein, G. Tosato, ETSAP, 2008, pp. 21 - 77.

[5] S. Simões, J. Cleto, P. Fortes, J. Seixas, G. Huppes, Cost of energy and environmental policy in Portuguese CO_2 abatement - scenario analysis to 2020. Energy Policy, 2008, Vol. 36, Issue 9, pp. 3598 - 3611.

[6] M. Labriet, H. Cabal, Y. Lechon, G. Giannakidis, A. Kanudia, The implementation of the EU renewable directive in Spain. Strategies and challenges. Energy Policy, 2010, Vol. 38, Issue 5, pp. 2272 - 2281.

[7] S. Proost, E. Delhaye, W. Nijs, D. van Regemorter, Will a radical transport pricing reform jeopardize the ambitious EU climate change objectives? Energy Policy, 2009, Vol. 37, Issue 10, pp. 3863 - 3871.

[8] M. Blesl, A. Das, U. Fahl, U. Remme, Role of energy efficiency standards in reducing CO2 emissions in Germany: An assessment with TIMES. Energy Policy, 2007, Vol. 35,

Issue 2, pp. 772 - 785.

[9] IEA, Technology Roadmap – Solar Photovoltaic Energy, OECD/International Energy Agency. Paris, France, 2010, pp. 7 – 9.

[10] IEA, Technology Roadmap – Concentrating Solar Power, OECD/International Energy Agency. Paris, France, 2010, pp. 27 - 28.

[11] IEA, Energy Technology Perspectives, OECD/International Energy Agency. Paris, France, 2008, pp. 400.

[12] LNEG, 2010. Personnel communication from Eng. Ana Estanqueiro from LNEG Unit of Solar, Wind and Ocean Energy. June 16, 2010.

Diversified analysis of renewable energy contribution for energy supply in Asian regions

Genku Kayo[1,*], Takashi Ikegami[2], Tomoki Ehara[3], Kazuyo Oyamada[3], Shuichi Ashina[1], Junichi Fujino[1]

[1] *National Institute for Environmental Studies (NIES), Ibaraki, Japan*
[2] *Institute of Industrial Science (IIS), Tokyo, Japan*
[3] *Mizuho Information and Research Institute (MHIR), Tokyo, Japan*
** Corresponding author. Tel: +81-29-850-2019, Fax: +81-29-850-2422, E-mail:kayo.genku@nies.go.jp*

Abstract: Renewable energy is one of the key drivers for reducing CO_2 emissions in the future. In order to support effective policy-making relating to renewable energy, estimation of available potentials mixed with all energy resources including fossil fuels is needed. However, previous research has sometimes focused on only one particular approach. Therefore, a diversified analysis of potential renewable energy contributions to energy supply in Asian regions was carried out in this paper. In order to estimate physical potential, a grid cell approach using geographical information system (GIS) data was adopted. Once the physical and technical potential had been estimated, the economic potential was then calculated. Socio-economic potential was analyzed using energy outlook data collected and reviewed from various publications in order to assess trends in energy demand and supply. The results indicate that almost all Asian countries will continue to develop and that the demand for energy will grow. With the aspect from potential amount, renewable energy supply is effective even though fossil fuels will continue to dominate totally energy mixes for the foreseeable future. In renewable energy supply, potential of solar is dominated and bears on wide implication compared with that of wind and biomass. To ensure the best possible results, further research should be carried out on the optimal schedule for the multi-phased introduction of renewable energy in long-term policy.

Keywords: *Solar energy potential, Wind energy potential, Biomass energy potential, Asian region*

1. Introduction

Renewable energy is one of the key drivers for reducing CO_2 emissions in the future. The third annual report (TAR) compiled by the IPCC expresses the relative potential of several phases of renewable energy in terms of physical, technological, socio-economic, economic and market potentials. In order to support effective policy-making relating to renewable energy, estimation of available potentials mixed with all energy resources including fossil fuels is needed. However, previous researches have sometimes focused on only one particular resource, for instance, solar energy (Hofman et al., 2002), wind energy (Grubb and Meyer, 1993) and biomass energy (Berndes et al., 2003). In this paper, diversified analysis of renewable energy contributions was carried out considering energy mix with fossil fuels and trends of energy demand. Renewable energy potentials were estimated in ten Asian regions. These regions included Japan (JPN), China (CHN), India (IND), Indonesia (IDN), Korea (KOR), Thailand (THA), Malaysia (MYS), Viet Nam (VNM), the Philippines (PHL) and Singapore (SGP).

1.1. Renewable energies

In this paper, three renewable energy sources were selected for investigation: solar, wind and biomass energy. It is expected that technologies to make use of these energy sources will be introduced into Asian countries in order to create a decentralized energy generation and supply system. Solar energy is included in this paper only in terms of the electricity generation provided by photovoltaic (PV) cells.

1.2. Definition

According to TAR (IPCC, 2001a), renewable energy can be described in terms of the following "potentials". The physical potential of a renewable energy source is the amount of that resource theoretically available in the area in question, and which can be considered suitable for production. This includes any constraints imposed by land use considerations or local site characteristics such as elevation and slope. The technical potential of a renewable energy source is the part of physical potential remaining after all losses due to conversion from the extractable primary energy source to secondary energy carriers or other forms of energy (electricity, fuel etc.) are taken into account. The socio-economic potential of a renewable energy source is the actual capacity for renewable energy use, taking into consideration the distribution of energy mixes and the growth of primary energy demand. The economic potential of a renewable energy source is the technical potential, based on the estimated production cost of a secondary form of energy which is competitive with a specified, locally relevant alternative. A flexible way to represent the economic potential is, therefore, in the form of energy production potential, expressed as a function of the production cost.

2. Methodology

2.1. Estimation of physical and technological potential

2.1.1. Data collection

In order to estimate physical potential, a grid cell approach using geographical information system (GIS) data was adopted. The physical potentials were estimated on a global basis using previously collected data such as insolation and wind speed measurements, land cover, elevation and wilderness area data. After calculation of the optimal inclination angle for solar PV cells in each grid cell, the total amounts of generation were estimated per cell and aggregated on a country-by-country basis. Table 1 shows the GIS data list that was used in this estimation process. (All the data used has been published on websites and made available for simulation purposes [5, 6, 7, 8, 9, 10, 11]).

Table 1. Data sources

Category	Data source	Original data provider
Land cover	MODIS/Terra Land Cover Type Yearly L3 Global 1km, Land Cover Type 1 (IGBP), 2005	NASA Land Processes Distributed Active Archive Center
Elevation	The Global Land One-km Base Elevation (GLOBE) Data, 1999	National Geophysical Data Center
Bathymetry	GEBCO One Minute Grid Version 2.00, 2006	General Bathymetric Chart of the Oceans
Wilderness	World Wilderness Areas, 1993	UNEP/GRID
Insolation	Surface Meteorology and Solar Energy Release 6.0 Data Set; Monthly averaged insolation incident on a horizontal surface, 2008	NASA Langley Research Center, Atmospheric Science Data Center
Wind Speed	Surface Meteorology and Solar Energy Release 5.0 Data Set; Monthly averaged wind speed at 50m above the surface, 2005	

2.1.2. Solar energy potential

Monthly and hourly solar energy potential in 3-by-3 arc-minute grid cells was calculated from averaged insolation data, averaged wind speed data, land cover type data, and so on. Compared with the previous method used (Bert. J. M. de Vries, 2007), extra parameters were included in the form of solar elevation angle, solar azimuth angle, land surface slope and elevation angle. In addition, the optimum inclination angle of each solar PV cell was calculated per grid cell and this information was also taken into account. The inclusion of these factors allowed a more accurate estimation to be made of the solar energy potential. The available area was determined using a suitability fraction, as shown in Table 2. For technical reasons, the area studied was limited to less than 5000m elevation and less than 60% slope. Solar energy potential, *EPS* [kWh/yr], was calculated using Eq. (1).

$$EPS_g = \sum_{M,T} I_{g,M,T} \cdot A_g \cdot \frac{e}{100} \qquad (1)$$

where *I* is the insolation intensity at the optimum inclination angle of solar PV [kW/m^2], *A* is the PV cell area [m^2], and *e* is the PV module efficiency (=13%). The subscripts *g*, *M* and *T* stand for the grid cell, month and time, respectively.

2.1.3. Wind energy potential

The wind turbine was assumed to be 80m high with a capacity of 2MW and rotors 90m in diameter. The available area was determined using a suitability fraction, as shown in Table 2, and restricted to less than 2000m elevation and less than 60% slope. Since the reference wind measurements provided by the surface meteorology dataset (NASA, 2005) were for a height of 50m, averaged wind speed was adjusted to a height of 80m, equal to that of the wind turbine. When the wind energy potential, *EPW* [kWh/yr], was calculated the probability distribution of wind speed *v* [m/s], the wind power correction factor *k,* and the availability rate j [%] were also taken into account, as shown in Eq. (2).

$$EPW_g = \sum_{v,LC} P(v) \cdot R(v) \cdot 8760 \cdot j \cdot k_{LC} \cdot (1-l) \cdot Nw_{g \cdot LC} \qquad (2)$$

where l is the loss rate, *LC* is the land cover, *P(v)* [kW] is the output of the wind turbine when the wind speed is *v* [m/s], and *R(v)* refers to the appearance probability distribution of the wind speed *v* [m/s]. Table 2 shows the parameter values for each type of land cover. Seventeen land cover categories were consolidated into four land use patterns. The suitability fraction values were one of the effective factors used in this estimation method. Therefore, in future, adequate suitability fractions should be estimated and modified by comparison with other, more precise calculations.

Table 2. Parameter values for each type of land cover

Land cover	Suitability Fraction [%]		Power Correction Factor [%]
	Solar	Wind	
All Forest, Closed Shrublands, Woody Savannas, Permanent Wetlands, Snow and Ice, Water Bodies	0	0	90
Urban and Built-Up Areas	1	0	90
Croplands, Natural Vegetation Mosaic	0	30	90
Open Shrublands, Savannas, Grasslands, Barren or Sparsely Vegetated Areas	1	50	95

2.1.4. Biomass energy potential

In the biomass energy potential calculation, twelve different resources (provided by the FAO statistical report, FAOSTAT, FAO, 2001) were taken into account. These resources included industrial round wood residues, pulp used for paper, sawn wood, mill residues, paper scrap, timber scrap, crop residues, sugarcane residues, bagasse, dung, kitchen refuse, and human feces. Each resource was assigned a different residual rate - defined as the fraction of the total amount available in production and able to be used for production purposes. Statistical data were, therefore, prepared in terms of volume or weight. The residual volumes were then converted to calorific values for calculation purposes.

2.1.5. Renewable energy potential grades

Renewable energy potentials were calculated and classified into three grades. When physical potentials were calculated, each grid cell was classified in terms of its renewable resource advantage. Grade I had some specific advantage in terms of its use as a renewable energy source, while grade III had some specific disadvantage associated with its use, due to location or climatic conditions. In the case of solar energy, the grade was determined by the insolation intensity received by each solar PV module [kWh/m^2/yr]. In the case of wind energy, the grade was determined by the utility operation rate, *UC* [%], defined by the percentage of annual electricity [TWh/yr] generated by full load operation throughout the year. The classified grades are shown in Table3 and 4.

2.2. Socio-economic potential estimation

Many institutes have published reports presenting statistical data or perspectives concerning the future of the Asian region, and this information is essential in order to estimate the contribution of renewable energies. However, because the Asian region is growing so rapidly and so dramatically, it is difficult to accurately construct future scenarios. Some reports published by international institutes (IPCC, 2001; IEA, 2009; EUROPEAN COMMISION, 2006; ADB, 2009; Greenpeace, 2008; Shell, 2008; Energy Research Institute, 2009; OECD, 2008 and so on) present various possible energy outlooks for future scenarios. Consequently, in this study, data relating to energy outlook were collected and reviewed in order to estimate expected trends in energy demand, supply and energy share in each country. After collecting data on the relevant parameters, maximum and minimum values were selected and a range of growth rates were established.

2.3. Economic potential estimation

After the calculations for physical and technical potential were completed, the production cost in each grid cell, *g*, was determined for each energy generation system. The production costs of solar energy, *CS* [USD/kWh], and wind energy, *CW* [USD/kWh], were calculated using Eq. (3) and Eq. (4).

$$CS_g = \frac{r}{1-(1+r)^{-LS}} \cdot \frac{(1+OM)\cdot INVS \cdot A_g}{EPS_g} \quad (3)$$

$$CW_g = \frac{r}{1-(1+r)^{-LW}} \cdot \frac{(1+OM)\cdot INVW \cdot A_g}{EPW_g} \quad (4)$$

where *OM* is the operation and maintenance cost expressed as a fraction of the investment cost, *r* is the discount rate, and *LS* or *LW* is the durable period. *EPS* and *EPW* are the energy potentials calculated using Eq. (1) or Eq. (2). *INVS* and *INVW* represent the cost of the system. In the case of solar energy, *INVS* was set at 780 [USD/m^2], which assumes 6 [USD/Wp]

included per PV module and BOS. *A* represents the area of the PV cell [m^2]. On the other hand, in the case of wind power, *INVW* was set at 760 [USD/kW], and *A* represents the construction area in each grid cell.

3. Results

3.1. Physical and technical potentials

3.1.1. Potential grades

Table 3 and 4 show the calculated results for physical and technical potential, broken down by grade. Comparing the three renewable energies studied shows that the solar energy potential is the largest, especially in grade II. China, India and Indonesia have some potential in grade I, reflecting good insolation conditions. However, regions such as Japan, China, Indonesia, Korea and Malaysia have more potential in grade III, overall, than in grade II. Wind energy potential is not as large as that of solar energy. Only China possesses significant potential in grade I. However, in the case of biomass energy, both China and India possess large potentials because of their large population and large plantation area. This physical potential analysis confirms that some countries have suitable renewable energy resources.

Table 3. Physical and technical potential, by grade (Solar Energy and Wind Energy)

Country code	Solar Energy Potential [TWh/yr]				Wind Energy Potential [TWh/yr]			
	Grade I 2200-2600 [kWh/m^2/y]	Grade II 1800-2200 [kWh/m^2/y]	Grade III 0-1800 [kWh/m^2/y]	Total	Grade I 40-100 [%]	Grade II 30-40 [%]	Grade III 0-30 [%]	Total
JPN	0	465	39,692	40,157	0	38	26	64
CHN	434	32,845	45,610	78,889	337	1,925	3,318	5,580
IND	4,255	46,136	169	50,560	0	177	721	898
IDN	5	1,625	3,699	5,329	0	0	45	45
KOR	0	3,759	6,604	10,363	0	0	17	17
THA	0	10,322	881	11,203	0	0	38	38
MYS	0	1,243	2,361	3,604	0	0	5	5
VNM	0	1,278	535	1,813	0	3	60	63
PHL	0	1,304	9	1,313	0	0	42	42
SGP	0	1,180	776	1,956	0	4	88	92

Table 4. Physical and technical potential, by grade (Biomass Energy)

Country code	Biomass Energy Potential [TWh/yr]			
	Grade I	Grade II	Grade III	Total
JPN	109	15	15	139
CHN	735	51	51	837
IND	577	8	8	593
IDN	121	7	7	135
KOR	25	3	3	31
THA	79	1	1	80
MYS	47	1	1	48
VNM	19	5	5	29
PHL	39	1	1	40
SGP	1	0	0	1

3.2. Socio-economic potentials

3.2.1. Review of expected energy demand in Asia

Fig. 1 shows expected total primary energy demand throughout Asia, as reported by IPCC (SRES2001, IPCC, 2001b). The curved lines indicate the forecasts simulated by several different models. The predicted maximum value in 2050 is approximately 3.84 times larger than the minimum value in 2050. The calculated results for physical and technical potentials are represented by the horizontal dashed lines in Fig. 1. The solar energy potentials, alone, can be seen to be large enough to meet the primary energy demand in all future scenarios. Wind energy potentials can also be seen to constitute an effective energy source. On the other hand, the biomass energy calculation shows that it is not large enough to constitute a major energy supply resource.

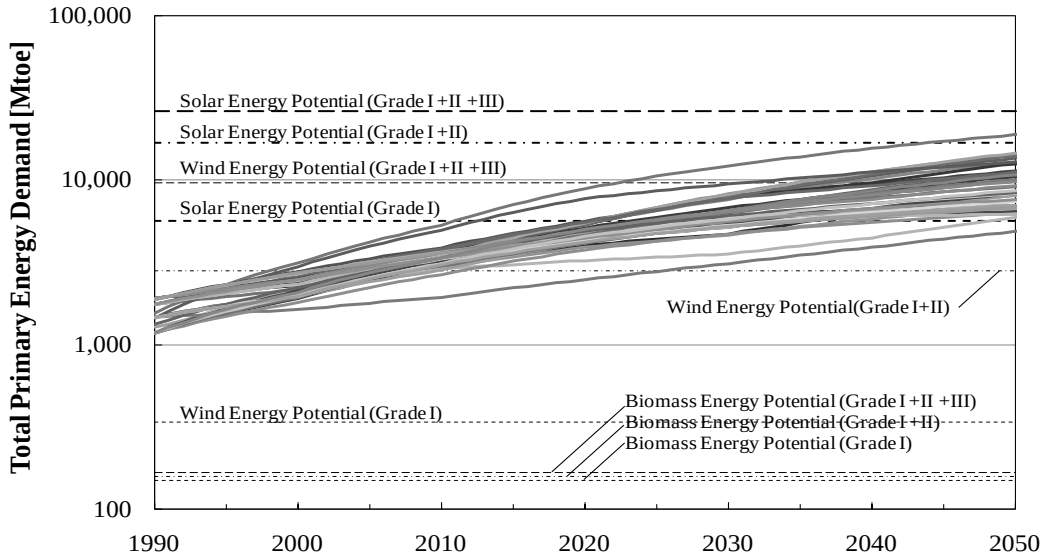

Fig. 1. Total primary energy forecast in published reports, and renewable energy potential

3.2.2. Renewable energy contributions in each region

Fig. 2 shows the outlook for primary energy supplies, fossil fuel supplies and renewable energies in three Asian regions: Japan, China and India. Each graph includes the maximum and minimum trends derived from the various reports collected and reviewed as part of this study. It can be seen that the renewable energy share is extremely small, overall. Fig. 2 also shows the calculation results obtained for physical and technical potentials (bold dashed lines). In the case of Japan and India, the solar energy potential (alone) exceeds the maximum predicted primary energy demand. On the other hand, China's energy growth is more rapid and larger than that of other Asian countries. Therefore, the renewable energy potential of China is not large enough to meet all of China's expected primary energy demand in the predicted maximum growth scenario. Renewable energy supply is effective even though fossil fuels will continue to dominate totally energy mixes for the foreseeable future.

3.3. Economic potentials

Fig. 3 shows the potential cost curve for three Asian regions: Japan, China and India. The horizontal axis (logarithmic scale) indicates the market potential. In the case of Japan, grade III solar energy shows most potential but has a high introduction cost. In contrast, the introduction cost of biomass energy is very low but the expected potential is small. In order to increase its share of renewable energy, Japan should, therefore, focus mainly on the installation of solar energy generation systems. In the case of China, the most potential is for grade II solar energy. The cost of grade III wind energy is more than 0.9USD/kWh higher

than other renewable resources. In India, grade I solar energy shows the most potential. Grade III wind energy also has a high cost, even in China and India. Consequently, solar energy should receive first priority for introduction and wind energy should be second. The potential for biomass energy is not as large, but its cost intensity is lower than either wind or solar power. Therefore, the immediate introduction of biomass energy systems could be an effective strategy in some Asian regions.

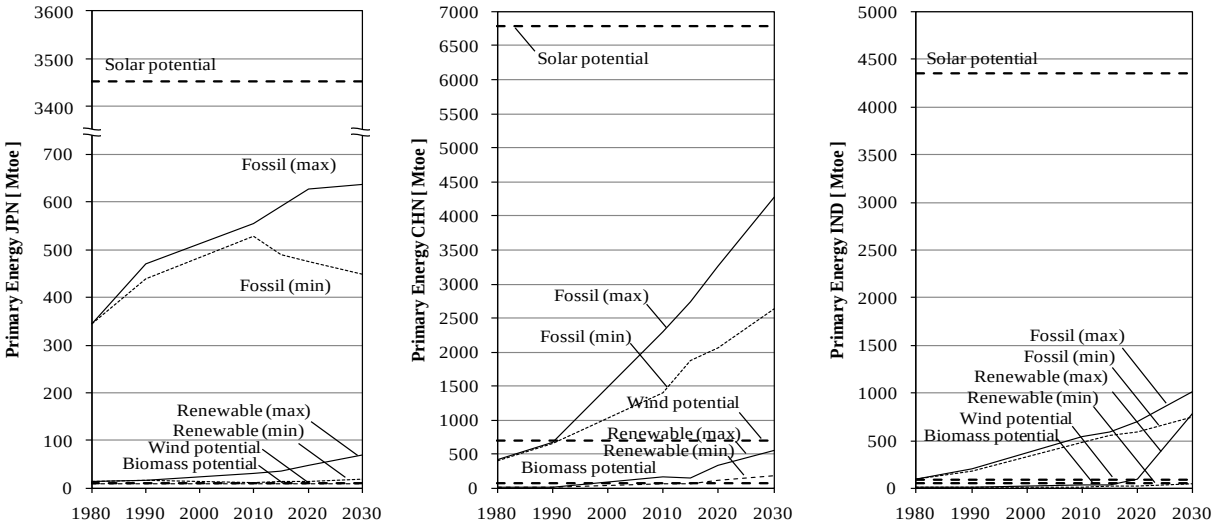

Fig. 2. Primary energy trends and renewable energy potentials in Japan (left), China (center), and India (right)

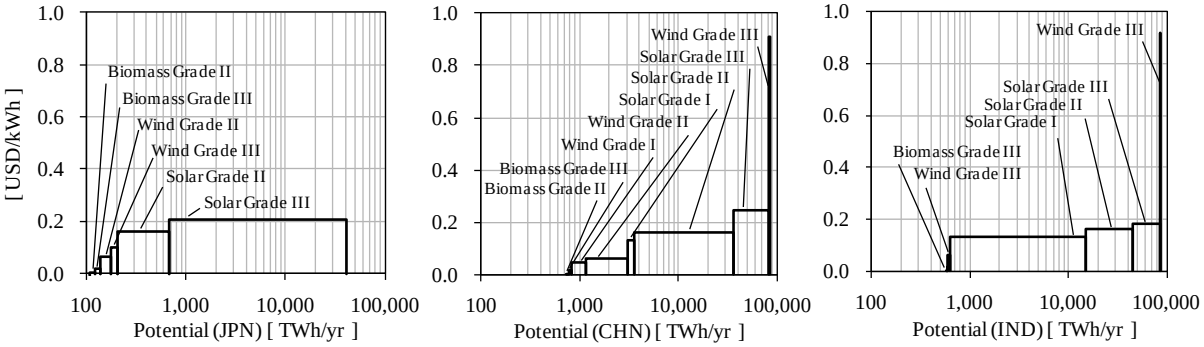

Fig. 3. Potential cost curves in Japan (left), China (center), and India (right)

4. Conclusions

Diversified analysis of potential renewable energy contributions to energy supply in Asian regions was carried out. As a result, estimates of renewable energy potential were refined, the socio-economic mechanisms associated with the introduction of renewable energy were calculated, and the relevant characteristics of each Asian country were analyzed. The results suggest that almost all Asian countries will continue to develop and that the demand for energy will grow drastically and rapidly. The results indicate that almost all Asian countries will continue to develop and that the demand for energy will grow. With the aspect from potential amount, renewable energy supply is effective even though fossil fuels will continue to dominate totally energy mixes fora the foreseeable future. In renewable energy supply, potential of solar is dominated and bears on wide implication compared with that of wind and biomass. To ensure the best possible results, further research should be carried out on the optimal schedule for the multi-phased introduction of renewable energy in long-term policy.

References

[1] IPCC 2001a, Climate Change 2001 – IPCC Third Assessment Report, Working Group III: Mitigation, 2001

[2] Hofman, Y., de Jager, D., Molenbroek, E., Schilig, F., Voogt, M., 2002. The Potential of Solar Electricity to Reduce CO2 Emissions. Ecofys, Utrecht.

[3] Grubb, M.J., Meyer, N.I., 1993. Wind energy: resources, systems, and regional strategies. In: Johansson, T.B., Kelly, H., Reddy, A.K.N., Williams, R.H. (Eds.), Renewable Energy: Sources for Fuels and Electricity. Island Press, Washington, DC.

[4] Berndes, G., Hoogwijk, M., van den Broek, R., 2003. The contribution of biomass in the future global energy supply: a review of 17 studies. Biomass and Bioenergy 25 (1), 1–27.

[5] MODIS/Terra Land Cover Type Yearly L3 Global 1km SIN Grid, 2005: Land Processes Distributed Active Archive Center (LPDAAC), U.S. Geological Survey (USGS).

[6] GLOBE: The Global Land One-km Base Elevation 30-sec. DEM, National Geophysical Data Center (NGDC), NESDIS, NOAA, U.S. Department of Commerce.

[7] Hastings, D. A. and Dunbar, P. K., 1999: Global Land One-km Base Elevation (GLOBE) Digital Elevation Model Documentation, Boulder, Colorado, NOAA National Geophysical Data Center, Publication KGRD 34.

[8] GEBCO One Minute Grid - Version 1.02, 2006: General Bathymetric Chart of Oceans.

[9] World Wilderness Areas, 1993: the Sierra Club and World Bank, as integrated by UNEP/GRID.

[10] Insolation Incident On A Horizontal Surface (22-year Monthly & Annual Average for July 1983 - June 2005), 2008: Surface meteorology and Solar Energy (SSE) Release 6.0 Data Set, Atmospheric Science Data Center, NASA Langley Research Center (LaRC).

[11] Wind Speed At 50m Above The Surface Of The Earth (10-year Monthly & Annual Average for July 1983 - June 1993), 2005: Surface meteorology and Solar Energy (SSE) Release 5 Data Set, Atmospheric Science Data Center, NASA Langley Research Center.

[12] Bert J.M. de Vries, Detlef P. van Vuuren, and Monique M. Hoogwijk, Renewable energy sources: Their global potential for the first-half of the 21st century at a global level: An integrated approach, Energy Policy, 35, 2007, 2590-2610

[13] FAO, FAOSTAT 2001 CD-ROM, Rome, 2001

[14] IPCC 2001b, Special Report on Emissions Scenarios, 2001

[15] IEA, World Energy Outlook, 2008

[16] EUROPEAN COMMISION, World Energy Technology Outlook 2050, 2006

[17] ADB, Energy Outlook for Asia and the Pacific, 2009

[18] Greenpeace, Energy Revolution Sustainable Energy Global Energy Outlook, 2008

[19] Shell, Shell Energy Scenarios to 2050, 2008

[20] OECD, OECD Environmental Outlook to 2030, 2008

Scenario analysis of the potential for CO_2 emission reduction in the Iranian cement industry

Farideh Atabi [1,*], Mohammad Sadegh Ahadi [2], Kiandokht Bahramian [3]

[1*] *Assistant Prof., Graduate School of Energy and the Environment, Science & Research Branch, Islamic Azad University, Tehran, Iran, P.O.Box: 14155/4933*
[2] *National Climate Change Office, Department of Environment, Tehran, Iran*
[3] *Environmental Engineer, Graduate School of Energy and the Environment, Science & Research Branch, Islamic Azad University, Tehran, Iran*
** Corresponding author. Tel: +989121341702, E-mail: far-atabi@jamejam.net*

Abstract: This article investigates the impact of various policies on the reduction of CO2 emissions from Iranian cement industry using a long range energy alternative planning (LEAP) model. A Business-as-Usual (BAU) scenario for the existing Iranian cement industry was applied. Moreover, the current and future demands for the cement industry were defined for 2005-2020. The current and future productivity of the cement industry was predicted in the BAU scenario. Then, three alternative scenarios were considered: replacement of heavy oil with natural gas, implementation of energy efficiency policies and integrated emission reduction, which includes all of the options over a 15-year period. The results indicated that in 2020, CO2 equivalent emissions would reach 61 million tons in the baseline scenario and 53 million tons in the integrated emission reduction scenario. If fuel switching were employed, the emissions would reach 58 million tons (4.9 % reduction) and in the energy efficiency scenario, the emissions would reach 55 million tons (9.8% reduction) in 2020. Therefore, the integrated scenario reduces the total CO2 equivalent emissions by 8 million tons (13% emission reduction).

Keywords: *CO_2 emission, cement industry, scenario analysis, energy model*

1. Introduction

Even though many countries have started to develop climate policies, scenario studies indicate that greenhouse gas emissions are likely to increase in the future in most regions around the world [1]. After the energy crisis of the 1970s, many researchers developed models to generate accurate predictions. Various models for prediction and the development of policies for mitigation can be divided into two groups: those used for mitigation in the energy sector, and those used to survey mitigation methods in the agriculture, forest and land use sectors [2]. One of the most important energy carriers in the industrial sector is natural gas, which plays a significant role in the reduction in the emission of environmental pollutants [3]. A study in Iran, evaluated the impacts of price reform and energy efficiency programs on the consumption of energy carriers and on GHG mitigation in the Iranian residential buildings sector using the LEAP model [4]. Research on substituting biomass with other energy carriers in Vietnam using the LEAP model, has shown that this fuel substitution leads to a 10.83 million-ton reduction in GHG emissions [5].

Another analysis of the environmental and economic impact of landfill gases (LFG) electricity generation in Korea using the LEAP model showed that LFG electricity generation would be an effective solution for CO_2 displacement over the medium term with additional energy profits and will reduce the global warming potential by a maximum of 75% when compared to spontaneous emissions of CH_4 [6]. Another study in Korea evaluated the environmental and economic aspects of chemical CO_2 absorption in power plants using this model; That study demonstrated that by applying various policies, the rate of CO_2 emissions will decrease by approximately 15% by 2014 [7]. Another study was also conducted to show the potential reduction in CO_2 emissions from oil refineries in Korea. Production analysis using the energy planning model showed that a 48% reduction in CO_2 emissions is feasible [8]. In this study, the energy demand of the Iranian cement industry is analysed with an

energy planning LEAP model. The effects of various policies on the baseline scenario and GHG mitigation scenario are also analysed and surveyed in the cement industry.

2. Methodology

Greenhouse gas emissions in the Iranian cement industry was surveyed in the format of a BAU scenario using the LEAP energy planning model. The results of employing different policies of energy efficiency and fuel switching on GHG mitigation in the format of mitigation scenario were then observed. Finally, the effectiveness of each policy applied in the cement industry over a 15-year period, from 2005 to 2020, was surveyed. In each scenario, the level of technological activity and energy intensity were specified, and in the activity data section, data relevant to consumption in the cement industry and the number of factories that use a specific resource, were defined in each scenario. Additionally, data describing the energy intensity of each type of fuel in each Factory were determined [9].

2.1. LEAP model

LEAP is an energy planning model that consists of an end-use structural model. Based on procedural analysis of the supply and demand network, the considered model describes technological energy carrier utilisation based on energy demand on one hand, and technological changes and therefore structural changes and efficiency of energy conversion systems as well as the rate and type of available primary energy resources on the other hand. This model consists of a hierarchical structure in which energy flows from the last point of usage (equipment and technology) toward higher levels. In fact, total energy demand is computed from each subcategory and category in a tree structure. In this model, the rate of total energy demand is computed according to Eq. 1.

$$\sum E_t = T_i \times I_i \tag{1}$$

where, E_t is the total energy demand (J), T_i is the data (i) activity level (ton), and I_i is energy intensity ($^{j}\!/\!_{ton}$) [6].

2.2. BAU scenario

In the (BAU) scenario, it is assumed that the current status of the Iranian cement industry will be maintained in the future, and that greenhouse gas emission in Iran's cement industry will be predicted by the main variables of BAU, such as the growth rate of cement production from 2005 to 2020, the type and rate of fuel consumption, the rate of technological changes and energy intensity.

In this scenario, 2005 was selected as the base year and all relevant information was gathered from this year [10]. Then, a BAU scenario was developed according to current plans as well as future policies, changes in cement production capacity, energy intensity, the fuel contribution that supplies the energy demand and other factors in the cement industry from 2005 to 2020. The GHG emission rate was assessed, and analysed. It was predicted that in the BAU scenario, the natural gas share of the total energy carriers, will increase from 63.11% in 2005 to 80% in the 2020 in the cement industry [11]. The amount of energy intensity of the whole cement industry in the country can be calculated using Eq. 2:

$$I_t = \sum c_i I_i \quad (2)$$

where, I_t is total energy intensity (j), I_i is energy intensity of respected technology (J/ton), and c_i is the technology (i) share in the total cement production in the country (%).

Energy demand as shown in Eq. 3 is calculated by multiplying cement production (activity data) by energy intensity:

$$E = \sum_{i=1}^{n} A_i \times I_i \quad (3)$$

where, E is energy demand (million GJ), A_i is cement production (million tons), and I_i is energy consumption for each activity (million GJ/ton).

The LEAP model is used to calculate the equivalent emission of CO_2 in the cement industry in three forms: (1) emission from direct consumption of energy carriers in cement industry, (2) emission from consumption of energy carriers in oil and gas refineries and power plants in order to supply the cement industry with both fuel and electricity (indirect), and (3) emissions from consumption of energy carriers in the industry, refineries and power plants to supply the energy demand to the cement industry (total emission).

2.3. Mitigation scenario

In the mitigation scenario, different policies to mitigate the energy demand are considered as input data for the LEAP model. Then, the model is compared with the BAU scenario by predicting the demands of energy carriers and the calculated mitigation in emissions. The policies surveyed here are fuel switching and more energy efficient technologies. In this scenario, it is assumed that all cement production units older than 20 years are replaced with new and efficient technologies and that energy efficient improvement plans are implemented on units that are 10 to 20 years old [12]. It is also assumed that the natural gas and biomass share in the mitigation scenario is 5% more than that in the BAU scenario in 2020. Energy carrier demand will increase 139% in this period.

3. Results and discussion

In Table 1, the average energy intensity for Iran's cement industry was calculated and presented separately based on the type of process. In the calculations, the average energy intensity weight was compared to the capacity of the entire cement industry in the country.

Table1. Energy intensity rate in the various cement industry technologies in Iran in 2005 [13]

Technology	Proportion of Total Production (percent)	Production (ton/yr)	Capacity (ton/day)	Fuel Consumption Intensity (kcal/kg.clinker)	Electricity Consumption Intensity (kWh/ton)
Dry high heater	5.14	1,600,500	4,850	1125	111
Dry pre heater	40.51	12,606,000	38,200	950	108
Dry pre heater & precalcinors	51.70	16,087,500	48,750	890	114
Mid dry pre calciners	0.64	198,000	600	1020	110
Wet process	2.01	627,000	1,900	2000	150
Total / Weighted average	100	31,119,000	94,300	949.6	112.1

To evaluate the changes in energy intensity, in addition to recognizing current infrastructures in each of the subsectors of the industry, the theoretical potential for increasing the efficiency of equipment and energy intensity of industrial products in developed countries is also needed. In the BAU scenario, the annual increase in energy demand reaches 11.51% and the demand for all energy carriers shows an annual increase of 10.7%.

It is predicted that the share of natural gas in the BAU scenario among all energy carriers in this industry will increase from 63.11% in 2005 to 80% in 2020. Meanwhile, the mitigation scenario shows a 5% increase in 2020 compared to the BAU scenario in the same year. Results from LEAP in Fig. 1 show that in the BAU scenario, emissions of CH_4, CO_2 and NO_x have also increased during this period; CO_2 has the highest increase.

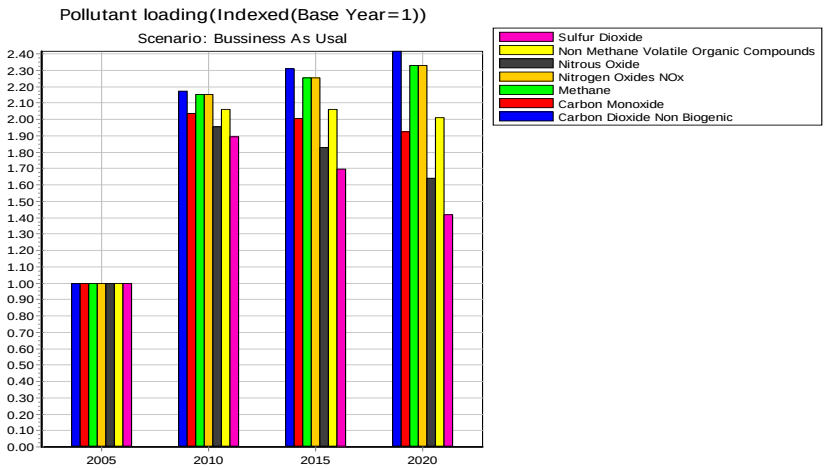

Fig.1. Prediction of the trends of the emission of pollutants and GHG (dimensionless) in the Iranian cement industry in the baseline scenario.

Meanwhile, the thermal energy demand in the mitigation scenario in 2020 shows a 33% reduction in the thermal energy demand compared to that of the BAU scenario. The emissions of all pollutants increase until 2010 and then decline because of the replacement of units that are older than 20 years with new and more efficient technologies. It should be noted that the emission of SO_2 and NO_x in 2020 are 40% and 10% less than the emission of these pollutants in the first year (2005) respectively, whereas, the emission of NO_x and SO_2 in the baseline scenario has increased by 40% and 65% , respectively. Therefore, after applying the

emission reduction policies (mitigation scenario), the emissions of SO_2 and NO_x show 80% and 75% reduction in 2020 respectively, compare to those of the BAU scenario.Table 2. shows the energy carriers in the BAU scenario and the mitigation scenarios.

Table 2. Comparison among the different energy carriers, that are needed in the Iranian cement industry in the year 2020 in the BAU and mitigation scenarios

Fuel	Share of the total demand (%) 2005	Share of the total demand (%) 2020	
		Mitigation scenario	BAU Scenario
Fuel oil	36.1	9.21	19.3
Natural gas	63.11	85	80
Diesel fuel	0.79	0.79	0.79
Biomass	0	5	0

As shown in Fig. 2, by implementing the policy of changing the process on one hand and the energy efficiency on the other hand, the amount of required energy carriers decreased from 340 million GJ in 2020 to 310 million GJ, and consequently, energy demand decreased by 11.5 percent.

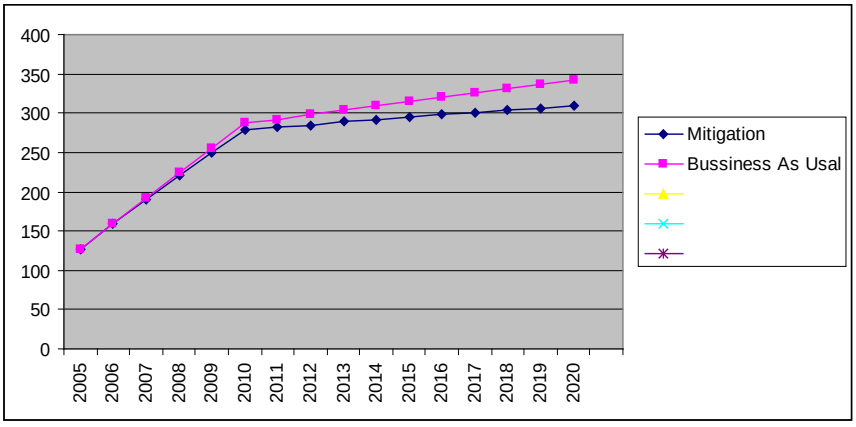

Fig. 2. Comparison of energy carriers demand in the baseline and mitigation scenarios in the Iranian cement industry (million GJ)

Results show that employing different policies regarding CO_2 emissions reduces these emissions from 16 million tons to 11 million tons in 2020. Fig. 3 shows a comparison of the CO_2 emissions in the BAU and mitigation scenarios in the Iranian cement industry.

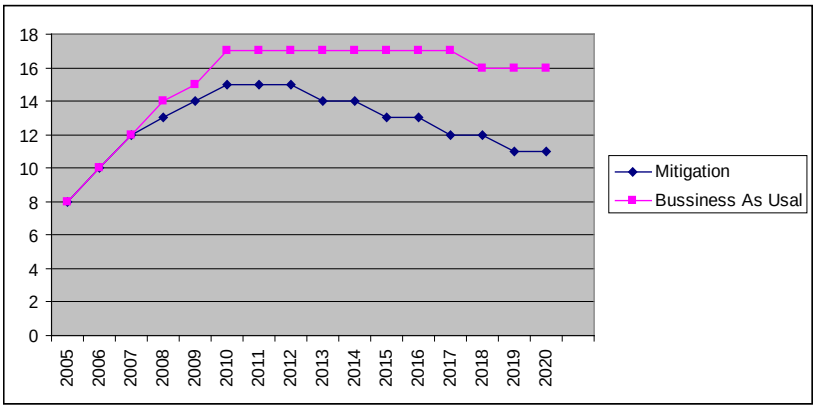

Fig.3. A comparison of CO2 emission in the BAU and mitigation scenarios in the Iranian cement industry (million tons).

As shown in Fig. 4, GHG emission (CO_2 equivalent) is reduced as a result of the efficiency policy and the fuel switching policy by 9.8% and 4.9%, respectively. However, emission reduction will be up to 13% by employing both policies**.**

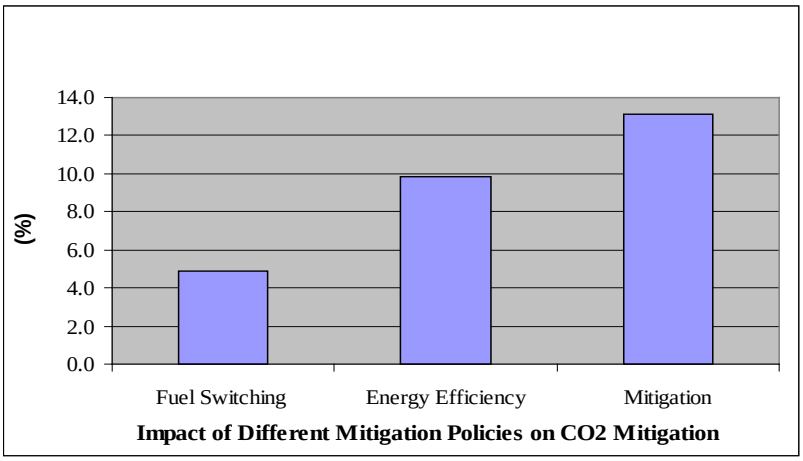

Fig. 4. Comparison of exerting different policies for GHGs (CO2 equivalent) reduction and integration of different scenarios in the Iranian cement industry

4. Conclusion

In this study, the process of technological changes that have improved the energy intensity in the Iranian cement industry specifically are used to predict the energy intensity in the BAU scenario and the mitigation scenario using LEAP software. To predict the greenhouse gas emissions rate in the different scenarios, the effects of the application of these actions on energy demand and fuel make-up are specified. A comparison of the effectiveness of different policies shows that the energy efficiency is more important than fuel switching in reducing CO_2 emissions.

Acknowledgement

The authors are especially grateful to Iran Fuel Conservation Company (IFCO) for its financial support.

References

[1] IPCC, 2000, Special Report on Emission Scenarios, A special report of working group III of Intergovernmental Panel on Climate Change, Cambridge University Press, Cambridge, UK

[2] IPCC, 1997, Technical Paper 2 , Second assessment report

[3] Ministry of energy, 2007, Energy balance, Energy Department, I.R.I

[4] Ahadi, M.S. et al., 2005, Policy making of energy resources in industry, National Climate Change Office, Department of Environment, Tehran, Iran

[5] Kumar Amit, et al., 2003, Greenhouse gas mitigation potential of biomass energy technologies in Vietnam using the long range energy alternative planning system model, Energy Policy Journal, No. 28, pp. 627-654

[6] Shin, H.C., Park J.W., Kim, H.S., Shin, E.S., Environmental and economic assessment of landfill in Korea using LEAP model, Energy Policy Journal, No. 33, 2005 , pp.1261-1270

[7] Song, HO-JUN, et al., 2007, Environmental and economic assessment of the chemical absorption, Energy Policy Journal, No. 35, pp. 5109-5116

[8] Sangwon Park, et al., 2007, Assessment of CO_2 and reduction potential in Korea petroleum using energy models, Energy Journal, No. 35,pp. 2419-2420

[9] Ministry of Industry, 2006, Cement production in 2020, Energy department, I.R.I

[10] Energy Efficiency Office, 2005, Report on energy efficiency in the cement industry, Ministry of Energy, I.R.I

[11] Institute for International Studies, 2004, Prediction of energy demand for in various energy sectors, Ministry of Oil, I.R.I

[12] Hoseini, S.A., 2009, Assessment of energy efficiency potential in cement industry, Cement Research Center, I.R.I

[13] Ministry of Energy, 2005, Report on energy intensity in the cement industry, Energy Department, I.R.I